FELIPE ALVES DE ALMEIDA

INDUÇÃO DO MECANISMO DE *QUORUM SENSING* POR AUTOINDUTOR-1 EM S*almonella enterica* E PROSPECÇÃO DE INIBIDORES

Tese apresentada à Universidade Federal de Viçosa, como parte das exigências do Programa de Pós-Graduação em Microbiologia Agrícola, para obtenção do título de *Doctor Scientiae*.

VIÇOSA
MINAS GERAIS – BRASIL
2018

Ficha catalográfica preparada pela Biblioteca Central da Universidade Federal de Viçosa - Câmpus Viçosa

T
A447i
2018

Almeida, Felipe Alves de, 1988-
Indução do mecanismo de *quorum sensing* por autoindutor-1 em *Salmonella enterica* e prospecção de inibidores / Felipe Alves de Almeida. – Viçosa, MG, 2018.
xii, 151 f. : il. (algumas color.) ; 29 cm.

Orientador: Maria Cristina Dantas Vanetti.
Tese (doutorado) - Universidade Federal de Viçosa.
Inclui bibliografia.

1. Bactérias patogênicas. 2. Proteínas. 3. Reação de oxidação-redução. 4. Tiol. 5. Biofilmes. 6. Inibidores. 7. Quorum sensing (Microbiologia). 8. Agentes anti-inflamatórios não esteróides. I. Universidade Federal de Viçosa. Departamento de Microbiologia. Programa de Pós-Graduação em Microbiologia Agrícola. II. Título.

CDD 22. ed. 579.344

FELIPE ALVES DE ALMEIDA

INDUÇÃO DO MECANISMO DE *QUORUM SENSING* POR AUTOINDUTOR-1 EM *Salmonella enterica* E PROSPECÇÃO DE INIBIDORES

Tese apresentada à Universidade Federal de Viçosa, como parte das exigências do Programa de Pós-Graduação em Microbiologia Agrícola, para obtenção do título de *Doctor Scientiae*.

APROVADA: 26 de fevereiro de 2018.

Uelinton Manoel Pinto
(Coorientador)

Tiago Antônio de Oliveira Mendes

Edvaldo Barros

Natan de Jesus Pimentel Filho

Maria Cristina Dantas Vanetti
(Orientadora)

A Deus e a todos que torceram por mim

DEDICO.

"...e ainda se vier, noites traiçoeiras
se a Cruz pesada for, Cristo estará comigo
e o mundo pode até
me fazer chorar
mas Deus me quer sorrindo..."
(Carlos Papae).

"Não devemos permitir que alguém saia da nossa
presença sem se sentir melhor e mais feliz."
(Madre Teresa de Calcutá).

"As pessoas acham que foco significa dizer sim
para a coisa na qual você está concentrado.
Significa dizer não para centenas de
outras boas ideias que existem.
Você precisa escolher com cuidado."
(Steve Jobs).

AGRADECIMENTOS

A Deus pela realização de mais esse sonho;

À Universidade Federal de Viçosa (UFV) e ao Departamento de Microbiologia, pela qualidade do ensino;

Ao Conselho Nacional de Desenvolvimento Científico e Tecnológico (CNPq), pela concessão da bolsa de doutorado;

À professora Maria Cristina Dantas Vanetti, pelos ensinamentos, pela amizade, compreensão e paciência que foram fundamentais para o êxito deste trabalho;

Ao meu coorientador professor Uelinton Manoel Pinto da Universidade de São Paulo (USP), pela disponibilidade, atenção e sugestões;

Ao meu coorientador professor Leandro Licursi de Oliveira, pela atenção, disponibilidade e ensinamentos;

Ao professor Hilário Cuquetto Mantovani da UFV, pela disponibilidade do Laboratório de Anaeróbios da UFV;

À professora Maria Cristina Baracat Pereira, pela atenção, pelas sugestões e por disponibilizar o Laboratório de Proteômica e Bioquímica de Proteínas para a realização dos experimentos de proteômica;

À Lanna Carrijo e Patrícia Fontes do Laboratório de Proteômica e Bioquímica de Proteínas, pela atenção, pelos ensinamentos e pela paciência em me ensinar;

Ao Professor Tiago Antônio de Oliveira Mendes da UFV, pela paciência, disponibilidade e, claro, todos os ensinamentos durante as análises dos dados e na disciplina de Bioinformática;

Ao Edvaldo Barros, pela paciência e disponibilidade em ensinar a analisar os dados de proteômica;

À professora Poliane Alfenas Zerbini da UFV, pela disponibilidade do Laboratório de Virologia da UFV;

Ao Renan Cascardo, pela paciência e ensinamentos durante a parte de biologia molecular;

Ao professor Maximiller Dal Bianco Lamas Costa da UFV, pelos ensinamentos e discussões sobre biologia molecular;

Ao professor Marcos Rogério Tótola e ao técnico Karlos Kalks da UFV, por disponibilizar o Laboratório de Biotecnologia e Biodiversidade Ambiental da UFV;

Ao Laboratório Nacional de Biociências (LNBio) do Centro Nacional de Pesquisa em Energia e Materiais (CNPEM) de Campinas-SP e aos funcionários, pela disponibilidade e apoio durante as análises de proteínas por espectrometria de massas;

Ao Núcleo de Análise de Biomoléculas (Nubiomol) da UFV, pelas análises dos dados de proteômica;

Ao Natan de Jesus Pimentel-Filho, pelas contribuições e pela disponibilidade;

À Maria Emilene Campos-Galvão, por iniciar a linha de pesquisa de *quorum sensing* por autoindutor-1 em *Salmonella* no Laboratório de Microbiologia de Alimentos da UFV;

À minha amiga Selda Bastos, pela amizade e pela disponibilidade em buscar as culturas na FIOCRUZ;

A todos os professores que, durante o mestrado e doutorado, contribuíram para minha formação;

Aos funcionários do Departamento de Microbiologia, pela amizade e disposição em ajudar, em especial, aos funcionários Aline, Danilo, Emília, Gabriel, Iraci, José Carlos, José Cesário, Letícia, Nilcéa, Paulo, Raquel, Sandra;

Ao Instituto de Laticínios Cândido Tostes da EPAMIG, por ter possibilitado o meu aperfeiçoamento em docência;

Aos funcionários do Departamento de Nutrição da UFJF de Governador Valadares, pelo apoio na finalização desta tese;

À minha mãe, Rosa Mônica, pelo amor, carinho e pela educação;

Ao meu pai, Cássio, pelo amor;

Ao meu irmão, Raphael, pela amizade e alegria e, claro, pelas horas de descontração;

Ao meu irmão, Gustavo, pela amizade;

Aos meus avós, Celma, Dirceu (*in memorian*), Gracy (*in memorian*) e Rubens (*in memorian*), pelo amor incondicional mesmo não entendendo o que é a pós-graduação e não estando fisicamente presentes;

À minha madrinha Elza (*in memorian*), pelo amor, por deixar a maior herança da minha vida que é a educação;

Aos meus tios e primos, pelo carinho e pela amizade;

A toda minha família, pela torcida e pelas orações;

Ao Matheus, pela amizade, pelo companheirismo e incentivo;

À minha eterna “Chaperona”, também chamada de Déborah Romaskevis, pelo companheirismo e pela amizade;

À minha “Brother” do *quorum sensing*, Deisy Guimarães, sempre disponível em ir trabalhar nas madrugadas e, claro, pelas inúmeras risadas e ajudas;

À minha amiga Elsa Fernandes e à sua família, que me acolheu de braços abertos na minha nova etapa da vida na Universidade Federal de Juiz de Fora (UFJF);

À minha amiga Nívea Vieira, por toda a amizade e ensinamentos nos trâmites de concursos públicos;

Às minhas amigas Érika Vargas, Mariana Alvim, Raquel Santos e Sofia Moreira, por toda amizade, companheirismo e apoio;

Aos meus amigos do Laboratório de Microbiologia de Alimentos da UFV, Claúdia, Cleonice, Cleriane, Deisy, Érika, Fábio, Fernanda, Gabriel, Leandro, Leonardo, Mayara, Natan, Ramila e Solimar, pelo carinho e ajuda nos experimentos;

Às minhas amigas do Laboratório de “Anaeróbicos”, Analice, Bianca, Cláudia, Déborah, Elsa, Isabela, Juliana, Sofia e Yasmin, pela amizade e ajuda nos experimentos;

Aos meus amigos do Laboratório de Virologia da UFV, Coxinha, Jonas, Paty, Rafael e Renan, pelos momentos de descontração;

Aos meus amigos Ana e Álvaro, pelos momentos de descontração;

Às minhas amigas Nati, Dora e Aparecida, pelas conversas e preocupação com meu bem-estar;

Aos meus amigos de Viçosa, Juiz de Fora e Governador Valadares pela amizade, pelo carinho, pelos momentos de alegria e descontração;

A todas as pessoas que, de alguma forma contribuíram e torceram por este sonho.

MUITO OBRIGADO!

BIOGRAFIA

FELIPE ALVES DE ALMEIDA, filho de Rosa Mônica Mattoso Alves e Cássio Murilo de Almeida, nasceu em Juiz de Fora - MG, em 10 de dezembro de 1988.

Em julho de 2011, graduou-se em Biomedicina pela Universidade Presidente Antônio Carlos em Juiz de Fora – MG.

Em março de 2012, ingressou no Programa de Pós-Graduação em Microbiologia Agrícola, na área de Microbiologia de Alimentos, na Universidade Federal de Viçosa submetendo-se à defesa de dissertação no dia 27 de fevereiro de 2014.

Em março de 2014, iniciou o curso de doutorado neste programa e área, submetendo-se à defesa de tese em 26 de fevereiro de 2018.

Em janeiro de 2018, entrou em exercício no cargo de Técnico em Alimentos e Laticínios no Departamento de Nutrição da Universidade Federal de Juiz de Fora *campus* Governador Valadares.

ÍNDICE

RESUMO

ALMEIDA, Felipe Alves de, D.Sc., Universidade Federal de Viçosa, fevereiro de 2018. **Indução do mecanismo de *quorum sensing* por autoindutor-1 em *Salmonella enterica* e prospecção de inibidores**. Orientadora: Maria Cristina Dantas Vanetti. Coorientadores: Leandro Licursi de Oliveira e Uelinton Manoel Pinto.

O mecanismo de *quorum sensing* em *Salmonella* pode ser mediado por três tipos de autoindutores (AI), denominados AI-1, AI-2 e AI-3. Contudo, o mecanismo por AI-1 neste patógeno é incompleto, pois não há síntese do AI-1, denominado acil homoserina lactona (AHL). Porém, *Salmonella* possui a proteína SdiA, homóloga a proteína LuxR, que permite detectar as AHLs produzidas por outras bactérias. A influência da AHL sobre a expressão de genes específicos de *Salmonella*, como os genes do operon *rck* e outros genes de virulência é reconhecida. Entretanto, poucos são os estudos que avaliaram a resposta global de *Salmonella* na presença de AHLs exógenas. Assim, os objetivos do presente estudo foram avaliar a influência da AHL sobre a resposta global de *Salmonella*, bem como avaliar a ligação destes AIs-1 à proteína SdiA e realizar a prospecção, *in silico,* de inibidores do mecanismo de *quorum sensing* por AI-1 em *Salmonella*. As análises globais dos perfis de proteínas, ácidos graxos e ácidos orgânicos extracelulares ao longo do tempo de cultivo de *Salmonella enterica* sorovar Enteritidis PT4 em anaerobiose na presença e ausência de *N*-dodecanoil homoserina lactona (C12-HSL), mostraram que estes perfis foram alterados na presença do AI. Além disso, os perfis de proteínas e ácidos graxos variaram menos ao longo do tempo de cultivo na presença de C12-HSL, ou seja, células cultivadas por 4 h (fase logarítmica) e por 36 h (fase estacionária) na presença do AI-1 apresentaram perfis de ácidos graxos e proteínas menos dispersos em comparação ao controle sem AHL, onde foi detectada grande variação destes perfis. Estes resultados indicam que as células na presença de C12-HSL estão mais preparadas para os estresses de fase estacionária, por haver a antecipação das alterações celulares que ocorrem nesta fase. Outro fato constatado é que as proteínas relacionadas ao processo de oxirredução, principalmente proteínas tiol, e a quantidade de tiol celular livre foram maiores em células cultivadas na presença de C12-HSL, indicando que este patógeno está mais preparado para uma possível condição de estresse oxidativo. A proteína SdiA de *Salmonella* Enteritidis foi modelada e verificou-se que as AHLs com cadeia acila mais longas têm mais afinidade a esta proteína, principalmente as AHLs com 12 carbonos. Além disso, as furanonas que são conhecidos inibidores do mecanismo de *quorum sensing*, também foram capazes de

ligar a SdiA de *Salmonella* com alta afinidade nas análises *in silico*. A prospecção de inibidores entre compostos de planta e anti-inflamatórios não esteroides (AINEs) por *docking* molecular também mostrou que a maioria dos compostos analisados foi capaz de ligar a proteína SdiA de *Salmonella*, com destaque para o Z-fitol e o lonazolaco. Os resultados do presente trabalho indicam caminhos para determinar as vias e, ou macromoléculas chaves do metabolismo influenciadas pelo mecanismo de *quorum sensing* por AI-1 em *Salmonella.* Além disso, os resultados obtidos *in silico* indicam potenciais compostos inibidores do *quorum sensing* para serem avaliados *in vitro*.

ABSTRACT

ALMEIDA, Felipe Alves de, D.Sc., Universidade Federal de Viçosa, February, 2018. **Induction of quorum sensing mechanism by autoinducer-1 in *Salmonella enterica* and prospection of inhibitors**. Adviser: Maria Cristina Dantas Vanetti. Co-Advisers: Leandro Licursi de Oliveira and Uelinton Manoel Pinto.

The mechanism of quorum sensing in *Salmonella* can be mediated by three types of autoinducers (AI), denominated AI-1, AI-2 and AI-3. However, the mechanism by AI-1 in this pathogen is incomplete, since it does not synthesize AI-1, called acyl homoserine lactone (AHL). On the other hand, *Salmonella* codes for the SdiA protein, a homologue of LuxR, which allows the detection of AHLs produced by other species of bacteria. The influence of AHL on the expression of *Salmonella*-specific genes such genes of the *rck* operon and other virulence genes is recognized. However, few studies have evaluated a global response of *Salmonella* in the presence of exogenous AHLs. Thus, the objectives of this study were to evaluate the influence of AHL on a global response of *Salmonella*, as well as to understand how these AI-1 bind to the SdiA protein and to carry out the prospection of inhibitors of the mechanism of quorum sensing by AI-1 in *Salmonella*. The global analyses of the protein, fatty acid and extracellular organic acid profiles throughout the cultivation time of *Salmonella enterica* serovar Enteritidis PT4 in anaerobic conditions in the presence and absence of *N*-dodecanoyl homoserine lactone (C12-HSL) showed that these profiles were changed in the presence of the AI. In addition, the protein and fatty acid profiles vary less throughout the cultivation time in the presence of C12-HSL, that is, the fatty acid and protein profiles of cells cultivated for 4 h (logarithmic phase) and for 36 h (stationary phase) in the presence of AI-1 were less dispersed in comparison to the control without AHL, which had great variation of these profiles. These results indicate that cells in the presence of C12-HSL are better suited for the stresses of the stationary phase, because there is the anticipation of cellular changes occurring at this stage. Another interesting fact is that proteins related to the oxidation-reduction process, especially thiol proteins and the levels of thiol were higher in cells cultivated in the presence of C12-HSL, indicating that this pathogen is more prepared for a possible condition of oxidative stress. The SdiA protein of *Salmonella* Enteritidis was modeled and it was found that AHLs with more carbons have more affinity to this protein, especially the AHLs with 12 carbons. In addition, the furanones that are known inhibitors of quorum sensing also have been able to bind to SdiA protein of *Salmonella* with high affinity. The prospection of inhibitors among

plant compounds and non-steroidal anti-inflammatory drugs (NSAIDs) by molecular docking also showed that most of the compounds analyzed were able to bind to SdiA protein of *Salmonella*, especially Z-phytol and lonazolac. The results of this work indicate ways to determine the key pathways and, or macromolecules of metabolism influenced by the mechanism of quorum sensing by AI-1 in *Salmonella*. These results obtained *in silico* indicate potential inhibitor compounds of the quorum sensing to be evaluated *in vitro*.

1. INTRODUÇÃO GERAL

Salmonella é um dos patógenos mais comumente veiculados por alimentos no mundo e alguns fatores de patogenicidade desta bactéria já foram descritos como sendo regulados pelo mecanismo de comunicação celular conhecido como *quorum sensing*. A comunicação por *quorum sensing* em *Salmonella* pode ser mediada por três tipos de autoindutores (AI), denominados AI-1, AI-2 e AI-3. Contudo, o mecanismo por AI-1 neste patógeno é incompleto, pois o mesmo não sintetiza o AI-1, denominado de acil homoserina lactona (AHL). Porém, *Salmonella* apresenta a proteína SdiA, homóloga a proteína LuxR, que permite detectar as AHLs produzidas por outras bactérias.

A influência da AHL sobre a expressão de genes específicos de *Salmonella*, como os genes do operon *rck* e outros genes de virulência e genes de formação de biofilme é reconhecida. Entretanto, poucos são os estudos que avaliaram uma resposta global de *Salmonella* na presença de AHLs exógenas, como mostrado no Capítulo 1. Estudos que abordassem análises globais dos metabólitos de *Salmonella* na presença do AI-1 poderiam contribuir para a compreensão das vantagens e desvantagens para este patógeno em responder às AHLs. Além disso, contribuiriam para a definição de vias e, ou macromoléculas chaves do metabolismo influenciados por estes AIs. Assim, os objetivos dos Capítulos 2 e 3 foram realizar análises globais do metabolismo de *Salmonella* na presença do AI-1 do mecanismo de *quorum sensing*.

Como genes de virulência e fatores de patogenicidade de *Salmonella* foram influenciados pelo *quorum sensing* mediado pelo AI-1, entender como as AHLs se ligam na proteína SdiA e buscar inibidores deste mecanismo pode ser uma estratégia para reduzir a patogenicidade e controlar processos de infecção por este patógeno. Assim, os objetivos dos Capítulos 4 e 5 foram o de avaliar a ligação de moléculas de *quorum sensing* e *quorum quenching* à proteína SdiA de *Salmonella*, bem como buscar compostos de plantas e anti-inflamatórios não esteroides (AINEs) com potencial anti-*quorum sensing* utilizando a técnica de *docking* molecular.

CAPÍTULO 1

Revisão: Mecanismo de *quorum sensing* por autoindutor-1 em *Salmonella*

Revisão: Mecanismo de *quorum sensing* por autoindutor-1 em *Salmonella*

Salmonella é um dos principais patógenos veiculados por alimentos em todo o mundo e, estatísticas do Centro de Controle e Prevenção de Doenças dos Estados Unidos (CDC) estimaram que, no período de 2000 a 2011, aproximadamente, 9,4 milhões das doenças de origem alimentar tiveram o agente etiológico identificado e, destas, *Salmonella* não tifoide foi a causa de 1.027.561 casos, 19.336 hospitalizações e 378 mortes (SCALLAN *et al.*, 2011). No Brasil, segundo dados do Ministério da Saúde, do total de surtos alimentares notificados no mesmo período, 19,16 % estavam associados à presença de *Salmonella* (BRASIL, 2011).

A capacidade de adaptar às condições estressantes manifestada por este patógeno está relacionada aos fatores de patogenicidade. Na maioria das vezes, estes fatores são codificados em regiões do DNA bacteriano denominadas de Ilhas de Patogenicidade (PAIs ou SPIs) (HUMPHREY *et al.*, 1996, 1998; ONG *et al.*, 2010). No gênero *Salmonella* já foram descritas 23 PAIs, as quais possuem estruturas e funções distintas relacionadas com a adaptação e a patogenicidade (HENSEL, 2004; HAYWARD *et al.*, 2013). Genes de patogenicidade pertencentes a estas PAIs tiveram sua expressão influenciada pelo mecanismo de *quorum sensing* (AHMER *et al.*, 1998; MICHAEL *et al.*, 2001; SMITH e AHMER, 2003; ABED *et al.*, 2014; CAMPOS-GALVÃO *et al.*, 2015b).

O *quorum sensing* é definido como um mecanismo de comunicação entre células que leva à expressão diferencial de genes em resposta a mudanças na densidade populacional (FUQUA *et al.*, 1994, 1996, 2001; KELLER e SURETTE, 2006; READING e SPERANDIO, 2006). Em *Salmonella*, este mecanismo pode ser mediado por três tipos diferentes de autoindutores (AI), AI-1, AI-2 e AI-3 (AHMER, 2004; SMITH *et al.*, 2004; WALTERS e SPERANDIO, 2006; AMMOR *et al.*, 2008). Os AIs-

1 são *N*-acil homoserina lactonas (AHLs) (MICHAEL *et al.*, 2001; SMITH e AHMER, 2003; AHMER, 2004; WALTERS e SPERANDIO, 2006), os AIs-2 são (2R, 4S)-2-metil-2,3,3,4-tetrahidroxitetrahidrofuranos (R-THMF) derivados das 4,5-dihidroxi-2,3-pentanodionas (DPD) (TAGA *et al.*, 2001) e os AIs-3 são moléculas produzidas pela microbiota gastrointestinal normal e hormônios da classe catecolamina, como adrenalina e noradrenalina, produzidos pelo hospedeiro (WALTERS e SPERANDIO, 2006; WALTERS *et al.*, 2006; ASAD e OPAL, 2008; HUGHES *et al.*, 2009; MOREIRA *et al.*, 2010).

A Figura 1 ilustra o sistema de *quorum sensing* por AI-1 em *Salmonella*.

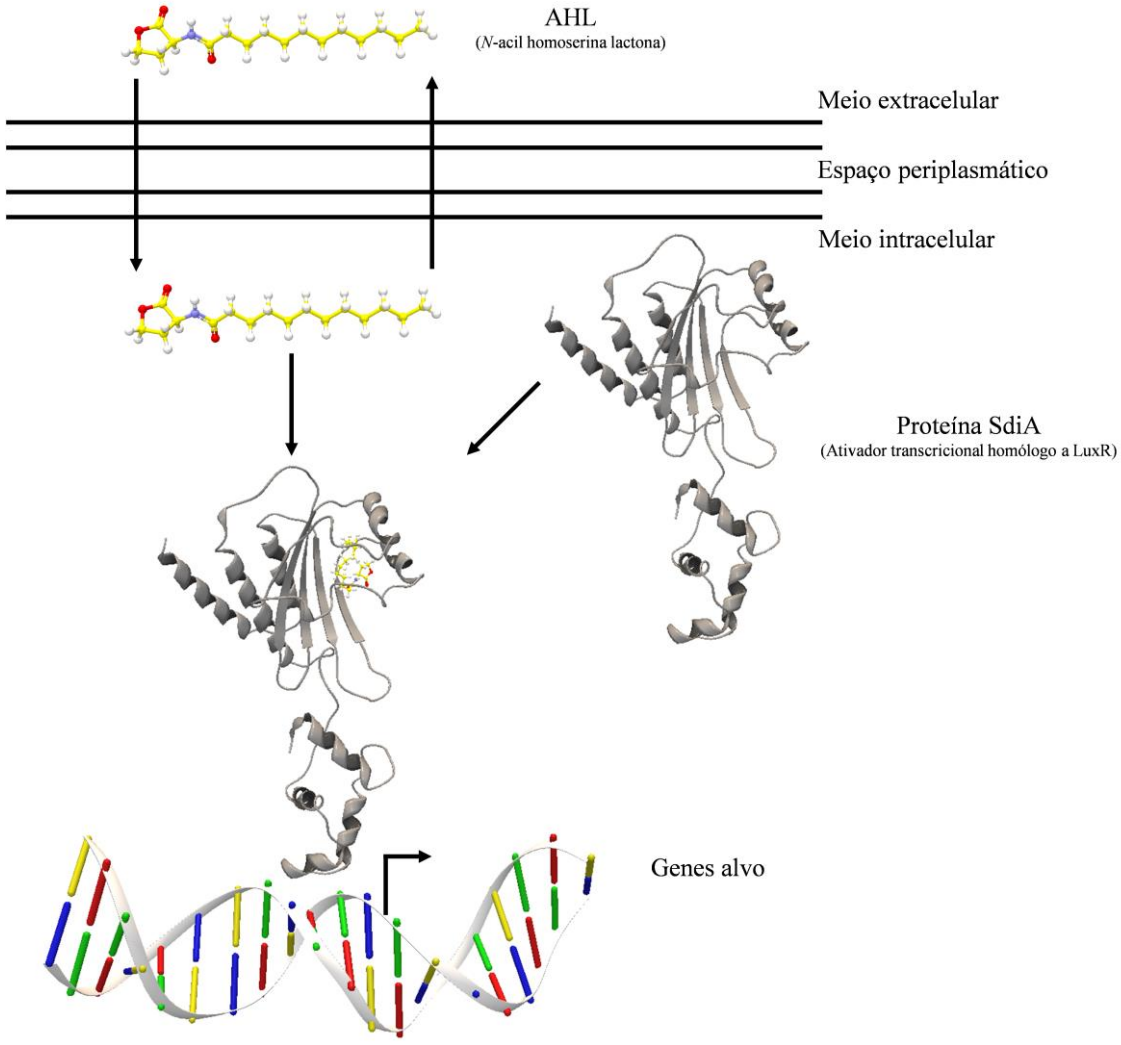

Figura 1. Sistema de *quorum sensing* por AI-1 em *Salmonella*. A AHL sintetizada por outras bactérias passa pela membrana e se liga à proteína SdiA, que por sua vez regula a expressão de genes alvo (Adaptada de AHMER, 2004; WALTERS e SPERANDIO, 2006).

O primeiro sistema *quorum sensing* mediado por AI-1 descrito no filo Proteobacteria depende de um par de proteínas chamadas LuxI (acil homoserina lactona sintase) e LuxR (ativador transcricional) ou proteínas homólogas. LuxI sintetiza AHLs, que também são chamadas de AI-1. Muitas Proteobacterias pertencentes à família Enterobacteriaceae, como *Salmonella* e *Escherichia coli*, não sintetizam AHL devido à ausência de LuxI ou homólogos (MICHAEL *et al.*, 2001; SMITH e AHMER, 2003; SABAG-DAIGLE e AHMER, 2012). Contudo, Carneiro (2017) mostrou que a concentração de *N*-dodecanoil homoserina lactona (C12-HSL) extracelular aumentou 1,64 vezes (32 nM) quando *Salmonella enterica* sorovar Enteritidis PT4 foi cultivada na presença de 50 nM desta molécula. Entretanto, quando cultivada na ausência deste AI, a C12-HSL não foi detectada. Estes dados sugerem que *Salmonella* pode ter uma sintase de AHL, ainda não identificada, com atividade regulada pelo AI.

Embora reconhecida por não sintetizar AI-1, *Salmonella* possui um homólogo de LuxR, conhecido como SdiA, que permite a detecção de AHLs sintetizadas por outras bactérias, como *Aeromonas hydrophila* e *Yersinia enterocolitica*, levando à regulação gênica (SMITH *et al.*, 2008; DYSZEL *et al.*, 2010). Estes AIs podem entrar e sair da célula por difusão ou através de bombas de efluxo dependendo do tipo de AHL (KAPLAN e GREENBERG, 1985; FUQUA *et al.*, 1994; PEARSON *et al.*, 1999; CASE *et al.*, 2008). Este AI se liga ao domínio N-terminal da proteína SdiA, alterando a afinidade de ligação do domínio C-terminal ao DNA e, consequentemente, regula a expressão de genes alvo (READING e SPERANDIO, 2006; NG e BASSLER, 2009; ATKINSON e WILLIAMS, 2009; NGUYEN *et al.*, 2015, ALMEIDA *et al.*, 2016). Michael *et al.* (2001) evidenciaram que a expressão do gene *sdiA* em *S. enterica* sorovar Typhimurium cultivada a 37 °C é induzida por uma concentração mínima de 1 nM, dependendo da AHL. Entretanto, Nguyen *et al.* (2015) mostraram que a presença de diferentes AHLs não altera a transcrição do gene *sdiA* de *E. coli* enterohemorrágica

(EHEC). Smith *et al.* (2008) também mostraram que o gene *sdiA* de *Salmonella* Typhimurium não foi ativado durante a passagem no trato gastrointestinal de camundongo, coelho, galinha, porco, porquinho-da-Índia e vaca, mas foi ativado em tartarugas colonizadas por *A. hydrophila* produtora de AHL. O gene *sdiA* de *Salmonella* Typhimurium também foi ativado durante a passagem pelo trato gastrointestinal de camundongos colonizados por *Y. enterocolitica* produtora de AHL, mas não quando colonizado por mutantes deste micro-organismo incapazes de sintetizar este AI (DYSZEL *et al.*, 2010). Quando o gene *yenI* de *Y. enterocolitica*, homólogo ao *luxI*, foi clonado em *Salmonella* Typhimurium, maior e imediata resistência às condições do trato gastrointestinal de camundongos foram observadas neste patógeno (DYSZEL *et al.*, 2010). Segundo os autores, esta diferença de ativação do gene *sdiA* no trato gastroinstinal dos organismos avaliados pode ser em função da presença ou não de bactérias que sintetizam AHLs, bem como em relação às interações e ao tempo de contato entre *Salmonella* Typhimurium e *Y. enterocolitica* necessário para ativar *sdiA*.

O fato de algumas bactérias gram-negativas não sintetizarem AHLs, mas responderem àquelas sintetizadas por outras bactérias, desperta a curiosidade sobre a função destas moléculas sinalizadoras nas bactérias não produtoras (SCHUSTER *et al.*, 2013). De acordo com Atkinson e Williams (2009), a ausência da sintase de AHL em *Salmonella* pode estar relacionada com a ecologia, uma vez que evitará a transferência de informação para outros micro-organismos presentes no meio. Além disso, não haverá o gasto energético com a síntese destas moléculas sinalizadoras. Entretanto, estas bactérias são favorecidas com as informações ambientais disponibilizadas no meio pelas outras bactérias. Considerando estas informações, ainda falta esclarecer quais seriam as alterações e vantagens que o *quorum sensing* por AI-1 promove em *Salmonella*. Segundo Di Cagno *et al.* (2011), as análises globais do proteoma e transcriptoma ajudariam a elucidar as influências do *quorum sensing* sobre a fisiologia celular e

revelar informações importantes sobre o comportamento microbiano, como vias e, ou macromoléculas chaves do metabolismo bacteriano.

A maioria dos estudos sobre o mecanismo de *quorum sensing* pelo AI-1 em *Salmonella* confirma a regulação da proteína SdiA, ligada ou não a AHLs, sobre os genes *pefI*, *srgD*, *srgA*, *srgB*, *rck* e *srgC* do operon *rck* (operon de resistência à morte mediada pelo sistema complemento) e do próprio operon *rck* presente no plasmídeo pSLT007 de *Salmonella* Typhimurium (AHMER *et al.*, 1998; MICHAEL *et al.*, 2001; SMITH e AHMER, 2003; NESSE *et al.*, 2011; ABED *et al.*, 2014). Ahmer *et al.* (1998) evidenciaram que a proteína SdiA de *Salmonella* Typhimurium é capaz de ativar parcialmente o promotor 2 do operon *ftsQAZ* e suprimir *ftsZ* responsável pela filamentação celular, ao contrário do que ocorre em *E. coli*. Estes resultados mostram que, apesar das proteínas SdiA de *Salmonella* e *E. coli* apresentarem alta similaridade (ALMEIDA *et al.*, 2016), elas podem não regular os mesmos genes alvo. Outros genes regulados por AHL em *Salmonella* estão relacionados com a patogenicidade como *hilA*, *invA* e *invF*, com a formação de biofilmes como *glgC*, *fliF*, *lpfA* e *fimF* e tiveram aumento na expressão após 7 h de cultivo em anaerobiose em caldo Triptona de Soja (TSB) contendo C12-HSL (CAMPOS-GALVÃO *et al.*, 2015b).

Além de reconhecer genes regulados por AHLs em *Salmonella*, alguns fenótipos são alterados quando o patógeno é cultivado na presença destes AIs. Nesse *et al.* (2011) mostraram que a invasão de células HEp-2 por *Salmonella* Typhimurium na presença de *N*-hexanoil homoserina lactone (C6-HSL) e *N*-octanoil homoserina lactone (C8-HSL) a 37 °C foi aumentada. A adição de C8-HSL juntamente com a presença do plasmídeo pRST98 que contém o gene de virulência *rck* em *S. enterica* sorovar Typhi, aumentou sua adesão em células HeLa após 1 h de incubação a 37 °C com 5 % gás carbônico (CO_2) (LIU *et al.*, 2014). A formação de biofilme por *Salmonella* Enteritidis PT4 578 em poliestireno foi regulada positivamente na presença de C12-HSL após 36 h de

cultivo em anaerobiose (CAMPOS-GALVÃO *et al.*, 2015b; ALMEIDA *et al.*, 2017a). Porém, não foi observada influência deste AI-1 sobre a adesão inicial das células em poliestireno (ALMEIDA *et al.*, 2017a) e nem sobre o crescimento planctônico (CAMPOS-GALVÃO *et al.*, 2015a; ALMEIDA *et al.*, 2017a). A formação de biofilme em poliestireno por *Salmonella* Typhimurium também foi influenciada pela presença de *N*-butiril homoserina lactone (C4-HSL) e C6-HSL, em condições de aerobiose (BAI e RAI, 2016).

Por outro lado, o sobrenadante livre de células de *Y. enterocolitica* e *Serratia proteamaculans* contendo AHLs, AI-2 e outros compostos não conhecidos alterou o crescimento de diferentes fagotipos de *Salmonella* Enteritidis e *Salmonella* Typhimurium em aerobiose (DOUROU *et al.*, 2011). O sobrenadante de *Pseudomonas aeruginosa* contendo AHLs e outros metabólitos também diminuiu o crescimento de nove sorovares de *S. enterica* (WANG *et al.*, 2013). Já o sobrenadante de *Hafnia alvei* contendo AHLs, bem como a adição de *N*-3-oxo-hexanoil homoserina lactona (3-oxo-C6-HSL) ao meio de cultivo em aerobiose não influenciou a formação de biofilme por *Salmonella* Typhimurium (BLANA *et al.*, 2017). Deve-se ressaltar que nestes estudos, os sobrenadantes livres de células de diferentes bactérias produtoras de AHLs contêm outros metabólitos que podem interferir na detecção do efeito desses AIs.

Smith e Ahmer (2003) observaram que as condições ambientais influenciaram na resposta de SdiA, uma vez que esta proteína apresentou atividade independente de AHL quando *Salmonella* Typhimurium foi cultivada a 30 °C, mas não a 37 °C. De acordo com Abed *et al.* (2014), a ativação do operon *rck* de *Salmonella* Typhimurium é independente de AI-1 e SdiA a 25 °C, mas dependente a 37 °C. Estes resultados podem ser explicados com a descoberta de Nguyen *et al.* (2015), os quais mostraram que SdiA em EHEC pode ser ativada independente da ligação da molécula de AHL e identificaram que uma molécula encontrada em procariotos e eucariotos chamada 1-

octanoil-*rac*-glicerol (OCL) pode ativar a SdiA. Entretanto, quando ligada a AHL, SdiA apresenta maior estabilidade e maior afinidade de ligação ao DNA. Almeida *et al.* (2016) mostraram *in silico*, que tanto OCL quanto AHLs, com ou sem modificações 3-oxo e com diferentes tamanhos de cadeia carbônica, são capazes de ligar à proteína SdiA modelada de *Salmonella* Enteritidis.

A fim de entender quais são as vantagens para este patógeno em responder a moléculas que não sintetiza e reconhecer vias e, ou macromoléculas chaves do metabolismo bacteriano, estudos tem buscado avaliar a influência do mecanismo de *quorum sensing* por AI-1 sobre uma resposta global em *Salmonella*. Resultados mostraram que as proteínas PheT, HtpG, PtsI, TalB, PmgI (ou GpmI), Eno, PykF e Adi foram mais abundantes na presença do AI-1 e as proteínas OmpA, OmpC, OmpD, GapA, Tsf, RpsB, RplE, RplB menos abundantes, bem como houve diferença no consumo de ácido fórmico extracelular por *Salmonella* Enteritidis na presença de C12-HSL, em anaerobiose (ALMEIDA *et al.*, 2017b). Segundo estes autores, as proteínas com abundâncias alteradas e a mudança no consumo de ácido fórmico estão correlacionadas com a antecipação da fase estacionária deste patógeno na presença da molécula do *quorum sensing*.

Resultados dos perfis de ácidos graxos e proteínas de *Salmonella* Enteritidis reforçam a hipótese de antecipação da fase estacionária na presença de AHL. Células cultivadas na presença de C12-HSL apresentaram o perfil de ácidos graxos e proteínas nas primeiras horas de cultivo semelhante aos das células em final de fase logarítmica e início de fase estacionária que cresceram na ausência deste AI-1 (ALMEIDA, 2018). Estes resultados indicam que a célula na presença de C12-HSL está mais preparada para superar os estresses relacionados com a fase estacionária de crescimento já nos períodos iniciais de cultivo. Entre as proteínas identificadas, as com função de oxirredução aumentaram na presença de AHL. Além disso, o teor de tiol livre celular também

aumentou nas fases iniciais de cultivo na presença de AHL e estas alterações podem conferir maior resistência ao estresse oxidativo. Carneiro (2017) mostrou que o perfil de metabólitos intracelulares de *Salmonella* Enteritidis na presença e na ausência do AI-1 foi diferente nos tempos iniciais de cultivo e esta diferença diminuiu ao longo do período de incubação em anaerobiose. Também foram observadas alterações das concentrações dos metabólitos intracelulares pertencentes às vias dos glicerolipídeos, aminoácidos e nucleotídeos de purina, bem como do consumo de glicose entre células cultivadas na presença e na ausência de C12-HSL (CARNEIRO, 2017).

Considerando que alguns genes e fatores de patogenicidade de *Salmonella* têm, reconhecidamente, suas expressões influenciadas pelo *quorum sensing* mediado por AI-1, a prospecção de inibidores deste mecanismo é de interesse. Campos-Galvão *et al.* (2015b) e Almeida *et al.* (2017a) mostraram que a formação de biofilme em poliestireno por *Salmonella* Enteritidis foi estimulada pela C12-HSL em anaerobiose após 36 h, mas reprimida pela presença concomitante de uma mistura de furanonas. Almeida *et al.* (2016) mostraram, através do *docking* molecular, que a maioria das furanonas com e sem bromo são capazes de se ligarem à proteína SdiA deste patógeno. Anteriormente, Gnanendra *et al.* (2013) haviam avaliado, por *docking* molecular, que C6-HSL halogenadas desenhadas por eles se ligaram à proteína SdiA de *Salmonella* Typhimurium e, possivelmente, tem potencial de inibição do mecanismo de *quorum sensing*.

A prospecção de inibidores do mecanismo de *quorum sensing* por AI-1 de *Salmonella* em compostos de plantas e anti-inflamatórios não esteroides (AINEs) por *docking* molecular pode consistir em estratégia interessante para redução da virulência de *Salmonella*. Em avaliação *in silico*, os compostos de plantas como o Z-fitol e os compostos classificados como metoxifenol (isoshogaol, shogaol e gingerol) e ácidos graxos (ácidos punícico, malválico, margárico e palmítico) destacaram-se como

possíveis agentes de *quorum quenching* (ALMEIDA, 2018). Entre os AINEs, destacaram-se o lonazolaco e outros compostos derivados do ácido acético (acemetacino, fentiazaco, oxametacino, aceclofenaco e indometacino) (ALMEIDA, 2018).

Diante da importância do mecanismo de *quorum sensing* mediado pelo AI-1 na regulação de alguns fenótipos em *Salmonella*, é necessário ampliar as informações a respeito dos processos controlados por essas moléculas. Estes estudos levariam a compreensão, de forma global, dos impactos no comportamento deste importante patógeno. Assim, a partir desses conhecimentos, será possível buscar estratégias de controle e inibição desse micro-organismo de interesse na indústria de alimentos e na área médica.

Referências bibliográficas

ABED, N.; GRÉPINET, O.; CANEPA, S.; HURTADO-ESCOBAR, G. A.; GUICHARD, N.; WIEDEMANN, A.; VELGE, P.; VIRLOGEUX-PAYANT, I. Direct regulation of the *pefI-srgC* operon encoding the Rck invasin by the quorum-sensing regulator SdiA in *Salmonella* Typhimurium. **Molecular Microbiology**, v. 94, n. 2, p. 254–271, 2014.

AHMER, B. M. M.; VAN REEUWIJK, J.; TIMMERS, C. D.; VALENTINE, P. J.; HEFFRON, F. *Salmonella* Typhimurium encodes an SdiA homolog, a putative quorum sensor of the LuxR family, that regulates genes on the virulence plasmid. **Journal of Bacteriology**, v. 180, n. 5, p. 1185–1193, 1998.

AHMER, B. M. M. Cell-to-cell signalling in *Escherichia coli* and *Salmonella enterica*. **Molecular Microbiology**, v. 52, n. 4, p. 933-945, 2004.

ALMEIDA, F. A.; PINTO, U. M.; VANETTI, M. C. D. Novel insights from molecular docking of SdiA from *Salmonella* Enteritidis and *Escherichia coli* with quorum sensing and quorum quenching molecules. **Microbial Pathogenesis**, v. 99, p. 178–190, 2016.

ALMEIDA, F. A.; PIMENTEL-FILHO, N. J.; PINTO, U. M.; MANTOVANI, H. C.; OLIVEIRA, L. L.; VANETTI, M. C. D. Acyl homoserine lactone-based quorum sensing stimulates biofilm formation by *Salmonella* Enteritidis in anaerobic conditions. **Archives of Microbiology**, v. 199, p. 475–486, 2017a.

ALMEIDA, F. A.; PIMENTEL-FILHO, N. J.; CARRIJO, L. C.; BENTO, C. B. P.; BARACAT-PEREIRA, M. C.; PINTO, U. M.; OLIVEIRA, L. L.; VANETTI, M. C. D. Acyl homoserine lactone changes the abundance of proteins and the levels of organic

acids associated with stationary phase in *Salmonella* Enteritidis. **Microbial Pathogenesis**, v. 102, p. 148–159, 2017b.

ALMEIDA, F. A. **Indução do mecanismo de *quorum sensing* por autoindutor-1 em *Salmonella enterica* e prospecção de inibidores**. Tese (Doutorado). Universidade Federal de Viçosa. Viçosa, MG, 151p., 2018.

AMMOR, M. S.; MICHAELIDIS, C.; NYCHAS, G.-J. E. Insights into the role of quorum sensing in food spoilage. **Journal of Food Protection**, v. 71, n. 7, p. 1510–1525, 2008.

ASAD, S.; OPAL, S. M. Bench-to-bedside review: Quorum sensing and the role of cell-to-cell communication during invasive bacterial infection. **Critical Care**, v. 12, n. 6, p. 236, 2008.

ATKINSON, S.; WILLIAMS, P. Quorum sensing and social networking in the microbial world. **Journal of the Royal Society Interface**, v. 6, n. 40, p. 959–978, 2009.

BAI, A. J.; RAI, V. H. Effect of small chain *N*-acyl homoserine lactone quorum sensing signals on biofilms of food-borne pathogens. **Journal of Food Science and Technology**, v. 53, n. 9, p. 3609–3614, 2016.

BLANA, V.; GEORGOMANOU, A.; GIAOURIS, E. Assessing biofilm formation by *Salmonella enterica* serovar Typhimurium on abiotic substrata in the presence of quorum sensing signals produced by *Hafnia alvei*. **Food Control**, v. 80, p. 83–91, 2017.

BRASIL. Ministério da Saúde. Secretaria de Vigilância em Saúde. Coordenação de Vigilância de Doenças de Transmissão Hídrica e Alimentar. **Dados epidemiológicos DTA – período 2000 a 2011**. 2011.

CAMPOS-GALVÃO, M. E. M.; LEITE, T. D. S.; RIBON, A. O. B.; ARAÚJO, E. F.; VANETTI, M. C. D. A new repertoire of informations about the quorum sensing system in *Salmonella enterica* serovar Enteritidis PT4. **Genetics and Molecular Research**, v. 14, n. 2, p. 4068–4084, 2015a.

CAMPOS-GALVÃO, M. E. M.; RIBON, A. O. B.; ARAÚJO, E. F.; VANETTI, M. C. D. Changes in the *Salmonella enterica* Enteritidis phenotypes in presence of acyl homoserine lactone quorum sensing signals. **Journal of Basic Microbiology**, v. 55, p.1-9, 2015b.

CARNEIRO, D. G. **Influência do mecanismo de *quorum sensing* no metabolismo de *Salmonella enterica***. Dissertação (Mestrado). Universidade Federal de Viçosa. Viçosa, MG, 49p., 2017.

CASE, R. J.; LABBATE, M.; KJELLEBERG, S. AHL-driven quorum-sensing circuits: their frequency and function among the Proteobacteria. **The ISME Journal**, v. 2, n. 4, p. 345–349, 2008.

Di CAGNO, R.; DE ANGELIS, M.; CALASSO, M.; GOBBETTI, M. Proteomics of the bacterial cross-talk by quorum sensing. **Journal of Proteomics**, v. 74, n. 1, p. 19–34, 2011.

DOUROU, D.; AMMOR, M. S.; SKANDAMIS, P. N.; NYCHAS, G. J. E. Growth of *Salmonella* Enteritidis and *Salmonella* Typhimurium in the presence of quorum sensing signalling compounds produced by spoilage and pathogenic bacteria. **Food Microbiology**, v. 28, n. 5, p. 1011–1018, 2011.

DYSZEL, J. L.; SMITH, J. N.; LUCAS, D. E.; SOARES, J. A.; SWEARINGEN, M. C.; VROSS, M. A.; YOUNG, G. M.; AHMER, B. M. M. *Salmonella enterica* serovar Typhimurium can detect acyl homoserine lactone production by *Yersinia enterocolitica* in mice. **Journal of Bacteriology**, v. 192, n. 1, p. 29–37, 2010.

FUQUA, W. C.; WINANS, S. C.; GREENBERG, E. P. Quorum sensing in bacteria: the LuxR-LuxI family of cell density-responsive transcriptional regulators. **Journal of Bacteriology**, v.176, n. 2, p. 269–275, 1994.

FUQUA, W. C.; WINANS, S. C.; GREENBERG, E. P. Census and consensus in bacterial ecosystems: the LuxR-LuxI family of quorum-sensing transcriptional regulators. **Annual Review of Microbiology**, v. 50, p. 727–751, 1996.

FUQUA, C.; PARSEK, M. R.; GREENBERG, E. P. Regulation of gene expression by cell-to-cell communication: acyl-homoserine lactone quorum sensing. **Annual Review of Genetics**, v. 35, p. 439–468, 2001.

GNANENDRA, S.; MOHAMED, S.; NATARAJAN, J. Identification of potent inhibitors for *Salmonella* Typhimurium quorum sensing via virtual screening and pharmacophore modeling. **Combinatorial Chemistry and High Throughput Screening**, v. 16, n. 10, p. 826–839, 2013.

HAYWARD, M. R.; JANSEN, V. A. A.; WOODWARD, M. J. Comparative genomics of *Salmonella enterica* serovars Derby and Mbandaka, two prevalent serovars associated with different livestock species in the UK. **BMC Genomics**, v. 14, n. 1, p. 365-383, 2013.

HENSEL, M. Evolution of pathogenicity islands of *Salmonella enterica*. **International Journal of Medical Microbiology**, v. 294, n. 2–3, p. 95–102, 2004.

HUGHES, D. T.; CLARKE, M. B.; YAMAMOTO, K.; RASKO, D. A.; SPERANDIO, V. The QseC adrenergic signaling cascade in Enterohemorrhagic *E. coli* (EHEC). **PLoS Pathogens**, v. 5, n. 8, p. e1000553, 2009.

HUMPHREY, T. J.; WILLIAMS, A.; MCALPINE, K.; LEVER, M. S.; GUARD-PETTER, J.; COX, J. M. Isolates of *Salmonella enterica* Enteritidis PT4 with enhanced heat and acid tolerance are more virulent in mice and more invasive in chickens. **Epidemiology and Infection**, v. 117, n. 1, p. 79–88, 1996.

HUMPHREY, T. J.; WILLIAMS, A.; MCALPINE, K.; JØRGENSEN, F.; O'BYRNE, C. Pathogenicity in isolates of *Salmonella enterica* serotype Enteritidis PT4 which differ in RpoS expression: effects of growth phase and low temperature. **Epidemiology and Infection**, v. 121, n. 2, p. 295–301, 1998.

KAPLAN, H. B.; GREENBERG, E. P. Diffusion of autoinducer is involved in

regulation of the *Vibrio fischeri* luminescence system. **Journal of Bacteriology**, v. 163, n. 3, p. 1210–1214, 1985.

KELLER, L.; SURETTE, M. G. Communication in bacteria: an ecological and evolutionary perspective. **Nature Reviews of Microbiology**, v. 4, n. 4, p. 249–258, 2006.

LIU, Z.; QUE, F.; LIAO, L.; ZHOU, M.; YOU, L.; ZHAO, Q.; LI, Y.; NIU, H.; WU, S.; HUANG, R. Study on the promotion of bacterial biofilm formation by a *Salmonella* conjugative plasmid and the underlying mechanism. **PLoS One**, v. 9, n. 10, p. e109808-e109819, 2014.

MICHAEL, B.; SMITH, J. N.; SWIFT, S.; HEFFRON, F.; AHMER, B. M. M. SdiA of *Salmonella enterica* is a LuxR homolog that detects mixed microbial communities. **Journal of Bacteriology**, v. 183, n. 19, p. 5733–5742, 2001.

MOREIRA, C. G.; WEINSHENKER, D.; SPERANDIO, V. QseC mediates *Salmonella enterica* serovar Typhimurium virulence *in vitro* and *in vivo*. **Infection and Immunity**, v. 78, n. 3, p. 914-926, 2010.

NESSE, L. L.; BERG, K.; VESTBY, L. K.; OLSAKER, I.; DJONNE, B. *Salmonella* Typhimurium invasion of HEp-2 epithelial cells *in vitro* is increased by *N*-acyl homoserine lactone quorum sensing signals. **Acta Veterinaria Scandinavica**, v. 53, p. 44-48, 2011.

NG, W.-L.; BASSLER, B. L. Bacterial quorum-sensing network architectures. **Annual Review of Genetics**, v. 43, p. 197–222, 2009.

NGUYEN, Y.; NGUYEN, N. X.; ROGERS, J. L.; LIAO, J.; MACMILLAN, J. B.; JIANG, Y.; SPERANDIO, V. Structural and mechanistic roles of novel chemical ligands on the SdiA quorum-sensing transcription regulator. **mBio**, v. 6, n. 2, p. e02429-e02438, 2015.

ONG, S. Y.; NG, F. L.; BADAI, S. S.; YURYEV, A.; ALAM, M. Analysis and construction of pathogenicity island regulatory pathways in *Salmonella enterica* serovar Typhi. **Journal of Integrative Bioinformatics**, v. 7, n. 1, p. 145-178, 2010.

PEARSON, J. P.; VAN DELDEN, C.; IGLEWSKI, B. H. Active efflux and diffusion are involved in transport of *Pseudomonas aeruginosa* cell-to-cell signals. **Journal of Bacteriology**, v. 181, n. 4, p. 1203–1210, 1999.

READING, N. C.; SPERANDIO, V. Quorum sensing: the many languages of bacteria. **FEMS Microbiology Letters**, v. 254, n. 1, p. 1–11, 2006.

SABAG-DAIGLE, A.; AHMER, B. M. M. ExpI and PhzI are descendants of the long lost cognate signal synthase for SdiA. **PLoS One**, v. 7, n. 10, p. e47720, 2012.

SCALLAN, E.; HOEKSTRA, R. M.; ANGULO, F. J.; TAUXE, R. V.; WIDDOWSON, M. A.; ROY, S. L.; JONES, J. L.; GRIFFIN, P. M. Foodborne illness acquired in the United States-major pathogens. **Emerging Infectious Diseases**, v. 17, n. 1, p. 7–15, 2011.

SCHUSTER, M.; SEXTON, D. J.; DIGGLE, S. P.; PETER GREENBERG, E. Acyl-homoserine lactone quorum sensing: from evolution to application. **Annual Review of Microbiology**, v. 67, n. 1, p. 43–63, 2013.

SMITH, J. N.; AHMER, B. M. M. Detection of other microbial species by *Salmonella*: expression of the SdiA regulon. **Journal of Bacteriology**, v. 185, n. 4, p. 1357–1366, 2003.

SMITH, J. L.; FRATAMICO, P. M.; NOVAK, J. S. Quorum sensing: a primer for food microbiologists. **Journal of Food Protection**, v. 67, n. 5, p. 1053–1070, 2004.

SMITH, J. N.; DYSZEL, J. L.; SOARES, J. A.; ELLERMEIER, C. D.; ALTIER, C.; LAWHON, S. D.; ADAMS, L. G.; KONJUFCA, V.; CURTISS, R.; SLAUCH, J. M.; AHMER, B. M. M. SdiA, an *N*-acylhomoserine lactone receptor, becomes active during the transit of *Salmonella enterica* through the gastrointestinal tract of turtles. **PLoS One**, v. 3, n. 7, p. e2826, 2008.

TAGA, M. E.; SEMMELHACK, J. L.; BASSLER, B. L. The LuxS-dependent autoinducer AI-2 controls the expression of an ABC transporter that functions in AI-2 uptake in *Salmonella* Typhimurium. **Molecular Microbiology**, v. 42, n. 3, p. 777-793, 2001.

WALTERS, M.; SPERANDIO, V. Quorum sensing in *Escherichia coli* and *Salmonella*. **International Journal of Medical Microbiology**, v. 296, n. 2-3, p. 125–131, 2006.

WALTERS, M.; SIRCILI, M. P.; SPERANDIO, V. AI-3 synthesis is not dependent on *luxS* in *Escherichia coli*. **Journal of Bacteriology**, v. 188, n. 16, p. 5668-5681, 2006.

WANG, H. H.; YE, K. P.; ZHANG, Q. Q.; DONG, Y.; XU, X. L.; ZHOU, G. H. Biofilm formation of meat-borne *Salmonella enterica* and inhibition by the cell-free supernatant from *Pseudomonas aeruginosa*. **Food Control**, v. 32, n. 2, p. 650–658, 2013.

CAPÍTULO 2

Acyl homoserine lactone changes the abundance of proteins and the levels of organic acids associated with stationary phase in *Salmonella* Enteritidis

Article published in Microbial Pathogenesis

Microbial Pathogenesis 102 (2017) 148–159

Contents lists available at ScienceDirect

Microbial Pathogenesis

journal homepage: www.elsevier.com/locate/micpath

Acyl homoserine lactone changes the abundance of proteins and the levels of organic acids associated with stationary phase in *Salmonella* Enteritidis

Felipe Alves de Almeida [a], Natan de Jesus Pimentel-Filho [b], Lanna Clícia Carrijo [c], Cláudia Braga Pereira Bento [d], Maria Cristina Baracat-Pereira [c], Uelinton Manoel Pinto [e], Leandro Licursi de Oliveira [f], Maria Cristina Dantas Vanetti [a, *]

[a] Department of Microbiology, Universidade Federal de Viçosa, Viçosa, MG, Brazil
[b] Center of Nature Science, Universidade Federal de São Carlos, Buri, SP, Brazil
[c] Department of Biochemistry and Molecular Biology, Universidade Federal de Viçosa, Viçosa, MG, Brazil
[d] Institute of Agrarian Science, Universidade Federal dos Vales do Jequitinhonha e Mucuri, Unaí, MG, Brazil
[e] Food Research Center, Department of Food and Experimental Nutrition, Faculty of Pharmaceutical Sciences, Universidade de São Paulo, São Paulo, SP, Brazil
[f] Department of General Biology, Universidade Federal de Viçosa, Viçosa, MG, Brazil

ARTICLE INFO

Article history:
Received 11 August 2016
Received in revised form
22 November 2016
Accepted 29 November 2016
Available online 1 December 2016

Keywords:
Autoinducer
Differentially abundant proteins
Formic acid
Starvation
Stationary phase

ABSTRACT

Quorum sensing (QS) is cell-cell communication mechanism mediated by signaling molecules known as autoinducers (AIs) that lead to differential gene expression. *Salmonella* is unable to synthesize the AI-1 acyl homoserine lactone (AHL), but is able to recognize AHLs produced by other microorganisms through SdiA protein. Our study aimed to evaluate the influence of AI-1 on the abundance of proteins and the levels of organic acids of *Salmonella* Enteritidis. The presence of *N*-dodecyl-homoserine lactone (C12-HSL) did not interfere on the growth or the total amount of extracted proteins of *Salmonella*. However, the abundance of the proteins PheT, HtpG, PtsI, Adi, TalB, PmgI (or GpmI), Eno, and PykF enhanced while the abundance of the proteins RplB, RplE, RpsB, Tsf, OmpA, OmpC, OmpD, and GapA decreased when *Salmonella* Enteritidis was anaerobically cultivated in the presence of C12-HSL. Additionally, the bacterium produced less succinic, lactic, and acetic acids in the presence of C12-HSL. However, the concentration of extracellular formic acid reached 20.46 mM after 24 h and was not detected when the growth was in the absence of AI-1. Considering the cultivation period for protein extraction, their abundance, process and function, as well as the levels of organic acids, we observed in cells cultivated in presence of C12-HSL a correlation with what is described in the literature as entry into the stationary phase of growth, mainly related to nitrogen and amino acid starvation and acid stress. Further studies are needed in order to determine the specific role of the differentially abundant proteins and extracellular organic acids secreted by *Salmonella* in the presence of quorum sensing signaling molecules.

1. Introduction

Salmonella enterica serovar Enteritidis is the most common serotype responsible for salmonellosis in many countries and, this pathogen is primarily transmitted by food [1–4]. The high virulence of this pathogen is associated with the presence of many pathogenicity islands encoding virulence factors [5–7].

Quorum sensing (QS) is a mechanism of cell-cell communication mediated by signaling molecules known as autoinducers (AIs) that leads to differential gene expression in response to changes in the population density among microbial cells or microbial and host cells [8–11]. In *Salmonella*, this mechanism can be achieved through three types of autoinducers (AIs) called AI-1, AI-2, and AI-3. Complete sets of QS systems composed of signal synthase and signal receptors are present in many bacteria [12].

The QS system mediated by AI-1 is present in Gram-negative

* Corresponding author. Department of Microbiology, Universidade Federal de Viçosa, Viçosa, MG 36570-900, Brazil.
E-mail address: mvanetti@ufv.br (M.C.D. Vanetti).

http://dx.doi.org/10.1016/j.micpath.2016.11.027
0882-4010/

bacteria, but in *Salmonella* it is incomplete. This pathogen is unable of synthesizing the AI-1 called acyl homoserine lactone (AHL) since neither *luxI* gene nor other homologues that codify for the AI-1 synthase are present in the bacterial genome. However, *Salmonella* is able to recognize AHLs synthesized by other microorganisms through SdiA protein, a transcriptional regulator homologous to LuxR which is the signal receptor [13–15]. The AHLs are internalized and bind to the ligand-binding domain (LBD) of SdiA which dimerizes and binds to DNA by using its DNA-binding domain (DBD) regulating expression of target genes [16]. The AI-2 is found in *Salmonella* where it is synthesized by LuxS and internalized by using products of the *lsr* operon [17–19]. In the QS mediated by AI-3 in *Salmonella*, the signal molecules are the hormones epinephrine and norepinephrine, synthesized by animal cells, which are sensed through proteins coded by the *qseBC* operon and *qseE* gene [12,20].

Autoinducers influence gene expression and protein abundance in *Salmonella,* consequently generating different phenotypes, including motility, biofilm formation as well as adhesion, invasion and survival in eukaryotic cells [12,15,21–27]. Campos-Galvão et al. [26] showed enhanced biofilm formation by *Salmonella* Enteritidis PT4 578 growing in the presence of 50 nM of AHLs with six, eight, ten and twelve carbons. However, the effect of *N*-dodecanoyl-DL-homoserine lactone (C12-HSL) on this phenotype was statistically higher than the other AHLs evaluated. These data were reinforced by the recently published study on molecular docking in which AHLs with twelve carbons presented greater affinity to SdiA of *Salmonella* Enteritidis PT4 578 than AHLs with ten, eight, six and four carbons side chains [28]. Liu et al. [25] reported that the presence of AI-1 increased the adhesion of *S. enterica* serovar Typhi to HeLa cells and biofilm formation in polystyrene. Similar results were observed for *Salmonella* Enteritidis in presence of AI-1, where biofilm formation in polystyrene was increased when cells were cultivated in anaerobic conditions [26,27]. Moreover, the *rck* operon of *Salmonella*, which is related to virulence, was more expressed in presence of the AI-1 as previously observed by other groups [14,29]. So far, only two studies evaluated the influence of QS in the abundance of proteins in *Salmonella*. In both cases, the effect of AI-2 on two strains of *S. enterica* serovar Typhimurium was tested, but no studies evaluated the influence of AI-1 on this bacterium [30,31].

Proteomics allows the determination of the global picture of proteins expressed by the genome and gives new insights into the behavior of bacteria during the QS phenomena [32]. Conventional two-dimensional gel electrophoresis (2-DE) in combination with advanced mass spectrometric techniques has facilitated the characterization of thousands of proteins using a single polyacrylamide gel. The 2-DE procedure allows easy visualization of protein isoforms and posttranslational modifications (PTMs) based on protein separation using two physical parameters such as isoelectric point and molecular weight, rendering this technology extremely informative [33].

Thus, considering the scarcity of information about the influence of AI-1 in *Salmonella*, our study aimed to evaluate the effect of this signaling molecule in the abundance of proteins and the levels of organic acids of *Salmonella* Enteritidis. The comparative analysis helps to understand the QS mechanism dependent upon AHL on the physiology of this pathogen.

2. Materials and methods

2.1. Bacterial strain

Salmonella enterica sorovar Enteritidis PT4 578, isolated from chicken meat, was provided by Fundação Oswaldo Cruz (FIOCRUZ, Rio de Janeiro, Brazil) and has been previously described [26,27,34]. Cultures were stored at −20 °C in Luria-Bertani (LB) broth [35] supplemented with 20% (v/v) of sterile glycerol.

2.2. Preparation of inoculum

Tryptone soy broth (TSB; Merck, Germany) was prepared under O_2-free conditions with a CO_2 filling and was dispensed into anaerobic bottles that were sealed with butyl rubber stoppers and then, autoclaved (anaerobic TSB) [36]. Before each experiment, cells were cultivated in anaerobic bottles containing 20 mL of anaerobic TSB for 24 h at 37 °C in a static-model anaerobic chamber (Coy Laboratory, USA) containing a mixture of H_2 (3–5%) and CO_2 (95–97%). Then, 1 mL of culture was transferred into 10 mL of anaerobic TSB and incubated at 37 °C in anaerobic chamber. After incubation for 4 h, exponentially growing cells were harvested by centrifugation at 5000*g* at 4 °C for 10 min (Sorvall, USA), washed with 0.85% saline, and the pellet resuspended in 0.85% saline. The inoculum was standardized to 0.1 of optical density at 600 nm (OD_{600nm}), approximately 10^7 colonies forming units per milliliter (CFU/mL), using a spectrophotometer (Thermo Fisher Scientific, Finland).

2.3. Preparation of HSL solution

N-dodecanoyl-DL-homoserine lactone (C12-HSL; PubChem CID: 11565426; Fluka, Switzerland) was suspended in acetonitrile (PubChem CID: 6342; Merck, Germany) at a concentration of 10 mM and further diluted to a working solution of 10 μM in acetonitrile. Control experiment was performed using acetonitrile. The final concentration of acetonitrile in the media was always less than 1% (v/v) to avoid interference in the growth and response of *Salmonella* to C12-HSL [14].

2.4. Effect of HSL on the growth of Salmonella

To evaluate the effect of C12-HSL on the growth of *Salmonella*, bottles containing 20 mL of anaerobic TSB supplemented with 50 nM of C12-HSL were inoculated with 2 mL of the standardized inoculum. Bottles were incubated at 37 °C for up to 12 h in anaerobic chamber. In established time points, the OD_{600nm} was determined using a spectrophotometer (Thermo Fisher Scientific, Finland).

2.5. Extraction and quantification of proteins of Salmonella

A standardized inoculum was added into anaerobic bottles containing 30 mL of anaerobic TSB supplemented with 50 nM of C12-HSL or the equivalent volume of acetonitrile as control and then, incubated at 37 °C in anaerobic chamber. After 7 h of incubation, the OD_{600nm} and CFU/mL were determined. Concomitantly, an aliquot of the media was centrifuged at 5000*g* at 4 °C for 15 min (Sorvall, USA). The cells in the pellet were resuspended in 1 mL of sterilized distilled water, transferred to 1.5 mL microtubes and once again centrifuged at 9500*g* at 4 °C for 30 min (Brikmann Instruments, Germany). The pellet was resuspended in 50 mM ammonium bicarbonate, 1 mM phenylmethylsulfonyl fluoride (PMSF) added of 1 mL of 2:1 trifluoroethanol:chloroform (TFE:$CHCl_3$), followed by vigorous agitation. Next, the mixture was kept at 0 °C for 1 h in ultrasound bath (100 W MSE 20 KHz), with mixing every 10 min. The material was centrifuged at 6500*g* at 4 °C for 4 min (Brikmann Instruments, Germany) to obtain three phases. The upper phase (composed by proteins soluble in TFE) and the central phase (composed by proteins insoluble in TFE) were collected. The mixture of both phases were dried in SpeedVac (Genevac, England) and resolubilized in 500 μL of a mixture of 5 M urea, 2 M tiourea, 4% (w/v) 3-[(3-cholamidopropyl)

dimethylammonio]-1-propanesulfonate (CHAPS), 40% (v/v) TFE, and 10 mM Tris-HCl (pH 8.8–9.0). Disulfide bonds of the proteins were reduced by 50 mM dithiothreitol (DTT) for 1 h at room temperature, and subsequently, alkylation was carried out by adding 100 mM acrylamide [37–39]. The protein extract was precipitated with 10% (w/v) trichloroacetic acid (TCA) and kept in ice for 30 min and then the material was centrifuged at 9500*g* for 10 min. The supernatant was discarded and the precipitate washed three times with cold acetone. After evaporation of the residual acetone at room temperature, the precipitate was resuspended in 700 μL of a mixture containing 7 M urea, 2 M thiourea, and 2% (w/v) CHAPS. Proteins were quantified using Coomassie blue dye [40] and then, the protein extracts were stored at −20 °C.

2.6. Separation of proteins by two-dimensional gel electrophoresis (2-DE)

2.6.1. Rehydration and sample loading

The protein extracts with 150 μg of proteins were loaded during the re-swelling process in a rehydration apparatus IPG BOX (GE Healthcare, Sweden) at 20 °C for 12 h. For the first dimension, 7 cm gel strips were used with a linear pH gradient ranging from 3 to 10 (Immobiline™ DryStrip; GE Healthcare, Sweden). To rehydrate each strip, 125 μL of a mixture containing the solubilized proteins in 40 mM DTT and 2% (v/v) IPG buffer plus DeStreak solution (GE Healthcare, Sweden) were used.

2.6.2. Isoelectric focusing (IEF)

The IEF was conducted in the equipment IPGphor III (GE Healthcare, Sweden). Electrophoresis conditions were: (i) 300 V for 12 h; (ii) 300 Vh in gradient until 1000 V; (iii) 2000 V in gradient for 1 h; (iv) 2000 Vh in one step of 2000 V; (v) 3000 V in gradient for 1.5 h; (vi) 3000 Vh in one step of 3000 V; (vii) 5000 V in gradient for 1.5 h; (viii) 3000 Vh in one step of 5000 V.

2.6.3. Equilibration of the gel strips

After the IEF, the strips were equilibrated in 10 mL equilibrating buffer 75 mM Tris-HCl pH 8.8, 6 M urea, 29.3% (v/v) glycerol, 2% (w/v) SDS and 0.002% (w/v) bromophenol blue in two 30 min stages in order to reduce and alkylate the proteins. In the first stage, 1% (w/v) DTT was added to the equilibrating buffer. In the second stage, 2.5% (w/v) iodoacetamide was added to the equilibrating buffer. The strips were then briefly incubated in running buffer and submitted to the second dimension of the 2-DE (SDS-PAGE).

2.6.4. Electrophoresis in polyacrylamide gel (SDS-PAGE)

The SDS-PAGE was based on Laemmli [41] in a 12% polyacrylamide gel with a Mini-Protean II Electrophoresis System (Bio-Rad Laboratories, EUA), using the broad range weight marker (6.5–200.0 kDa, Bio-Rad, USA). Separation was performed at 80 V for 30 min and then, at 60 V until the bromophenol blue reached the gel lower limit.

2.6.5. Fixation and staining of the gel

The 2D gels were fixed in solution containing 10% (v/v) acetic acid and 50% (v/v) methanol for 30 min and were stained in a solution containing 8% (w/v) ammonium sulfate, 0.8% (v/v) phosphoric acid, 0.08% (w/v) Coomassie blue G-250, and 30% (v/v) methanol for 72 h. After this step, the gels were washed and maintained in 5% (v/v) acetic acid.

2.6.6. Analysis of the protein spots

The 2D stained gels were then photo-digitalized in an Image Scanner III (GE Healthcare, Sweden) in transparent mode, resolution of 300 dpi, green color filter and with updated calibration. For the comparative analysis of the images, the software ImageMaster 2D Platinum 7.5 (GE Healthcare, Sweden) was used. Image analysis included spot detection, spot measurement, background subtraction and spot matching of three biological replicate gels. Prior to performing spot matching between gel images, one gel image was selected as reference and the used parameters were: contrast equal to - 1, smooth equal to 2, minimum area equal to 20 and saliency equal to 30. The amount of protein of each spot was expressed as the volume of that spot which was defined as the sum of the intensities of all the pixels that make up that spot. To correct the variability and to reflect the quantitative variations of protein spots, the spot volumes were normalized as the percentage (%) of the total volume considering all the spots in the gel. The analysis of variance (ANOVA) for protein spots were followed by the software ImageMaster 2D Platinum 7.5 (GE Healthcare, USA) and the fold change was calculated as the ratio of the % volume of the treatment with C12-HSL by the control. The spots with *p*-value less than 0.05 ($p < 0.05$) and intensities less than 0.8-fold or more than 1.2-fold (fold changed <0.8 or >1.2), as well as when the protein spot was not detected in one of the treatments, which we defined as less than 1.0-fold or more than 1.0-fold (fold changed <1.0 or >1.0), were considered differentially abundant proteins [42].

2.7. Identification of differentially abundant proteins by mass spectrometry

2.7.1. In-gel protein digestion

The protein spots with significant expression changes were excised from stained 2D gels and were submitted to trypsinolysis according to Shevchenko et al. [43] with modifications suggested by Pereira et al. [44]. For the tryptic digestion Sequencing Grade Modified Trypsin, Porcine (Promega, USA) was used. The samples, containing tryptic peptides, were concentrated until about 5 μL in a SpeedVac Concentrator (Thermo Fisher Scientific, Finland) and were added of 5 μL of 0.1% (v/v) trifluoroacetic acid (TFA). Subsequently, samples were desalted in ZipTip® C18 columns (Millipore, USA), concentrated in a SpeedVac Concentrator and resuspended in 5 μL of 0.1% (v/v) TFA.

2.7.2. Mass spectrometry

Mass spectra of the tryptic peptides were performed using a matrix assisted laser desorption/ionization – time of flight/time of flight (MALDI-TOF/TOF) mass spectrometer, model Ultraflex III (Bruker Daltonics, Germany). The samples of tryptic peptides were mixed with α-cyano-4-hydroxycinnamic acid (Bruker Daltonics, Germany) in a proportion of 1:1.

2.7.3. Identification of proteins

The mass spectra obtained were processed using Flex Analysis software (version 3.3; Bruker Daltonics, Germany) and the peaks lists in *.xml* and *.mgf* format were generated by BioTools software (version 3.2; Bruker Daltonics, Germany). These were used for identification of the proteins by the peptide mass fingerprinting (PMF) method and by the peptide fragment fingerprinting (PFF) method using the Mascot software (version 2.4.0; Matrix Science, United Kingdom) against the knowledgebase UniProtKB (http://www.uniprot.org/). For the search, the following parameters were considered: taxonomy *Salmonella* and all entries (separately), monoisotopic mass, trypsin, allow up to one missed cleavage site, peptide tolerance equal to 0.5 Da, MS/MS tolerance equal to 0.5 Da, peptide charge equal to +1, fixed modification for carbamidomethylation of cysteine residues and variable modification for oxidation of methionine residues. The identifications of the proteins from the PFF by Mascot software were validated by Scaffold software (version 3.6.4; Proteome Software, USA). Peptide

identifications were accepted if they could be established at greater than 90% probability as specified by the Peptide Prophet algorithm [45]. Protein identifications were accepted if they could be established at greater than 90% probability and contained at least one identified peptide by the Protein Prophet algorithm [46].

2.8. Gene ontology (GO) analysis and protein-protein interactions (PPI) network

The GO annotations for differentially abundant proteins were acquired by European Bioinformatics Institute (http://www.ebi.ac.uk/QuickGO/). Then, the PPI network was generated for proteins of the *Salmonella* Typhimurium LT2 with the confidence interactions greater than 0.4 using the STRING database version 10.0 (http://string-db.org/ [47]).

2.9. Quantification of extracellular organic acids and ethanol

A standardized inoculum of *Salmonella* was added into anaerobic bottles containing 20 mL of anaerobic TSB supplemented with 50 nM C12-HSL or acetonitrile as control and incubated at 37 °C for up to 36 h in anaerobic chamber. After incubation for 2, 7, 24, and 36 h, 2 mL samples were centrifuged at 12,000*g* for 10 min and the cell-free culture supernatants were treated as described by Siegfried et al. [48]. The extracellular organic acids and ethanol were determined as described by Bento et al. [49]. The high-performance liquid chromatography (HPLC) apparatus coupled to a refractive index (Dionex Corporation, USA) was calibrated with the standard curve of the following organic acids: succinic, lactic, acetic, formic, propionic, valeric, isovaleric, butyric, and isobutyric acids as well as ethanol. All acids were prepared to a final concentration of 10 mM, except isovaleric acid (5 mM) and acetic acid (20 mM). Ethanol was prepared to a final concentration of 150 mM.

2.10. Statistics

Experiments were carried out in three biological replicates. All data were subjected to analysis of variance (ANOVA) followed by Tukey's test using the Statistical Analysis System and Genetics Software® [50] and the software ImageMaster 2D Platinum 7.5 (GE Healthcare, USA) for proteins analysis. A $p < 0.05$ was considered to be statistically significant.

3. Results and discussion

3.1. Growth of Salmonella in the presence of HSL

The presence of 50 nM of C12-HSL in the medium did not interfere on the *Salmonella* Enteritidis PT4 578 growth during 12 h of incubation (Fig. 1). The concentration of C12-HSL used in this study is much higher than the necessary concentration to induce *sdiA* gene expression in *Salmonella* Typhimurium which, according to Michael et al. [14], can be as low as 1.0 nM. These results corroborate with those found by Campos-Galvão et al. [34] for the same pathogen growing in the presence of different AHLs. Others studies have shown that the growth rate of different serovars of *S. enterica* during the exponential phase decreased in the presence of the cell free supernatants (CFSs) of *Yersinia enterocolitica* and *Serratia proteamaculans* [51] or *Pseudomonas aeruginosa* [52] containing AHLs. However, it is necessary to consider that these CFSs had other unknown metabolites and the inhibitory effect cannot be exclusively attributed to the AHLs.

3.2. HSL changes the abundance of proteins in Salmonella

Changes in the abundance of proteins in *Salmonella* Enteritidis PT4 578 were evaluated in anaerobic TSB supplemented with C12-HSL at 37 °C for 7 h. At this time, *Salmonella* Enteritidis was in early stationary phase of growth and the OD_{600nm} and log CFU/mL in the presence of C12-HSL (0.167 ± 0.008 and 9.1 ± 0.1, respectively) did not differ ($p > 0.05$) to the control treatment (0.165 ± 0.001 and 9.1 ± 0.1, respectively) (Fig. 1). The total proteins extracted from the cells supplemented with C12-HSL (3.98 ± 0.58 μg/μL) did not differ ($p > 0.05$) to the control treatment (4.07 ± 0.21 μg/μL), without this AI-1.

Analysis of the 2-DE gel prepared with protein extracted from early stationary phase growing cells in the presence or absence of C12-HSL showed a total of 184 protein spots, with 39 spots differentially abundant between treatments (Fig. 2). Of these, the abundance of 10 spots was decreased in the presence of C12-HSL ($p < 0.05$ and fold changed < 0.8 as well as < 1.0) whereas, the abundance rate of 29 spots was increased ($p < 0.05$ and fold changed > 1.2 as well as > 1.0) when compared with the control treatment (Table 1). From the 39 differentially abundant protein spots removed from the gels, 21 were identified (53.8%) and validated by Scaffold software (Table 2).

Of the 21 identified proteins, 90.5% (19 proteins) had theoretical and experimental isoeletric points (pI) ranging between 4.0 and 7.0. However, three proteins were identified in more than one spot such as OmpA (spots 41 and 42), Adi (spots 100, 101 and 102), and PykF (spots 171, 173 and 174) (Table 2). Kint et al. [31] also reported the identification of the proteins LuxS and FljB, differentially abundant in wild-type and *luxS* mutant *Salmonella* Typhimurium, in two different spots. These authors observed that the molecular mass (MM) of LuxS was similar in both spots where the protein was identified, but the pI values were different and *a posteriori* analysis revealed that this protein showed posttranslational modifications (PTMs) [31]. PTMs of proteins can change their pI and/or their MM resulting in isoforms that separate in different spots in 2D gels [31,53].

The abundance of the proteins PheT, HtpG, PtsI, Adi, TalB, PmgI (or GpmI), Eno, and PykF enhanced while the abundance of the proteins RplB, RplE, RpsB, Tsf, OmpA, OmpC, OmpD, and GapA decreased when *Salmonella* Enteritidis was cultivated in the

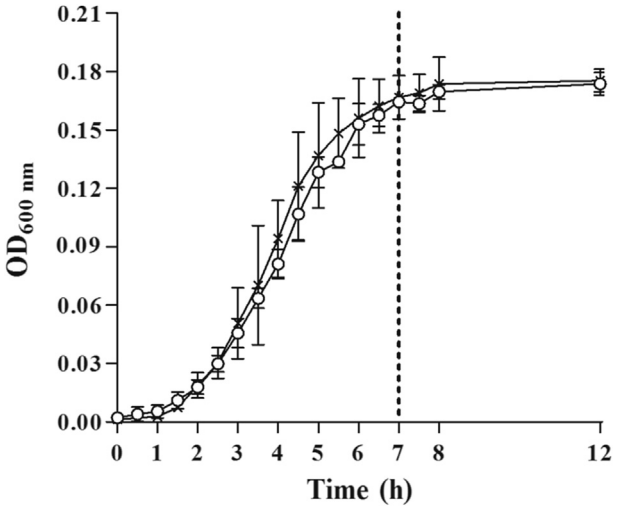

Fig. 1. Growth of *Salmonella* Enteritidis PT4 578 in the presence of C12-HSL. *Salmonella* was anaerobically cultivated in TSB at 37 °C for 12 h in the presence of acetonitrile (open cycle) or 50 nM of C12-HSL (crossed line). The dashed line indicates the time of collection of cells for protein extraction. Error bars indicate standard error.

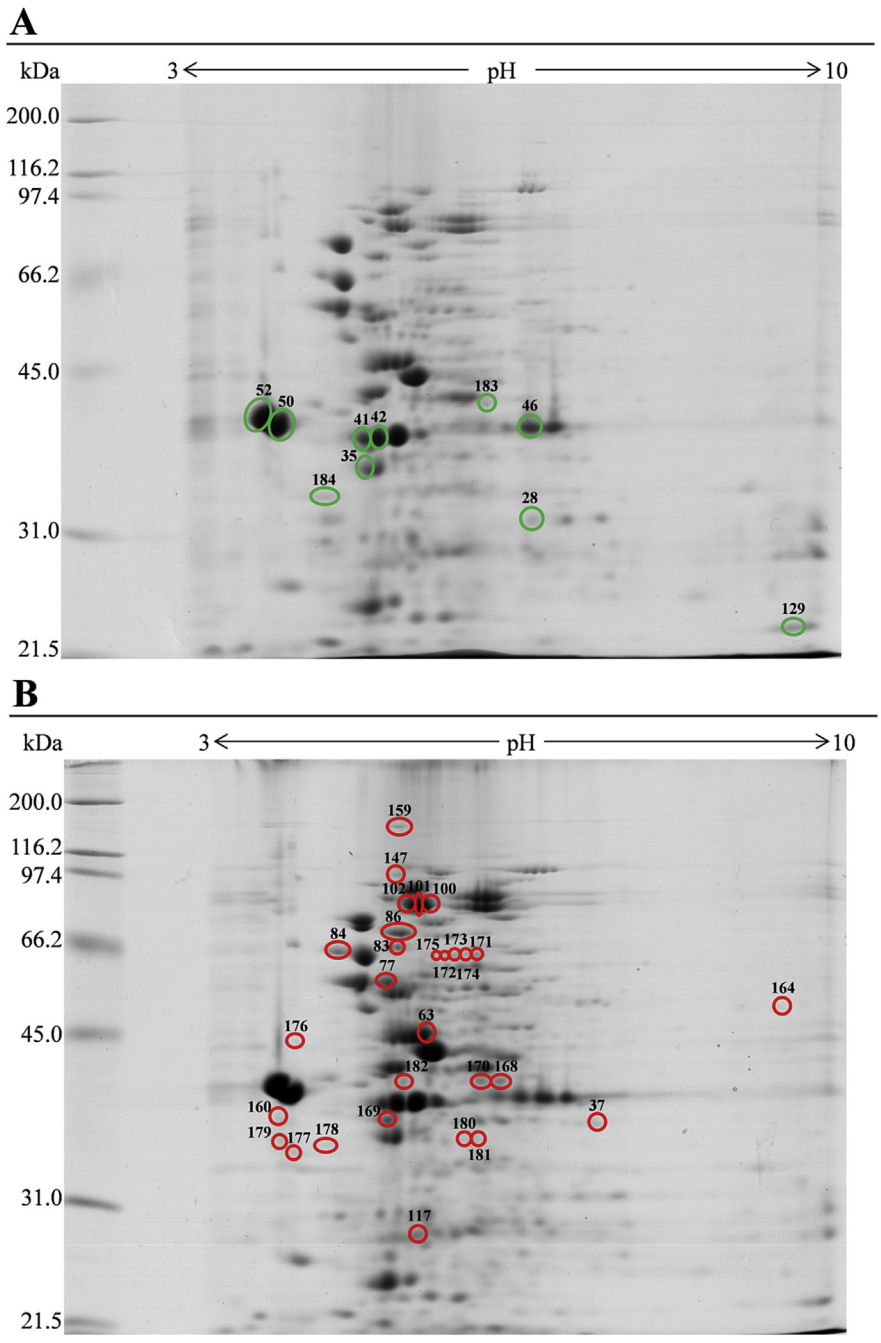

Fig. 2. Representative 2D gels of protein extracts of *Salmonella* Enteritidis PT4 578 anaerobically cultivated in TSB at 37 °C for 7 h in the absence (A) or presence (B) of 50 nM of C12-HSL. Proteins with significantly ($p < 0.05$ and fold changed > 1.2 as well as > 1.0) increased abundance rates following C12-HSL treatment are surrounded by red circle. The green-encircled spots represent proteins whose abundance was significantly ($p < 0.05$ and fold changed < 0.8 as well as < 1.0) decreased. The numbers on the circles are the references of each protein spot. (For interpretation of the references to colour in this figure legend, the reader is referred to the web version of this article.)

presence of C12-HSL (Fig. 3). We have only found proteomic studies related to the role of AI-2 mediated QS system in *Salmonella*. Soni et al. [30] showed that the LuxS/AI-2-mediated system in *Salmonella* Typhimurium controls the increased abundance of proteins such as Tig, YaeT, PhoP, GpmI, TrxB, and an unidentified protein, while PfkA decreased in wild-type *Salmonella* Typhimurium when compared to *luxS* mutant. On the other hand, when mutant cells were cultivated in the presence of AI-2, the abundance of PfkA, Tig, YaeT, PhoP, TalB, GpmI, TrxB, Pta, YiiM, and an unidentified protein enhanced while the abundance of GroL, OmpF and RpoA descreased [30]. Kint et al. [31] observed a decrease in the abundance of FljB in *luxS* mutant of *Salmonella* Typhimurium compared to wild-type cells.

The proteins identified in the present study were classified into the following four categories, based on their process according to the GO annotations: (i) translation: PheT, RplB, RplE, RpsB, and Tsf, (ii) transport: OmpA, OmpC, OmpD, and PtsI (iii) metabolic process: TalB, GapA, PmgI, Eno, and PykF, and (iv) stress response: HtpG and Adi. We then grouped the proteins based on their functions (Fig. 3).

Thus, considering the cultivation period for extracting the proteins as well as their abundance and function, we observed a correlation with what is described in the literature for cells entering into

Table 1
Differentially abundant protein spots of *Salmonella* Enteritidis PT4 growing in TSB for 7 h in the presence of C12-HSL.

Spot	Experimental	Mean % spot volume ± SE		Fold changed (% spot's volume with C12-HSL/Control)	Total
	pI/MM (kDa)	Control	C12-HSL		
184	4.47/33.882	0.409 ± 0.073[a]	ND[b]	<1.00	10
183	6.27/41.739	0.097 ± 0.016[a]	ND[b]	<1.00	
129	9.52/23.452	0.330 ± 0.079[a]	0.106 ± 0.027[b]	0.32	
28	6.77/32.188	0.312 ± 0.015[a]	0.160 ± 0.037[b]	0.51	
41	4.91/38.583	1.805 ± 0.099[a]	1.061 ± 0.112[b]	0.59	
46	6.73/39.653	2.914 ± 0.118[a]	1.931 ± 0.147[b]	0.66	
35	4.96/35.910	0.965 ± 0.048[a]	0.678 ± 0.097[b]	0.70	
42	5.10/38.583	3.992 ± 0.134[a]	2.909 ± 0.198[b]	0.73	
50	4.03/39.653	7.355 ± 0.407[a]	5.509 ± 0.538[b]	0.75	
52	3.86/40.475	10.110 ± 0.322[a]	7.964 ± 0.138[b]	0.79	
37	7.33/36.905	0.059 ± 0.003[b]	0.079 ± 0.004[a]	1.34	29
63	5.42/46.910	1.378 ± 0.125[b]	1.875 ± 0.112[a]	1.36	
77	4.97/58.092	0.575 ± 0.087[b]	0.843 ± 0.019[a]	1.47	
102	5.21/82.975	0.768 ± 0.069[b]	1.127 ± 0.126[a]	1.47	
101	5.31/82.975	0.881 ± 0.075[b]	1.334 ± 0.113[a]	1.51	
84	4.47/65.808	0.353 ± 0.022[b]	0.555 ± 0.024[a]	1.57	
86	5.09/72.248	0.630 ± 0.061[b]	1.050 ± 0.097[a]	1.67	
100	5.41/82.975	0.910 ± 0.183[b]	1.680 ± 0.246[a]	1.85	
164	9.30/51.893	0.028 ± 0.009[b]	0.055 ± 0.006[a]	1.99	
160	3.84/37.542	0.076 ± 0.003[b]	0.153 ± 0.024[a]	2.01	
147	5.05/95.991	0.047 ± 0.007[b]	0.104 ± 0.018[a]	2.21	
117	5.34/28.944	0.096 ± 0.029[b]	0.216 ± 0.023[a]	2.25	
83	5.07/65.808	0.134 ± 0.013[b]	0.399 ± 0.035[a]	2.98	
159	5.09/150.199	0.045 ± 0.013[b]	0.162 ± 0.016[a]	3.61	
180	5.83/35.437	ND[b]	0.040 ± 0.008[a]	>1.00	
175	5.49/62.593	ND[b]	0.047 ± 0.016[a]	>1.00	
174	5.86/62.204	ND[b]	0.052 ± 0.004[a]	>1.00	
178	4.31/35.100	ND[b]	0.053 ± 0.016[a]	>1.00	
172	5.59/62.204	ND[b]	0.066 ± 0.020[a]	>1.00	
171	5.97/62.593	ND[b]	0.072 ± 0.015[a]	>1.00	
181	5.97/35.550	ND[b]	0.073 ± 0.014[a]	>1.00	
176	3.99/43.728	ND[b]	0.078 ± 0.028[a]	>1.00	
173	5.72/62.204	ND[b]	0.080 ± 0.014[a]	>1.00	
168	6.23/40.381	ND[b]	0.092 ± 0.037[a]	>1.00	
179	3.79/35.437	ND[b]	0.095 ± 0.010[a]	>1.00	
170	6.02/40.381	ND[b]	0.099 ± 0.031[a]	>1.00	
182	5.15/40.253	ND[b]	0.129 ± 0.047[a]	>1.00	
177	3.97/34.326	ND[b]	0.164 ± 0.037[a]	>1.00	
169	4.99/37.053	ND[b]	0.242 ± 0.005[a]	>1.00	
Total differentially abundant proteins					**39**

MM = Molecular Mass; pI = Isoeletric point; Mean = mean of the three biological replicates; SE = Standard Error; ND = not detected.
Average followed by different letters in the same for each spot differ at 5% probability ($p < 0.05$) by Tukey's test.
< 1.00 or >1.00 indicate that the protein was not detected in one of the conditions.

stationary phase, mainly related to nitrogen and amino acid starvation and, acid stress. These data corroborate with those reported for *E. coli* in response to nutrient limitation in the presence of AHL, where the $\sigma^{s/38}$ (RpoS) of RNA polymerase, which is specific in stationary phase, was more abundant [54,55]. In *Burkholderia pseudomallei*, 60 genes have been shown to be controlled by AHL and most of these genes are also co-regulated by RpoS and associated with stationary phase [56]. In addition, in three species of the genus *Burkholderia*, AHLs have been shown to anticipate the responses to the stresses of stationary phase leading to increased cellular survival [57]. Van Delden et al. [58] demonstrated that the expression of both *lasR* and *rhlR* genes and AHL synthesis are prematurely activated during the stringent response induced by overexpression of *relA* in *P. aeruginosa* PAO1, independently of cell density.

Initially, the abundance of PheT (Phenylalanine-tRNA ligase beta subunit or Phenylalanine-tRNA synthetase beta subunit) was enhanced by 2.21 fold in *Salmonella* Enteritidis PT4 growing in the presence of the autoinducer (Fig. 3). This protein is the β subunit of the enzyme $\alpha_2\beta_2$ heterotetrameric and PheS is the α subunit of that enzyme, responsible for charging the $tRNA^{Phe}$ with the L-phenylalanine [59]. PheS is located in the same operon of PheT. However, this last protein was not identified in our gels. In *E. coli*, the synthesis of phenylalanyl-soluble RNA synthetase enhanced twice when cells were cultivated under phenylalanine limitation [60]. Putzer and Laalami [61] reported that *pheST* genes were repressed 2.5 fold under conditions in which the cellular concentration of charged $tRNA^{Phe}$ was decreased. Thus, the arrival of uncharged $tRNA^{Phe}$ in the ribosomes enhances the synthesis of nucleotides guanosine tetraphosphate (ppGpp) and pentaphosphate (pppGpp) by RelA resulting in stringent response [62–66].

The incapacity of charging tRNA caused by nitrogen and amino acid starvation leads to a reduction in ribosomal protein synthesis and rRNA, as well as degradation of rRNA, dimerization, inactivation and ultimately degradation of the ribosomes [67–70]. Thus, four proteins related to translation processes were less abundant in the presence of C12-HSL, namely RplB (50S ribosomal protein L2), RplE (50S ribosomal protein L5), and RpsB (30S ribosomal protein S2) with the function of structural constituent of ribosome, and the Tsf or EF-Ts (Elongation factor Ts) with the function of translational elongation (Fig. 3). Aseev et al. [71] showed that the promoter of the operon *rpsB-tsf* in *E. coli* was negatively regulated by (p)ppGpp during amino acid starvation. Moreover, during the stringent response, the cell blockage of DNA synthesis inhibits stable RNAs and membrane components as well as leads to a rapid production

Table 2
Identification of differentially abundant proteins by *Salmonella* Enteritidis PT4 growing for 7 h in the presence of C12-HSL.

No. Spot	Access number[a]	Identified protein[a]	Protein name[a]	Gene name[a]	Gene locus[a]	Theoretical[b]	Experimental	Peptide mass fingerprinting (PMF)			Peptide fragment fingerprinting (PFF)			
						pI/MM (kDa)		Score	Match	Coverage (%)	Score	Match	Exclusive peptide	Coverage (%)
28	P66541	30S ribosomal protein S2	RpsB	*rpsB*	STM0216	6.61/26.741	6.77/32.188	33	12	42	135	3	2	13
35	P64052	Elongation factor Ts	Tsf	*tsf*	STM0217	5.13/30.338	4.96/35.910	37	9	27	229	4	1	15
41	P02936	Outer membrane protein A	OmpA	*ompA*	STM1070	5.60/37.491	4.91/38.583	47	18	52	205	3	2	9
42	P02936	Outer membrane protein A	OmpA	*ompA*	STM1070	5.60/37.491	5.10/38.583	84	15	47	255	4	2	9
46	P0A1P0	Glyceraldehyde-3-phosphate dehydrogenase	GapA	*gapA*	STM1290	6.33/35.564	6.73/39.653	41	11	38	290	5	2	16
50	P37592	Outer membrane porin protein OmpD	OmpD	*nmpC*	STM1572	4.66/39.671	4.03/39.653	56	10	32	211	5	2	13
52	P0A263	Outer membrane protein C	OmpC	*ompC*	STM2267	4.61/41.311	3.86/40.475	35	8	25	440	4	4	14
63	P64076	Enolase	Eno	*eno*	STM2952	5.25/45.570	5.42/46.910	46	9	26	91	3	1	6
77	Q8ZL56	2,3-bisphosphoglycerate-independent phosphoglycerate mutase	PmgI or GpmI	*pmgI*	STM3704	5.05/56.219	4.97/58.092	71	21	50	171	3	2	5
84	P0A249	Phosphoenolpyruvate-protein phosphotransferase	PtsI or EI	*ptsI*	STM2432	4.75/63.344	4.47/65.808	115	24	40	278	8	2	9
86	P58480	Chaperone protein HtpG	HtpG	*htpG*	STM0487	5.11/71.457	5.09/72.248	65	22	39	450	6	5	13
100	Q8ZKE3	Arginine decarboxylase	Adi	*adi*	STM4296	5.24/84.250	5.41/82.975	85	25	38	348	7	4	10
101	Q8ZKE3	Arginine decarboxylase	Adi	*adi*	STM4296	5.24/84.250	5.31/82.975	90	25	39	262	5	2	7
102	Q8ZKE3	Arginine decarboxylase	Adi	*adi*	STM4296	5.24/84.250	5.21/82.975	80	18	30	334	8	4	9
129	P62405	50S ribosomal protein L5	RplE	*rplE*	STM3428	9.40/20.304	9.52/23.452	102	18	71	392	9	3	38
147	P15434	Phenylalanine-tRNA ligase beta subunit	PheT	*pheT*	STM1338	5.12/87.226	5.05/95.991	28	16	21	92	2	1	3
169	P66955	Transaldolase	TalB	*talB*	STM0007	5.10/35.149	4.99/37.053	62	13	47	151	3	1	7
171	P77983	Pyruvate kinase	PykF	*pykF*	STM1378	5.52/48.622	5.97/62.593	38	11	18	104	3	1	2
173	P77983	Pyruvate kinase	PykF	*pykF*	STM1378	5.52/48.622	5.72/62.204	36	6	11	117	1	1	2
174	P77983	Pyruvate kinase	PykF	*pykF*	STM1378	5.52/48.622	5.86/62.204	41	8	19	100	1	1	2
184	P60428	50S ribosomal protein L2	RplB	*rplB*	STM3437	10.93/ 29.801	4.47/33.882	56	17	50	212	6	2	21

PI/MM = Isoeletric point/Molecular Mass.
[a] Corresponds to knowledgebase UniProtKB (http://www.uniprot.org/) reference of *Salmonella enterica* serovar Typhimurium LT2 [96].
[b] Theoretical pI/MM values for monoisotopic obtained from ExPASy bioinformatics tool “Compute pI/Mw” (http://web.expasy.org/compute_pi/).

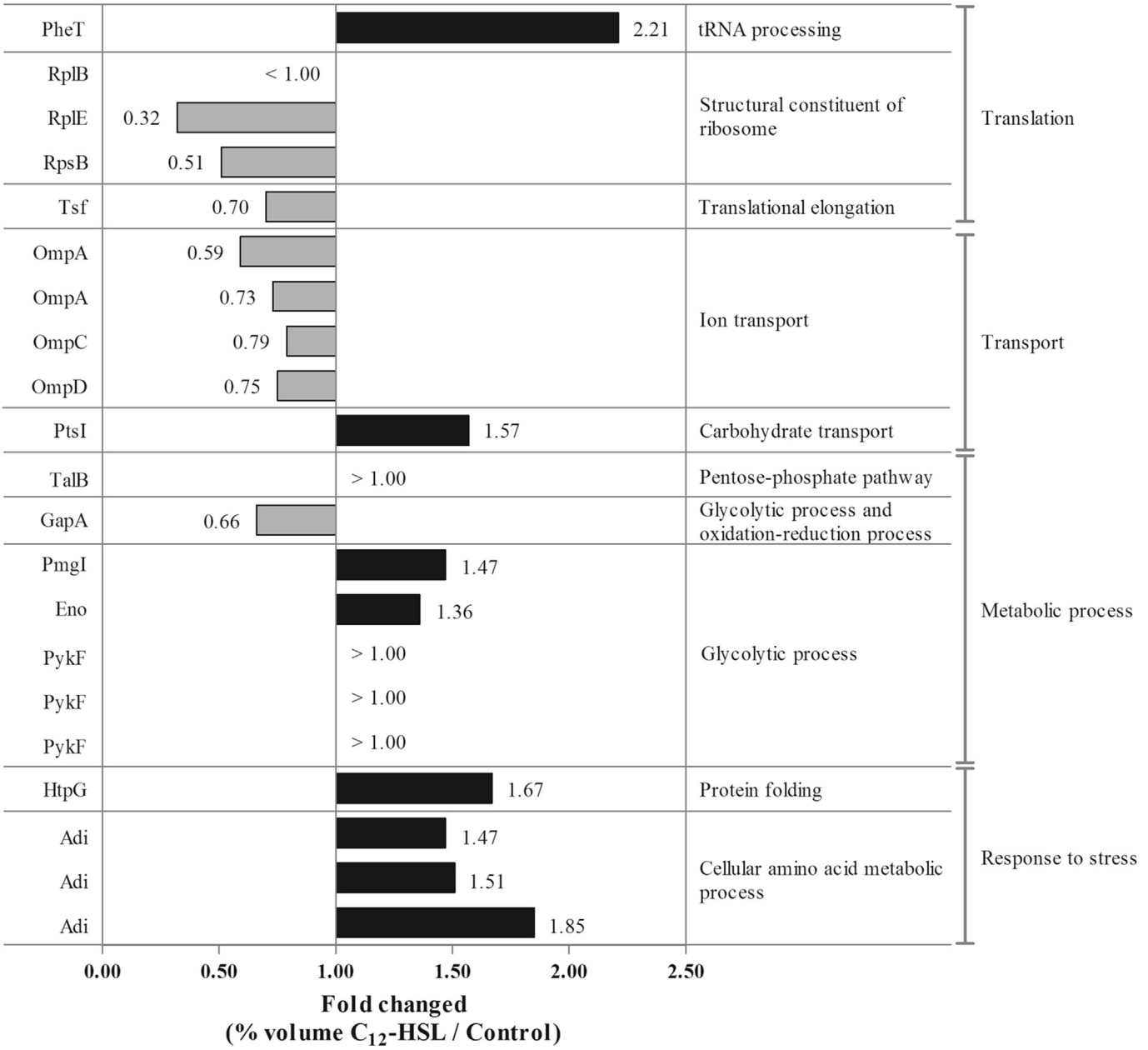

Fig. 3. Differentially abundant proteins identified and grouped as to the process and function according to Gene Ontology (GO) annotations (European Bioinformatics Institut). Proteins with enhanced abundance following C12-HSL treatments ($p < 0.05$ and fold changed > 1.2 as well as > 1.0) are shown in black bars and the proteins which abundance decreased following C12-HSL treatments ($p < 0.05$ and fold changed < 0.8 as well as < 1.0) are shown in grey bars.

of factors that are crucial for stress resistance, amino acid biosynthesis and directs the cellular energy resources [62,63,65,66].

One way for the cell to obtain energy is by increasing glucose uptake by the phosphotransferase system (PTS), where the enzyme I (EI) receives phosphate from phosphoenolpyruvate (PEP) and then, phosphorylates the histidine protein, HPr. The phosphorylation cascade continues with the phosphorylation of different domains of the enzyme II (EII) and then, glucose into glucose-6-phosphate (G6P) [72]. In *Salmonella* Enteritidis PT4, the presence of C12-HSL enhanced in 1.57 fold the abundance of PtsI protein (Phosphoenolpyruvate-protein phosphotransferase) or EI (Phosphotransferase system, enzyme I) (Fig. 3), suggesting an increase in the glucose uptake and therefore directing G6P to many metabolic pathways such as the pentose-phosphate pathway and the glycolytic pathway for amino acid biosynthesis. Nishio et al. [73] showed that the increased expression of *ptsI* gene enhanced the uptake rate and the specific usage of glucose by *E. coli*.

Interestingly, two proteins that have glyceraldehyde-3-phosphate (GAP) as a substrate in common in different metabolic pathways were differentially abundant. TalB (Transaldolase) from the pentose-phosphate pathway was more abundant in *Salmonella* Enteritidis growing in the presence of C12-HSL, while GapA (Glyceraldehyde-3-phosphate dehydrogenase) from the glycolytic pathway and related to the oxidation-reduction process was less abundant (Fig. 3). However, the abundance of the proteins PmgI or GpmI (2,3-bisphosphoglycerate-independent phosphoglycerate mutase), Eno (Enolase), and PykF (Pyruvate kinase) all belonging to the glycolytic pathway, but downstream of GAP, increased in the presence of C12-HSL (Fig. 3).

In the glycolytic pathway, GAP is transformed by GapA into 1,3-

bisphospho-D-glycerate (1,3PG), which in turn is transformed into PEP through the participation of several enzymes including PmgI (or GpmI) and Eno. Then, two pyruvate kinases, PykA and PykF, catalyze the conversion of PEP into pyruvate (PYR) coupled to the synthesis of ATP which is the point of flux control in the glycolytic pathway. Soni et al. [30] showed that GpmI and TalB were more abundant in wild-type *Salmonella* Typhimurium as well as in *luxS* mutant cultivated in the presence of AI-2 when compared with the *luxS* mutant in the absence of AI-2.

The abundance of outer membrane proteins (OMPs), OmpA (Outer membrane protein A), OmpC (Outer membrane protein C), and OmpD (Outer membrane porin protein OmpD) reduced when *Salmonella* Enteritidis was cultivated in the presence of C12-HSL (Fig. 3). The OMPs are involved in the ion transport, adhesion and invasion of macrophages, and are recognized by bacteriophages and by the immune system. Because of that, this group of proteins is widely used in the studies for vaccine elaboration [74–79]. Studies have reported that the level of expression of OMPs is controlled by membrane and environmental stresses such as nutrient limitation and concentration of some antibiotics [77,80–82].

The chaperone HtpG (Chaperone protein HtpG or Heat shock protein HtpG) was 1.67 fold more abundant in the presence of C12-HSL (Fig. 3). This protein is an *hsp*90 homologue more abundant in *Salmonella* Typhimurium in response to the bactericidal/permeability increasing protein (BPI) from human neutrophils [83], and the *htpG* gene was more abundant in *Salmonella* Typhimurium following exposure to antimicrobial peptides present in the tonsils, ileum and/or ileocaecal lymph nodes of pigs [84].

The Adi protein (Arginine decarboxylase) involved in the cellular amino acid metabolic process was 1.85 fold more abundant in *Salmonella* Enteritidis PT4 in medium supplemented with HSL (Fig. 3). This protein is part of the system of resistance to arginine-dependent acid stress (AR3) of *Salmonella* that is activated anaerobically in order to increase intracellular pH, since AdiA or SpeA (Arginine decarboxylase) decarboxylate L-arginine consuming an intracellular proton H^+ forming carbon dioxide (CO_2) and agmatine [85,86]. Van Houdt et al. [87] showed that in the presence of 0.5 mM C6-HSL, the *gadA* promoter (Glutamate decarboxylase A) in *E. coli* was strongly upregulated after 8 and 60 h of growth in LB broth acidified to pH 4.0 (with HCl) at 30 °C. This response is associated with increases in the acid tolerance dependent on *sdiA* [87]. Kieboom and Abee [86] showed that this system is important for the survival of *Salmonella* Typhimurium in mineral medium with pH 2.5 by adding arginine in anaerobiosis, inducing an enhancement in the expression of the gene *adiA*. Furthermore, this gene was positively controlled by $\sigma^{S/38}$ in *Salmonella* Typhimurium leading to synthesis of polyamines [88]. In addition, the polyamines increased the biofilm formation, stress resistance and virulence in *Salmonella* [89–92].

Moreover, the PPI network of these proteins showed a *p*-value of 1e-09 for enrichment (Fig. 4). This small value indicates that the

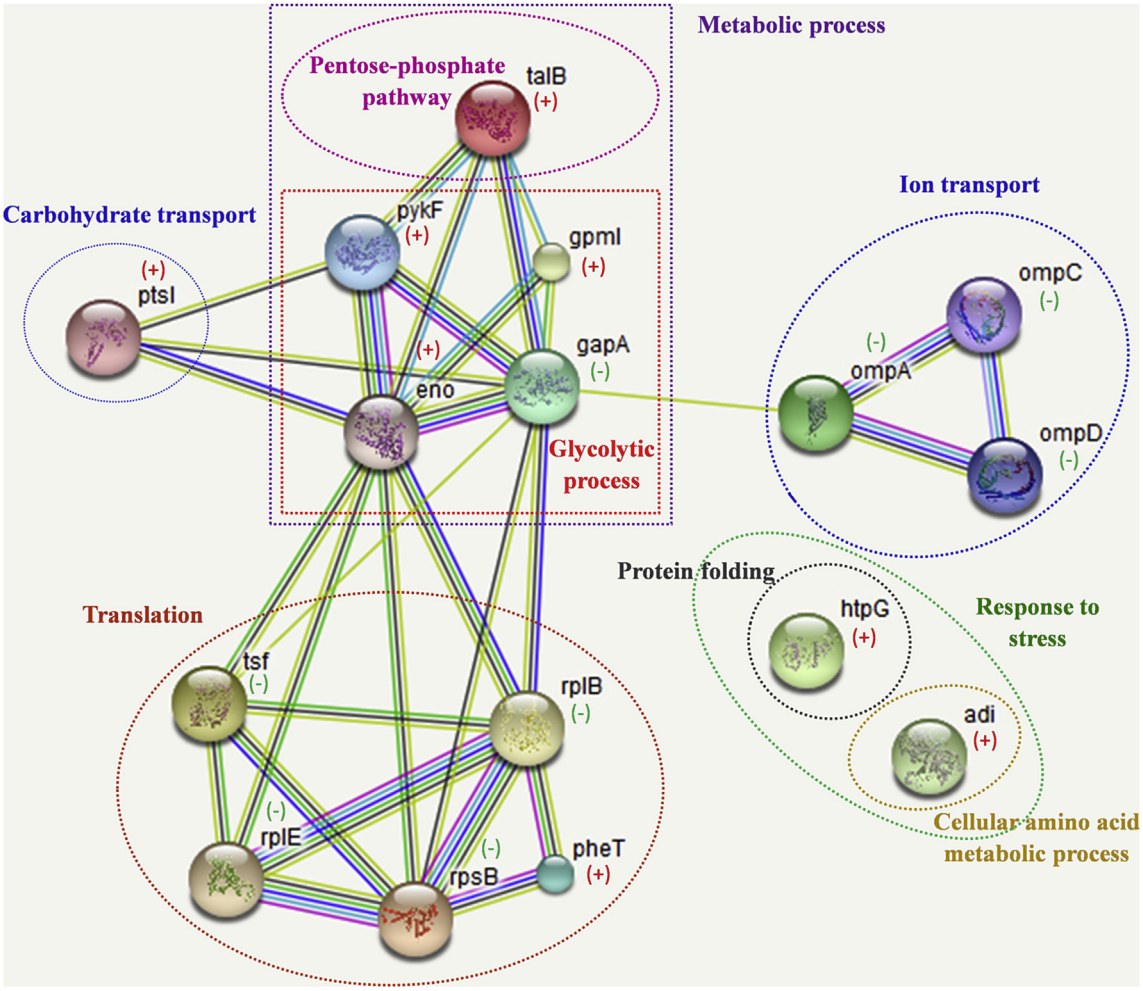

Fig. 4. The PPI network in relation to the differentially abundant proteins of *Salmonella* Enteritidis in the presence of C12-HSL. The boxes with dashed line delimite the proteins of the same process or with the same functions (written with the same colors of the boxes). (+), proteins with significantly ($p < 0.05$ and fold changed > 1.2 as well as > 1.0) increased abundance rates following C12-HSL treatment; (−), proteins whose abundance was significantly ($p < 0.05$ and fold changed < 0.8 as well as < 1.0) decreased.

Table 3
Concentration of extracellular organic acids and ethanol.

Time (h)	Succinic acid (mM)		Lactic acid (mM)		Acetic acid (mM)		Formic acid (mM)		Ethanol (mM)	
	Control	C12-HSL	Control	C12-HSL	Control	C12-HSL	Control	C12-HSL	Control	C12-HSL
2	0.87^{D}	0.93^{C}	0.11^{D}	0.74^{C}	5.03^{D}	4.97^{C}	0.00^{B}	0.00^{C}	15.46^{B}	15.18^{B}
7	8.33^{C}	8.65^{B}	9.57^{C}	10.16^{B}	30.89^{C}	30.97^{B}	60.13^{A}	57.59^{A}	17.02^{A}	16.52^{A}
24	10.61^{B}	10.73^{A}	27.02^{B}	27.74^{A}	34.29^{B}	34.91^{A}	0.00^{bB}	20.46^{aB}	17.26^{A}	16.84^{A}
36	12.22^{aA}	11.05^{bA}	31.84^{aA}	28.44^{bA}	37.13^{aA}	35.24^{bA}	0.00^{B}	0.00^{C}	12.91^{C}	13.09^{C}

The comparisons can be drawn between treatments or throughout time. Average followed by different lower case letters in the same line (between treatments) and followed by different capital letters in the columns (throughout time) differs at 5% probability ($p < 0.05$) by Tukey's test. Where a lower case letter is not shown, no statistical difference between control and C12-HSL was observed.

proteins have more interactions among themselves than what would be expected for a random set of proteins of similar size as well as the proteins are at least partially biologically connected as a group [47].

3.3. HSL changes the levels of organic acids and ethanol of *Salmonella*

Although C12-HSL alters the pattern of proteins expression, especially proteins related to metabolic processes in *Salmonella* Enteritidis PT4 growing at 37 °C for 7 h in anaerobic TSB, the levels of extracellular organic acids and ethanol were not altered in the same conditions and time cultivation (Table 3). Moreover, considering that succinic, lactic, acetic, and formic acids were identified in both conditions, *Salmonella* Enteritidis PT4 may activate the mixed-acid pathway fermentation. The organic acids: propionic, valeric, isovaleric, butyric, and isobutyric acids were not identified in the samples evaluated.

There was a gradual increase in the concentrations of succinic, lactic, and acetic acids along the growth of *Salmonella* (Table 3). However, the concentration of these acids reached a plateau after 24 h incubation in the presence of C12-HSL. In addition, formic acid and ethanol concentrations did not follow a regular pattern throughout time. On the other hand, comparing between the treatments, only at 36 h of incubation a significantly lower concentration of succinic, lactic, and acetic acids were produced in treatment containing AI-1 in relation to the control without this signaling molecule. Different to what was observed for the other extracellular organic acids, the concentration of formic acid had a pick at 7 h incubation and decreased in later time points. However, in the control treatment extracellular formic acid was not detected at 24 h of incubation while for cells treated with C12-HSL, extracellular formic acid reached 20.46 mM ($p < 0.05$).

Thus, the results show that C12-HSL interferes with energy metabolism of *Salmonella* Enteritidis PT4 during its growth and, consequently, in the extracellular levels of organic acids. These acids can also be present in the environment as in the mammalian gastrointestinal tract where they regulate invasion genes [93,94]. In *Salmonella* Typhimurium, formic acid enhances the expression of the regulators *hilA* and *hilD* of the *Salmonella* pathogenicity island 1 (SPI1) that contains genes associated with invasion thereby enhancing invasion of epithelial cells [94]. Furthermore, Barker et al. [95] showed that the organic acids, mainly formic acid, protect *E. coli* and *Salmonella* cells in stationary phase from a potent antimicrobial peptide. It would be interesting to test the infectivity of *Salmonella in vivo* in the presence and absence of C12-HSL.

4. Conclusion

The results show that AI-1 changes the abundance of proteins and the levels of organic acids of *Salmonella* Enteritidis PT4 in anaerobic condition. Thus, considering the cultivation period for extracting the proteins as well as their abundance and function, we observed a correlation with what is described in the literature for cells entering into stationary phase, mainly related to nitrogen and amino acid starvation and, acid stress. In addition, formic acid remains longer in the supernatant of cells growing in the presence of AHL. However, more studies are needed to determine the specific role of the differentially abundant proteins and the extracellular organic acids secreted by *Salmonella* growing in the presence of AHL. It is still not clear what is the advantage for *Salmonella* to control its proteins and organic acids synthesis through quorum sensing by exogenous AI-1. However, it is important to know and understand the effects of AHLs on the physiology of this pathogen in order to find ways to eliminate it and hence reduce the numbers of associated foodborne outbreaks.

Acknowledgements

Felipe Alves de Almeida was supported by a fellowship from Conselho Nacional de Desenvolvimento Científico e Tecnológico and this research was supported by Fundação de Amparo à Pesquisa do Estado de Minas Gerais, Coordenação de Aperfeiçoamento de Pessoal de Nível Superior, Financiadora de Estudos e Projetos, Sistema Nacional de Laboratórios em Nanotecnologias (SisNANO) and Ministério da Ciência, Tecnologia e Informação (MCTI). The authors thank the Núcleo de Análise de Biomoléculas (Nubiomol) of Universidade Federal de Viçosa for the equipments and softwares for protein analysis.

References

[1] S.E. Majowicz, J. Musto, E. Scallan, F.J. Angulo, M. Kirk, S.J. O'Brien, et al., The global burden of nontyphoidal *Salmonella* gastroenteritis, Clin. Infect. Dis. 50 (2010) 882–889, http://dx.doi.org/10.1086/650733.
[2] M.M. Nunes, A.L.A.A. Mota, E.D. Caldas, Investigation of food and water microbiological conditions and foodborne disease outbreaks in the Federal District, Brazil, Food Control. 34 (2013) 235–240, http://dx.doi.org/10.1016/j.foodcont.2013.04.034.
[3] M. Chironna, S. Tafuri, M.S. Gallone, A. Sallustio, D. Martinelli, R. Prato, et al., Outbreak of *Salmonella infantis* gastroenteritis among people who had eaten at a hash house in southern Italy, Public Health 128 (2014) 438–443, http://dx.doi.org/10.1016/j.puhe.2014.02.002.
[4] R. Freeman, G. Dabrera, C. Lane, N. Adams, L. Browning, T. Fowler, et al., Association between use of proton pump inhibitors and non-typhoidal salmonellosis identified following investigation into an outbreak of *Salmonella* Mikawasima in the UK, 2013, Epidemiol. Infect. 144 (2015) 968–975, http://dx.doi.org/10.1017/S0950268815002332.
[5] M. Hensel, Evolution of pathogenicity islands of *Salmonella enterica*, Int. J. Med. Microbiol. 294 (2004) 95–102, http://dx.doi.org/10.1016/j.ijmm.2004.06.025.
[6] S.Y. Ong, F.L. Ng, S.S. Badai, A. Yuryev, M. Alam, Analysis and construction of pathogenicity island regulatory pathways in *Salmonella enterica* serovar Typhi, J. Integr. Bioinform 7 (2010), http://dx.doi.org/10.2390/biecoll-jib-2010-145.
[7] M.R. Hayward, V.A.A. Jansen, M.J. Woodward, Comparative genomics of *Salmonella enterica* serovars Derby and Mbandaka, two prevalent serovars associated with different livestock species in the UK, BMC Genomics 14 (2013) 365, http://dx.doi.org/10.1186/1471-2164-14-365.
[8] W.C. Fuqua, S.C. Winans, E.P. Greenberg, Quorum sensing in bacteria: the LuxR-LuxI family of cell density-responsive transcriptional regulators, J. Bacteriol. 176 (1994) 269–275.
[9] C. Fuqua, M.R. Parsek, E.P. Greenberg, Regulation of gene expression by cell-

to-cell communication: acyl-homoserine lactone quorum sensing, Annu. Rev. Genet. 35 (2001) 439–468, http://dx.doi.org/10.1146/annurev.genet.35.102401.090913.
[10] C. Fuqua, S.C. Winans, E.P. Greenberg, Census and consensus in bacterial ecosystems: the LuxR-LuxI family of quorum-sensing transcriptional regulators, Annu. Rev. Microbiol. 50 (1996) 727–751, http://dx.doi.org/10.1146/annurev.micro.50.1.727.
[11] L. Keller, M.G. Surette, Communication in bacteria: an ecological and evolutionary perspective, Nat. Rev. Microbiol. 4 (2006) 249–258, http://dx.doi.org/10.1038/nrmicro1383.
[12] M. Walters, V. Sperandio, Quorum sensing in *Escherichia coli* and *Salmonella*, Int. J. Med. Microbiol. 296 (2006) 125–131, http://dx.doi.org/10.1016/j.ijmm.2006.01.041.
[13] B.M. Ahmer, J. Van Reeuwijk, C.D. Timmers, P.J. Valentine, F. Heffron, *Salmonella* Typhimurium encodes an SdiA homolog, a putative quorum sensor of the LuxR family, that regulates genes on the virulence plasmid, J. Bacteriol. 180 (1998) 1185–1193.
[14] B. Michael, J.N. Smith, S. Swift, F. Heffron, B.M.M. Ahmer, SdiA of *Salmonella enterica* is a LuxR homolog that detects mixed microbial communities, J. Bacteriol. 183 (2001) 5733–5742, http://dx.doi.org/10.1128/JB.183.19.5733-5742.2001.
[15] J.N. Smith, B.M.M. Ahmer, Detection of other microbial species by *Salmonella*: expression of the SdiA regulon, J. Bacteriol. 185 (2003) 1357–1366, http://dx.doi.org/10.1128/JB.185.4.1357-1366.2003.
[16] Y. Nguyen, N.X. Nguyen, J.L. Rogers, J. Liao, J.B. Macmillan, Y. Jiang, et al., Structural and mechanistic roles of novel chemical ligands on the SdiA quorum-sensing transcription regulator, MBio 6 (2015) e02429, http://dx.doi.org/10.1128/mBio.02429-14.
[17] M.E. Taga, J.L. Semmelhack, B.L. Bassler, The LuxS-dependent autoinducer AI-2 controls the expression of an ABC transporter that functions in AI-2 uptake in *Salmonella* Typhimurium, Mol. Microbiol. 42 (2001) 777–793.
[18] M.E. Taga, B.L. Bassler, Chemical communication among bacteria, Proc. Natl. Acad. Sci. U.S.A. 100 (2003) 14549–14554, http://dx.doi.org/10.1073/pnas.1934514100.
[19] K.B. Xavier, B.L. Bassler, Regulation of uptake and processing of the quorum-sensing autoinducer AI-2 in *Escherichia coli*, J. Bacteriol. 187 (2005) 238–248, http://dx.doi.org/10.1128/JB.187.1.238-248.2005.
[20] D.T. Hughes, V. Sperandio, Inter-kingdom signalling: communication between bacteria and their hosts, Nat. Rev. Microbiol. 6 (2008) 111–120, http://dx.doi.org/10.1038/nrmicro1836.
[21] M.B. Miller, B.L. Bassler, Quorum sensing in bacteria, Annu. Rev. Microbiol. 55 (2001) 165–199, http://dx.doi.org/10.1146/annurev.micro.55.1.165.
[22] A.M. Prouty, W.H. Schwesinger, J.S. Gunn, Biofilm formation and interaction with the surfaces of gallstones by *Salmonella* spp, Infect. Immun. 70 (2002) 2640–2649, http://dx.doi.org/10.1128/IAI.70.5.2640-2649.2002.
[23] J.N. Smith, J.L. Dyszel, J.A. Soares, C.D. Ellermeier, C. Altier, S.D. Lawhon, et al., SdiA, an *N*-acylhomoserine lactone receptor, becomes active during the transit of *Salmonella enterica* through the gastrointestinal tract of turtles, PLoS One 3 (2008) e2826, http://dx.doi.org/10.1371/journal.pone.0002826.
[24] P.R. Jesudhasan, M.L. Cepeda, K. Widmer, S.E. Dowd, K.A. Soni, M.E. Hume, et al., Transcriptome analysis of genes controlled by *luxS*/autoinducer-2 in *Salmonella enterica* serovar Typhimurium, Foodborne Pathog. Dis. 7 (2010) 399–410, http://dx.doi.org/10.1089/fpd.2009.0372.
[25] Z. Liu, F. Que, L. Liao, M. Zhou, L. You, Q. Zhao, et al., Study on the promotion of bacterial biofilm formation by a *Salmonella* conjugative plasmid and the underlying mechanism, PLoS One 9 (2014) e109808, http://dx.doi.org/10.1371/journal.pone.0109808.
[26] M.E.M. Campos-Galvão, A.O.B. Ribon, E.F. Araújo, M.C.D. Vanetti, Changes in the *Salmonella enterica* Enteritidis phenotypes in presence of acyl homoserine lactone quorum sensing signals, J. Basic Microbiol. 56 (2015) 493–501, http://dx.doi.org/10.1002/jobm.201500471.
[27] F.A. Almeida, N.J. Pimentel-Filho, U.M. Pinto, H.C. Mantovani, L.L. Oliveira, M.C.D. Vanetti, Acyl homoserine lactone-based quorum sensing stimulates biofilm formation by *Salmonella* Enteritidis in anaerobic conditions (in press), Arch. Microbiol. (2016), http://dx.doi.org/10.1007/s00203-016-1313-6.
[28] F.A. Almeida, U.M. Pinto, M.C.D. Vanetti, Novel insights from molecular docking of SdiA from *Salmonella* Enteritidis and *Escherichia coli* with quorum sensing and quorum quenching molecules, Microb. Pathog. 99 (2016) 178–190, http://dx.doi.org/10.1016/j.micpath.2016.08.024.
[29] N. Abed, O. Grépinet, S. Canepa, G. a Hurtado-Escobar, N. Guichard, A. Wiedemann, et al., Direct regulation of the *pefI-srgC* operon encoding the Rck invasin by the quorum-sensing regulator SdiA in *Salmonella* Typhimurium, Mol. Microbiol. 94 (2014) 254–271, http://dx.doi.org/10.1111/mmi.12738.
[30] K.A. Soni, P.R. Jesudhasan, M. Cepeda, B. Williams, M. Hume, W.K. Russell, et al., Autoinducer AI-2 is involved in regulating a variety of cellular processes in *Salmonella* Typhimurium, Foodborne Pathog. Dis. 5 (2008) 147–153, http://dx.doi.org/10.1089/fpd.2007.0050.
[31] G. Kint, K.A. Sonck, G. Schoofs, D. De Coster, J. Vanderleyden, S.C. De Keersmaecker, 2D proteome analysis initiates new insights on the *Salmonella* Typhimurium LuxS protein, BMC Microbiol. 9 (2009) 198, http://dx.doi.org/10.1186/1471-2180-9-198.
[32] R. Di Cagno, M. De Angelis, M. Calasso, M. Gobbetti, Proteomics of the bacterial cross-talk by quorum sensing, J. Proteomics 74 (2011) 19–34, http://dx.doi.org/10.1016/j.jprot.2010.09.003.
[33] F. Chevalier, Highlights on the capacities of "Gel-based" proteomics, Proteome Sci. 8 (2010) 23, http://dx.doi.org/10.1186/1477-5956-8-23.
[34] M.E.M. Campos-Galvão, T.D.S. Leite, A.O.B. Ribon, E.F. Araújo, M.C.D. Vanetti, A new repertoire of informations about the quorum sensing system in *Salmonella enterica* serovar Enteritidis PT4, Genet. Mol. Res. 14 (2015) 4068–4084, http://dx.doi.org/10.4238/2015.April.27.22.
[35] J.H. Miller, Experiments in Molecular Genetics, Cold Spring Harbor Laboratory Press, Cold Spring Harbor, NY, 1972.
[36] J.R. Lima, A.O.B. Ribon, J.B. Russell, H.C. Mantovani, Bovicin HC5 inhibits wasteful amino acid degradation by mixed ruminal bacteria *in vitro*, FEMS Microbiol. Lett. 292 (2009) 78–84, http://dx.doi.org/10.1111/j.1574-6968.2008.01474.x.
[37] J.M.P. Deshusses, J.A. Burgess, A. Scherl, Y. Wenger, N. Walter, V. Converset, et al., Exploitation of specific properties of trifluoroethanol for extraction and separation of membrane proteins, Proteomics 3 (2003) 1418–1424, http://dx.doi.org/10.1002/pmic.200300492.
[38] R.O. Ebanks, A. Dacanay, M. Goguen, D.M. Pinto, N.W. Ross, Differential proteomic analysis of *Aeromonas salmonicida* outer membrane proteins in response to low iron and *in vivo* growth conditions, Proteomics 4 (2004) 1074–1085, http://dx.doi.org/10.1002/pmic.200300664.
[39] B.L. Nunn, S.A. Shaffer, A. Scherl, B. Gallis, M. Wu, S.I. Miller, et al., Comparison of a *Salmonella* Typhimurium proteome defined by shotgun proteomics directly on an LTQ-FT and by proteome pre-fractionation on an LCQ-DUO, Genomics Proteom. 5 (2006) 154–168, http://dx.doi.org/10.1093/bfgp/ell024.
[40] M.M. Bradford, A rapid and sensitive method for the quantitation of microgram quantities utilizing the principle of protein-dye binding, Anal. Biochem. 72 (1976) 248–254, http://dx.doi.org/10.1016/0003-2697(76)90527-3.
[41] U.K. Laemmli, Cleavage of structural proteins during the assembly of the head of bacteriophage T4, Nature 227 (1970) 680–685, http://dx.doi.org/10.1038/227680a0.
[42] Y. Ye, H. Li, N. Ling, Y. Han, Q. Wu, X. Xu, et al., Identification of potential virulence factors of *Cronobacter sakazakii* isolates by comparative proteomic analysis, Int. J. Food Microbiol. 217 (2016) 182–188, http://dx.doi.org/10.1016/j.ijfoodmicro.2015.08.025.
[43] A. Shevchenko, H. Tomas, J. Havlis, J.V. Olsen, M. Mann, In-gel digestion for mass spectrometric characterization of proteins and proteomes, Nat. Protoc. 1 (2006) 2856–2860, http://dx.doi.org/10.1038/nprot.2006.468.
[44] M.P. Pereira, B.C. Gouvêa, F.C. Marcelino-Guimarães, H.J.O. Ramos, M.A. Moreira, E.G. Barros, Proteomic analysis of soybean leaves in a compatible and an incompatible interaction with *Phakopsora pachyrhizi*, Organelles Proteom. 1 (2013) 16–27, http://dx.doi.org/10.2478/orpr-2013-0004.
[45] A. Keller, A.I. Nesvizhskii, E. Kolker, R. Aebersold, Empirical statistical model to estimate the accuracy of peptide identifications made by MS/MS and database search, Anal. Chem. 74 (2002) 5383–5392, http://dx.doi.org/10.1021/ac025747h.
[46] A.I. Nesvizhskii, A. Keller, E. Kolker, R. Aebersold, A statistical model for identifying proteins by tandem mass spectrometry, Anal. Chem. 75 (2003) 4646–4658, http://dx.doi.org/10.1021/ac0341261.
[47] D. Szklarczyk, A. Franceschini, S. Wyder, K. Forslund, D. Heller, J. Huerta-Cepas, et al., STRING v10: protein-protein interaction networks, integrated over the tree of life, Nucleic Acids Res. 43 (2015) D447–D452, http://dx.doi.org/10.1093/nar/gku1003.
[48] R. Siegfried, H. Ruckemann, G. Stumpf, Method for the determination of organic acids in silage by high performance liquid chromatography, Landwirt Forsch 37 (1984) 298–304.
[49] C.B.P. Bento, A.C. Azevedo, E. Detmann, H.C. Mantovani, Biochemical and genetic diversity of carbohydrate-fermenting and obligate amino acid-fermenting hyper-ammonia-producing bacteria from Nellore steers fed tropical forages and supplemented with casein, BMC Microbiol. 15 (2015) 28, http://dx.doi.org/10.1186/s12866-015-0369-9.
[50] D.F. Ferreira, SISVAR: a computer statistical analysis system, Cienc. e Agrotecnologia 35 (2011) 1039–1042.
[51] D. Dourou, M.S. Ammor, P.N. Skandamis, G.J.E. Nychas, Growth of *Salmonella* Enteritidis and *Salmonella* Typhimurium in the presence of quorum sensing signalling compounds produced by spoilage and pathogenic bacteria, Food Microbiol. 28 (2011) 1011–1018, http://dx.doi.org/10.1016/j.fm.2011.02.004.
[52] H.-H. Wang, K.-P. Ye, Q.-Q. Zhang, Y. Dong, X.-L. Xu, G.-H. Zhou, Biofilm formation of meat-borne *Salmonella enterica* and inhibition by the cell-free supernatant from *Pseudomonas aeruginosa*, Food Control. 32 (2013) 650–658, http://dx.doi.org/10.1016/j.foodcont.2013.01.047.
[53] B.D. Halligan, V. Ruotti, W. Jin, S. Laffoon, S.N. Twigger, E.A. Dratz, ProMoST (Protein Modification Screening Tool): a web-based tool for mapping protein modifications on two-dimensional gels, Nucleic Acids Res. 32 (2004) 638–644, http://dx.doi.org/10.1093/nar/gkh356.
[54] G.W. Huisman, R. Kolter, Sensing starvation: a homoserine lactone-dependent signaling pathway in *Escherichia coli*, Science 265 (1994) 537–539, http://dx.doi.org/10.1126/science.7545940.
[55] R. Hengge-Aronis, Signal transduction and regulatory mechanisms involved in control of the σ^S (RpoS) subunit of RNA polymerase, Microbiol. Mol. Biol. Rev. 66 (2002) 373–395, http://dx.doi.org/10.1128/MMBR.66.3.373-395.2002.
[56] P. Wongtrakoongate, S. Tumapa, S. Tungpradabkul, Regulation of a quorum sensing system by stationary phase sigma factor RpoS and their co-regulation of target genes in *Burkholderia pseudomallei*, Microbiol. Immunol. 56 (2012) 281–294, http://dx.doi.org/10.1111/j.1348-0421.2012.00447.x.
[57] E. Goo, C.D. Majerczyk, J.H. An, J.R. Chandler, Y.-S. Seo, H. Ham, et al., Bacterial

quorum sensing, cooperativity, and anticipation of stationary-phase stress, Proc. Natl. Acad. Sci. U.S.A. 109 (2012) 19775–19780, http://dx.doi.org/10.1073/pnas.1218092109.
[58] C. Van Delden, R. Comte, A.M. Bally, Stringent response activates quorum sensing and modulates cell density-dependent gene expression in *Pseudomonas aeruginosa*, J. Bacteriol. 183 (2001) 5376–5384, http://dx.doi.org/10.1128/JB.183.18.5376-5384.2001.
[59] M.M. Champion, C.S. Campbell, D.A. Siegele, D.H. Russell, J.C. Hu, Proteome analysis of *Escherichia coli* K-12 by two-dimensional native-state chromatography and MALDI-MS, Mol. Microbiol. 47 (2003) 383–396, http://dx.doi.org/10.1046/j.1365-2958.2003.03294.x.
[60] G. Nass, F.C. Neidhardt, Regulation of formation of aminoacyl-ribonucelic acid synthetases in *Escherichia coli*, Biochim. Biophys. Acta 134 (1967) 347–359.
[61] H. Putzer, S. Laalami, Regulation of the expression of aminoacyl-tRNA synthetases and translation factors, Transl. Mech. 107 (2003) 388–415.
[62] K. Potrykus, M. Cashel, ppGpp: still magical? Annu. Rev. Microbiol. 62 (2008) 35–51, http://dx.doi.org/10.1146/annurev.micro.62.081307.162903.
[63] Z.D. Dalebroux, M.S. Swanson, ppGpp: magic beyond RNA polymerase, Nat. Rev. Microbiol. 10 (2012) 203–212, http://dx.doi.org/10.1038/nrmicro2720.
[64] V. Shyp, S. Tankov, A. Ermakov, P. Kudrin, B.P. English, M. Ehrenberg, et al., Positive allosteric feedback regulation of the stringent response enzyme RelA by its product, EMBO Rep. 13 (2012) 835–839, http://dx.doi.org/10.1038/embor.2012.106.
[65] D.R. Brown, G. Barton, Z. Pan, M. Buck, S. Wigneshweraraj, Nitrogen stress response and stringent response are coupled in *Escherichia coli*, Nat. Commun. 5 (2014) 4115, http://dx.doi.org/10.1038/ncomms5115.
[66] D.R. Brown, G. Barton, Z. Pan, M. Buck, S. Wigneshweraraj, Combinatorial stress responses: direct coupling of two major stress responses in *Escherichia coli*, Microb. Cell. 1 (2014) 315–317, http://dx.doi.org/10.15698/mic2014.09.168.
[67] A. Wada, Growth phase coupled modulation of *Escherichia coli* ribosomes, Genes Cells 3 (1998) 203–208, http://dx.doi.org/10.1046/j.1365-2443.1998.00187.x.
[68] M.P. Deutscher, Degradation of stable RNA in bacteria, J. Biol. Chem. 278 (2003) 45041–45044, http://dx.doi.org/10.1074/jbc.R300031200.
[69] B.J. Paul, W. Ross, T. Gaal, R.L. Gourse, rRNA transcription in *Escherichia coli*, Annu. Rev. Genet. 38 (2004) 749–770, http://dx.doi.org/10.1146/annurev.genet.38.072902.091347.
[70] M.P. Deutscher, Degradation of RNA in bacteria: comparison of mRNA and stable RNA, Nucleic Acids Res. 34 (2006) 659–666, http://dx.doi.org/10.1093/nar/gkj472.
[71] L.V. Aseev, L.S. Koledinskaya, I.V. Boni, Dissecting the extended "-10" *Escherichia coli rpsB* promoter activity and regulation *in vivo*, Biochem. Biokhim. 79 (2014) 776–784, http://dx.doi.org/10.1134/S0006297914080057.
[72] P.W. Postma, J.W. Lengeler, G.R. Jacobson, Phosphoenolpyruvate: carbohydrate phosphotransferase systems of bacteria, Microbiol. Rev. 57 (1993) 543–594.
[73] Y. Nishio, Y. Usuda, K. Matsui, H. Kurata, Computer-aided rational design of the phosphotransferase system for enhanced glucose uptake in *Escherichia coli*, Mol. Syst. Biol. 4 (2008) 160, http://dx.doi.org/10.1038/msb4100201.
[74] R.S. Negm, T.G. Pistole, Macrophages recognize and adhere to an OmpD-like protein of *Salmonella* Typhimurium, FEMS Immunol, Med. Microbiol. 20 (1998) 191–199.
[75] H. Nikaido, Molecular basis of bacterial outer membrane permeability revisited, Microbiol. Mol. Biol. Rev. 67 (2003) 593–656.
[76] B. Hara-Kaonga, T.G. Pistole, OmpD but not OmpC is involved in adherence of *Salmonella enterica* serovar Typhimurium to human cells, Can. J. Microbiol. 50 (2004) 719–727, http://dx.doi.org/10.1139/w04-056.
[77] S.G.J. Smith, V. Mahon, M.A. Lambert, R.P. Fagan, A molecular swiss army knife: OmpA structure, function and expression, FEMS Microbiol. Lett. 272 (2007) 1–11, http://dx.doi.org/10.1111/j.1574-6968.2007.00778.x.
[78] S.B. Berger, X. Romero, C. Ma, G. Wang, W.A. Faubion, G. Liao, et al., SLAM is a microbial sensor that regulates bacterial phagosome functions in macrophages, Nat. Immunol. 11 (2010) 920–927, http://dx.doi.org/10.1038/ni.1931.
[79] J.S. Lee, I.D. Jung, C.-M. Lee, J.W. Park, S.H. Chun, S.K. Jeong, et al., Outer membrane protein a of *Salmonella enterica* serovar Typhimurium activates dendritic cells and enhances Th1 polarization, BMC Microbiol. 10 (2010) 263, http://dx.doi.org/10.1186/1471-2180-10-263.
[80] L.P. Randall, M.J. Woodward, The multiple antibiotic resistance (*mar*) locus and its significance, Res. Vet. Sci. 72 (2002) 87–93, http://dx.doi.org/10.1053/rvsc.2001.0537.
[81] T. Ferenci, Maintaining a healthy SPANC balance through regulatory and mutational adaptation, Mol. Microbiol. 57 (2005) 1–8, http://dx.doi.org/10.1111/j.1365-2958.2005.04649.x.
[82] M. Castillo-Keller, P. Vuong, R. Misra, Novel mechanism of *Escherichia coli* porin regulation, J. Bacteriol. 188 (2006) 576–586, http://dx.doi.org/10.1128/JB.188.2.576-586.2006.
[83] S.-Y. Qi, Y. Li, A. Szyroki, I.G. Giles, A. Moir, C.D. O'Connor, *Salmonella* Typhimurium responses to a bactericidal protein from human neutrophils, Mol. Microbiol. 17 (1995) 523–531, http://dx.doi.org/10.1111/j.1365-2958.1995.mmi_17030523.x.
[84] A. Van Parys, F. Boyen, B. Leyman, E. Verbrugghe, F. Haesebrouck, F. Pasmans, Tissue-specific *Salmonella* Typhimurium gene expression during persistence in pigs, PLoS One 6 (2011) e24120, http://dx.doi.org/10.1371/journal.pone.0024120.
[85] Y. Nakada, Y. Jiang, T. Nishijyo, Y. Itoh, C.D. Lu, Molecular characterization and regulation of the *aguBA* operon, responsible for agmatine utilization in *Pseudomonas aeruginosa* PAO1, J. Bacteriol. 183 (2001) 6517–6524, http://dx.doi.org/10.1128/JB.183.22.6517-6524.2001.
[86] J. Kieboom, T. Abee, Arginine-dependent acid resistance in *Salmonella enterica* serovar Typhimurium, J. Bacteriol. 188 (2006) 5650–5653, http://dx.doi.org/10.1128/JB.00323-06.
[87] R. Van Houdt, A. Aertsen, P. Moons, K. Vanoirbeek, C.W. Michiels, *N*-acyl-L-homoserine lactone signal interception by *Escherichia coli*, FEMS Microbiol. Lett. 256 (2006) 83–89, http://dx.doi.org/10.1111/j.1574-6968.2006.00103.x.
[88] C. Lévi-Meyrueis, V. Monteil, O. Sismeiro, M.A. Dillies, M. Monot, B. Jagla, et al., Expanding the RpoS/σ^S-network by RNA sequencing and identification of σ^S-controlled small RNAs in *Salmonella*, PLoS One 9 (2014) e96918, http://dx.doi.org/10.1371/journal.pone.0096918.
[89] L. Jelsbak, L.E. Thomsen, I. Wallrodt, P.R. Jensen, J.E. Olsen, Polyamines are required for virulence in *Salmonella enterica* serovar Typhimurium, PLoS One 7 (2012) 1–10, http://dx.doi.org/10.1371/journal.pone.0036149.
[90] C. Schroll, J.P. Christensen, H. Christensen, S.E. Pors, L. Thorndahl, P.R. Jensen, et al., Polyamines are essential for virulence in *Salmonella enterica* serovar Gallinarum despite evolutionary decay of polyamine biosynthesis genes, Vet. Microbiol. 170 (2014) 144–150, http://dx.doi.org/10.1016/j.vetmic.2014.01.034.
[91] L.L. Nesse, K. Berg, L.K. Vestby, Effects of norspermidine and spermidine on biofilm formation by potentially pathogenic *Escherichia coli* and *Salmonella enterica* wild-type strains, Appl. Environ. Microbiol. 81 (2015) 2226–2232, http://dx.doi.org/10.1128/AEM.03518-14.
[92] I.C. Espinel, P.R. Guerra, L. Jelsbak, Multiple roles of putrescine and spermidine in stress resistance and virulence of *Salmonella enterica* serovar Typhimurium, Microb. Pathog. 95 (2016) 117–123, http://dx.doi.org/10.1016/j.micpath.2016.03.008.
[93] S.D. Lawhon, R. Maurer, M. Suyemoto, C. Altier, Intestinal short-chain fatty acids alter *Salmonella* Typhimurium invasion gene expression and virulence through BarA/SirA, Mol. Microbiol. 46 (2002) 1451–1464, http://dx.doi.org/10.1046/j.1365-2958.2002.03268.x.
[94] Y. Huang, M. Suyemoto, C.D. Garner, K.M. Cicconi, C. Altier, Formate acts as a diffusible signal to induce *Salmonella* invasion, J. Bacteriol. 190 (2008) 4233–4241, http://dx.doi.org/10.1128/JB.00205-08.
[95] H.C. Barker, N. Kinsella, A. Jaspe, T. Friedrich, C.D. O'Connor, Formate protects stationary-phase *Escherichia coli* and *Salmonella* cells from killing by a cationic antimicrobial peptide, Mol. Microbiol. 35 (2000) 1518–1529, http://dx.doi.org/10.1046/j.1365-2958.2000.01820.x.
[96] M. McClelland, K.E. Sanderson, J. Spieth, S.W. Clifton, P. Latreille, L. Courtney, et al., Complete genome sequence of *Salmonella enterica* serovar Typhimurium LT2, Nature 413 (2001) 852–856, http://dx.doi.org/10.1038/35101614.

CAPÍTULO 3

Levels of thiol and proteins related to the oxidation-reduction process are altered by quorum sensing in *Salmonella*

Article formatted according to PLoS Pathogens

Full title: Levels of thiol and proteins related to the oxidation-reduction process are altered by quorum sensing in *Salmonella*

Short title: Quorum sensing and oxidation-reduction process in *Salmonella*

Felipe Alves de Almeida[ab], Deisy Guimarães Carneiro[a], Tiago Antônio de Oliveira Mendes[c], Edvaldo Barros[d], Uelinton Manoel Pinto[e], Leandro Licursi de Oliveira[f], Maria Cristina Dantas Vanetti[a]*

[a]Department of Microbiology, Universidade Federal de Viçosa, Viçosa - MG, Brazil;

[b]Department of Nutrition, Universidade Federal de Juiz de Fora, Governador Valadares - MG, Brazil;

[c]Department of Biochemistry and Molecular Biology, Universidade Federal de Viçosa, Viçosa - MG, Brazil;

[d]Núcleo de Análise de Biomoléculas, Universidade Federal de Viçosa, Viçosa - MG, Brazil;

[e]Food Research Center, Department of Food and Experimental Nutrition, Faculty of Pharmaceutical Sciences, Universidade de São Paulo, São Paulo – SP, Brazil;

[f]Department of General Biology, Universidade Federal de Viçosa, Viçosa - MG, Brazil.

*Corresponding author: Department of Microbiology, Universidade Federal de Viçosa, Viçosa - MG 36570-900, Brazil.

Telephone: + 55 31 3899-2954

E-mail address: mvanetti@ufv.br

Author contributions

Conceived and designed the experiments: FAdA, DGC, LLdO and MCDV. Performed the experiments: FAdA and DGC. Analyzed the data: FAdA, TAdOM and EB. Contributed reagents/materials/analysis tools: LLdO and MCDV. Wrote the paper: FAdA, TAdOM, UMP and MCDV.

Abstract

Quorum sensing is a communication mechanism among cells that leads to differential gene expression in response to changes in population density. *Salmonella* is unable to synthesize the autoinducer-1 (AI-1), *N*-acyl homoserine lactone (AHL), but is able to recognize AHLs produced by other microorganisms through SdiA protein. Our study aimed to evaluate the fatty acid and protein profiles of *Salmonella enterica* serovar Enteritidis PT4 578 throughout time of cultivation in the presence and absence of AHL. The presence of *N*-dodecanoyl-homoserine lactone (C12-HSL) altered the fatty acid and protein profiles of *Salmonella* cultivated during 4, 6, 7, 12 and 36 h in anaerobic condition. The profiles of *Salmonella* Enteritidis at logarithmic phase of growth (4 h of cultivation), in the presence of C12-HSL, were similar to those of cells at late stationary phase (36 h). In addition, these cells have less variation along growth, indicating that quorum sensing anticipates a stationary phase response. The presence of C12-HSL increased the abundance of thiol proteins such as Tpx, Q7CR42, Q8ZP25, YfgD, AhpC, NfsB, YdhD and TrxA, as well as the levels of free cellular thiol after 6 h of cultivation, possibly preparing the cells for an oxidative stress response. The LuxS protein of the AI-2 quorum sensing mechanism was differentially abundant and may indicate a cross response between the communication mechanisms mediated by AI-1 and AI-2 in *Salmonella*, depending on the growth phase. The NfsB protein had its abundance increased in the presence of C12-HSL in all the evaluated times, indicating that the cells

may be susceptible to the action of nitrofurans or that AHLs present a certain toxicity or mutagenicity activity to the cell.

Keywords: acyl homoserine lactone; cyclopropane; oxidation-reduction; sulfhydryl; thiol protein.

Author summary

Salmonella is an enteric pathogen that infects both humans and animals. Gastrointestinal diseases of infectious origin caused by the ingestion of food contaminated by this pathogen constitute a major public health problem. Quorum sensing is a mechanism of communication between cells that leads to differential expression of genes in response to changes in population density, mainly genes encoding virulence factors. This communication is often mediated by molecules called *N*-acyl homoserine lactone (AHL). *Salmonella* is unable to synthesize AHLs but able to recognize those produced by other bacteria. Our study aimed to evaluate the fatty acids and protein profiles of *Salmonella enterica* serovar Enteritidis PT4 578 throughout time of cultivation in the presence and absence of AHL. AHL altered the fatty acids and proteins of *Salmonella*, mimicking conditions of the stationary phase. Thus, the presence of AHLs seems to anticipate a stress response to the stationary phase. In addition, increased the abundance of thiol proteins and the levels of free cellular thiol possibly preparing the cells for an oxidative stress was also related to the presence of the AHL.

1. Introduction

Quorum sensing is a mechanism of inter-cellular communication that leads to differential expression of genes in response to changes in population density [1, 2]. In the Proteobacteria phylum, a pair of proteins called LuxI (acyl homoserine lactone

synthase) and LuxR (transcriptional activator) or homologous proteins are responsible for this mechanism. LuxI synthesizes *N*-acyl homoserine lactones (AHLs) that are also called autoinducer-1 (AI-1). In contrast, many Proteobacteria belonging to the Enterobacteriaceae family, such as *Salmonella* and *Escherichia coli*, do not synthesize AHL because they lack LuxI homologues [3-5]. However, a homologue of LuxR, known as SdiA, is present and allows the detection of AHLs synthesized by other microorganisms such as *Aeromonas hydrophila* and *Yersinia enterocolitica*, leading to gene regulation [6, 7].

According to Atkinson and Williams [8], the absence of AHL synthase in *Salmonella* and *E. coli* may be related to ecological aspects, since it will avoid the transfer of information to other microorganisms present in the medium and there will be no energy expenditure with the synthesis of these signalling molecules. However, these bacteria are favored by the environmental information provided by others in the medium. Thus, what are the real advantages and alterations that quorum sensing mediated by AI-1 causes in *Salmonella*? According to Di Cagno et al. [9], the global analyses of the proteome and transcriptome should help to elucidate the influences of quorum sensing on the cellular physiology.

Most of studies have found that the *pefI*, *srgD*, *srgA*, *srgB*, *rck* e *srgC* genes of the operon *rck* (resistant to complement killing) and the *rck* operon present in plasmids and related to the virulence of *Salmonella enterica* serovar Typhimurium are regulated by AHL [3, 5, 10]. Campos-Galvão et al. [11] also showed that the *hilA*, *invA* and *invF* genes of the Pathogenicity Islands 1 (SPI-1) of *Salmonella enterica* serovar Enteritidis PT4, and *glgC*, *fliF*, *lpfA* and *fimF* genes involved in biofilm formation were most expressed in the presence of *N*-dodecanoyl homoserine lactone (C12-AHL).

Almeida et al. [12] performed global analysis on the influence of AHL on the abundance of proteins and the levels of extracellular organic acids of *Salmonella*

Enteritidis. These authors showed that the abundance of the PheT, HtpG, PtsI, TalB, PmgI, Eno, PykF and Adi proteins increased and the abundance of the OmpA, OmpC, OmpD, GapA, Tsf, RpsB, RplE and RplB proteins decreased at 7 h of cultivation in the presence of AI-1, in addition to having changes in consumption of formate. According to the authors, these observed changes are correlated with those described in the literature as entry into the stationary phase of growth. In other bacteria, this effect was confirmed through global analysis during growth, as in the case of the transcriptome analysis of *Pseudomonas aeruginosa* [13] and *Burkholderia thailandensis* [14], as well as the metabolite analysis of *Burkholderia glumae*, *Burkholderia pseudomallei* and *B. thailandensis* [15].

Knowledge of the changes in overall *Salmonella* physiology due to the presence of AHLs during growth is still virtually unknown. Thus, this work aimed to evaluate physiological aspects of *Salmonella* such as the overall protein profile as well as the fatty acid composition of the cells during growth of the organism in the presence and in the absence of AHL. This is the first work that carefully examines the effect of AHL throughout growth in anaerobic conditions and the first to show that levels of thiol and proteins related to the oxidation-reduction stress response are altered by quorum sensing in *Salmonella*.

2. Results and Discussion

2.1. HSL alters the fatty acid profile of *Salmonella* throughout time

The fatty acid profile of *Salmonella* cells cultivated in the absence and presence of C12-HSL was evaluated by gas chromatograph equipped with flame ionization detector. The results showed that C12-HSL altered the fatty acid composition of *Salmonella* cultivated during 4, 6, 7, 12 and 36 h in anaerobic TSB, with major changes mainly at 4 h of cultivation (Table 1).

Table 1. Fatty acid profile of *Salmonella* Enteritidis PT4 578 anaerobically cultivated in TSB at 37 °C in the presence or absence of C12-HSL.

Classification	Fatty acids	Time (h)									
		4		6		7		12		36	
		Control	C12-HSL	Control	C12-HSL	Control	C12-HSL	Control	C12-HSL	Control	C12-HSL
Saturated	12:00	4.80^{A}	4.72^{A}	4.69^{AB}	4.61^{AB}	4.46^{C}	4.65^{AB}	4.31^{C}	4.38^{B}	4.50^{BC}	4.50^{AB}
	14:00	6.68^{E}	6.85^{E}	9.21^{D}	9.21^{D}	9.82^{C}	10.21^{C}	11.04^{B}	11.46^{B}	11.84^{A}	12.10^{A}
	16:00	35.17^{D}	34.76^{C}	36.28^{aC}	35.66^{bBC}	36.71^{B}	36.68^{AB}	37.72^{A}	37.63^{A}	38.09^{A}	37.87^{A}
	18:00	0.58	0.74	0.50	0.48	0.53^{a}	0.47^{b}	0.47	0.46	0.47	0.47
	19:00	$\mathbf{0.49^{A}}$	**0.50**	$\mathbf{0.52^{A}}$	**0.49**	$\mathbf{0.44^{AB}}$	**0.48**	$\mathbf{0.34^{B}}$	**0.41**	$\mathbf{0.46^{AB}}$	**0.48**
Cyclopropane	**17:0 cyclo ω7c**	$\mathbf{15.52^{aB}}$	$\mathbf{14.43^{bB}}$	$\mathbf{16.64^{AB}}$	$\mathbf{17.18^{A}}$	$\mathbf{16.87^{A}}$	$\mathbf{16.86^{A}}$	$\mathbf{17.40^{A}}$	$\mathbf{16.89^{A}}$	$\mathbf{16.38^{AB}}$	$\mathbf{16.22^{A}}$
	19:0 cyclo ω8c	$\mathbf{11.21^{aC}}$	$\mathbf{9.42^{bB}}$	$\mathbf{15.18^{B}}$	$\mathbf{15.45^{A}}$	$\mathbf{16.74^{A}}$	$\mathbf{15.88^{A}}$	$\mathbf{16.87^{A}}$	$\mathbf{16.34^{A}}$	$\mathbf{14.47^{B}}$	$\mathbf{14.54^{A}}$
Monounsaturated	**16:1 ω6c/16:1 ω7c**	$\mathbf{2.87^{bA}}$	$\mathbf{3.56^{aA}}$	$\mathbf{0.80^{B}}$	$\mathbf{0.82^{B}}$	$\mathbf{0.75^{B}}$	$\mathbf{0.70^{B}}$	$\mathbf{0.53^{B}}$	$\mathbf{0.57^{B}}$	$\mathbf{0.77^{B}}$	$\mathbf{0.70^{B}}$
	17:1 ω7c	$\mathbf{0.00^{C}}$	$\mathbf{0.00^{B}}$	$\mathbf{0.31^{aA}}$	$\mathbf{0.26^{bA}}$	$\mathbf{0.24^{B}}$	$\mathbf{0.30^{A}}$	$\mathbf{0.23^{B}}$	$\mathbf{0.27^{A}}$	$\mathbf{0.28^{AB}}$	$\mathbf{0.30^{A}}$
	18:1 ω6c/18:1 ω7c	$\mathbf{12.28^{bA}}$	$\mathbf{14.93^{aA}}$	$\mathbf{3.10^{B}}$	$\mathbf{3.31^{B}}$	$\mathbf{2.21^{C}}$	$\mathbf{2.30^{C}}$	$\mathbf{1.39^{D}}$	$\mathbf{1.47^{D}}$	$\mathbf{1.27^{D}}$	$\mathbf{1.23^{D}}$
	18:1 ω7c 11-methyl	$\mathbf{0.76^{AB}}$	**0.71**	$\mathbf{0.93^{A}}$	**0.83**	$\mathbf{0.76^{AB}}$	**0.84**	$\mathbf{0.57^{B}}$	**0.69**	$\mathbf{0.83^{A}}$	**0.86**
Polyunsaturated	20:2 ω6,9c	0.58	0.50	0.84	0.71	0.58	0.69	0.75	0.57	0.69	0.67
Hydroxy	**18:1 2OH**	$\mathbf{0.00^{C}}$	$\mathbf{0.00^{B}}$	$\mathbf{0.35^{A}}$	$\mathbf{0.31^{A}}$	$\mathbf{0.24^{AB}}$	$\mathbf{0.27^{A}}$	$\mathbf{0.20^{B}}$	$\mathbf{0.24^{A}}$	$\mathbf{0.29^{AB}}$	$\mathbf{0.30^{A}}$
Unresolved	14:0 3OH/16:1 iso I	8.05^{BC}	7.97^{BC}	9.51^{A}	9.67^{A}	8.74^{AB}	8.68^{B}	7.41^{bC}	7.70^{aC}	8.58^{B}	8.66^{BC}
	18:0 anteiso/18:2 ω6,9c	$\mathbf{1.01^{A}}$	**0.91**	$\mathbf{0.89^{AB}}$	**0.78**	$\mathbf{0.70^{B}}$	**0.77**	$\mathbf{0.60^{B}}$	**0.71**	$\mathbf{0.86^{AB}}$	**0.85**
	19:1 ω6c/19:1 ω7c/19:0 cyclo	$\mathbf{0.00^{C}}$	$\mathbf{0.00^{B}}$	$\mathbf{0.26^{A}}$	$\mathbf{0.22^{A}}$	$\mathbf{0.21^{AB}}$	$\mathbf{0.23^{A}}$	$\mathbf{0.18^{B}}$	$\mathbf{0.21^{A}}$	$\mathbf{0.21^{AB}}$	$\mathbf{0.24^{A}}$

The comparisons can be drawn between treatments or throughout time. Average followed by different lower case letters in the same line (between treatments at the same time) and followed by different capital letters in the columns (throughout time for each treatment, separately) differs at 5% probability ($p < 0.05$) by Tukey's test. Where a letter is not shown, no statistical difference between samples was observed;

Main results discussed in the text are shown in bold.

The concentration of the fatty acids 19:00 and 18:1 ω7c 11-methyl, as well as, an unresolved mixture of the 18:0 anteiso/18:2 ω6,9c did not change throughout the time in the presence of C12-HSL, while such differences were observed in the control samples (Table 1). Also, after 6 h of cultivation, there was no difference in the concentration of the fatty acids 17:0 cyclo ω7c, 19:0 cyclo ω8c, 17:1 ω7c and 18:1 2OH, as well as, an unresolved mixture of the 19:1 ω6c/19:1 ω7c/19:0 cyclo in the treatment with C12-HSL (Table 1). Interestingly, the maintenance of the cyclopropane fatty acids 17:0 cyclo ω7c and 19:0 cyclo ω8c could indicate that the cells are prepared for a possible stress condition. It is noteworthy that the cyclopropane fatty acids 17:0 cyclo and 19:0 cyclo are formed by transmethylation of *cis* monounsaturated fatty acids 16:1 ω7c and 18:1 ω7c, respectively, when the cell enters in stationary phase [16]. This modification helps in reducing the impact of environment stresses such as starvation, heavy metal addition, organic compound toxicity and increased temperature on membrane fluidity [17-21]. An example of the effect of fatty acids modification on bacterial cell membrane related to stress condition was presented by Guckert et al. [19] who observed an increase in the proportions of cyclopropane fatty acids during nutrient deprivation stress in *Vibrio cholerae.*

The Principal Component Analysis (PCA) allowed to evaluate the quality of the triplicates and to understand the global difference of levels and types of fatty acids among samples stimulated by C12-HSL and the controls (Fig 1). The variation between the replicates was lower than the variation between times, indicating that saponification, methylation, extraction and analysis of fatty acids by gas chromatography were adequate (Fig 1).

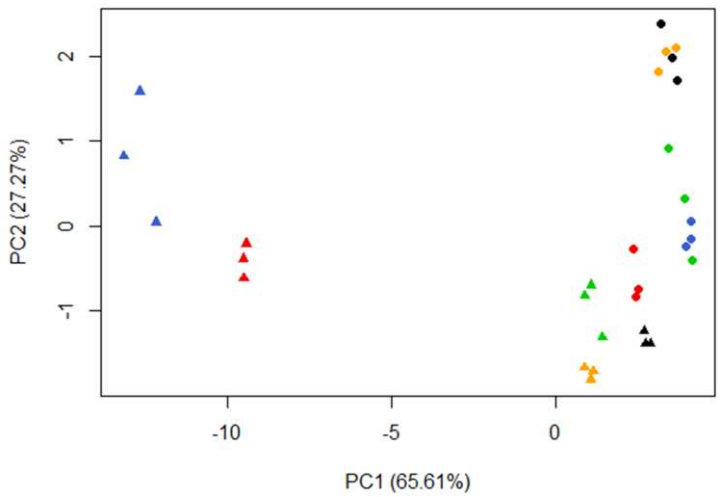

Fig 1. PCA analysis of fatty acids from *Salmonella* Enteritidis PT4 578 anaerobically cultivated in TSB at 37 °C in the presence or absence of C12-HSL. PCA of the percentages of the triplicates of fatty acid profile of *Salmonella* with control (filled triangle) and C12-HSL (filled circle) treatment. The colors represent the times 4 h (red), 6 h (blue), 7 h (green), 12 h (orange) and 36 h (black) for each triplicate individually.

The PCA analysis also showed that there was a high dispersion between of the global profile of fatty acids identified in *Salmonella* for the control and treatment with C12-HSL, in all times under analysis. However, the dispersion tended to reduce over time of growth as can be observed on Fig 1. On the other hand, the fatty acids identified in *Salmonella* in the presence of C12-HSL tended to be less dispersed throughout the growth than in the absence of the quorum sensing molecule (Fig 1). Thus, the cells in the logarithmic (4 h) and stationary (36 h) phases of growth had the fatty acid profile more similar in the presence of AI-1, indicating that they might be more prepared for possible stress early on during growth in the presence of the signaling molecule, but even more so during the stationary phase. This behavior suggests that quorum sensing in *Salmonella* induces an early profile of fatty acids which is typical of stationary phase of growth, even in situations where the cell density is low. According to Schuster et al. [22], this early preparation of the cells has a high cost of fitness, but leads to more resistance should a stress condition arrive.

Another observation that can be extracted from the data is that the fatty acid composition of *Salmonella* cells growing in the presence of C12-HSL for 4 h is quite

similar to cells cultured in the absence of this autoinducer after 7 h of cultivation (Fig 1). At this time of cultivation (7 h), these cells are already in the stationary phase of growth and prepared to support stressful conditions (results not shown).

2.2. HSL alters the protein profile of *Salmonella* throughout the time

The protein profile of *Salmonella* cells cultivated either in the absence or in the presence of C12-HSL was evaluated by UPLC coupled with a Q-Tof (UPLC-Q-Tof or LC-MS). Similarly to what has been observed in fatty acids composition analysis, the presence of C12-HSL altered the protein profile of *Salmonella* during growth in TSB under anaerobic conditions (Fig 2).

The PCA of the proteomic data showed that the variation among replicates was much lower than the variation among times, indicating that the extraction, quantification, trypsin digestion and analysis by UPLC-Q-Tof of the proteins were suitable for a proper comparison (Fig 2A). The PCA analysis showed a similar dispersion of the profile to that one observed with the fatty acid analysis, which indicates a higher dispersion of the proteins in the control group compared to the treatment with C12-HSL in all the evaluated times (Fig 2A). The identified proteins of *Salmonella* in the presence of C12-HSL tended to be less dispersed throughout growth than in the absence of the quorum sensing molecule (Fig 2A). Moreover, a heatmap prepared by using the logarithm of average normalized of total ion current (TIC) values of the triplicates of each protein showed, in a global way, changes in the relative levels of each protein of *Salmonella* over time of growth forming two major clades (Fig 2B). The figure shows that the protein profile of *Salmonella* cultivated in the absence of C12-HSL for 4 h presented more variations and, this observation was confirmed by the dendrogram which resulted from cluster analysis by agglomerative hierarchical methods (Fig 2C).

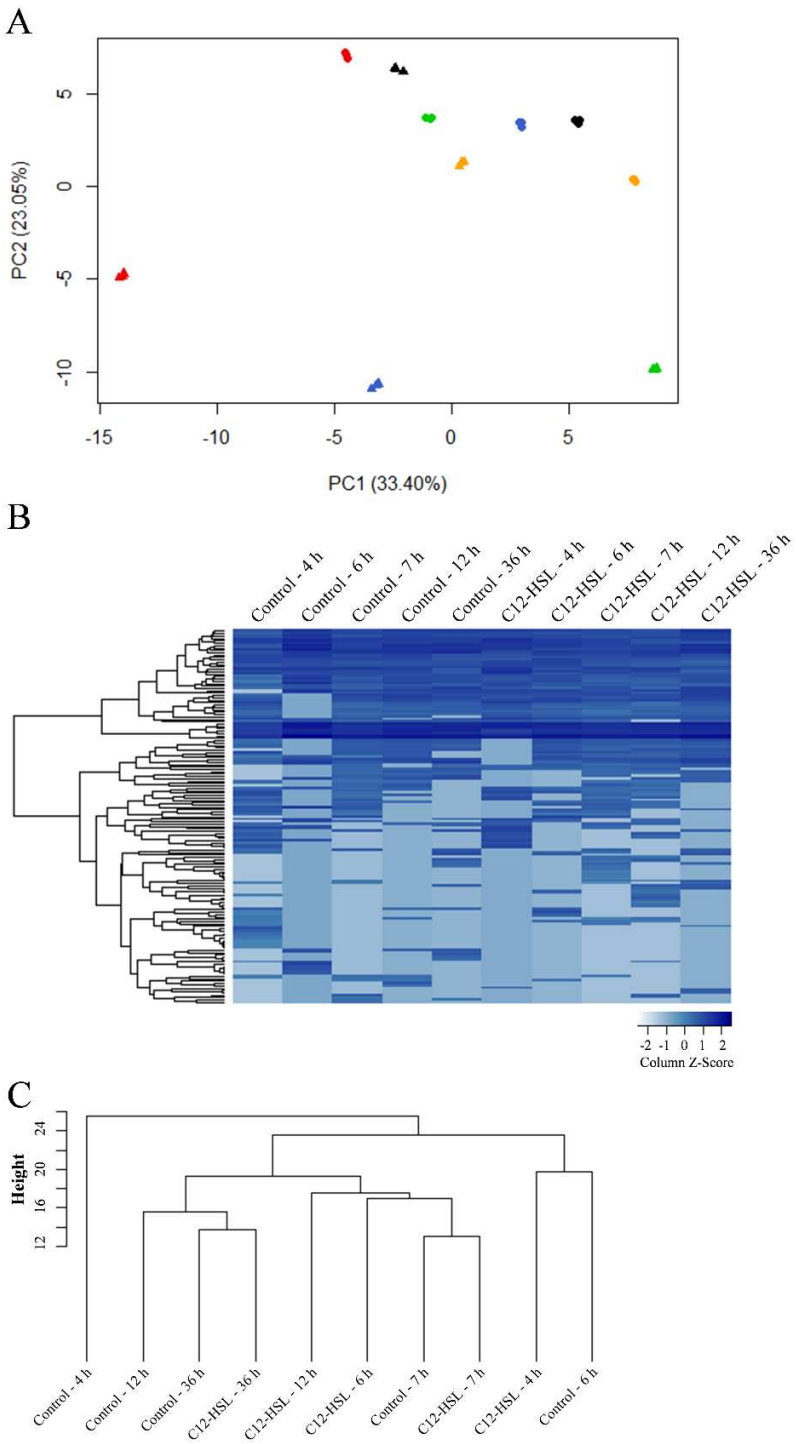

Fig 2. PCA, heatmap and dendrogram analyses of proteis from *Salmonella* Enteritidis PT4 578 anaerobically cultivated in TSB at 37 °C in the presence or absence of C12-HSL. (A) PCA of the logarithm of normalized TIC values of the triplicates of protein profile with control (filled triangle) and C12-HSL (filled circle) treatment. The colors represent the times 4 h (red), 6 h (blue), 7 h (green), 12 h (orange) and 36 h (black) for each triplicate individually. **(B)** Heatmap of the logarithm of average normalized TIC values of the triplicates for each protein identified. Each row corresponds to a unique protein, and each column the average of the triplicate values. The color scale ranges from low abundance (light blue) to high abundance (dark blue). **(C)** Dendrogram of the logarithm of average normalized TIC values of the triplicates for each protein identified. The height of the arms is proportional to the difference in the abundance profile of the proteins.

Interestingly, the PCA, the heatmap and the dendrogram analyses together showed that the addition of C12-HSL at the beginning of *Salmonella* growth resulted in smaller protein profile variations over time of growth when compared with the control. These results indicate that the AI-1 regulates proteins which usually have their abundance influenced by the growth phase in this pathogen. Thus, the fatty acid and the protein profiles presented the same behavior indicating that AI-1 molecule anticipates a stationary phase response. These results corroborate with our previous observation under identical conditions, in which the differentially abundant proteins and organic acids of *Salmonella* cultivated for 7 h in the presence of C12-HSL correlated with what has been described in the literature as entry into the stationary phase of growth, mainly in relation to nitrogen and amino acid starvation as well as acid stress [12]. Schuster et al. [13] showed that genes with expression influenced by the growth phase in *Pseudomonas aeruginosa* were repressed by quorum sensing during the late logarithmic and stationary phases. Goo et al. [15] showed that quorum sensing anticipates and influences the survival to the stress of the stationary phase of *B. glumae*, *B. pseudomallei* and *B. thailandensis*. In addition, the genes involved in transcription and translation of *B. pseudomallei* in stationary phase were co-regulated by RpoS protein (RNA polymerase sigma factor) and quorum sensing [23].

The statistical analyses of the identified proteins of *Salmonella* cultivated in the absence and presence of C12-HSL for 4, 6, 7, 12 and 36 h in anaerobic TSB are shown in Table 2 and S1 Table (Supporting information).

Table 2. Statistical analysis of proteins identified from *Salmonella* Enteritidis PT4 578 anaerobically cultivated in TSB at 37 °C in the presence or absence of C12-HSL.

Protein	Protein name	Gene	Process	Time (h)									
				4		6		7		12		36	
				Log_2 FC	$-Log_{10}$ *p*	Log_2 FC	$-Log_{10}$ *p*	Log_2 FC	$-Log_{10}$ *p*	Log_2 FC	$-Log_{10}$ *p*	Log_2 FC	$-Log_{10}$ *p*
ATP synthase subunit delta	Q7CPE5	*atpH*	Biosynthetic	-11.566	1.060	8.687	3.470	1.157	2.760	ND	ND	ND	ND
Acetyl-CoA carboxylase, BCCP subunit	Q7CPM1	*accB*	Biosynthetic	2.049	0.841	ND	ND	-10.547	1.542	ND	ND	-1.505	1.241
Acyl carrier protein	P0A6B1	*acpP*	Biosynthetic	1.930	1.139	-0.409	0.737	-0.439	0.714	-0.277	1.882	-0.452	1.297
ATP synthase subunit beta	Q7CPE2	*atpD*	Biosynthetic	ND	ND	ND	ND	-7.974	1.357	ND	ND	ND	ND
Cell division protein FtsZ	Q8ZRU0	*ftsZ*	Cell division	ND	ND	ND	ND	-7.378	1.542	8.561	1.296	ND	ND
Cell division protein ZapB	Q8ZKP1	*zapB*	Cell division	-9.554	2.451	10.650	2.037	-0.305	0.317	-0.300	0.554	0.912	1.133
Protein phosphatase CheZ	P07800	*cheZ*	Chemotaxis	-8.243	4.181	2.733	0.940	3.359	0.506	0.029	0.023	9.365	1.026
Aspartate ammonia-lyase	Q7CPA1	*aspA*	Metabolic process	ND	ND	ND	ND	6.377	1.508	ND	ND	ND	ND
Arginine decarboxylase	Q8ZKE3	*adi*	Metabolic process	ND	ND	ND	ND	ND	ND	ND	ND	-8.168	1.714
Shikimate kinase 1	P63601	*aroK*	Metabolic process	-10.245	2.324	7.418	1.665	0.677	0.288	1.517	1.882	ND	ND
2-iminobutanoate/2-iminopropanoate deaminase	Q7CP78	*ridA*	Metabolic process	2.789	1.273	-3.083	3.151	-0.235	0.865	-2.437	0.866	-0.781	1.249
Autonomous glycyl radical cofactor	Q7CQ05	*grcA*	Metabolic process	0.816	1.306	0.940	2.063	0.511	1.542	0.072	0.162	-0.513	1.714
Pyruvate formate lyase I, induced anaerobically	Q7CQU1	*pflB*	Metabolic process	ND	ND	11.573	0.825	-0.159	1.542	ND	ND	ND	ND
Lactoylglutathione lyase	P0A1Q2	*gloA*	Metabolic process	-6.833	0.914	ND	ND	ND	ND	ND	ND	ND	ND
Enolase	P64076	*eno*	Metabolic process	-1.074	1.640	-0.551	0.328	-0.417	0.506	1.104	0.668	0.180	0.140
Glyceraldehyde-3-phosphate dehydrogenase	P0A1P0	*gapA*	Metabolic process	ND	ND	ND	ND	ND	ND	9.405	1.107	ND	ND
Phosphoglycerate kinase	P65702	*pgk*	Metabolic process	-0.310	0.812	0.108	0.113	0.746	1.988	-0.487	1.719	0.562	1.987
Triosephosphate isomerase	Q8ZKP7	*tpiA*	Metabolic process	-11.938	2.806	-11.340	2.011	-0.216	0.169	8.235	0.996	ND	ND
Adenylate kinase	P0A1V4	*adk*	Metabolic process	0.221	0.329	1.820	1.810	0.091	0.215	-0.451	1.037	-1.271	1.260
Deoxyribose-phosphate aldolase	Q8ZJV8	*deoC*	Metabolic process	-7.031	0.839	ND	ND	-0.630	0.925	ND	ND	7.796	0.767
Pyrimidine/purine nucleoside phosphorylase	Q8ZRE7	*ppnP*	Metabolic process	ND	ND	ND	ND	ND	ND	8.356	1.530	ND	ND
Acetate kinase	P63411	*ackA*	Metabolic process	-8.530	2.435	9.037	2.391	0.800	0.511	8.469	1.882	ND	ND
Ribose-5-phosphate isomerase A	P66692	*rpiA*	Metabolic process	-8.886	3.352	ND	ND	0.426	0.481	ND	ND	-0.871	1.020
6,7-dimethyl-8-ribityllumazine synthase	P66038	*ribH*	Metabolic process	-10.296	2.100	8.466	2.208	-0.989	0.842	-0.515	1.415	9.901	1.243
Flagellar hook protein FlgE	P0A1J1	*flgE*	Motility	ND	ND	ND	ND	-8.339	1.048	ND	ND	-6.615	1.054
Flagellar hook-associated protein 3	P16326	*flgL*	Motility	-6.794	1.152	ND	ND	ND	ND	ND	ND	ND	ND
Flagella synthesis protein FlgN	P0A1J7	*flgN*	Motility	-9.157	1.970	ND	ND	-0.528	0.735	-0.138	0.125	8.395	4.679
Flagellar hook-associated protein 2	B5R7H2	*fliD*	Motility	ND	ND	ND	ND	7.292	2.329	ND	ND	ND	ND
Flagellin	B5R7H3	*fljB*	Motility	0.012	0.034	-0.297	1.298	0.179	1.542	-0.076	0.940	0.316	1.016

Table 2. Continuation.

Protein	Protein name	Gene	Process	Time (h)									
				4		6		7		12		36	
				Log_2 FC	$-Log_{10}$ *p*	Log_2 FC	$-Log_{10}$ *p*	Log_2 FC	$-Log_{10}$ *p*	Log_2 FC	$-Log_{10}$ *p*	Log_2 FC	$-Log_{10}$ *p*
[2FE-2S] ferredoxin	Q7CQ13	*fdx*	Oxidation-reduction	-0.511	0.404	ND	ND	10.435	2.995	1.162	1.696	-8.019	1.577
Flavodoxin 1	Q8ZQX1	*fldA*	Oxidation-reduction	ND	ND	ND	ND	ND	ND	9.103	1.504	9.307	1.054
Glutaredoxin 1	P0A1P8	*grxA*	Oxidation-reduction	ND	ND	10.883	0.737	ND	ND	ND	ND	-0.839	0.547
Glutaredoxin 3	Q7CPH7	*grxC*	Oxidation-reduction	ND	ND	ND	ND	ND	ND	ND	ND	8.107	1.078
Hydrogenase-3, iron-sulfur subunit	Q7CPY1	*hycB*	Oxidation-reduction	-7.993	1.393	ND	ND	ND	ND	ND	ND	ND	ND
Protease involved in processing C-terminal end of HycE	Q8ZMJ3	*hycI*	Oxidation-reduction	ND	ND	ND	ND	0.469	0.605	-1.598	1.076	0.655	0.668
Glutaredoxin	Q7CQK9	*ydhD*	Oxidation-reduction	-1.224	0.976	9.653	1.513	-0.180	1.357	1.196	1.179	-0.311	1.054
Alkyl hydroperoxide reductase subunit C	P0A251	*ahpC*	Oxidation-reduction	-0.080	0.233	0.592	1.393	-0.625	1.154	0.305	0.488	-0.400	0.430
Thioredoxin dependent thiol peroxidase	Q7CQ23	*bcp*	Oxidation-reduction	ND	ND	ND	ND	ND	ND	ND	ND	8.506	1.054
Thiol:disulfide interchange protein DsbC	P55890	*dsbC*	Oxidation-reduction	ND	ND	-8.491	0.940	ND	ND	ND	ND	ND	ND
Oxygen-insensitive NAD(P)H nitroreductase	P15888	*nfsB*	Oxidation-reduction	8.325	4.181	9.274	1.111	0.590	1.542	9.311	1.719	1.708	2.151
Superoxide dismutase [Fe]	P0A2F4	*sodB*	Oxidation-reduction	ND	ND	ND	ND	1.417	1.979	-1.254	0.738	ND	ND
Superoxide dismutase [Cu-Zn] 1	P0CW86	*sodC1*	Oxidation-reduction	11.567	2.324	0.060	0.082	-0.093	0.098	0.866	1.107	0.151	0.747
Putative thiol-alkyl hydroperoxide reductase	Q7CR42	STM0402	Oxidation-reduction	-0.931	3.817	1.287	1.810	-0.538	1.542	-0.294	0.689	-0.746	0.767
Putative thiol-disulfide isomerase and thioredoxin	Q8ZP25	STM1790	Oxidation-reduction	-9.429	1.436	10.287	2.011	0.629	2.192	1.026	1.719	-0.532	1.000
Probable thiol peroxidase	Q8ZP65	*tpx*	Oxidation-reduction	-9.378	1.761	1.394	1.606	0.131	0.434	0.191	0.911	0.295	0.968
Thioredoxin 1	P0AA28	*trxA*	Oxidation-reduction	0.284	0.274	-0.518	0.812	0.792	1.542	-1.247	1.525	-0.567	1.836
Arsenate reductase	Q8ZN68	*yfgD*	Oxidation-reduction	-9.881	1.761	9.480	1.565	-0.553	1.154	-0.854	1.152	-0.491	0.668
Fimbrial protein	P12061	*sefA*	Pathogenesis	1.178	3.123	-0.109	0.677	-0.236	3.658	-0.321	1.359	-0.228	0.747
Non-specific acid phosphatase	P26976	*phoN*	Pathogenesis	ND	ND	-9.715	2.323	ND	ND	ND	ND	ND	ND
Major outer membrane lipoprotein 1	Q7CQN4	*lpp1*	Pathogenesis	ND	ND	-8.366	1.046	ND	ND	ND	ND	ND	ND
Ecotin	Q8ZNH4	*eco*	Pathogenesis	1.515	1.561	10.403	1.629	0.246	3.740	-0.399	0.571	1.421	3.339
Peptidyl-prolyl cis-trans isomerase	Q8ZLL6	*fkpA*	Protein folding	1.695	2.381	0.213	1.810	-0.265	1.501	0.945	1.415	-0.773	1.304
Peptidyl-prolyl cis-trans isomerase	Q8XFG8	*ppiB*	Protein folding	-8.726	2.358	7.501	1.665	ND	ND	ND	ND	ND	ND
Peptidyl-prolyl cis-trans isomerase	Q8ZLL4	*slyD*	Protein folding	0.401	1.152	1.340	1.072	0.691	1.542	0.560	0.883	-0.362	0.404
Trigger factor	P66932	*tig*	Protein folding	-1.402	1.238	0.665	0.451	0.708	1.105	-0.426	1.485	-0.730	1.971
Chaperone protein DnaK	Q56073	*dnaK*	Protein folding	-2.246	1.390	0.407	0.928	-0.040	0.142	0.166	0.289	-0.627	0.809
60 kDa chaperonin	P0A1D3	*groL*	Protein folding	0.758	0.661	-0.350	0.139	2.690	4.349	-1.241	0.765	-0.108	0.067
10 kDa chaperonin	P0A1D5	*groS*	Protein folding	0.969	1.188	0.433	0.865	0.037	0.178	0.076	0.585	0.182	1.840
Protein GrpE	Q7CPZ4	*grpE*	Protein folding	-9.471	1.122	7.826	0.799	8.528	0.842	ND	ND	-1.209	1.972
Small heat shock protein IbpA	Q7CPF1	*ibpA*	Protein folding	ND	ND	ND	ND	ND	ND	ND	ND	-7.675	1.054
Chaperone protein Skp	P0A1Z2	*skp*	Protein folding	ND	ND	ND	ND	-10.241	1.299	9.656	0.990	ND	ND
Chaperone SurA	Q7CR87	*surA*	Protein folding	-7.111	2.324	ND	ND	ND	ND	ND	ND	ND	ND

Table 2. Continuation.

Protein	Protein name	Gene	Process	Time (h)									
				4		6		7		12		36	
				Log_2 FC	$-Log_{10}$ *p*	Log_2 FC	$-Log_{10}$ *p*	Log_2 FC	$-Log_{10}$ *p*	Log_2 FC	$-Log_{10}$ *p*	Log_2 FC	$-Log_{10}$ *p*
Iron-sulfur cluster insertion protein ErpA	Q7CR66	*erpA*	Protein maturation	ND	ND	-7.504	1.598	ND	ND	ND	ND	ND	ND
Fe/S biogenesis protein NfuA	Q8ZLI7	*nfuA*	Protein maturation	2.317	1.761	0.908	0.593	-0.996	1.048	-1.033	1.106	-0.700	0.767
Iron-sulfur cluster assembly scaffold protein IscU	Q7CQ11	*nifU*	Protein maturation	9.913	1.176	-1.624	1.512	-8.446	1.151	9.074	1.271	ND	ND
S-ribosylhomocysteine lyase	Q9L4T0	*luxS*	Quorum sensing	-0.240	0.614	11.588	1.665	0.421	0.914	0.761	1.076	0.039	0.097
Single-stranded DNA-binding protein 1	P0A2F6	*ssb*	Response to stress	-7.772	1.761	ND	ND	8.250	1.368	ND	ND	ND	ND
UPF0234 protein YajQ	Q8ZRC9	*yajQ*	Response to stress	-7.420	2.808	8.948	0.625	ND	ND	ND	ND	ND	ND
Universal stress protein G	P67093	*uspG*	Response to stress	ND	ND	9.407	2.079	0.013	0.039	1.175	1.107	0.198	1.026
Putative outer membrane protein	Q7CPS4	*ygiW*	Response to stress	ND	ND	6.498	1.320	-7.298	2.011	-6.702	1.296	ND	ND
Putative molecular chaperone (Small heat shock	Q8ZPY6	STM1251	Response to stress	ND	ND	ND	ND	ND	ND	9.601	1.882	0.157	0.078
RNA polymerase-binding transcription factor DksA	P0A1G5	*dksA*	Transcription	ND	ND	ND	ND	7.810	2.307	8.954	0.727	-7.468	2.038
Cold shock-like protein CspC	P0A9Y9	*cspC*	Transcription	11.820	1.185	0.813	0.987	2.846	2.329	-1.023	0.571	-0.194	0.767
RNA chaperone, negative regulator of cspA	Q7CQZ5	*cspE*	Transcription	ND	ND	-8.997	1.858	ND	ND	ND	ND	-8.747	1.840
Transcriptional repressor of emrAB operon	Q7CPY9	*emrR*	Transcription	-7.967	1.060	7.639	2.079	7.947	1.745	7.095	1.485	ND	ND
Transcriptional repressor of iron-responsive genes (Fur family) (Ferric uptake regulator)	Q7CQY3	*fur*	Transcription	0.175	0.574	8.426	1.998	-0.134	0.248	0.544	1.076	0.459	0.253
Transcription elongation factor GreA	P64281	*greA*	Transcription	-1.164	1.352	10.895	1.810	-0.544	0.776	-0.501	1.754	0.006	0.011
DNA-binding protein H-NS	P0A1S2	*hns*	Transcription	-3.346	2.381	-1.089	0.898	0.174	0.248	0.042	0.022	-0.278	0.809
DNA-binding protein HU-alpha	P0A1R6	*hupA*	Transcription	1.714	2.363	0.140	0.593	0.646	1.729	0.940	0.990	-0.633	1.826
Virulence transcriptional regulatory protein PhoP	P0DM78	*phoP*	Transcription	-10.751	1.390	8.923	1.046	0.758	2.854	0.030	0.019	0.955	5.924
Regulator of nucleoside diphosphate kinase	Q7CQZ7	*rnk*	Transcription	-7.467	2.747	ND	ND	-0.012	0.019	-6.467	1.037	ND	ND
DNA-directed RNA polymerase subunit alpha	P0A7Z7	*rpoA*	Transcription	-0.255	2.435	2.402	1.998	-0.135	0.851	-1.706	0.561	-1.425	1.297
DNA-directed RNA polymerase subunit omega	P0A803	*rpoZ*	Transcription	-1.482	1.796	8.487	1.998	-1.524	2.995	0.738	0.554	-0.963	2.151
DNA-binding protein	B5RBI8	SG2019	Transcription	-7.989	2.381	ND	ND	6.415	2.307	0.535	0.328	ND	ND
Transcriptional regulator SlyA	P40676	*slyA*	Transcription	ND	ND	ND	ND	-0.341	0.142	-8.648	1.327	-2.417	1.026
DNA-binding protein StpA	P0A1S4	*stpA*	Transcription	0.152	0.125	ND	ND	ND	ND	8.362	3.372	ND	ND
Nucleoid-associated protein YbaB	P0A8B8	*ybaB*	Transcription	0.454	0.416	0.312	0.255	-0.286	0.349	-9.610	1.037	-0.817	1.249
Transcription modulator YdgT	Q7CQK5	*ydgT*	Transcription	-9.106	2.324	ND	ND	ND	ND	ND	ND	ND	ND
Inorganic pyrophosphatase	P65748	*ppa*	Transcription	-10.551	1.376	-2.442	0.737	0.540	0.598	0.730	0.480	-0.911	2.335
Modulator of Rho-dependent transcription termination	Q8ZRN4	*rof*	Transcription	ND	ND	ND	ND	0.720	1.072	-0.815	0.616	-0.751	0.981
Regulator of ribonuclease activity A	P67651	*rraA*	Transcription	ND	ND	ND	ND	7.518	2.329	ND	ND	ND	ND
Stringent starvation protein B	Q7CPN4	*sspB*	Transcription	ND	ND	ND	ND	7.192	2.063	ND	ND	ND	ND

Table 2. Continuation.

Protein	Protein name	Gene	Process	Time (h)									
				4		6		7		12		36	
				Log_2 FC	$-Log_{10}$ *p*	Log_2 FC	$-Log_{10}$ *p*	Log_2 FC	$-Log_{10}$ *p*	Log_2 FC	$-Log_{10}$ *p*	Log_2 FC	$-Log_{10}$ *p*
Peptide deformylase	Q8ZLM7	*def*	Translation	-8.092	2.806	ND	ND	-8.530	1.503	-8.086	1.719	ND	ND
Ribosome recycling factor	P66738	*rrf or frr*	Translation	-2.277	3.208	0.989	1.558	0.444	0.506	1.071	1.330	0.602	1.026
Stationary-phase-induced ribosome-associated protein	Q7CQJ0	*sra*	Translation	ND	ND	-9.400	2.414	-9.252	1.151	0.305	0.238	-2.258	1.840
Ribosome associated factor	Q7CQ00	*yfiA*	Translation	ND	ND	-7.943	2.079	ND	ND	-8.664	2.295	-9.657	1.387
Translation initiation factor IF-1	P69226	*infA*	Translation	ND	ND	ND	ND	8.689	0.617	7.127	1.719	ND	ND
Translation initiation factor IF-3	P33321	*infC*	Translation	-10.818	1.790	8.352	1.512	ND	ND	-7.574	1.754	-7.938	2.417
50S ribosomal protein L1	P0A2A3	*rplA*	Translation	-0.903	1.148	-8.794	2.134	9.181	1.039	ND	ND	ND	ND
50S ribosomal protein L3	P60446	*rplC*	Translation	9.334	2.324	ND	ND	ND	ND	ND	ND	ND	ND
50S ribosomal protein L6	P66313	*rplF*	Translation	0.593	1.957	-0.186	0.328	ND	ND	7.572	0.841	-9.383	1.241
50S ribosomal protein L9	Q8ZK80	*rplI*	Translation	0.306	2.454	-0.381	1.665	0.147	0.183	-0.995	1.359	-0.361	1.026
50S ribosomal protein L10	P0A297	*rplJ*	Translation	-0.425	0.870	9.051	2.011	0.557	0.637	1.216	1.396	9.329	1.220
50S ribosomal protein L11	P0A7K0	*rplK*	Translation	0.564	1.152	-9.100	1.288	9.783	0.846	ND	ND	-8.354	1.971
50S ribosomal protein L7/L12	P0A299	*rplL*	Translation	1.043	1.148	0.832	1.665	0.408	0.615	-1.167	0.990	0.692	0.668
50S ribosomal protein L15	P66073	*rplO*	Translation	-10.938	4.151	ND	ND	ND	ND	ND	ND	ND	ND
50S ribosomal protein L17	Q7CPL7	*rplQ*	Translation	-0.782	1.990	3.526	4.757	0.467	0.466	9.427	0.677	-0.123	0.055
50S ribosomal protein L18	Q7CPL6	*rplR*	Translation	1.375	2.324	ND	ND	-0.275	0.235	9.705	1.182	ND	ND
50S ribosomal protein L19	P0A2A1	*rplS*	Translation	-0.533	0.420	ND	ND	ND	ND	10.169	0.909	ND	ND
50S ribosomal protein L24	P60626	*rplX*	Translation	-0.441	0.873	11.243	3.470	1.216	0.773	-0.730	1.107	0.442	0.305
50S ribosomal protein L25	Q7CQ71	*rplY*	Translation	-0.776	1.230	7.944	1.598	0.984	1.542	0.793	0.382	-0.605	0.707
50S ribosomal protein L28	P0A2A5	*rpmB*	Translation	-1.746	2.358	9.704	1.095	0.537	0.297	8.210	1.025	ND	ND
50S ribosomal protein L29	P66170	*rpmC*	Translation	-1.525	1.640	8.702	1.677	1.191	0.481	-0.900	2.043	0.539	0.280
50S ribosomal protein L30	P0A2A7	*rpmD*	Translation	ND	ND	ND	ND	ND	ND	ND	ND	-9.619	2.532
50S ribosomal protein L31	P66191	*rpmE*	Translation	ND	ND	ND	ND	ND	ND	10.159	1.074	ND	ND
50S ribosomal protein L33	P0A7P2	*rpmG*	Translation	ND	ND	8.313	2.037	ND	ND	7.849	1.076	ND	ND
50S ribosomal protein L34	P0A7P8	*rpmH*	Translation	-7.903	2.324	ND	ND	ND	ND	9.446	1.053	ND	ND
30S ribosomal protein S1	Q7CQT9	*rpsA*	Translation	-3.033	4.181	ND	ND	1.901	1.525	-1.215	0.505	ND	ND
30S ribosomal protein S2	P66541	*rpsB*	Translation	-7.096	1.761	ND	ND	ND	ND	ND	ND	ND	ND
30S ribosomal protein S4	O54297	*rpsD*	Translation	-0.643	0.937	ND	ND	ND	ND	8.864	0.990	ND	ND
30S ribosomal protein S5	P0A7W4	*rpsE*	Translation	-1.050	0.941	-8.356	1.776	ND	ND	ND	ND	ND	ND
30S ribosomal protein S6	P66593	*rpsF*	Translation	-9.552	1.680	6.762	1.521	0.510	0.344	ND	ND	ND	ND
30S ribosomal protein S7	P0A2B3	*rpsG*	Translation	-0.345	1.761	ND	ND	-0.539	0.666	ND	ND	ND	ND
30S ribosomal protein S8	P0A7X0	*rpsH*	Translation	-1.382	2.297	2.600	2.902	0.735	1.542	0.112	0.285	-2.163	2.532
30S ribosomal protein S10	P67904	*rpsJ*	Translation	0.303	0.245	-0.520	0.495	0.125	0.142	-1.227	0.585	ND	ND

Table 2. Continuation.

Protein	Protein name	Gene	Process	Time (h)									
				4		6		7		12		36	
				Log_2 FC	$-Log_{10}$ *p*	Log_2 FC	$-Log_{10}$ *p*	Log_2 FC	$-Log_{10}$ *p*	Log_2 FC	$-Log_{10}$ *p*	Log_2 FC	$-Log_{10}$ *p*
30S ribosomal protein S11	O54296	*rpsK*	Translation	1.423	1.139	ND	ND	ND	ND	ND	ND	ND	ND
30S ribosomal protein S13	Q8ZLM1	*rpsM*	Translation	0.283	0.242	ND	ND	ND	ND	ND	ND	ND	ND
30S ribosomal protein S14	P66409	*rpsN*	Translation	-0.353	0.568	7.881	1.810	-0.451	2.036	2.427	0.990	ND	ND
30S ribosomal protein S18	Q8ZK81	*rpsR*	Translation	-12.161	2.208	ND	ND	ND	ND	ND	ND	ND	ND
30S ribosomal protein S19	P66491	*rpsS*	Translation	0.149	0.404	ND	ND	ND	ND	ND	ND	ND	ND
30S ribosomal protein S20	P0A2B1	*rpsT*	Translation	1.295	4.181	1.915	1.348	0.834	1.072	1.105	0.776	-1.148	1.054
Elongation factor P	P64036	*efp*	Translation	-9.275	1.432	ND	ND	ND	ND	ND	ND	ND	ND
Elongation factor Ts	P64052	*tsf*	Translation	-0.212	0.451	1.346	1.596	0.609	1.154	-0.872	1.754	-2.134	2.151
Elongation factor Tu	P0A1H5	*tufA*	Translation	-3.968	1.957	2.390	2.077	-0.543	0.598	-0.425	0.147	-0.140	0.096
Histidine-binding periplasmic protein	P02910	*hisJ*	Transport	-9.017	1.957	-1.073	0.737	-0.934	0.522	9.351	1.331	0.646	0.920
PTS system glucose-specific EIIA component	P0A283	*crr*	Transport	-0.304	0.841	-2.267	3.151	-1.073	1.822	-0.399	1.485	0.063	0.257
Multiphosphoryl transfer protein	P17127	*fruB*	Transport	ND	ND	-7.368	1.542	ND	ND	ND	ND	ND	ND
Phosphocarrier protein HPr	P0AA07	*ptsH*	Transport	8.437	1.230	7.848	3.151	0.504	0.481	1.948	0.711	-9.520	0.737
Glutamine high-affinity transporter	Q7CQW0	*glnH*	Transport	ND	ND	ND	ND	ND	ND	-7.105	1.102	ND	ND
Ferritin	Q8ZNU4	*ftn*	Transport	-10.668	2.044	9.884	2.902	1.148	0.945	ND	ND	10.071	1.054
Protein-export protein SecB	Q7CPH8	*secB*	Transport	-7.460	1.409	10.905	1.252	ND	ND	ND	ND	ND	ND
Outer membrane protein A	P02936	*ompA*	Transport	1.039	2.044	0.063	0.113	-0.312	0.482	0.140	0.207	0.693	1.987
Outer membrane channel	Q8ZLZ4	*tolC*	Transport	ND	ND	ND	ND	10.139	0.594	ND	ND	-0.744	0.767
BssS protein family	A0A1V9AFN8	ABA47_0691	Unclassified	-8.706	2.381	ND	ND	0.807	0.663	0.364	0.253	ND	ND
Uncharacterized protein	A0A1F2JWR0	HMPREF 3126_08675	Unclassified	ND	ND	ND	ND	ND	ND	-9.642	1.719	ND	ND
Uncharacterized protein	A0A1R2IBX3	R567_04560	Unclassified	ND	ND	ND	ND	8.671	0.842	ND	ND	-7.007	0.967
Uncharacterized protein	B5RBG9	SG1997	Unclassified	-7.908	1.098	-9.302	1.665	ND	ND	7.916	0.779	ND	ND
Putative periplasmic protein	Q8ZPY8	STM1249	Unclassified	ND	ND	ND	ND	1.332	1.094	7.565	1.882	9.917	1.431
UPF0253 protein YaeP	P67551	*yaeP*	Unclassified	ND	ND	ND	ND	8.765	1.985	ND	ND	ND	ND
Putative cytoplasmic protein	Q8ZQ41	*yccJ*	Unclassified	ND	ND	ND	ND	9.189	0.663	9.850	1.719	-9.249	2.067
Uncharacterized protein	Q7CQR0	*ycfF*	Unclassified	ND	ND	ND	ND	ND	ND	7.127	1.107	ND	ND
Putative cytoplasmic protein	Q7CQJ6	*ydfZ*	Unclassified	-1.164	1.244	0.884	2.134	0.262	2.329	-0.047	0.221	-0.048	0.063
Putative cytoplasmic protein	Q7CQB7	*yecF*	Unclassified	-9.069	0.706	ND	ND	ND	ND	ND	ND	6.772	1.342
UPF0265 protein YeeX	P67605	*yeeX*	Unclassified	-12.867	2.813	10.455	1.629	1.293	0.890	-0.540	0.696	8.884	1.714
Putative cytoplasmic protein	Q7CQ33	*yfcZ*	Unclassified	1.467	1.409	-0.175	0.344	0.415	1.314	-0.656	1.562	0.010	0.029

Table 2. Continuation.

Protein	Protein name	Gene	Process	Time (h)									
				4		6		7		12		36	
				Log_2 FC	$-Log_{10}$ *p*	Log_2 FC	$-Log_{10}$ *p*	Log_2 FC	$-Log_{10}$ *p*	Log_2 FC	$-Log_{10}$ *p*	Log_2 FC	$-Log_{10}$ *p*
Putative cytoplasmic protein	Q8ZKH3	*yjbR*	Unclassified	ND	ND	ND	ND	ND	ND	7.963	1.687	ND	ND
Uncharacterized protein	I3W485	-	Unclassified	ND	ND	8.155	1.028	ND	ND	8.028	0.859	ND	ND

ND = not detected;

Log_2 FC = logarithm in base two of fold changed (ratio of the average normalized TIC values of the treatment with C12-HSL by the control);

$-Log_{10}$ *p* = negative logarithm of *p*-value;

Gray background and black letter = increased abundance of protein in C12-HSL and detected in both treatments (Log_2 FC > 0.585 and $-Log_{10}$ > 1.301);

Gray background and red letter = increased abundance of protein in C12-HSL and detected only in the treatment with C12-HSL (Log_2 FC > 0.585);

Yellow background and black letter = decreased abundance of protein in C12-HSL and detected in both treatments (Log_2 FC < -0.585 and $-Log_{10}$ > 1.301);

Yellow background and red letter = decreased abundance of protein in C12-HSL and detected only in the control treatment (Log_2 FC < -0.585).

The results showed that at 4 and 6 h of incubation, a higher percentage of differentially expressed proteins was observed in comparison with other times (Table 3).

Table 3. Number and percentage of differentially abundant proteins in comparison to the total proteins identified from *Salmonella* Enteritidis PT4 578 anaerobically cultivated in TSB at 37 °C in the presence C12-HSL.

Time (h)	Proteins identified						
	Abundance increased		Abundance decreased		Differentially abundant		Total
	Number	%	Number	%	Number	%	Number
4	17	15.5	55	50.0	72	65.5	110
6	51	54.8	16	17.2	67	72.0	93
7	31	28.7	11	10.2	42	38.9	108
12	36	34.0	14	13.2	50	47.2	106
36	16	17.8	23	25.6	39	43.4	90

In addition, more proteins had their abundance decreased at 4 h in the presence of AHL (50.0%), while an opposite trend was observed at 6 h (54.8%). The greatest number of differentially abundant proteins at the initial times can be due to the addition of AI-1 at the beginning of the cultivation. In AHL-producing bacteria, such as *B. thailandensis* and *P. aeruginosa*, the genes were regulated at the end of the logarithmic and beginning of the stationary phase of growth due to the accumulation of signaling molecules in the medium [13, 14, 24]. Schuster et al. [13] showed that genes involved in carbohydrate utilization or nutrient transport were the most repressed by quorum sensing and during the late logarithmic and stationary phases of *P. aeruginosa.*

The differentially abundant proteins were grouped in order to perform an analysis of enrichment of biological processes based on Gene Ontology (GO) annotations, as shown on Fig 3. The proteins related to translation, transcription, oxidation-reduction, metabolic, unclassified, protein folding and transport processes had their abundance affected by C12-HSL in all the studied time points.

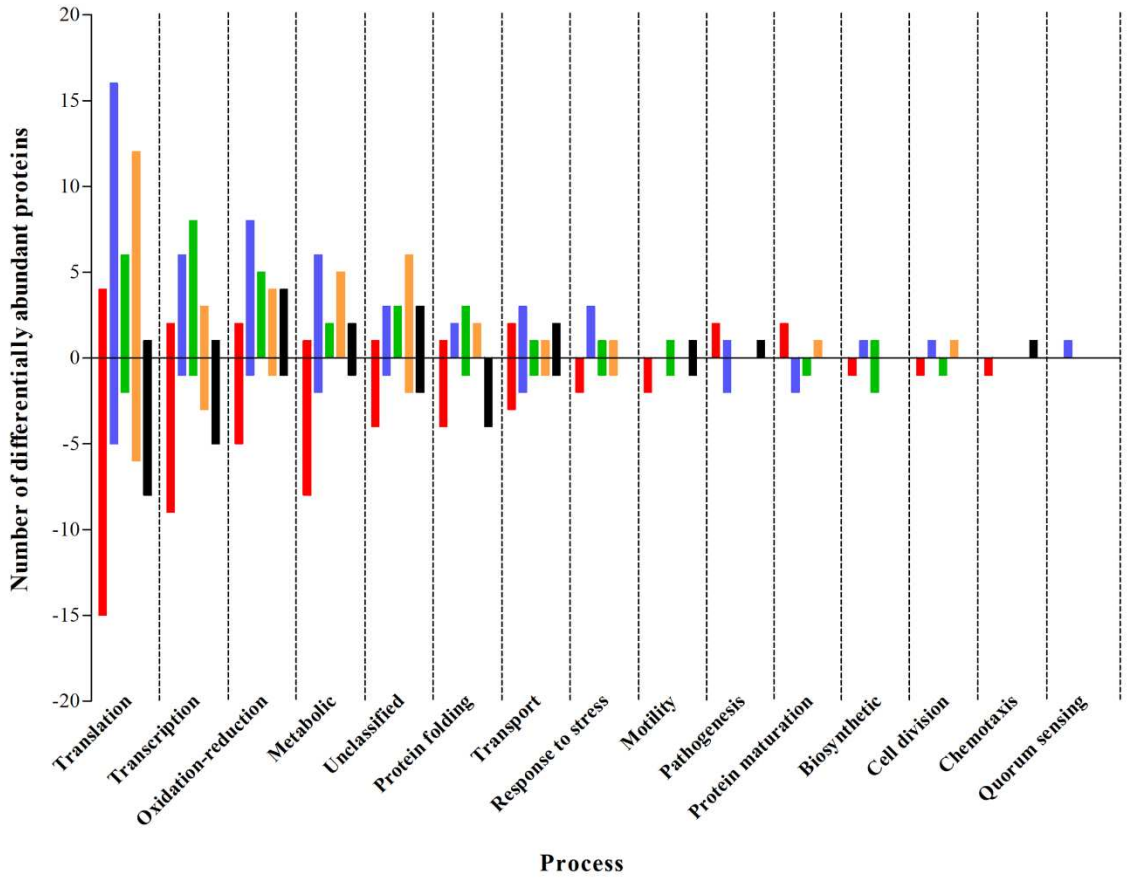

Fig 3. Number of differentially abundant proteins grouped according to the process on Gene Ontology (GO) annotations (European Bioinformatics Institute). The colors represent the times 4 h (red), 6 h (blue), 7 h (green), 12 h (orange) and 36 h (black). The Y-axis represents the number of differentially abundant proteins identified: above zero the number the proteins in which the abundance increased in the presence of C12-HSL compared to the control and below zero represents the proteins in which the abundance decreased in the presence of C12-HSL.

An important protein identified is the LuxS protein (S-ribosylhomocysteine lyase) which participates in the quorum sensing mechanism through production of autoinducer-2 (Table 2 and Fig 3). This protein was identified only in the presence of 50 nM of the C12-HSL at 6 h of cultivation, that is, at the end of the logarithmic phase of growth of *Salmonella*. This result indicates that there can be a cross response between quorum sensing mechanisms mediated by AI-1 and AI-2 in *Salmonella* depending of the growth phase. Interactions between the different mechanisms of quorum sensing present in *P. aeruginosa* have been described leading to a hierarchical activation of these mechanisms [25-27] and also to the synthesis of inductive and inhibitory molecules [28]. The existence of multiple arrangements between the different

mechanisms of quorum sensing might play important role in processing of environmental cues and thus, dictating desired and robust collective response [29].

Among the identified proteins, a greater number of proteins involved in transcription process showed a variation of their abundance in the presence of C12-HSL (Fig 3). Since transcription is an essential step in gene expression and the transcriptional regulation determines the molecular machinery for developmental plasticity, homeostasis and adaptation [30], a network of interaction between the proteins related to the transcription process and “regulation of transcription, DNA-templated” was generated (Fig 4A).

The PPI network showed an average local clustering coefficient of 0.636 and a *p*-value of <1.06e-10 for enrichment indicating that the proteins have more interactions among themselves than what would be expected for a random set of proteins of similar size. This result also indicates that these proteins are, at least, partially biologically connected as a group [31]. The RpoA (DNA-directed RNA polymerase subunit alpha) and Hns (DNA-binding protein H-NS) proteins were the central nodes of two networks that are connected through them (Fig 4A). The RpoA protein had its abundance increased at 6 h of cultivation of *Salmonella* Enteritidis in the presence of C12-HSL (Fig 4B). Soni et al. [32] showed that the abundance this protein decreased in late logarithmic phase of growth of *Salmonella* Typhimurium in the presence of AI-2. In addition, these proteins were identified in all the time points evaluated in this study (Fig 4B). Thus, the variations of the abundance of proteins with a "regulation of transcription, DNA-templated" function between the treatments and throughout the time of cultivation of *Salmonella* can be responsible for regulating the abundance of the other proteins that have been identified (Figs 3 and 4B).

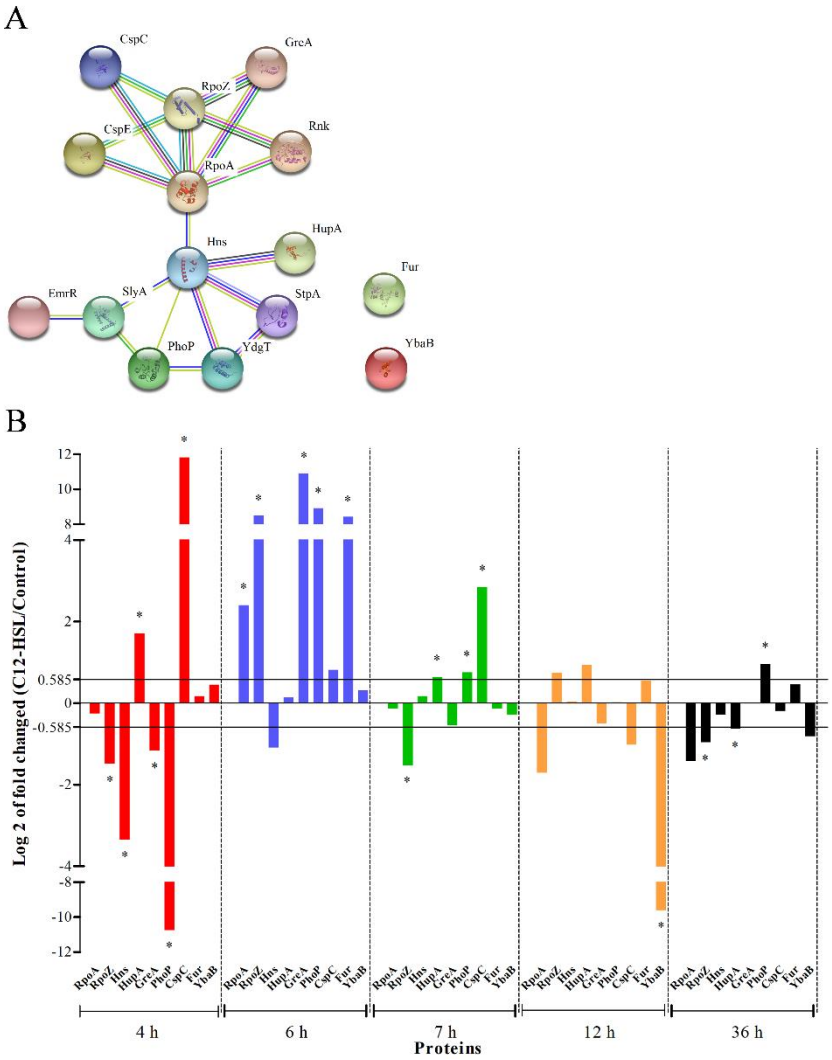

Fig 4. Proteins related to transcription process and "regulation of transcription, DNA-templated" function from *Salmonella* Enteritidis PT4 578, anaerobically cultivated in TSB at 37 °C in the presence or absence of C12-HSL. (A) The network of interactions among the proteins of the transcription process and "regulation of transcription, DNA-templated" function and **(B)** the logarithm in base two of fold changed of the proteins that were identified at all times and in at least one of the treatments. * averages significant difference ($p < 0.05$).

2.3. Levels of thiol and proteins related to the oxidation-reduction process are altered by HSL in *Salmonella*

The proteins of oxidation-reduction process had their abundance affected by the presence of C12-HSL in all times of cultivation (Fig 3). In fact, at 4 h of cultivation with in the signaling molecule, a greater number of proteins with decreased abundance was observed in comparison to the control treatment (Fig 3). Conversely, an inverse relationship was observed at 6 h of cultivation, indicating that cells cultivated in this

period in the presence of C12-HSL are more prepared to resist to an oxidative stress condition than cells cultivated in the absence of this molecule. The proteins related to the oxidative process can be considered crucial to maintenance of the cellular redox balance, as well as to anticipate resistance to a possible oxidative stress due to excessive production of reactive oxygen/nitrogen species (ROS/RNS) [33-35].

In other bacteria, quorum sensing has been associated to oxidative stress response. For instance, in *P. aeruginosa*, the expression of *katA* (catalase) and *sodA* (superoxide dismutase) genes and, concomitantly, the activities of the catalase and superoxide dismutase enzymes were up-regulated by quorum sensing [36]. In addition, Garcia-Contreras et al. [37] showed that resistance of *P. aeruginosa* to oxidative stress by the addition of hydrogen peroxide (H_2O_2) was enhanced by quorum sensing, increasing the production of catalase and NADPH dehydrogenases. In our study, the SodC1 (Superoxide dismutase [Cu-Zn] 1) also had its abundance increased at 4 h of incubation, while SodB (Superoxide dismutase [Fe]) protein had its abundance increased at 7 h when in the presence of C12-HSL (Table 2). The quorum sensing via BpsIR (a system homologous to LuxIR) and *N*-octanoyl-homoserine lactone (C8-HSL) also inscreased resistance to oxidative stress of *B. pseudomallei*, as well as the expression of the *dpsA* gene (DNA-binding protein from starved cells) [38]. The Dps is a non-specific DNA-binding protein involved in resistance to oxidative stress and it is an abundant protein in stationary phase of growth in *E. coli* [39, 40].

Afterwards, a network of interaction between the proteins of the oxidation-reduction process was generated (Fig 5A). The PPI network showed an average local clustering coefficient of 0.609 and a *p*-value of <1e-16 for enrichment. These results indicate that the proteins have more interactions among themselves than what would be expected for a random set of proteins of similar size and also that these proteins are at least partially biologically connected as a group [31].

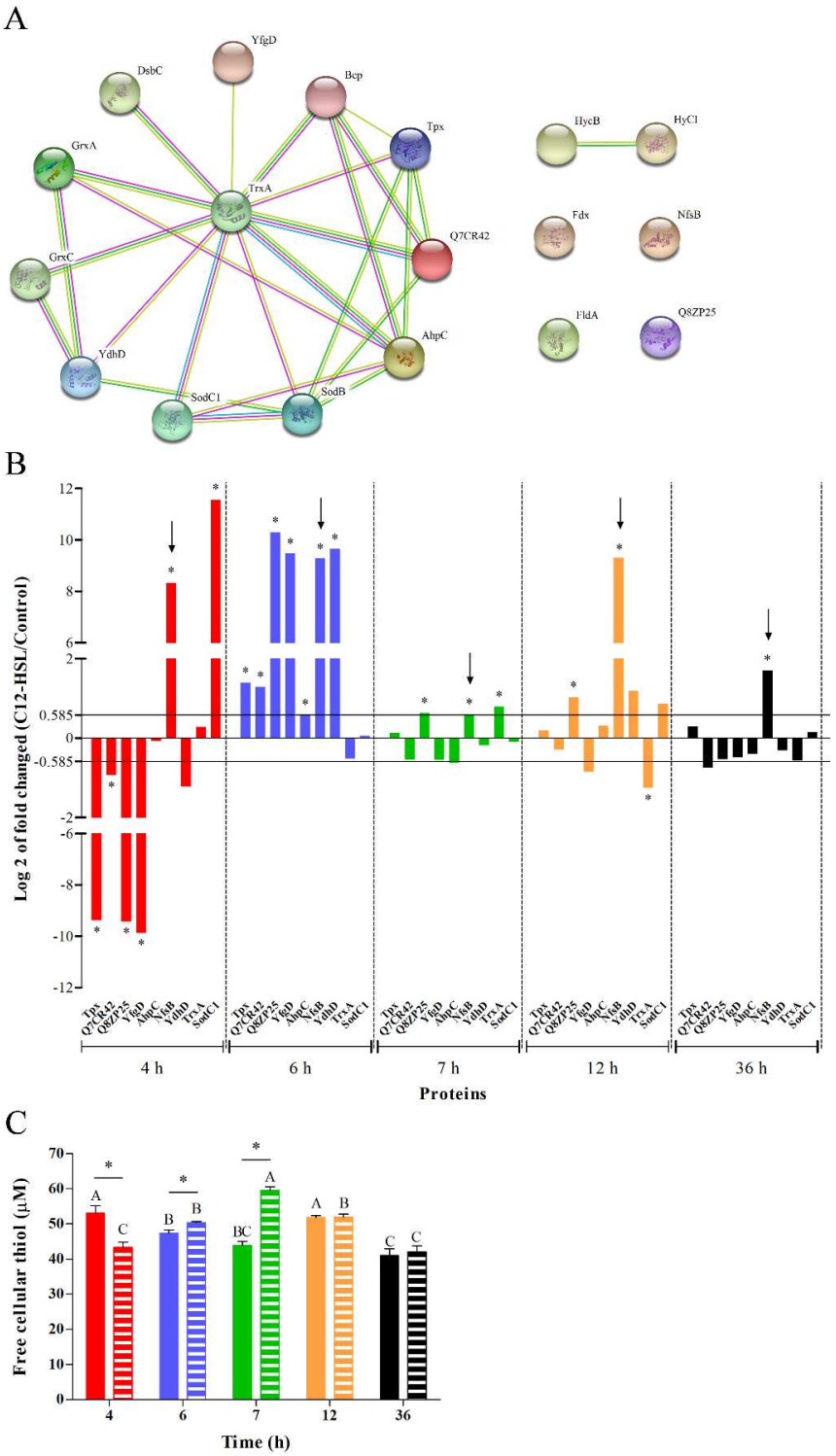

Fig 5. Identified proteins related to the oxidation-reduction process and quantification of free cellular thiol in *Salmonella* Enteritidis PT4 578 anaerobically cultivated in TSB at 37 °C in the presence or absence of C12-HSL. (A) The network of interactions among the proteins of oxidation-reduction process and **(B)** the logarithm in base two of fold changed of the proteins that were identified at all times and in at least one of the treatments, as well as **(C)** the quantification of free cellular thiol in absence (filled bars) and presence of C12-HSL (striped bars). * averages significant difference ($p < 0.05$); Black arrows show the NfsB protein; Averages of the levels of thiol followed by asterisk (between treatments at the same time) and followed by different capital letters (throughout time for each treatment, separately) differs at 5% probability ($p < 0.05$) by Tukey's test. Where an asterisk or letter is not shown, no statistical difference between samples was observed; Error bars indicate standard error.

Interestingly, the TrxA protein (Thioredoxin 1) stands out as being a central node of the main edge by interacting with most of the proteins used to generate the network (Fig 5A). This protein also had its increased abundance at 7 h of cultivation of *Salmonella* Enteritidis in the presence of 50 nM C12-HSL in anaerobic conditions, but its abundance was lower at 12 h (Fig 5B). The TrxA protein had its increased abundance in planktonic and biofilm cells of *Salmonella* Enteritidis exposed to benzalkonium chloride [41, 42]. This protein is known to be essential to activate the gene transcription of the pathogenicity island 2 (SPI-2) of *Salmonella* Typhimurium and consequently, for resistance during infection of mice [43-45]. In addition, the *srgA* gene (Thiol: disulfide interchange protein) is located in the *rck* operon (Resistance to complement killing) regulated by SdiA protein of *Salmonella* Typhimurium binding to AHLs [5]. The SgrA protein contains regions conserved among other oxidoreductases in the thioredoxin superfamily, such as TrxA [46].

Thioredoxin is an oxidoreductase that participates in redox reactions by oxidation of its thiol active-sites which are then reduced by NADPH. It also exerts control over the activity of target proteins via reversible thiol-disulfide exchange reactions by the thioredoxin and glutaredoxin systems [35, 47-50]. This protein also has a regulatory mechanism independent of thiol redox activity, which thioredoxin interacts with other proteins and forms a functional complex [48]. The thiol, also known as mercaptan or sulfhydryl, –SH side chain of cysteine is susceptible to reactions with ROS or RNS species, giving rise to a range of post-translational oxidative modifications by thiol proteins, including reversible (intra-protein disulfides, inter-protein disulfides, S-sulfenation, S-nitrosation, S-thiolation, S-sulfhydration, S-sulfenamidation) and non-reversible hyper-oxidized (S-sulfination, S-sulfonation) redox states. In addition, in some cases it can alter the structure and activity of proteins that contain cysteine residues [34, 35, 51].

From nine proteins used for the generation of the network (Fig 5A), eight are or have some relation with thiol proteins such as: Tpx (Probable thiol peroxidase), Q7CR42 (Putative thiol-alkyl hydroperoxide reductase), Q8ZP25 (Putative thiol-disulfide isomerase and thioredoxin), YfgD (Arsenate reductase), AhpC (Alkyl hydroperoxide reductase subunit C), NfsB (Oxygen-insensitive NAD(P)H nitroreductase), YdhD (Glutaredoxin) and TrxA (Thioredoxin 1) proteins. The thiol proteins: Tpx, Q7CR42, Q8ZP25 and YfgD had their abundance decreased at 4 h of cultivation of *Salmonella* Enteritidis in the presence of the 50 nM C12-HSL (Fig 5B). On the other hand, at 6 h of cultivation, the Tpx, Q7CR42, Q8ZP25, YfgD, AhpC, NfsB and YdhD proteins had their abundance increased, as well as Q8ZP25, NfsB and TrxA proteins at 7 h (Fig 5B). In addition, more thiol proteins had their abundances altered at 4, 6 and 7 h of culture, which refer to the logarithmic phase up to the early stationary phase of growth compared to the times of 12 and 36 h where the cells were in stationary phase for a long time (Fig 5B).

The quantification of free cellular thiol showed a correlation with the abundance of thiol proteins at each time and treatment (Figs 5B and 5C). At 4 h of cultivation, a lower level of thiol was observed in the treatment with the quorum sensing molecule as well as a lower abundance of the thiol proteins in comparison to the control treatment. Subsequently, at 6 and 7 h a reverse situation was observed and the highest level of thiol observed in cells cultivated in presence of C12-HSL at 7 h (59.53 μM) (Fig 5C). Then, at 12 and 36 h no differences in the levels of thiol were observed correlating with the number of differentially abundant thiol proteins which was greatly reduced. In addition, for the same treatment throughout the time of cultivation of *Salmonella*, the levels of thiol increased up to 7 h of cultivation in the presence of C12-HSL and decreased after this time (Fig 5C). On the other hand, in the absence of this AHL, the level of thiol varied throughout the time without a trend (Fig 5C). These results showed that quorum

sensing alters not only the abundance of thiol proteins but also the levels of thiol, indicating that resistance to possible oxidative stress can be mediated by thiol proteins and thiol depending on the period of growth in the presence of the signaling molecule. This is the first time that the relationship between thiol proteins and levels of free cellular thiol with quorum sensing is reported.

Variations in the abundance of thiol proteins and levels of free cellular thiol due to the growth phase of *Salmonella* and the presence of acyl homoserine lactone can be related to changes in the structure of the SdiA protein (LuxR homologue) which could alter its ability to bind DNA and, consequently, activate transcription. On the other hand, the thiol proteins and thiol could prevent structural alterations of the SdiA protein caused by ROS/RNS. This rationale is possible because the cysteine residues (C) and their respective positions (C45, C122, C142, and C232) present in the SdiA protein of *Salmonella* Enteritidis PT4 578 could be susceptible to oxidative stress [52]. The C232 is the main conserved residue among LuxR family proteins [53] and it is involved in the interaction between the Ligand-binding domain (LBD) with DNA-binding domain (DBD) and DBD-DBD [54].

Kafle et al. [55] evaluated all cysteine residues of the LasR protein (a LuxR homologue) of *P. aeruginosa* to infer their redox sensitivity and to probe the connection between stress response and the activity of that protein. The C79 residue is important for ligand recognition and folding of this domain which further potentiates DNA binding, but it does not seem to be sensitive to oxidative stress when bound to its native ligand. The C201 and C203 residues in the DBD form a disulfide bond when treated with hydrogen peroxide, and this bond appears to disrupt the DNA binding activity of the transcription factor. Mutagenesis of either of these cysteines leads to expression of a protein that no longer binds DNA. Thus, these authors provided a possible mechanism for oxidative stress response by the cysteine residues of the LasR protein in *P.*

aeruginosa and indicated that multiple cysteines within the protein can be useful targets for disabling its activity.

The presence of C12-HSL increased the abundance of thiol proteins, such as oxidoreductases, which can change the structure of this AHL and inactivate it. Some oxidoreductases synthesized by *Rhodococcus erythropolis* and *Bacillus megaterium*, as well as by eukaryotic cells, are able to inactivate AHLs by oxidation or reduction of its acyl side chain [56-59]. In fact, this is one of the known mechanisms of quorum quenching [56].

Finally, the NfsB protein (or NfnB or NfsI) was the only protein that had its abundance increased at all cultivation times in the presence of C12-HSL compared to the control treatment in *Salmonella* (Fig 5B). This result indicates that *Salmonella* cultivated in the presence of this quorum sensing molecule can be susceptible to the action of nitrofurans or C12-HSL has a certain toxicity or mutagenicity activity to the cell. The NfsB protein is a flavin mononucleotide-containing flavoprotein that can use either NADH or NADPH as a source of reducing power in order to reduce the nitro moiety of nitrofurans, yielding biologically inactive end products. This process occurs through a sequence of intermediates, including nitroso and hydroxylamine states, which are assumed to be responsible for toxicity [60, 61]. *E. coli* and *Salmonella* Typhimurium containing the *nfsA* and *nfsB* genes are more sensitive to nitrofurans, which are widely used as antimicrobial agents [62, 63]. Carroll et al. [64] also showed that the introduction of plasmids carrying the *nfsA* and *nfsB* genes into *Salmonella* Typhimurium increased sensibility to nitrofuran compounds with mutagenic potential.

Gomi et al. [65] showed that 10 μg/mL of C12-HSL derived from *Chromobacterium violaceum* induced the production of tumor necrosis factor-α (TNF-α) and interleukin-1β (IL-1β) by mouse RAW264.7 cells and IL-8 by human THP-1 cells, while C4, C6, C7, C8, C10 and C14-HSL did not induce. The C12-HSL and C12-

oxo-HSL also decreased the levels of putrescine of human epidermal cells (HaCat) and, consequently, decreased the rate of cell proliferation [66]. John et al. [67] showed that *N*-3-oxo-tetradecanoyl-homoserine lactone (3-oxo-C14-HSL) produced by *Acinetobacter baumannii* had a dose-dependent cytotoxic effect on human cervical cancer cells (HeLa), adenocarcinoma human alveolar basal epithelial cells (A549), Dukes' type C colorectal adenocarcinoma cells (HCT15) and Dukes' type B colorectal adenocarcinoma cells (SW480), with induction of apoptosis and reduced viability and proliferation of these cells in the presence of AHL. In addition, these authors showed that 3-oxo-C14-HSL was able to decrease the growth and to induce the enhancement of biofilm by of *Staphylococcus aureus*, but had no effect on *Staphylococcus epidermidis*, coagulase-negative *Staphylococcus* and *E. coli*.

In addition, the NfsB protein can be used with a biomarker for the presence of the AI-1 in *Salmonella*, due to being more abundant in the presence of this molecule in all the evaluated times. This result can be extrapolated to other microorganisms because nitroreductases homologous to NfsA and NfsB are found in many members of the Enterobacteriaceae family [68].

In conclusion, the fatty acid and protein profiles of *Salmonella* Enteritidis PT4 578 in logarithmic phase of growth at 4 h of cultivation were similar to the profiles of cells in late stationary phase at 36 h in the presence of C12-HSL. These profiles varied less along their growth in the presence of AI-1, indicating that quorum sensing anticipates a stationary phase response. In addition, the presence of this signaling molecule increased the abundance of thiol proteins and the levels of free cellular thiol after 6 h of cultivation which can prepare the cells for a possible oxidative stress. On the other hand, this increase may lead to modifications in the structure of the AHL or SdiA protein which, consequently, could alter the binding affinities in SdiA or DNA.

It is necessary to highlight two proteins identified in all evaluated times. The LuxS protein of the AI-2 quorum sensing mechanism was differentially abundant at one of the times and may indicate a cross response between the quorum sensing mechanisms mediated by AI-1 and AI-2 in *Salmonella* depending on the growth phase. The NfsB protein had its abundance increased in the presence of C12-HSL in all the evaluated times, indicating that the cells may be susceptible to the action of nitrofurans or this molecule has a certain toxicity or mutagenicity to the cell. Further studies are needed in order to determine the specific role of the thiol proteins, as well as the LuxS and NfsB proteins of *Salmonella* in the presence of AI-1.

3. Materials and methods

3.1. Bacterial strain

Salmonella enterica serovar Enteritidis phage type 4 (PT4) 578 (GenBank: MF066708.1), isolated from chicken meat, was provided by Fundação Oswaldo Cruz (FIOCRUZ, Rio de Janeiro, Brazil). Cultures were stored at −20 °C in Luria-Bertani (LB) broth [69] supplemented with 20% (v/v) of sterilized glycerol.

3.2. Preparation of inoculum

Inoculum was preparated according to Almeida et al. [12, 70]. Tryptone soy broth (TSB; Sigma-Aldrich, India) was prepared with CO_2 under O_2-free conditions, dispensed in anaerobic bottles that were sealed with butyl rubber stoppers and then autoclaved (anaerobic TSB). Before each experiment, cells were cultivated in 20 mL of anaerobic TSB for 24 h at 37 °C. Then, 1.0 mL was transferred into 10 mL of anaerobic TSB and incubated at 37 °C. After 4 h of incubation, exponentially growing cells were harvested by centrifugation at 5000 *g* at 4 °C for 10 min (Sorvall, USA), washed with 0.85% saline, and the pellet resuspended in 0.85% saline. The inoculum was

standardized to 0.1 of optical density at 600 nm (OD_{600nm}) (approximately 10^7 CFU/mL) using a spectrophotometer (Thermo Fisher Scientific, Finland).

3.3. Preparation of HSL solution

N-dodecanoyl-DL-homoserine lactone (C12-HSL; PubChem CID: 11565426; Fluka, Switzerland) was suspended in acetonitrile (PubChem CID: 6342; Merck, Germany) at a concentration of 10 mM and further diluted to a working solution of 10 μM in acetonitrile. Control experiment was performed using acetonitrile with final concentration in the media less than 1% (v/v) to avoid interference in the growth and response of *Salmonella* to C12-HSL [3].

3.4. Fatty acid profile analysis of *Salmonella*

3.4.1. Saponification, methylation and extraction of fatty acids

An aliquot of 10 mL of the standardized inoculum was added into anaerobic bottles containing 90 mL of anaerobic TSB supplemented with 50 nM of C12-HSL or the equivalent volume of acetonitrile as control and then, incubated at 37 °C. After 4, 6, 7, 12, 24 and 36 h of incubation, the OD_{600nm} was determined. Concomitantly, 10 mL of the media was centrifuged at 5000 *g* at 4 °C for 15 min (Sorvall, USA). The cells in the pellet were resuspended in 1 mL of sterilized distilled water, and once again, centrifuged at 5000 *g* at 4 °C for 10 min. The pellet was transferred to glass tubes free of fatty acids and then, the fatty acids were saponified, methylated, and extracted by the procedure of the Sherlock® Analysis Manual (version 6.2; MIDI, USA) [71].

3.4.2. Analysis and identification of fatty acids

The cellular fatty acid composition was determined by 7890A gas chromatograph equipped with flame ionization detector (Agilent Technologies, USA).

Afterwards, the fatty acids were identified in the Sherlock® Microbial Identification System software by the procedure of the Sherlock® Analysis Manual (version 6.2; MIDI, USA) [71].

3.4.3. Statistical analysis

Experiments were carried out in three biological replicates. The values of the triplicates were used for Principal Component Analysis (PCA) using RStudio software (version 1.0.143; USA). All data were subjected to analysis of variance (ANOVA) followed by Tukey's test using the Statistical Analysis System and Genetics Software® [72]. A $p < 0.05$ was considered to be statistically significant.

3.5. Protein profile analysis of *Salmonella*

3.5.1. Extraction and quantification of proteins

An aliquot of 10 mL of the standardized inoculum was added into anaerobic bottles containing 90 mL of anaerobic TSB supplemented with 50 nM of C12-HSL or the equivalent volume of acetonitrile as control and then, incubated at 37 °C. After 4, 6, 7, 12 and 36 h of incubation, the OD_{600nm} was determined and 10 mL of the media was centrifuged at 5000 *g* at 4 °C for 15 min (Sorvall, USA). The cells in the pellet were resuspended in 1 mL of sterilized distilled water, transferred to 1.5 mL microtubes and once again centrifuged at 9500 *g* at 4 °C for 30 min (Brikmann Instruments, Germany). The pellet was resuspended in 1 mL of Tris-HCl 50 mM, pH 8.0 added of 1 mM phenylmethylsulfonyl fluoride (PMSF) and 1 mM dithiothreitol (DTT). Next, the mixture was kept in ice for 1 min, then 1 min in ultrasound bath (154 W, 37 KHz; Unique, Brazil) and this cycle was repeated five times. Posteriorly, five cycles of 1 min in ice, 1 min in vortex and 8 min in ultrasound bath were performed. The mixture was centrifuged at 9500 *g* at 4 °C for 30 min, the supernatant containing the intracellular

proteins was transferred to 1.5 mL microtube and were stored at −20 °C. The pellet was resuspended in 100 µL of ammonium bicarbonate 50 mM and 1 mL of 2:1 trifluoroethanol:chloroform (TFE:$CHCl_3$) was added. Then, the mixture was submitted again for five cycles on ice and ultrasound bath and five cycles on ice, vortex and ultrasound bath as previously described. The mixture was centrifuged at 9500 *g* at 4 °C for 4 min to obtain three phases. The upper phase, composed by proteins soluble in TFE, was transferred to 1.5 mL microtubes and was dried in SpeedVac (Genevac, England). The supernatant with intracellular proteins was transferred to microtube containing the proteins soluble in TFE. The protein extract was precipitated with 10% (w/v) trichloroacetic acid (TCA) and kept on ice for 30 min and after that, the material was centrifuged at 9500 *g* at 4 °C for 10 min. The supernatant was discarded and the precipitate washed three times with cold acetone. After evaporation of the residual acetone at room temperature, the precipitate was resuspended in 400 µL of ammonium bicarbonate 50 mM. Proteins were quantified using Coomassie blue dye [73] and the protein extracts were stored at -20 °C.

3.5.2. In-solution protein digestion

The trypsin digestion of proteins in solution was performed according to Villen and Gygi [74], with modifications. An aliquot of the extract containing 10 µg of protein was transferred to 1.5 mL microtube and the final volume was adjusted to 150 µL with ammonium bicarbonate 50 mM and 150 µL of urea 8 M were added. The disulfide bonds of the proteins were reduced by 5 mM DTT for 25 min at 56 °C and the protein mixture was cooled to room temperature. Then, the alkylation was carried out by adding 14 mM iodoacetamide and followed by incubation for 30 min at room temperature in the dark. The free iodoacetamide was quenched by adding 5 mM DTT with further incubated for 15 min at room temperature in the dark. The concentration of urea in the

protein mixture was reduced to 1.6 M by diluting it in 1:5 in ammonium bicarbonate 50 mM with the addition of 1mM calcium chloride. An aliquot containing 20 ng of trypsin (Sequencing grade modified trypsin; Promega, USA) in ammonium bicarbonate 50 mM was added to a final ratio of 1:50 of trypsin:protein and it was incubated for 16 h at 37 °C. After the incubation, the solution was cooled to room temperature and the enzymatic reaction was quenched with 1% (v/v) trifluoroacetic acid (TFA) until pH 2.0. After centrifugation at 2500 *g* for 10 min at room temperature, the supernatant containing the peptides was collected.

3.5.3. Peptide desalting

The supernatant containing the peptides was desalted according to Rappsilber et al. [75], with modifications. Two membranes of octadecyl (C18; 3M EMPORE™, USA) were packed in each stage tip to load 10 µg of digested proteins. The stage tip was conditioned with 100 µL of 100% (v/v) methanol and was equilibrated with 100 µL 0.1% (v/v) formic acid. After that, the supernatant containing the peptides was loaded two times onto the stage tip and this was washed 10 times with 100 µL of 0.1% (v/v) formic acid. The peptides were eluted with 200 µL of 80% (v/v) acetonitrile containing 0.1% (v/v) formic acid. In each previous step, the stage tip was centrifuged at 400 *g* for 2 min (Eppendorf, Germany). The eluate was dried in SpeedVac (Thermo Fisher Scientific, Finland), resuspended in 22.5 µL of 0.1% (v/v) formic acid and stored at -20 °C.

3.5.4. Mass spectrometric analysis

The solution containing the peptides was centrifuged at 9000 *g* for 5 min and 15 µL of the supernatant was transferred to vials. An aliquot of 4.5 µL of peptides, equivalent to 2 µg of protein, was separated by C18 (100 mm x 100 mm) RP-nanoUPLC (nanoAcquity; Waters, USA) coupled with a Q-Tof Premier mass

spectrometer (Waters, USA) with nanoelectrospray source at a flow rate of 0.6 μL.min^{-1}. The gradient was 2 – 90% (v/v) acetonitrile in 0.1% (v/v) formic acid over 45 min. The nanoelectrospray voltage was set to 3.0 kV, a cone voltage of 50 V and the source temperature was 80 °C. The instrument was operated in the 'top three' mode, in which one MS spectrum is acquired followed by MS/MS of the top three most-intense peaks detected. After MS/MS fragmentation, the ion was placed on exclusion list for 60 s.

3.5.5. Identification and quantification of proteins

The spectra were acquired using software MassLynx (version 4.1; Waters) and the *.raw* data files were converted to a peak list format *.mgf* without summing the scans by the software Mascot Distiller (version 2.3.2.0; Matrix Science, United Kingdom) and searched against the knowledgebase UniProtKB using the Mascot software (version 2.4.0; Matrix Science, United Kingdom). For the search, the following parameters were considered: taxonomy *Salmonella* and all entries (separately), monoisotopic mass, trypsin, allow up to one missed cleavage site, peptide charge +2, +3 and +4, fixed modification for carbamidomethylation of cysteine residues and variable modification for oxidation of methionine residues, peptide tolerance equal to 0.1 Da, MS/MS tolerance equal to 0.1 Da, ESI-QUA-TOF for instrument. The identifications of the proteins by Mascot software were validated and the proteins were quantified by Scaffold software (version 4.7.2; Proteome Software, USA). For the protein validation, peptide and protein identifications were accepted if they could be established at greater than 90% probability as specified by the Peptide Prophet algorithm [76] and by the Protein Prophet algorithm [77], respectively. In addition, the proteins should contain at least one identified peptide. For the protein quantitation, the quantitative value of total ion current (TIC) of each protein was normalized by sum total of TIC. For the unidentified proteins, a TIC value of 0.05 was adopted (cut off of method sensibility).

3.5.6. Statistical analysis

Experiments were carried out in three biological replicates. The logarithms of normalized TIC values of the triplicates were used for Principal Component Analysis (PCA) as well as the logarithms of average normalized TIC values of the triplicates of each protein which were used to construct the heatmap and dendrogram using RStudio software. The significance of difference of normalized TIC values between the samples were calculated by T-test with correction for multiple hypotheses by false discovery rate (FDR) using RStudio software. The fold changed was calculated as the ratio of the average normalized TIC values of the treatment with C12-HSL by the control and the result was showed as logarithm in base two. The proteins with *p*-value less than 0.05 ($p < 0.05$; negative logarithm of *p*-value > 1.301) and fold changed less than 0.667-fold or more than 1.500-fold (logarithm in base two of fold changed < -0.585 or > 0.585) were considered differentially abundant proteins [78]. Moreover, when the protein was not detected in one of the treatments, the *p*-value was not considered and the fold-changed was calculated by adopting a TIC value of 0.05 (cut off of method sensibility) for the sample in which the protein was not identified, being this protein also considered differentially abundant.

3.5.7. Bioinformatics analysis

The Gene Ontology (GO) annotations of the process and function of the differentially abundant proteins were acquired with the tool QuickGO implemented by European Bioinformatics Institute (http://www.ebi.ac.uk/QuickGO/). Then, the PPI network was generated for some proteins of the *Salmonella* Typhimurium LT2 with the confidence interactions greater than 0.4 using the STRING database version 10.5 (http://string-db.org/, [31]).

3.6. Quantification of free cellular thiol

3.6.1. Extraction of free cellular thiol

The pellet was obtained as described in item 3.5.1. The pellet was resuspended in 250 µL of sterilized distilled water. Next, the mixture was kept on ice for 1 min, 1 min mixed by vortex for 1 min and treated with ultrasound (400 W, 20 KHz; Sonics & Materials Inc., USA) for 30 s; and this cycle was repeated five times. The mixture was then centrifuged at 9500 *g* at 4 °C for 15 min and the supernatant containing the free cellular thiol was used immediately.

3.6.2. Quantification of free cellular thiol

The quantification of free cellular thiol was performed according to Ellman [79] and Riddles et al. [80], with modifications. For each 25 µL of the supernatant or standard, 5 µL of 0.4% (w/v) 5,5′-dithiobis(2-nitrobenzoic acid) (DTNB or Ellman's reagent; Sigma, USA) in buffer sodium phosphate 0.1 M pH 8.0 containing 1mM EDTA and 250 µL of the buffer sodium phosphate were added in microplate. The microplate was incubated at room temperature for 15 min and the absorbance at 412 nm measured by using a spectrophotometer (Thermo Fisher Scientific, Finland). The free cellular thiol was quantified by using cysteine hydrochloride monohydrate (Sigma, USA) as standard at concentrations of 0.0 to 1.5 mM. The obtained equation was as follows: absorbance = (0.9421 x concentration) + 0.0432, with $R^2 = 0.9936$.

3.6.3. Statistical analysis

Experiments were carried out in three biological replicates and the quantification of free cellular thiol was normalized by OD_{600nm}. All data were subjected to analysis of variance (ANOVA) followed by Tukey's test using the Statistical Analysis System and Genetics Software® [72]. A $p < 0.05$ was considered to be statistically significant.

Acknowledgements

Felipe Alves de Almeida was supported by a fellowship from Conselho Nacional de Desenvolvimento Científico e Tecnológico (CNPq) and this research has been supported by Fundação de Amparo à Pesquisa do Estado de Minas Gerais (FAPEMIG), Coordenação de Aperfeiçoamento de Pessoal de Nível Superior (CAPES), Financiadora de Estudos e Projetos (Finep), Sistema Nacional de Laboratórios em Nanotecnologias (SisNANO) and Ministério da Ciência, Tecnologia e Informação (MCTI). The authors acknowledge the Mass Spectrometry Facility at Brazilian Biosciences National Laboratory (LNBio), CNPEM, Campinas, Brazil and the Núcleo de Análise de Biomoléculas (Nubiomol) at Universidade Federal de Viçosa, Viçosa, Brazil for their support on mass spectrometry and data analysis. The authors thank Professor Marcos Rogério Tótola of Department of Microbiology at Universidade Federal de Viçosa for equipment and software for fatty acids analysis. The funders had no role in study design, data collection and analysis, decision to publish, or preparation of the manuscript.

References

[1] Fuqua WC, Winans SC, Greenberg EP. Quorum sensing in bacteria: the LuxR-LuxI family of cell density-responsive transcriptional regulators. J Bacteriol. 1994;176: 269-275. doi: 10.1128/jb.176.2.269-275.1994

[2] Reading NC, Sperandio V. Quorum sensing: the many languages of bacteria. FEMS Microbiol Lett. 2006;254: 1-11. doi: 10.1111/j.1574-6968.2005.00001.x

[3] Michael B, Smith JN, Swift S, Heffron F, Ahmer BM. SdiA of *Salmonella enterica* is a LuxR homolog that detects mixed microbial communities. J Bacteriol. 2001;183: 5733-5742. doi: 10.1128/JB.183.19.5733-5742.2001

[4] Sabag-Daigle A, Ahmer BM. ExpI and PhzI are descendants of the long lost cognate signal synthase for SdiA. PLoS One. 2012;7: e47720-e47723. doi: 10.1371/journal.pone.0047720

[5] Smith JN, Ahmer BM. Detection of other microbial species by *Salmonella*: expression of the SdiA regulon. J Bacteriol. 2003;185: 1357-1366. doi: 10.1128/JB.185.4.1357-1366.2003

[6] Dyszel JL, Soares JA, Swearingen MC, Lindsay A, Smith JN, Ahmer BM. *E. coli* K-12 and EHEC genes regulated by SdiA. PLoS One. 2010;5: e8946-e8950. doi: 10.1371/journal.pone.0008946

[7] Smith JN, Dyszel JL, Soares JA, Ellermeier CD, Altier C, Lawhon SD, et al. SdiA, an *N*-acylhomoserine lactone receptor, becomes active during the transit of *Salmonella enterica* through the gastrointestinal tract of turtles. PLoS One. 2008;3: e2826-e2833. doi: 10.1371/journal.pone.0002826

[8] Atkinson S, Williams P. Quorum sensing and social networking in the microbial world. J R Soc Interface. 2009;6: 959-978. doi: 10.1098/rsif.2009.0203

[9] Di Cagno R, De Angelis M, Calasso M, Gobbetti M. Proteomics of the bacterial cross-talk by quorum sensing. J Proteomics. 2011;74: 19-34. doi: 10.1016/j.jprot.2010.09.003

[10] Ahmer BM, Van Reeuwijk J, Timmers CD, Valentine PJ, Heffron F. *Salmonella* Typhimurium encodes an SdiA homolog, a putative quorum sensor of the LuxR family, that regulates genes on the virulence plasmid. J Bacteriol. 1998;180: 1185-1193.

[11] Campos-Galvão ME, Ribon AO, Araujo EF, Vanetti MCD. Changes in the *Salmonella enterica* Enteritidis phenotypes in presence of acyl homoserine lactone quorum sensing signals. J Basic Microbiol. 2015;56: 493-501. doi: 10.1002/jobm.201500471

[12] Almeida FA, Pimentel-Filho NJ, Carrijo LC, Bento CBP, Baracat-Pereira MC, Pinto UM, et al. Acyl homoserine lactone changes the abundance of proteins and the levels of organic acids associated with stationary phase in *Salmonella* Enteritidis. Microb Pathog. 2017;102: 148-159. doi: 10.1016/j.micpath.2016.11.027

[13] Schuster M, Lostroh CP, Ogi T, Greenberg EP. Identification, timing, and signal specificity of *Pseudomonas aeruginosa* quorum-controlled genes: a transcriptome analysis. J Bacteriol. 2003;185: 2066-2079. doi: 10.1128/JB.185.7.2066–2079.2003

[14] Majerczyk C, Brittnacher M, Jacobs M, Armour CD, Radey M, Schneider E, et al. Global analysis of the *Burkholderia thailandensis* quorum sensing-controlled regulon. J Bacteriol. 2014;196: 1412-1424. doi: 10.1128/JB.01405-13

[15] Goo E, Majerczyk CD, An JH, Chandler JR, Seo YS, Ham H, et al. Bacterial quorum sensing, cooperativity, and anticipation of stationary-phase stress. Proc Natl Acad Sci USA. 2012;109: 19775-19780. doi: 10.1073/pnas.1218092109

[16] Law JH, Zalkin H, Kaneshiro T. Transmethylation of fatty acids. Biochim Biophys Acta. 1962;70: 143-151. doi: 10.1016/0006-3002(63)90734-0

[17] Chen YY, Ganzle MG. Influence of cyclopropane fatty acids on heat, high pressure, acid and oxidative resistance in *Escherichia coli*. Int J Food Microbiol. 2016;222: 16-22. doi: 10.1016/j.ijfoodmicro.2016.01.017

[18] Grogan DW, Cronan JE. Cyclopropane ring formation in membrane lipids of bacteria. Microbiol Mol Biol Rev. 1997;61: 429-441.

[19] Guckert JB, Hood MA, White DC. Phospholipid ester-linked fatty acid profile changes during nutrient deprivation of *Vibrio cholerae*: increases in the trans/cis ratio and proportions of cyclopropyl fatty acids. Appl Environ Microbiol. 1986; 52; 794-801.

[20] Kaur A, Chaudhary A, Kaur A, Choudhary R, Kaushik R. Phospholipid fatty acid - A bioindicator of environment monitoring and assessment in soil ecosystem. Curr Sci. 2005;89: 1103-1112.

[21] Zhang YM, Rock CO. Membrane lipid homeostasis in bacteria. Nat Rev Microbiol. 2008;6: 222–233. doi: 10.1038/nrmicro1839

[22] Schuster M, Sexton DJ, Hense BA. Why quorum sensing controls private goods. Front Microbiol. 2017;8: 885-900. doi: 10.3389/fmicb.2017.00885

[23] Wongtrakoongate P, Tumapa S, Tungpradabkul S. Regulation of a quorum sensing system by stationary phase sigma factor RpoS and their co-regulation of target genes in *Burkholderia pseudomallei*. Microbiol Immunol. 2012;56: 281-294. doi: 10.1111/j.1348-0421.2012.00447.x

[24] Wagner VE, Bushnell D, Passador L, Brooks AI, Iglewski BH. Microarray analysis of *Pseudomonas aeruginosa* quorum-sensing regulons: effects of growth phase and environment. J Bacteriol. 2003;185: 2080-2095. doi: 10.1128/JB.185.7.2080–2095.2003

[25] An D, Danhorn T, Fuqua WC, Parsek MR. Quorum sensing and motility mediate interactions between *Pseudomonas aeruginosa* and *Agrobacterium tumefaciens* in biofilm cocultures. Proc Natl Acad Sci USA. 2006;103: 3828-3833. doi: 10.1073/pnas.0511323103

[26] Kaufmann GF, Sartorio R, Lee SH, Rogers CJ, Meijler MM, Moss JA, et al. Revisiting quorum sensing: discovery of additional chemical and biological functions for 3-oxo-*N*-acylhomoserine lactones. Proc Natl Acad Sci USA. 2005;102: 309-314. doi: 10.1073/pnas.0408639102

[27] Xavier JB, Kim W, Foster KR. A molecular mechanism that stabilizes cooperative secretions in *Pseudomonas aeruginosa*. Mol Microbiol. 2011;79: 166-179. doi: 10.1111/j.1365-2958.2010.07436.x

[28] Lazazzera BA. Quorum sensing and starvation: signals for entry into stationary phase. Curr Opin Microbiol. 2000;3: 177-182.

[29] Prajapat MK, Saini S. Logic of two antagonizing intra-species quorum sensing systems in bacteria. Biosystems. 2018;165: 88-98. doi: 10.1016/j.biosystems.2018.01.004

[30] Balleza E, Lopez-Bojorquez LN, Martinez-Antonio A, Resendis-Antonio O, Lozada-Chavez I, Balderas-Martinez YI, et al. Regulation by transcription factors in bacteria: beyond description. FEMS Microbiol Rev. 2009;33: 133-151. doi: 10.1111/j.1574-6976.2008.00145.x

[31] Szklarczyk D, Franceschini A, Wyder S, Forslund K, Heller D, Huerta-Cepas J, et al. STRING v10: protein-protein interaction networks, integrated over the tree of life. Nucleic Acids Res. 2015;43: D447-D452. doi: 10.1093/nar/gku1003

[32] Soni KA, Jesudhasan PR, Cepeda M, Williams B, Hume M, Russell WK, et al. Autoinducer AI-2 is involved in regulating a variety of cellular processes in *Salmonella* Typhimurium. Foodborne Pathog Dis. 2008;5: 147-153. doi: 10.1089/fpd.2007.0050

[33] Jones DP. Redefining oxidative stress. Antioxid Redox Signal. 2006;8: 1865-1879. doi: 10.1089/ars.2006.8.1865

[34] Rudyk O, Eaton P. Biochemical methods for monitoring protein thiol redox states in biological systems. Redox Biol. 2014;2: 803-813. doi: 10.1016/j.redox.2014.06.005

[35] Landeta C, Boyd D, Beckwith J. Disulfide bond formation in prokaryotes. Nat Microbiol. 2018;3: 270-280. doi: 10.1038/s41564-017-0106-2

[36] Hassett DJ, Ma JF, Elkins JG, McDermott TR, Ochsner UA, West SE, et al. Quorum sensing in *Pseudomonas aeruginosa* controls expression of catalase and superoxide dismutase genes and mediates biofilm susceptibility to hydrogen peroxide. Mol Microbiol. 1999;34: 1082-1093. doi: 10.1046/j.1365-2958.1999.01672.x

[37] Garcia-Contreras R, Nunez-Lopez L, Jasso-Chavez R, Kwan BW, Belmont JA, Rangel-Vega A, et al. Quorum sensing enhancement of the stress response promotes resistance to quorum quenching and prevents social cheatin. ISME J. 2014;9: 115-125. doi: 10.1038/ismej.2014.98

[38] Lumjiaktase P, Diggle SP, Loprasert S, Tungpradabkul S, Daykin M, Camara M, et al. Quorum sensing regulates *dpsA* and the oxidative stress response in *Burkholderia pseudomallei*. Microbiology. 2006;152: 3651-3659. doi: 10.1099/mic.0.29226-0

[39] Almiron M, Link AJ, Furlong D, Kolter R. A novel DNA-binding protein with regulatory and protective roles in starved *Escherichia coli*. Genes Dev. 1992;6: 2646-2654.

[40] Martinez A, Kolter R. Protection of DNA during oxidative stress by the nonspecific DNA-binding protein Dps. J Bacteriol. 1997;179: 5188-5194. doi: 10.1128/jb.179.16.5188-5194.1997

[41] Mangalappalli-Illathu AK, Korber DR. Adaptive resistance and differential protein expression of *Salmonella enterica* serovar Enteritidis biofilms exposed to benzalkonium chloride. Antimicrob Agents Chemother. 2006;50: 3588-3596. doi: 10.1128/AAC.00573-06

[42] Mangalappalli-Illathu AK, Vidovic S, Korber DR. Differential adaptive response and survival of *Salmonella enterica* serovar Enteritidis planktonic and biofilm cells exposed to benzalkonium chloride. Antimicrob Agents Chemother. 2008;52: 3669-3680. doi: 10.1128/AAC.00073-08

[43] Bjur E, Eriksson-Ygberg S, Aslund F, Rhen M. Thioredoxin 1 promotes intracellular replication and virulence of *Salmonella enterica* serovar Typhimurium. Infect Immun. 2006;74: 5140-5151. doi: 10.1128/IAI.00449-06

[44] Peters SE, Paterson GK, Bandularatne ES, Northen HC, Pleasance S, Willers C, et al. *Salmonella enterica* serovar Typhimurium *trxA* mutants are protective against virulent challenge and induce less inflammation than the live-attenuated vaccine strain SL3261. Infect Immun. 2010;78: 326-336. doi: 10.1128/IAI.00768-09

[45] Song M, Kim JS, Liu L, Husain M, Vazquez-Torres A. Antioxidant defense by thioredoxin can occur independently of canonical thiol-disulfide oxidoreductase enzymatic activity. Cell Reports. 2016;14: 2901-2911. doi: 10.1016/j.celrep.2016.02.066

[46] Bouwman CW, Kohli M, Killoran A, Touchie GA, Kadner RJ, Martin NL. Characterization of SrgA, a *Salmonella enterica* serovar Typhimurium virulence plasmid-encoded paralogue of the disulfide oxidoreductase DsbA, essential for biogenesis of plasmid-encoded fimbriae. J Bacteriol. 2003;185: 991-1000.

[47] Jakob U, Muse W, Eser M, Bardwell JCA. Chaperone activity with a redox switch. Cell. 1999;96: 341-352. doi: 10.1016/S0092-8674(00)80547-4

[48] Kumar JK, Tabor S, Richardson CC. Proteomic analysis of thioredoxin-targeted proteins in *Escherichia coli*. Proc Natl Acad Sci USA. 2004;101: 3759-3764. doi: 10.1073/pnas.0308701101

[49] Rietsch A, Bessette P, Georgiou G, Beckwith J. Reduction of the periplasmic disulfide bond isomerase, DsbC, occurs by passage of electrons from cytoplasmic thioredoxin. J Bacteriol. 1997;179: 6602-6608. doi: 10.1128/jb.179.21.6602-6608.1997

[50] Zheng M, Aslund F, Storz G. Activation of the OxyR transcription factor by reversible disulfide bond formation. Science. 1998;279: 1718-1721. doi: 10.1126/science.279.5357.1718

[51] Danon A. Redox reactions of regulatory proteins: do kinetics promote specificity? Trends Biochem Sci. 2002;27: 197-203. doi: 10.1016/S0968-0004(02)02066-2

[52] Campos-Galvão MEM, Leite TD, Ribon AO, Araujo EF, Vanetti MCD. A new repertoire of informations about the quorum sensing system in *Salmonella enterica* serovar Enteritidis PT4. Genet Mol Res. 2015;14: 4068-4084. doi: 10.4238/2015.April.27.22

[53] Almeida FA, Pinto UM, Vanetti MCD. Novel insights from molecular docking of SdiA from *Salmonella Enteritidis* and *Escherichia coli* with quorum sensing and quorum quenching molecules. Microb Pathog. 2016;99: 178-190. doi: 10.1016/j.micpath.2016.08.024

[54] Nguyen Y, Nguyen NX, Rogers JL, Liao J, MacMillan JB, Jiang Y, et al. Structural and mechanistic roles of novel chemical ligands on the SdiA quorum-sensing transcription regulator. mBio. 2015;6: e02429-e02438. doi: 10.1128/mBio.02429-14

[55] Kafle P, Amoh AN, Reaves JM, Suneby EG, Tutunjian KA, Tyson RL, et al. Molecular insights into the impact of oxidative stress on the quorum-sensing regulator protein LasR. J Biol Chem. 2016;291: 11776-11786. doi: 10.1074/jbc.M116.719351

[56] Uroz S, Chhabra SR, Cámara M, Williams P, Oger P, Dessaux Y. *N*-acylhomoserine lactone quorum-sensing molecules are modified and degraded by *Rhodococcus erythropolis* W2 by both amidolytic and novel oxidoreductase activities. Microbiology. 2005;151: 3313-3322. doi: 10.1099/mic.0.27961-0

[57] Chowdhary PK, Keshavan N, Nguyen HQ, Peterson JA, González JE, Haines DC. *Bacillus megaterium* CYP102A1 oxidation of acyl homoserine lactones and acyl homoserines. Biochemistry. 2007;46: 14429-14437. doi: 10.1021/bi701945j

[58] Bijtenhoorn P, Mayerhofer H, Müller-Dieckmann J, Utpatel C, Schipper C, Hornung C, et al. A Novel metagenomic short-chain dehydrogenase/reductase attenuates *Pseudomonas aeruginosa* biofilm formation and virulence on *Caenorhabditis elegans*. PLoS ONE. 2011;6: e26278-e26292. doi: 10.1371/journal.pone.0026278

[59] Pietschke C, Treitz C, Forêt S, Schultze A, Künzel S, Tholey A, et al. Host modification of a bacterial quorum-sensing signal induces a phenotypic switch in bacterial symbionts. Proc Natl Acad Sci USA. 2017;114: E8488-E8497. doi: 10.1073/pnas.1706879114

[60] Bryant DW, McCalla DR, Leeksma M, Laneuville P. Type I nitroreductases of *Escherichia coli*. Can J Microbiol. 1981;27: 81-86.

[61] Michael NP, Brehm JK, Anlezark GM, Minton NP. Physical characterisation of the *Escherichia coli* B gene encoding nitroreductase and its over-expression in *Escherichia coli* K12. FEMS Microbiol Lett. 1994;124: 195-202.

[62] García V, Montero I, Bances M, Rodicio R, Rodicio MR. Incidence and genetic bases of nitrofurantoin resistance in clinical isolates of two successful multidrug-resistant clones of *Salmonella enterica* serovar Typhimurium: Pandemic "DT 104" and pUO-StVR2. Microb Drug Resist. 2017;23: 405-412. doi: 10.1089/mdr.2016.0227

[63] Whiteway J, Koziarz P, Veall J, Sandhu N, Kumar P, Hoecher B, et al. Oxygen-insensitive nitroreductases: analysis of the roles of *nfsA* and *nfsB* in development of resistance to 5-nitrofuran derivatives in *Escherichia coli*. J Bacteriol. 1998;180: 5529-5539.

[64] Carroll CC, Warnakulasuriyarachchi D, Nokhbeh MR, Lambert IB. *Salmonella* Typhimurium mutagenicity tester strains that overexpress oxygen-insensitive nitroreductases *nfsA* and *nfsB*. Mutat Res. 2002;501: 79-98. doi: 10.1016/S0027-5107(02)00018-0

[65] Gomi K, Kikuchi T, Tokue Y, Fujimura S, Uehara A, Takada H, et al. Mouse and human cell activation by *N*-dodecanoyl-DL-homoserine lactone, a *Chromobacterium violaceum* autoinducer. Infection and Immunity. 2006;74: 7029–7031. doi: 10.1128/IAI.00038-06

[66] Kristiansen S, Bjarnsholt T, Adeltoft D, Ifversen P, Givskov M. The *Pseudomonas aeruginosa* autoinducer dodecanoyl-homoserine lactone inhibits the putrescine synthesis in human cells. APMIS. 2008;116: 361-371. doi: 10.1111/j.1600-0463.2008.00966.x

[67] John J, Saranathan R, Adigopula LN, Thamodharan V, Singh SP, Lakshmi TP, et al. The quorum sensing molecule *N*-acyl homoserine lactone produced by *Acinetobacter baumannii* displays antibacterial and anticancer properties. Biofouling. 2016;32: 1029-1047. doi: 10.1080/08927014.2016.1221946

[68] Rau J, Stolz A. Oxygen-insensitive nitroreductases NfsA and NfsB of *Escherichia coli* function under anaerobic conditions as lawsone-dependent Azo reductases. Appl Environ Microbiol. 2003;69: 3448-3455. doi: 10.1128/AEM.69.6.3448–3455.2003

[69] Miller JH. Experiments in Molecular Genetics. New York: Cold Spring Harbor Laboratory Press; 1972.

[70] Almeida FA, Pimentel-Filho NJ, Pinto UM, Mantovani HC, Oliveira LL, Vanetti MCD. Acyl homoserine lactone-based quorum sensing stimulates biofilm formation by *Salmonella* Enteritidis in anaerobic conditions. Arch Microbiol. 2017;199: 475-486. doi: 10.1007/s00203-016-1313-6

[71] Sherlock® Analysis Manual. Microbial Identification System. 6.2 version. United States of America: MIDI, Inc.; 2012.

[72] Ferreira DF. Sisvar: a computer statistical analysis system. Ciênc Agrotec. 2011;35: 1039-1042.

[73] Bradford MM. A rapid and sensitive method for the quantitation of microgram quantities of protein utilizing the principle of protein-dye binding. Anal Biochem. 1976;72: 248-254. doi: 10.1016/0003-2697(76)90527-3

[74] Villen J, Gygi SP. The SCX/IMAC enrichment approach for global phosphorylation analysis by mass spectrometry. Nat Protoc. 2008;3: 1630-1638. doi: 10.1038/nprot.2008.150

[75] Rappsilber J, Mann M, Ishihama Y. Protocol for micro-purification, enrichment, pre-fractionation and storage of peptides for proteomics using StageTips. Nat Protoc. 2007;2: 1896-1906. doi: 10.1038/nprot.2007.261

[76] Keller A, Nesvizhskii AI, Kolker E, Aebersold R. Empirical statistical model to estimate the accuracy of peptide identifications made by MS/MS and database search. Anal Chem. 2002;74: 5383-5392. doi: 10.1021/ac025747h

[77] Nesvizhskii AI, Keller A, Kolker E, Aebersold R. A statistical model for identifying proteins by tandem mass spectrometry. Anal Chem. 2003;75: 4646-4658. doi: 10.1021/ac0341261

[78] Lago M, Monteil V, Douche T, Guglielmini J, Criscuolo A, Maufrais C, et al. Proteome remodelling by the stress sigma factor RpoS/σS in *Salmonella*: identification of small proteins and evidence for post-transcriptional regulation. Sci Rep. 2017;7: 2127-2141. doi: 10.1038/s41598-017-02362-3

[79] Ellman GL. Tissue sulfhydryl groups. Arch Biochem Biophys. 1959;82: 70-77.

[80] Riddles PW, Blakeley RL, Zerner B. Ellman's reagent: 5,5'-dithiobis(2-nitrobenzoic acid)-a reexamination. Anal Biochem. 1979;94: 75-81.

Supporting information

S1 Table. Organism, gene, protein, molecular mass (MM), isoeletric point (pI), process and function of proteins identified from *Salmonella* Enteritidis PT4 578 anaerobically cultivated in TSB at 37 °C in the presence or absence of C12-HSL.

Organism	Gene	Gene name	Protein	Protein name	MM (KDa)	pI	Process	Function
Salmonella Typhimurium str. LT2	*atpH*	STM3868	ATP synthase subunit delta	Q7CPE5	19.514	4.89	Biosynthetic	ATP
Salmonella Typhimurium str. LT2	*accB*	STM3379	Acetyl-CoA carboxylase, BCCP subunit	Q7CPM1	16.733	4.66	Biosynthetic	Fatty acid
Salmonella Typhimurium str. LT2	*acpP*	STM1196	Acyl carrier protein	P0A6B1	8.634	3.98	Biosynthetic	Fatty acid
Salmonella Typhimurium str. LT2	*atpD*	STM3865	ATP synthase subunit beta	Q7CPE2	50.309	4.90	Biosynthetic	Unclassified
Salmonella Typhimurium str. LT2	*ftsZ*	STM0133	Cell division protein FtsZ	Q8ZRU0	40.299	4.66	Cell division	FtsZ-dependent cytokinesis
Salmonella Typhimurium str. LT2	*zapB*	STM4088	Cell division protein ZapB	Q8ZKP1	9.307	4.59	Cell division	FtsZ-dependent cytokinesis
Salmonella Typhimurium str. LT2	*cheZ*	STM1915	Protein phosphatase CheZ	P07800	23.905	4.39	Chemotaxis	Phosphoprotein phosphatase
Salmonella Typhimurium str. LT2	*aspA*	STM4326	Aspartate ammonia-lyase	Q7CPA1	52.880	5.15	Metabolic process	Aspartate ammonia-lyase
Salmonella Typhimurium str. LT2	*adi*	STM4296	Arginine decarboxylase	Q8ZKE3	84.837	5.17	Metabolic process	Cellular amino acid metabolic
Salmonella Typhimurium str. LT2	*aroK*	STM3487	Shikimate kinase 1	P63601	19.458	5.27	Metabolic process	Cellular amino acid metabolic
Salmonella Typhimurium str. LT2	*ridA*	STM4458	2-iminobutanoate/2-iminopropanoate deaminase	Q7CP78	13.624	5.13	Metabolic process	Cellular amino acid metabolic
Salmonella Typhimurium str. LT2	*grcA*	STM2646	Autonomous glycyl radical cofactor	Q7CQ05	14.392	5.10	Metabolic process	Formate C-acetyltransferase
Salmonella Typhimurium str. LT2	*pflB*	STM0973	Pyruvate formate lyase I, induced anaerobically	Q7CQU1	85.293	5.75	Metabolic process	Formate C-acetyltransferase
Salmonella Typhimurium str. LT2	*gloA*	STM1435	Lactoylglutathione lyase	P0A1Q2	14.869	4.90	Metabolic process	Glutathione metabolic process
Salmonella Typhimurium str. LT2	*eno*	STM2952	Enolase	P64076	45.627	5.25	Metabolic process	Glycolytic process
Salmonella Typhimurium str. LT2	*gapA*	STM1290	Glyceraldehyde-3-phosphate dehydrogenase	P0A1P0	35.735	6.33	Metabolic process	Glycolytic process
Salmonella Typhimurium str. LT2	*pgk*	STM3069	Phosphoglycerate kinase	P65702	41.278	5.09	Metabolic process	Glycolytic process
Salmonella Typhimurium str. LT2	*tpiA*	STM4081	Triosephosphate isomerase	Q8ZKP7	26.900	5.68	Metabolic process	Glycolytic process
Salmonella Typhimurium str. LT2	*adk*	STM0488	Adenylate kinase	P0A1V4	23.530	5.53	Metabolic process	Nucleotide biosynthetic
Salmonella Typhimurium str. LT2	*deoC*	STM4567	Deoxyribose-phosphate aldolase	Q8ZJV8	27.895	5.87	Metabolic process	Nucleotide biosynthetic
Salmonella Typhimurium str. LT2	*ppnP*	STM0391	Pyrimidine/purine nucleoside phosphorylase	Q8ZRE7	10.152	5.01	Metabolic process	Nucleotide biosynthetic
Salmonella Typhimurium str. LT2	*ackA*	STM2337	Acetate kinase	P63411	43.572	5.93	Metabolic process	Organic acid metabolic
Salmonella Typhimurium str. LT2	*rpiA*	STM3063	Ribose-5-phosphate isomerase A	P66692	22.938	5.08	Metabolic process	Pentose-phosphate shunt
Salmonella Typhimurium str. LT2	*ribH*	STM0417	6,7-dimethyl-8-ribityllumazine synthase	P66038	15.998	5.10	Metabolic process	Riboflavin biosynthetic process
Salmonella Typhimurium str. LT2	*flgE*	STM1177	Flagellar hook protein FlgE	P0A1J1	42.185	4.77	Motility	Bacterial-type flagellum-dependent cell motility
Salmonella Typhimurium str. LT2	*flgL*	STM1184	Flagellar hook-associated protein 3	P16326	34.154	4.83	Motility	Bacterial-type flagellum-dependent cell motility
Salmonella Typhimurium str. LT2	*flgN*	STM1171	Flagella synthesis protein FlgN	P0A1J7	15.979	5.34	Motility	Bacterial-type flagellum-dependent cell motility
Salmonella Gallinarum str. 287/91	*fliD*	SG1095	Flagellar hook-associated protein 2	B5R7H2	49.926	5.12	Motility	Bacterial-type flagellum-dependent cell motility
Salmonella Gallinarum str. 287/91	*fljB*	SG1096	Flagellin	B5R7H3	52.950	4.90	Motility	Bacterial-type flagellum-dependent cell motility

S1 Table. Continuation.

Organism	Gene	Gene name	Protein	Protein name	MM (KDa)	pI	Process	Function
Salmonella Typhimurium str. LT2	*fdx*	STM2538	[2FE-2S] ferredoxin	Q7CQ13	12.780	4.40	Oxidation-reduction	Electron carrier
Salmonella Typhimurium str. LT2	*fldA*	STM0694	Flavodoxin 1	Q8ZQX1	19.796	4.22	Oxidation-reduction	Electron carrier
Salmonella Typhimurium str. LT2	*grxA*	STM0872	Glutaredoxin 1	P0A1P8	10.089	5.63	Oxidation-reduction	Electron carrier
Salmonella Typhimurium str. LT2	*grxC*	STM3702	Glutaredoxin 3	Q7CPH7	9.301	6.70	Oxidation-reduction	Electron carrier
Salmonella Typhimurium str. LT2	*hycB*	STM2852	Hydrogenase-3, iron-sulfur subunit	Q7CPY1	22.610	6.63	Oxidation-reduction	Electron carrier
Salmonella Typhimurium str. LT2	*hycI*	STM2845	Protease involved in processing C-terminal end of HycE	Q8ZMJ3	17.097	4.00	Oxidation-reduction	Electron carrier
Salmonella Typhimurium str. LT2	*ydhD*	STM1433	Glutaredoxin	Q7CQK9	13.071	4.84	Oxidation-reduction	Electron carrier
Salmonella Typhimurium str. LT2	*ahpC*	STM0608	Alkyl hydroperoxide reductase subunit C	P0A251	20.848	5.03	Oxidation-reduction	Oxidoreductase
Salmonella Typhimurium str. LT2	*bcp*	STM2491	Thioredoxin dependent thiol peroxidase	Q7CQ23	17.769	5.16	Oxidation-reduction	Oxidoreductase
Salmonella Typhimurium str. LT2	*dsbC*	STM3043	Thiol:disulfide interchange protein DsbC	P55890	26.047	7.11	Oxidation-reduction	Oxidoreductase
Salmonella Typhimurium str. LT2	*nfsB*	STM0578	Oxygen-insensitive NAD(P)H nitroreductase	P15888	23.997	5.40	Oxidation-reduction	Oxidoreductase
Salmonella Typhimurium str. LT2	*sodB*	STM1431	Superoxide dismutase [Fe]	P0A2F4	21.352	5.58	Oxidation-reduction	Oxidoreductase
Salmonella Typhimurium str. LT2	*sodC1*	STM1044	Superoxide dismutase [Cu-Zn] 1	P0CW86	18.529	6.48	Oxidation-reduction	Oxidoreductase
Salmonella Typhimurium str. LT2	STM0402	STM0402	Putative thiol-alkyl hydroperoxide reductase	Q7CR42	22.417	5.24	Oxidation-reduction	Oxidoreductase
Salmonella Typhimurium str. LT2	STM1790	STM1790	Putative thiol-disulfide isomerase and thioredoxin	Q8ZP25	15.052	4.69	Oxidation-reduction	Oxidoreductase
Salmonella Typhimurium str. LT2	*tpx*	STM1682	Probable thiol peroxidase	Q8ZP65	18.185	4.93	Oxidation-reduction	Oxidoreductase
Salmonella Typhimurium str. LT2	*trxA*	STM3915	Thioredoxin 1	P0AA28	11.913	4.67	Oxidation-reduction	Oxidoreductase
Salmonella Typhimurium str. LT2	*yfgD*	STM2495	Arsenate reductase	Q8ZN68	13.426	5.60	Oxidation-reduction	Oxidoreductase
Salmonella Enteritidis	*sefA*	sefA	Fimbrial protein	P12061	16.524	9.65	Pathogenesis	Cell adhesion
Salmonella Typhimurium str. LT2	*phoN*	STM4319	Non-specific acid phosphatase	P26976	18.478	9.01	Pathogenesis	Dephosphorylation
Salmonella Typhimurium str. LT2	*lpp1*	STM1377	Major outer membrane lipoprotein 1	Q7CQN4	8.443	9.36	Pathogenesis	Lipid modification
Salmonella Typhimurium str. LT2	*eco*	STM2262	Ecotin	Q8ZNH4	18.320	6.59	Pathogenesis	Serine-type endopeptidase inhibitor
Salmonella Typhimurium str. LT2	*fkpA*	STM3453	Peptidyl-prolyl cis-trans isomerase	Q8ZLL6	28.927	8.39	Protein folding	Peptidyl-prolyl cis-trans isomerase
Salmonella Typhimurium str. LT2	*ppiB*	STM0536	Peptidyl-prolyl cis-trans isomerase	Q8XFG8	18.243	5.52	Protein folding	Peptidyl-prolyl cis-trans isomerase
Salmonella Typhimurium str. LT2	*slyD*	STM3455	Peptidyl-prolyl cis-trans isomerase	Q8ZLL4	21.117	4.77	Protein folding	Peptidyl-prolyl cis-trans isomerase
Salmonella Typhimurium str. LT2	*tig*	STM0447	Trigger factor	P66932	48.037	4.84	Protein folding	Peptidyl-prolyl cis-trans isomerase
Salmonella Typhimurium str. LT2	*dnaK*	STM0012	Chaperone protein DnaK	Q56073	69.273	4.83	Protein folding	Unfolded protein binding
Salmonella Typhimurium str. LT2	*groL*	STM4330	60 kDa chaperonin	P0A1D3	57.421	4.85	Protein folding	Unfolded protein binding
Salmonella Typhimurium str. LT2	*groS*	STM4329	10 kDa chaperonin	P0A1D5	10.312	5.36	Protein folding	Unfolded protein binding
Salmonella Typhimurium str. LT2	*grpE*	STM2681	Protein GrpE	Q7CPZ4	21.827	4.69	Protein folding	Unfolded protein binding
Salmonella Typhimurium str. LT2	*ibpA*	STM3809	Small heat shock protein IbpA	Q7CPF1	15.740	5.23	Protein folding	Unfolded protein binding
Salmonella Typhimurium str. LT2	*skp*	STM0225	Chaperone protein Skp	P0A1Z2	17.894	9.76	Protein folding	Unfolded protein binding
Salmonella Typhimurium str. LT2	*surA*	STM0092	Chaperone SurA	Q7CR87	47.221	6.73	Protein folding	Unfolded protein binding

S1 Table. Continuation.

Organism	Gene	Gene name	Protein	Protein name	MM (KDa)	pI	Process	Function
Salmonella Typhimurium str. LT2	*erpA*	STM0204	Iron-sulfur cluster insertion protein ErpA	Q7CR66	12.263	4.15	Protein maturation	Iron-sulfur cluster assembly
Salmonella Typhimurium str. LT2	*nfuA*	STM3511	Fe/S biogenesis protein NfuA	Q8ZLI7	21.152	4.52	Protein maturation	Iron-sulfur cluster assembly
Salmonella Typhimurium str. LT2	*nifU*	STM2542	Iron-sulfur cluster assembly scaffold protein IscU	Q7CQ11	13.983	4.78	Protein maturation	Iron-sulfur cluster assembly
Salmonella Typhimurium str. LT2	*luxS*	STM2817	S-ribosylhomocysteine lyase	Q9L4T0	19.467	5.71	Quorum sensing	S-ribosylhomocysteine lyase
Salmonella Typhimurium str. LT2	*ssb*	STM4256	Single-stranded DNA-binding protein 1	P0A2F6	19.062	5.46	Response to stress	Cellular response to DNA damage stimulus
Salmonella Typhimurium str. LT2	*yajQ*	STM0435	UPF0234 protein YajQ	Q8ZRC9	18.308	5.60	Response to stress	Cellular response to DNA damage stimulus
Salmonella Typhimurium str. LT2	*uspG*	STM0614	Universal stress protein G	P67093	15.891	6.18	Response to stress	Protein autoadenylation and autophosphorylation
Salmonella Typhimurium str. LT2	*ygiW*	STM3176	Putative outer membrane protein	Q7CPS4	13.993	5.03	Response to stress	Protein, cellulose and peptidoglycan binding
Salmonella Typhimurium str. LT2	STM1251	STM1251	Putative molecular chaperone (Small heat shock protein)	Q8ZPY6	17.540	5.42	Response to stress	Unclassified
Salmonella Typhimurium str. LT2	*dksA*	STM0186	RNA polymerase-binding transcription factor DksA	P0A1G5	17.733	5.06	Transcription	Amino acid biosynthesis
Salmonella Typhimurium str. LT2	*cspC*	STM1837	Cold shock-like protein CspC	P0A9Y9	7.398	6.54	Transcription	Regulation of transcription, DNA-templated
Salmonella Typhimurium str. LT2	*cspE*	STM0629	RNA chaperone, negative regulator of cspA	Q7CQZ5	7.447	8.09	Transcription	Regulation of transcription, DNA-templated
Salmonella Typhimurium str. LT2	*emrR*	STM2813	Transcriptional repressor of emrAB operon	Q7CPY9	20.752	6.07	Transcription	Regulation of transcription, DNA-templated
Salmonella Typhimurium str. LT2	*fur*	STM0693	Transcriptional repressor of iron-responsive genes (Fur family) (Ferric uptake regulator)	Q7CQY3	17.229	5.56	Transcription	Regulation of transcription, DNA-templated
Salmonella Typhimurium str. LT2	*greA*	STM3299	Transcription elongation factor GreA	P64281	17.702	4.75	Transcription	Regulation of transcription, DNA-templated
Salmonella Typhimurium str. LT2	*hns*	STM1751	DNA-binding protein H-NS	P0A1S2	15.590	5.32	Transcription	Regulation of transcription, DNA-templated
Salmonella Typhimurium str. LT2	*hupA*	STM4170	DNA-binding protein HU-alpha	P0A1R6	9.515	9.57	Transcription	Regulation of transcription, DNA-templated
Salmonella Typhimurium str. LT2	*phoP*	STM1231	Virulence transcriptional regulatory protein PhoP	P0DM78	25.617	5.28	Transcription	Regulation of transcription, DNA-templated
Salmonella Typhimurium str. LT2	*rnk*	STM0616	Regulator of nucleoside diphosphate kinase	Q7CQZ7	15.042	4.47	Transcription	Regulation of transcription, DNA-templated
Salmonella Typhimurium str. LT2	*rpoA*	STM3415	DNA-directed RNA polymerase subunit alpha	P0A7Z7	36.717	4.98	Transcription	Regulation of transcription, DNA-templated
Salmonella Typhimurium str. LT2	*rpoZ*	STM3741	DNA-directed RNA polymerase subunit omega	P0A803	10.230	4.87	Transcription	Regulation of transcription, DNA-templated
Salmonella Gallinarum str. 287/91	SG2019	SG2019	DNA-binding protein	B5RBI8	14.956	5.63	Transcription	Regulation of transcription, DNA-templated
Salmonella Typhimurium str. LT2	*slyA*	STM1444	Transcriptional regulator SlyA	P40676	16.469	6.23	Transcription	Regulation of transcription, DNA-templated
Salmonella Typhimurium str. LT2	*stpA*	STM2799	DNA-binding protein StpA	P0A1S4	15.478	7.93	Transcription	Regulation of transcription, DNA-templated
Salmonella Typhimurium str. LT2	*ybaB*	STM0485	Nucleoid-associated protein YbaB	P0A8B8	12.064	5.01	Transcription	Regulation of transcription, DNA-templated
Salmonella Typhimurium str. LT2	*ydgT*	STM1461	Transcription modulator YdgT	Q7CQK5	8.375	6.03	Transcription	Regulation of transcription, DNA-templated
Salmonella Typhimurium str. LT2	*ppa*	STM4414	Inorganic pyrophosphatase	P65748	19.778	5.01	Transcription	RNA degradation
Salmonella Typhimurium str. LT2	*rof*	STM0237	Modulator of Rho-dependent transcription termination	Q8ZRN4	9.778	4.48	Transcription	RNA degradation
Salmonella Typhimurium str. LT2	*rraA*	STM4089	Regulator of ribonuclease activity A	P67651	17.478	4.07	Transcription	RNA degradation
Salmonella Typhimurium str. LT2	*sspB*	STM3341	Stringent starvation protein B	Q7CPN4	18.210	4.36	Transcription	RNA degradation

S1 Table. Continuation.

Organism	Gene	Gene name	Protein	Protein name	MM (KDa)	pI	Process	Function
Salmonella Typhimurium str. LT2	*def*	STM3406	Peptide deformylase	Q8ZLM7	19.384	5.02	Translation	Peptide deformylase
Salmonella Typhimurium str. LT2	*rrf or frr*	STM0219	Ribosome recycling factor	P66738	20.600	7.77	Translation	Ribosome binding
Salmonella Typhimurium str. LT2	*sra*	STM1565	Stationary-phase-induced ribosome-associated protein	Q7CQJ0	5.366	11.33	Translation	Ribosome binding
Salmonella Typhimurium str. LT2	*yfiA*	STM2665	Ribosome associated factor	Q7CQ00	12.645	6.59	Translation	Ribosome binding
Salmonella Typhimurium str. LT2	*infA*	STM0953	Translation initiation factor IF-1	P69226	8.244	9.22	Translation	RNA binding
Salmonella Typhimurium str. LT2	*infC*	STM1334	Translation initiation factor IF-3	P33321	20.638	9.54	Translation	RNA binding
Salmonella Typhimurium str. LT2	*rplA*	STM4150	50S ribosomal protein L1	P0A2A3	24.713	9.64	Translation	Structural constituent of ribosome
Salmonella Typhimurium str. LT2	*rplC*	STM3440	50S ribosomal protein L3	P60446	22.291	9.79	Translation	Structural constituent of ribosome
Salmonella Typhimurium str. LT2	*rplF*	STM3425	50S ribosomal protein L6	P66313	18.905	9.71	Translation	Structural constituent of ribosome
Salmonella Typhimurium str. LT2	*rplI*	STM4394	50S ribosomal protein L9	Q8ZK80	15.774	6.75	Translation	Structural constituent of ribosome
Salmonella Typhimurium str. LT2	*rplJ*	STM4151	50S ribosomal protein L10	P0A297	17.846	9.04	Translation	Structural constituent of ribosome
Salmonella Typhimurium str. LT2	*rplK*	STM4149	50S ribosomal protein L11	P0A7K0	14.923	9.64	Translation	Structural constituent of ribosome
Salmonella Typhimurium str. LT2	*rplL*	STM4152	50S ribosomal protein L7/L12	P0A299	12.291	4.60	Translation	Structural constituent of ribosome
Salmonella Typhimurium str. LT2	*rplO*	STM3421	50S ribosomal protein L15	P66073	14.957	11.18	Translation	Structural constituent of ribosome
Salmonella Typhimurium str. LT2	*rplQ*	STM3414	50S ribosomal protein L17	Q7CPL7	14.443	11.05	Translation	Structural constituent of ribosome
Salmonella Typhimurium str. LT2	*rplR*	STM3424	50S ribosomal protein L18	Q7CPL6	12.762	10.46	Translation	Structural constituent of ribosome
Salmonella Typhimurium str. LT2	*rplS*	STM2673	50S ribosomal protein L19	P0A2A1	13.122	10.80	Translation	Structural constituent of ribosome
Salmonella Typhimurium str. LT2	*rplX*	STM3429	50S ribosomal protein L24	P60626	11.309	10.21	Translation	Structural constituent of ribosome
Salmonella Typhimurium str. LT2	*rplY*	STM2224	50S ribosomal protein L25	Q7CQ71	10.535	9.52	Translation	Structural constituent of ribosome
Salmonella Typhimurium str. LT2	*rpmB*	STM3728	50S ribosomal protein L28	P0A2A5	9.102	11.42	Translation	Structural constituent of ribosome
Salmonella Typhimurium str. LT2	*rpmC*	STM3432	50S ribosomal protein L29	P66170	7.256	9.98	Translation	Structural constituent of ribosome
Salmonella Typhimurium str. LT2	*rpmD*	STM3422	50S ribosomal protein L30	P0A2A7	6.510	10.96	Translation	Structural constituent of ribosome
Salmonella Typhimurium str. LT2	*rpmE*	STM4096	50S ribosomal protein L31	P66191	7.942	9.51	Translation	Structural constituent of ribosome
Salmonella Typhimurium str. LT2	*rpmG*	STM3727	50S ribosomal protein L33	P0A7P2	6.368	10.25	Translation	Structural constituent of ribosome
Salmonella Typhimurium str. LT2	*rpmH*	STM3839	50S ribosomal protein L34	P0A7P8	5.377	13.00	Translation	Structural constituent of ribosome
Salmonella Typhimurium str. LT2	*rpsA*	STM0981	30S ribosomal protein S1	Q7CQT9	61.250	4.89	Translation	Structural constituent of ribosome
Salmonella Typhimurium str. LT2	*rpsB*	STM0216	30S ribosomal protein S2	P66541	26.799	6.62	Translation	Structural constituent of ribosome
Salmonella Typhimurium str. LT2	*rpsD*	STM3416	30S ribosomal protein S4	O54297	23.528	10.02	Translation	Structural constituent of ribosome
Salmonella Typhimurium str. LT2	*rpsE*	STM3423	30S ribosomal protein S5	P0A7W4	17.592	10.11	Translation	Structural constituent of ribosome
Salmonella Typhimurium str. LT2	*rpsF*	STM4391	30S ribosomal protein S6	P66593	15.163	5.26	Translation	Structural constituent of ribosome
Salmonella Typhimurium str. LT2	*rpsG*	STM3447	30S ribosomal protein S7	P0A2B3	17.579	10.30	Translation	Structural constituent of ribosome
Salmonella Typhimurium str. LT2	*rpsH*	STM3426	30S ribosomal protein S8	P0A7X0	14.175	9.44	Translation	Structural constituent of ribosome
Salmonella Typhimurium str. LT2	*rpsJ*	STM3441	30S ribosomal protein S10	P67904	11.759	9.85	Translation	Structural constituent of ribosome

S1 Table. Continuation.

Organism	Gene	Gene name	Protein	Protein name	MM (KDa)	pI	Process	Function
Salmonella Typhimurium str. LT2	*rpsK*	STM3417	30S ribosomal protein S11	O54296	13.936	11.33	Translation	Structural constituent of ribosome
Salmonella Typhimurium str. LT2	*rpsM*	STM3418	30S ribosomal protein S13	Q8ZLM1	13.210	10.78	Translation	Structural constituent of ribosome
Salmonella Typhimurium str. LT2	*rpsN*	STM3427	30S ribosomal protein S14	P66409	11.658	11.16	Translation	Structural constituent of ribosome
Salmonella Typhimurium str. LT2	*rpsR*	STM4393	30S ribosomal protein S18	Q8ZK81	9.123	10.78	Translation	Structural constituent of ribosome
Salmonella Typhimurium str. LT2	*rpsS*	STM3436	30S ribosomal protein S19	P66491	10.410	10.52	Translation	Structural constituent of ribosome
Salmonella Typhimurium str. LT2	*rpsT*	STM0043	30S ribosomal protein S20	P0A2B1	9.649	11.18	Translation	Structural constituent of ribosome
Salmonella Typhimurium str. LT2	*efp*	STM4334	Elongation factor P	P64036	20.667	4.90	Translation	Translation elongation factor
Salmonella Typhimurium str. LT2	*tsf*	STM0217	Elongation factor Ts	P64052	30.453	5.13	Translation	Translation elongation factor
Salmonella Typhimurium str. LT2	*tufA*	STM3445	Elongation factor Tu	P0A1H5	43.427	5.30	Translation	Translation elongation factor
Salmonella Typhimurium str. LT2	*hisJ*	STM2354	Histidine-binding periplasmic protein	P02910	28.476	6.03	Transport	Amino acid transport
Salmonella Typhimurium str. LT2	*crr*	STM2433	PTS system glucose-specific EIIA component	P0A283	18.236	4.73	Transport	Carbohydrate transport
Salmonella Typhimurium str. LT2	*fruB*	STM2206	Multiphosphoryl transfer protein	P17127	39.569	4.87	Transport	Carbohydrate transport
Salmonella Typhimurium str. LT2	*ptsH*	STM2431	Phosphocarrier protein HPr	P0AA07	9.114	5.65	Transport	Carbohydrate transport
Salmonella Typhimurium str. LT2	*glnH*	STM0830	Glutamine high-affinity transporter	Q7CQW0	27.245	8.44	Transport	Ionotropic glutamate receptor
Salmonella Typhimurium str. LT2	*ftn*	STM1935	Ferritin	Q8ZNU4	19.324	4.89	Transport	Iron ion transport
Salmonella Typhimurium str. LT2	*secB*	STM3701	Protein-export protein SecB	Q7CPH8	17.462	4.26	Transport	Protein transport
Salmonella Typhimurium str. LT2	*ompA*	STM1070	Outer membrane protein A	P02936	37.606	5.60	Transport	Structural molecule
Salmonella Typhimurium str. LT2	*tolC*	STM3186	Outer membrane channel	Q8ZLZ4	53.653	5.42	Transport	Structural molecule
Salmonella Enteritidis	ABA47_0691	ABA47_0691	BssS protein family	A0A1V9AFN8	9.256	4.66	Unclassified	Unclassified
Salmonella sp. str. HMSC13B08	HMPREF 3126_08675	HMPREF 3126_08675	Uncharacterized protein	A0A1F2JWR0	-	-	Unclassified	Unclassified
Salmonella Enteritidis	R567_04560	R567_04560	Uncharacterized protein	A0A1R2IBX3	8.597	10.29	Unclassified	Unclassified
Salmonella Gallinarum str. 287/91	SG1997	SG1997	Uncharacterized protein	B5RBG9	8.584	10.37	Unclassified	Unclassified
Salmonella Typhimurium str. LT2	STM1249	STM1249	Putative periplasmic protein	Q8ZPY8	12.681	6.21	Unclassified	Unclassified
Salmonella Typhimurium str. LT2	*yaeP*	STM0238	UPF0253 protein YaeP	P67551	7.266	4.66	Unclassified	Unclassified
Salmonella Typhimurium str. LT2	*yccJ*	STM1118	Putative cytoplasmic protein	Q8ZQ41	8.684	4.74	Unclassified	Unclassified
Salmonella Typhimurium str. LT2	*ycfF*	STM1205	Uncharacterized protein	Q7CQR0	13.261	5.74	Unclassified	Unclassified
Salmonella Typhimurium str. LT2	*ydfZ*	STM1509	Putative cytoplasmic protein	Q7CQJ6	7.275	9.09	Unclassified	Unclassified
Salmonella Typhimurium str. LT2	*yecF*	STM1949	Putative cytoplasmic protein	Q7CQB7	8.234	4.85	Unclassified	Unclassified
Salmonella Typhimurium str. LT2	*yeeX*	STM2059	UPF0265 protein YeeX	P67605	13.065	9.10	Unclassified	Unclassified
Salmonella Typhimurium str. LT2	*yfcZ*	STM2390	Putative cytoplasmic protein	Q7CQ33	10.281	4.13	Unclassified	Unclassified
Salmonella Typhimurium str. LT2	*yjbR*	STM4251	Putative cytoplasmic protein	Q8ZKH3	13.377	6.05	Unclassified	Unclassified
Salmonella Salamae	-	-	Uncharacterized protein	I3W485	38.615	9.29	Unclassified	Unclassified

CAPÍTULO 4

Novel insights from molecular docking of SdiA from *Salmonella* Enteritidis and *Escherichia coli* with quorum sensing and quorum quenching molecules

Article published in Microbial Pathogenesis

Microbial Pathogenesis 99 (2016) 178–190

Contents lists available at ScienceDirect

Microbial Pathogenesis

journal homepage: www.elsevier.com/locate/micpath

Novel insights from molecular docking of SdiA from *Salmonella* Enteritidis and *Escherichia coli* with quorum sensing and quorum quenching molecules

Felipe Alves de Almeida [a], Uelinton Manoel Pinto [b], Maria Cristina Dantas Vanetti [a, *]

[a] Department of Microbiology, Laboratory of Food Microbiology, Universidade Federal de Viçosa, Viçosa, MG, 36570-900, Brazil
[b] Food Research Center, Department of Food and Experimental Nutrition, Faculty of Pharmaceutical Sciences, Universidade de São Paulo, São Paulo, SP, Brazil

ARTICLE INFO

Article history:
Received 24 May 2016
Received in revised form
4 July 2016
Accepted 22 August 2016
Available online 24 August 2016

Keywords:
1-Octanoyl-*rac*-glycerol
Acyl homoserine lactone
Autoinducer
Furanone
LuxR family proteins
Molecular modeling

ABSTRACT

Quorum sensing is a cell-to-cell communication mechanism leading to differential gene expression in response to high population density. The autoinducer-1 (AI-1) type quorum sensing system is incomplete in *Escherichia coli* and *Salmonella* due to the lack of the AI-1 synthase (LuxI homolog) responsible for acyl homoserine lactone (AHL) synthesis. However, these bacteria encode the AHL receptor SdiA (a LuxR homolog) leading to gene regulation in response to AI-1 produced by other bacteria. This study aimed to model the SdiA protein of *Salmonella enterica* serovar Enteritidis PT4 578 based on three crystallized SdiA structures from Enterohemorrhagic *E. coli* (EHEC) with different ligands. Molecular docking of these predicted structures with AHLs, furanones and 1-octanoyl-*rac*-glycerol were also performed. The available EHEC SdiA structures provided good prototypes for modeling SdiA from *Salmonella*. The molecular docking of these proteins showed that residues Y63, W67, Y71, D80 and S134 are common binding sites for different quorum modulating signals, besides being conserved among other LuxR type proteins. We also show that AHLs with twelve carbons presented better binding affinity to SdiA than AHLs with smaller side chains in our docking analysis, regardless of the protein structures used. Interestingly, the conformational changes provided by AHL binding resulted in structural models with increased affinities to brominated furanones. These results suggest that the use of brominated furanones to inhibit phenotypes controlled by quorum sensing in *Salmonella* and EHEC may present a good strategy since these inhibitors seem to specifically compete with AHLs for binding to SdiA in both pathogens.

1. Introduction

Quorum sensing is a mechanism of communication among cells leading to differential gene expression in response to changes in population density [1,2]. In phylum Proteobacteria, a pair of proteins LuxI (acyl homoserine lactone synthase) and LuxR (transcription activator) or their homologous proteins is responsible for this mechanism in which LuxI derivatives synthesizes the autoinducer-1 (AI-1) called *N*-acyl homoserine lactones (AHLs) [1,3–5]. Some proteobacteria belonging to the family Enterobacteriaceae, such as *Escherichia coli* and *Salmonella*, do not synthesize AHL due to the absence of LuxI homologues. However, these microorganisms encode a transcription factor of the LuxR family, named SdiA [6], which responds to AHLs produced by other bacterial species and synthetic AHLs [7–11]. In this regard, quorum sensing in *Salmonella* and *E. coli* resembles the paracrine signaling found in mammalian systems [12].

In AI-1 type quorum sensing system, when the population reaches a high density, the AHLs are internalized and bind to the ligand-binding domain (LBD) of the LuxR type proteins which dimerize and bind to DNA by using their DNA-binding domain (DBD) regulating expression of target genes [13–16]. In *Salmonella*, AHLs regulate phenotypes such as adhesion to HeLa cells, biofilm formation on polystyrene, invasion of HEp-2 epithelial cells and survival in rabbit and guinea pig serum [17–19]. Similarly in *E. coli*, these molecules regulate adhesion to HEp-2 epithelial cells, biofilm formation on polystyrene and resistance to acidic pH [20–22].

* Corresponding author.
E-mail address: mvanetti@ufv.br (M.C.D. Vanetti).

http://dx.doi.org/10.1016/j.micpath.2016.08.024
0882-4010/

On the other hand, there have been reports of phenotypes regulated by SdiA protein in the absence of AHLs in *Salmonella* and *E. coli* [8,10,16,23,24]. For instance, SdiA of Enterohemorrhagic *E. coli* O157:H7 (EHEC) is constitutively activated by the binding of molecule 1-octanoyl-*rac*-glycerol (OCL) in the absence of AHLs [16]. The OCL molecule is a monoglycerol present in prokaryotes and eukaryotes and is used as an energy source, and substrate for the synthesis of membrane and a signaling molecule [25,26]. However, the activation of SdiA from EHEC by AHLs conferred greater stability and affinity to DNA, albeit not affecting *sdiA* gene transcription [16]. Additionally, these authors observed conformational changes of EHEC SdiA protein complexed with different ligands such as: OCL in the absence of AHLs; *N*-(3-oxo-hexanoyl)-L-homoserine lactone (3-oxo-C6-HSL) and; *N*-(3-oxo-octanoyl)-L-homoserine lactone (3-oxo-C8-HSL). More studies are needed to elucidate the exact functions of AHLs on the physiology of these microorganisms since a great level of complexity is seen as revealed by these previous works.

The structures of SdiA protein of EHEC crystallized with different ligands contain information about the atomic coordinates, structural factors, ligands and cofactors [16]. For this reason, these structures become interesting prototypes for the modeling of SdiA protein from *Salmonella* which has not been crystallized yet, and subsequently conduct studies of molecular docking with quorum sensing and quorum quenching molecules.

Molecular docking and protein modeling prediction are commonly used in quorum sensing studies in the search for auto-inducer and inhibitors as well as to predict their binding sites [27–41]. Gnanendra et al. [30] performed molecular modeling of *Salmonella enterica* serovar Typhimurium SdiA protein by using the structure of CviR from *Chromobacterium violaceum*, which was the available model at the time. These authors then used molecular docking to predict the AHL binding sites. Gnanendra et al. [32] also conducted a molecular docking study with halogenated AHLs, suggesting that those could be potential quorum sensing inhibitors in *Salmonella* Typhimurium.

Furanones are AHL antagonistic compounds in gram-negative bacteria, since they present structural similarity to these auto-inducers due to the homoserine lactone ring, but hinder transcriptional regulation by a mechanism still not fully understood [42–48]. The inhibitory effect of different brominated and non-brominated furanones on biofilm formation by *Salmonella* Typhimurium [47], *Salmonella enterica* serovar Agona [48] and *Salmonella enterica* serovar Enteritidis [19] has been reported as well as their effect on biofilm formation and motility in *E. coli* [49].

In the present study, SdiA protein of *Salmonella* Enteritidis PT4 578 has been modeled on the basis of three crystallized SdiA structures from EHEC with different ligands. We then performed molecular docking of these different structures with OCL, AHLs and furanones in order to predict their binding affinity and to identify the potential binding residues. Due to the importance of the phenotypes regulated by AHLs in *Salmonella* and EHEC, this study provides insights for the guided search for quorum sensing inhibitors as well as contributes to the understanding of the inhibitor and autoinducer binding mechanisms in *Salmonella* Enteritidis.

2. Materials and methods

The experimental strategy employed in this study in order to create the SdiA molecular model of *Salmonella* Enteritidis, from available EHEC SdiA crystal structures, and to evaluate the molecular docking of different quorum sensing and quorum quenching molecules is depicted on Fig. 1 and fully described herein.

2.1. Target amino acid sequence of SdiA protein

The amino acid sequence of SdiA of *Salmonella enterica* serovar Enteritidis PT4 578 (GenBank: AGZ95694.1 [50]) was obtained from the National Centre for Biotechnology Information database (NCBI; http://www.ncbi.nlm.nih.gov/).

2.2. Search of homologous proteins to Salmonella Enteritidis SdiA

The tools "BLAST" and "Find and Model Structure" of the CLC Drug Discovery Workbench 2.5 software (http://www.clcbio.com/products/clc-drug-discovery-workbench/) were used to search homologous amino acid sequences with the SdiA protein of *Salmonella* Enteritidis PT4 578 (GenBank: AGZ95694.1) in the RCSB Protein Data Bank database (PDB; http://www.rcsb.org/pdb/home/home.do). The five parameters: resolution (Å), free R-value, E-value, percentage of identity and coverage were evaluated in this step. The amino acid sequences of proteins with more than 50% identity were extracted and aligned by "ClustalW" tool of the CLC Drug Discovery Workbench 2.5 software.

2.3. Molecular modeling and validation of Salmonella Enteritidis SdiA protein

The molecular modeling of SdiA protein of *Salmonella* Enteritidis was performed by the CLC Drug Discovery Workbench 2.5 software based on the protein with the higher percentage of convergence. The structures of *Salmonella* Enteritidis PT4 578 modeled from EHEC were identified with their template code of PDB plus the letter "S". Then, the generated macromolecular structure of SdiA protein of *Salmonella* Enteritidis (4Y13-S, 4Y15-S and 4Y17-S) and its template from EHEC (PDB: 4Y13, 4Y15 and 4Y17 [16]) were superposed and validated by using three different approaches. First we validated the structures by using the Ramachandran Plot Analysis (RAMPAGE [51]) at Crystallography and Biocomputing Group of the University of Cambridge, Department of Biochemistry server (http://mordred.bioc.cam.ac.uk/~rapper/rampage.php), then at the Verify3D [52], and finally by ERRAT [53] at Structure Analysis and Verification server version 4 (SAVES server; http://services.mbi.ucla.edu/SAVES/).

2.4. Comparison the generated macromolecular structure of SdiA protein with its template

The generated macromolecular structures of SdiA protein of *Salmonella* Enteritidis and their templates of EHEC [16] were superposed to compare the ligand-binding domain (LBD) and the DNA-binding domain (DBD).

2.5. Amino acid conservation of SdiA proteins

The amino acid sequences of SdiA protein of *Salmonella* Enteritidis PT4 578 (GenBank: AGZ95694.1) and EHEC (UniProtKB: Q8XBD0) were aligned by "ClustalW" tool of the CLC Drug Discovery Workbench 2.5 software.

2.6. Molecular docking of SdiA proteins with different molecules

The molecular docking of SdiA proteins of *Salmonella* Enteritidis and EHEC were performed with quorum sensing and quorum quenching molecules (Table 1) by using the "Dock Ligands" tool of the CLC Drug Discovery Workbench 2.5 software, with 1000 interactions for each ligand being performed. The generated score mimics the potential energy change when the protein and the ligand come together based on hydrogen bonds, metal ions and

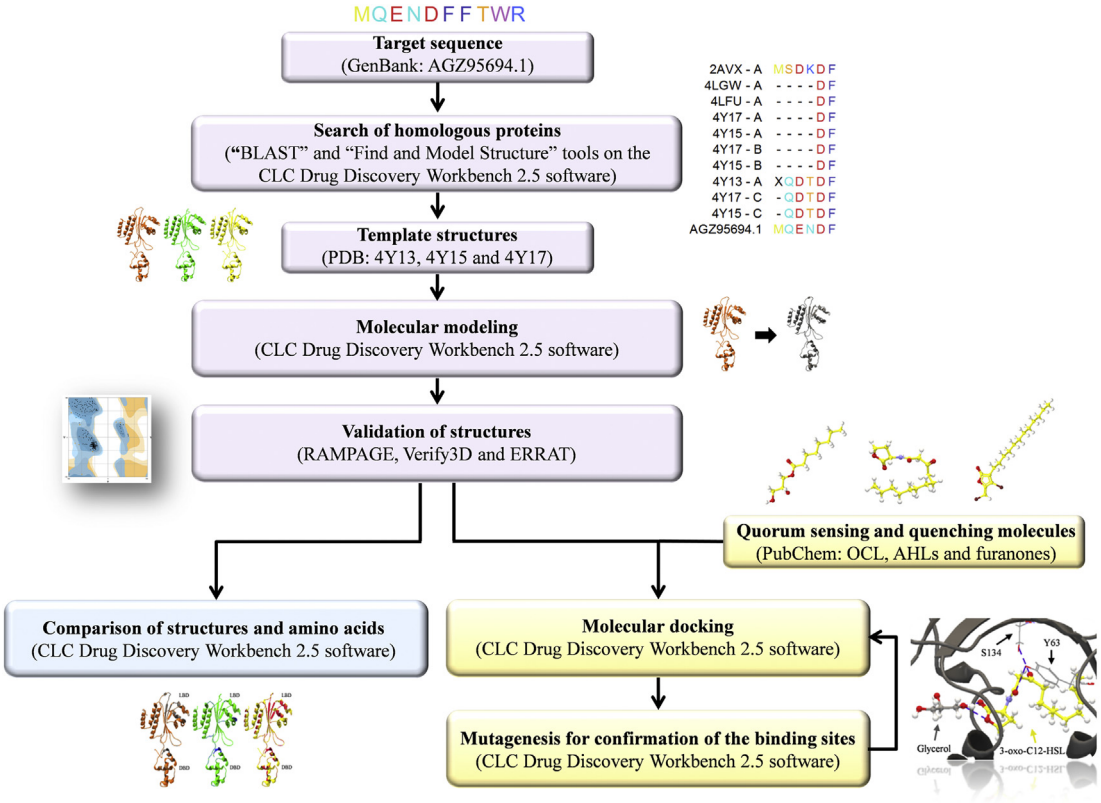

Fig. 1. Experimental strategy used to evaluate the molecular docking of SdiA from *Salmonella* Enteritidis and *Escherichia coli* with quorum modulating molecules. Different steps are color coded as: purple - molecular modeling, blue - comparison of the structures and the amino acid sequences and, yellow - molecular docking. The databases, tools and softwares used in the different steps are indicated in brackets. (For interpretation of the references to colour in this figure legend, the reader is referred to the web version of this article.)

steric interactions, where lower scores (more negative) correspond to higher binding affinities. The five best scores of the docking were used in each macromolecular structure, allowing the inspection of the binding sites of SdiA with ligands and cofactors.

2.7. Mutagenesis prediction of SdiA binding sites

An *in silico* leucine scanning mutagenesis was performed for each binding site of SdiA proteins with ligands and cofactors in the CLC Drug Discovery Workbench 2.5 software. Mutated proteins were docked with quorum sensing and quorum quenching molecules by using the above described software in order to confirm the binding sites as performed in previous studies [54–56].

3. Results and discussion

3.1. SdiA homologous proteins

The search for homologous proteins to the SdiA protein of *Salmonella* Enteritidis PT4 578 (GenBank: AGZ95694.1) by the "Find and Model Structure" and "BLAST" tools showed that 10 proteins from the PDB database have more than 63.7% identity, all of which are SdiA proteins from *E. coli* (Table 2). It is noteworthy that *Salmonella* SdiA structure is not available in the PDB database. The amino acid sequences of the C chains of 4Y15 and 4Y17 structures and the A chain of 4Y13 structure of EHEC had the highest percentage of coverage, 99.58%, and greater than 69.04% identity with SdiA protein of *Salmonella* Enteritidis PT4 578 (Table 2). This result was confirmed by alignment of the amino acid sequences of all proteins listed in Table 1 (please see Fig. S1, supplementary material). Gnanendra et al. [30] previously showed that the A chain of CviR, a LuxR type protein from *C. violaceum* (PDB: 3QP5), was the sequence available at that time with the most homology to SdiA protein of *Salmonella* Typhimurium, exhibiting 40% identity and E-value of 4e-15 by "BLASTP" tool.

Thus, the A chain of 4Y13 structure and the C chains of 4Y15 and 4Y17 structures of EHEC were selected for the molecular modeling of SdiA protein of *Salmonella* Enteritidis because they had the highest percentage of coverage, providing more refined information about the atomic coordinates, structural factors, ligands and cofactors. These structures are SdiA protein of EHEC (UniProtKB: Q8XBD0) complexed with different ligands. For instance, 4Y13 structure is bound to OCL; the 4Y15 structure is bound to 3-oxo-C6-HSL; and the 4Y17 structure is bound to 3-oxo-C8-HSL [16].

3.2. Molecular modeling and validation of SdiA predicted structures

The generated macromolecular structures of SdiA protein of *Salmonella* Enteritidis from molecular modeling were superposed to the respective template of EHEC, which showed a good alignment of both the LBD in *N*-terminal end and DBD in C-terminal end (Fig. 2). Furthermore, these structures were validated by checking the stereo chemical parameters with three softwares: RAMPAGE, Verify3D and ERRAT (Table 3). The Ramachandran Plot Analysis showed that more than 95.9% of the residues of all structures analyzed were in favored region (Table 3 and Fig. 3). In addition, all the structures had more than 85.7% of the amino acid residues with scores greater than or equal to 0.2 in the Verify3D (Table 3). These results indicate that there is compatibility between an atomic model (3D) with its own amino acid sequence (1D) by assigning a structural class based on its location, environment and comparing the results to good structures [52].

Table 1
Quorum sensing and quorum quenching molecules used in the molecular docking of SdiA proteins.

Group	Type	Molecule	IUPAC nomenclature	PubChem CID[a]	Reference
OCL	–	1-octanoyl-*rac*-glycerol	2,3-dihydroxypropyl octanoate	3033877	[16]
AHL	Unmodified in 3-oxo	*N*-butyryl-DL-homoserine lactone	*N*-(2-oxooxolan-3-yl)butanamide	443433	[44]
		N-hexanoyl-DL-homoserine lactone	*N*-(2-oxooxolan-3-yl)hexanamide	3462373	[19,44,50]
		N-octanoyl-DL-homoserine lactone	*N*-(2-oxooxolan-3-yl)octanamide	3474204	[19,44,50]
		N-decanoyl-DL-homoserine lactone	*N*-(2-oxooxolan-3-yl)decanamide	11644562	[19,44,50]
		N-dodecanoyl-DL-homoserine lactone	*N*-(2-oxooxolan-3-yl)dodecanamide	11565426	[19,50]
	Modified in 3-oxo	*N*-(3-oxohexanoyl)-L-homoserine lactone	3-oxo-*N*-[(3S)-2-oxooxolan-3-yl]hexanamide	688505	[16,44,45,64]
		N-(3-oxooctanoyl)-L-homoserine lactone	3-oxo-*N*-[(3S)-2-oxooxolan-3-yl]octanamide	127293	[16,44]
		N-(3-oxodecanoyl)-L-homoserine lactone	3-oxo-*N*-[(3S)-2-oxooxolan-3-yl]decanamide	10221060	[44]
		N-(3-oxododecanoyl)-L-homoserine lactone	3-oxo-*N*-[(3S)-2-oxooxolan-3-yl]dodecanamide	3246941	[64]
Furanone	Non-brominated	3-methyl-2(5H)-furanone	3-Methyl-2(5H)-furanone	30945	[19]
		3-butyl-2(5H)-furanone	4-butyl-2H-furan-5-one	11768654	[47]
		2-methyl tetrahydro-3-furanone	2-methyloxolan-3-one	18522	[19]
		2,2-dimethyl-3(2H)-furanone	2,2-dimethylfuran-3-one	147604	[19]
		2(5H)-furanone	2H-furan-5-one	10341	[19]
	Brominated	4-bromo-5-(bromomethylene)-2(5H)-furanone	4-bromo-5-(bromomethylidene)furan-2-one	67228456	[45,47,64]
		5-bromomethylene-2(5H)-furanone	5-(bromomethylidene)furan-2-one	67228360	[44,45,47,64]
		5-dibromomethylene-2(5H)-furanone	5-(dibromomethylidene)furan-2-one	315069	[47]
		3-ethyl-5-(dibromomethylene)furan-2(5H)-one	5-(dibromomethylidene)-3-ethylfuran-2-one	11140550	[47]
		4-bromo-3-butyl-5-(dibromomethylene)furan-2(5H)-one	4-bromo-3-butyl-5-(dibromomethylidene)furan-2-one	362385	[47]
		4-bromo-5-(bromomethylene)-3-ethyl-2(5H)-furanone	(5Z)-4-bromo-5-(bromomethylidene)-3-ethylfuran-2-one	12051732	[47]
		4-bromo-5-(bromomethylene)-3-butyl-2(5H)-furanone	(5Z)-4-bromo-5-(bromomethylidene)-3-butylfuran-2-one	9839657	[47]
		4-bromo-5-(bromomethylene)-3-hexyl-2(5H)-furanone	(5Z)-4-bromo-5-(bromomethylidene)-3-hexylfuran-2-one	16127328	[47]
		4-bromo-5-(bromomethylene)-3-octyl-2(5H)-furanone	(5Z)-4-bromo-5-(bromomethylidene)-3-octylfuran-2-one	52950214	[47]
		4-bromo-5-(bromomethylene)-3-decyl-2(5H)-furanone	(5Z)-4-bromo-5-(bromomethylidene)-3-decylfuran-2-one	52946441	[47]
		4-bromo-5-(bromomethylene)-3-dodecyl-2(5H)-furanone	(5Z)-4-bromo-5-(bromomethylidene)-3-dodecylfuran-2-one	10180544	[47]

International Union of Pure and Applied Chemistry (IUPAC).
1-octanoyl-*rac*-glycerol (OCL).
Acyl homoserine lactone (AHL).
[a] Compound Identifier of PubChem database (PubChem CID; https://pubchem.ncbi.nlm.nih.gov/).

Moreover, all the structures showed a threshold higher than the cut off of 91% in ERRAT, except the generated 4Y15-S structure of SdiA protein from *Salmonella* that showed 87.0% of the protein above the acceptable limit (Table 3). Gnanendra et al. [30] considered values of 92.6% at Verify3D and 73.2% at ERRAT as reliable and with good quality in the validation of generated structure of SdiA protein of *Salmonella* Typhimurium based on the CviR protein from *C. violaceum*. Furthermore, the results of the structures of SdiA of EHEC used as template in molecular modeling of the present study are in agreement with those found by Nguyen et al. [16]. Thus, all the results of validation by Ramachandran Plot Analysis, Verify-3D and ERRAT confirm that the generated macromolecular structures of SdiA from *Salmonella* Typhimurium and their templates were acceptable to be used in further studies.

3.3. Comparison the generated macromolecular structures of SdiA proteins with their templates

All the generated macromolecular structures of the SdiA protein of *Salmonella* Enteritidis (Fig. 4A and B) and their EHEC templates (Fig. 4C and D) were superposed separately. These superpositions showed that the LBD and DBD had slight conformational changes depending upon the presence or absence of AHL, as well as in relation to the size of the AHL carbon chain (Fig. 4). These results corroborate with those found for the same protein of EHEC [16] and for TraR, another LuxR type protein [57,58]. In addition, Nguyen et al. [16] showed the conformational change of DBD of SdiA protein of EHEC in the presence of AHLs increased its stability and affinity for DNA. In fact, they showed that this stability and DNA affinity were even greater for AHLs with longer carbon chains. However, these authors reported that the conformation of the DBD in the presence of OCL and the absence of AHLs is also capable of regulating gene expression, confirming previous studies performed in the absence of AHLs [8,10,23,24,59,60].

3.4. Amino acid conservation of SdiA proteins

The amino acid sequences of SdiA protein of *Salmonella* Enteritidis PT4 578 and EHEC were aligned (Fig. 5). This comparison showed that 71.66% (172) of the amino acid residues were conserved between SdiA protein of *Salmonella* Enteritidis and EHEC. Besides, many of these conserved residues were also described as conserved among other LuxR type proteins participating in interactions between the domains of these proteins (Fig. 5) [6,16,30,50,61]. In addition, 15 amino acid residues were described by Gnanendra et al. [30], Yao et al. [62] and Nguyen et al. [16] as binding sites for different ligands between SdiA protein of *Salmonella* Enteritidis, *E. coli* and EHEC, respectively (Fig. 5). However, only the residues W67, Y71, and D80 were common binding sites among these studies while residue Y63 was common among *E. coli* studies. Moreover, it is noteworthy that the binding of OCL in the SdiA protein of EHEC may be mediated by glycerol as a cofactor [16].

Table 2
SdiA homologous proteins to *Salmonella* Enteritidis PT4 578 obtained from PDB database.

Number PDB	Chain	Protein complex	Organism	Resolution (Å)	Free R-value	Tools				
						"BLAST"		"Find and model structure"		
						E-value	% Identity	E-value	% Identity	% Coverage
4Y15	C	SdiA in complex with 3-oxo-C6-homoserine lactone	EHEC	2.84	0.25	2.20e-109	71.55	1.34e-129	71.55	99.58
4Y17	C	SdiA in complex with 3-oxo-C8-homoserine lactone	EHEC	2.84	0.27	2.38e-109	71.55	1.83e-129	71.55	99.58
4Y13	A	SdiA in complex with 1-octanoyl-*rac*-glycerol	EHEC	3.10	0.24	4.58e-103	69.04	1.10e-122	69.04	99.58
4Y15	B	SdiA in complex with 3-oxo-C6-homoserine lactone	EHEC	2.84	0.25	1.25e-108	72.03	9.22e-129	72.03	98.33
4Y17	B	SdiA in complex with 3-oxo-C8-homoserine lactone	EHEC	2.84	0.27	1.25e-108	72.03	9.22e-129	72.03	98.33
4Y15	A	SdiA in complex with 3-oxo-C6-homoserine lactone	EHEC	2.84	0.25	1.56e-108	72.03	1.04e-128	72.03	98.33
4Y17	A	SdiA in complex with 3-oxo-C8-homoserine lactone	EHEC	2.84	0.27	1.56e-108	72.03	1.04e-128	72.03	98.33
4LFU	A	Crystal structure of *Escherichia coli* SdiA in the space group C2	*E. coli*	2.26	0.28	1.62e-108	72.03	1.30e-128	72.03	98.33
4LGW	A	Crystal structure of *Escherichia coli* SdiA in the space group P6522	*E. coli*	2.70	0.27	1.35e-108	72.03	1.49e-128	72.03	98.33
2AVX	A	Solution structure of *E. coli* SdiA1-171	*E. coli*	Pending	Pending	3.48e-67	63.74	3.41e-78	63.74	71.25

3.5. Molecular docking of SdiA proteins of Salmonella Enteritidis and EHEC

The generated 4Y13-S structure of SdiA protein of *Salmonella* Enteritidis modeled from the SdiA protein of EHEC complexed with OCL, in the absence of AHL, showed the highest binding affinity to *N*-(3-oxododecanoyl)-L-homoserine lactone (3-oxo-C12-HSL) with a score of −70.32 (Table 4). This molecule bound to Y63 and S134 residues of the protein and with glycerol (Fig. 6A). The molecules with greater affinity to this structure were AHLs with twelve carbons with or without 3-oxo modification, followed by AHLs with ten and eight carbons (Table 4). These data corroborate those found by Campos-Galvão et al. [19] that showed enhanced biofilm formation by *Salmonella* Enteritidis PT4 578 growing in the presence of 50 nM of AHLs with six, eight, ten and twelve carbons. However, the effect of *N*-dodecanoyl-DL-homoserine lactone (C12-HSL) on this phenotype was statistically higher than the other AHLs evaluated. Gnanendra et al. [30] showed that 3-oxo AHLs with six carbons had higher binding affinities to SdiA of *Salmonella* Typhimurium when compared AHLs with eight carbons without 3-oxo modification. This result might reflect the use of CviR structure by those authors when modeling SdiA, since CviR is more specific to AHLs with shorter carbon side chains, which would likely interfere in the modeled SdiA structure. We, however, have modeled *Salmonella* SdiA from a more conserved protein from EHEC which supposedly generates a more robust model. Moreover, Gnanendra et al. [30] showed that the R60, W67, Y71, D80 and W95 residues were conserved binding sites of the different AHLs unlike what we have observed in this study, where the Y63 residue was the most conserved (Table 4).

The brominated furanones with twelve, ten, eight, six and four carbons had higher scores in relation to all other furanones (Table 4). Furthermore, four out of five non-brominated furanones bound to W67 residue of 4Y13-S structure *Salmonella* Enteritidis PT4 578 (Table 4). Campos-Galvão et al. [19] showed that when a mixture of four non-brominated furanones was added concurrently with C12-HSL, biofilms by *Salmonella* Enteritidis PT4 578 were not observed. Thus, the results of the molecular docking showed that three of these four furanones used by Campos-Galvão et al. [19] bound in the modeled 4Y13-S structure of SdiA protein of *Salmonella* Enteritidis. This result indicates a competition between the AHL and furanones for the W67 residue which is a common binding site for these molecules, despite furanones havin lower score than C12-HSL. Similar results were found by Yang et al. [27] and Husain et al. [41] in which the molecular docking of LasR of *Pseudomonas aeruginosa* presented free binding energy higher with 3-oxo-C12-HSL than with quorum sensing inhibiting compounds such as chlorzoxazone, ceftazidime, nifuroxazide, and salicylic acid.

Corroborating our previous results, the 4Y15-S and 4Y17-S structures of SdiA protein of *Salmonella* Enteritidis PT4 578 modeled from the SdiA protein of EHEC complexed with 3-oxo-C6-HSL and 3-oxo-C8-HSL showed a similar pattern of binding affinities to the molecules evaluated in comparison with 4Y13-S structure (Table 4). The modeled 4Y15-S and 4Y17-S *Salmonella* structures also showed higher binding affinities to AHL with twelve carbons, such as −85.00 between 4Y15-S structure and C12-HSL and −86.30 between 4Y17-S structure and 3-oxo-C12-HSL (Table 4). The molecules with the second highest score affinity to these structures were brominated furanones with twelve carbons, followed by those AHL with ten, eight and six carbons and finally OCL (Table 4). In addition, the W67 and Y71 residues were the most common binding sites for brominated furanones in these structures (Table 4). Thus, the conformational changes of 4Y15-S and 4Y17-S structures of *Salmonella* Enteritidis resulting from the binding with AHLs resulted in structures with higher predicted affinities to brominated furanones. This is likely due to optimization of the binding site in the presence of AHL which forms a tight pocket in these structures as compared with that model with OCL which would show an open chamber formation in the absence of AHL [16] and possibly not perfectly accommodating the bulky inhibitor. The Y63, W67, Y71, D80 and S134 residues were common binding sites when the five best scores of each molecule resulting from molecular docking with the three structures of SdiA protein of *Salmonella* Enteritidis were compared (Table 4). The only difference was the presence of glycerol in the 4Y13-S structure as a binding site, which may bind at Q72 residue. Gnanendra et al. [30] also showed by molecular docking that the R60, W67, Y71, D80, V82, L83, W95 and V119 residues of modeled structure of SdiA protein of *Salmonella* Typhimurium were binding sites of different AHLs. Thus, the W67, Y71 and D80 residues are common binding sites between that and

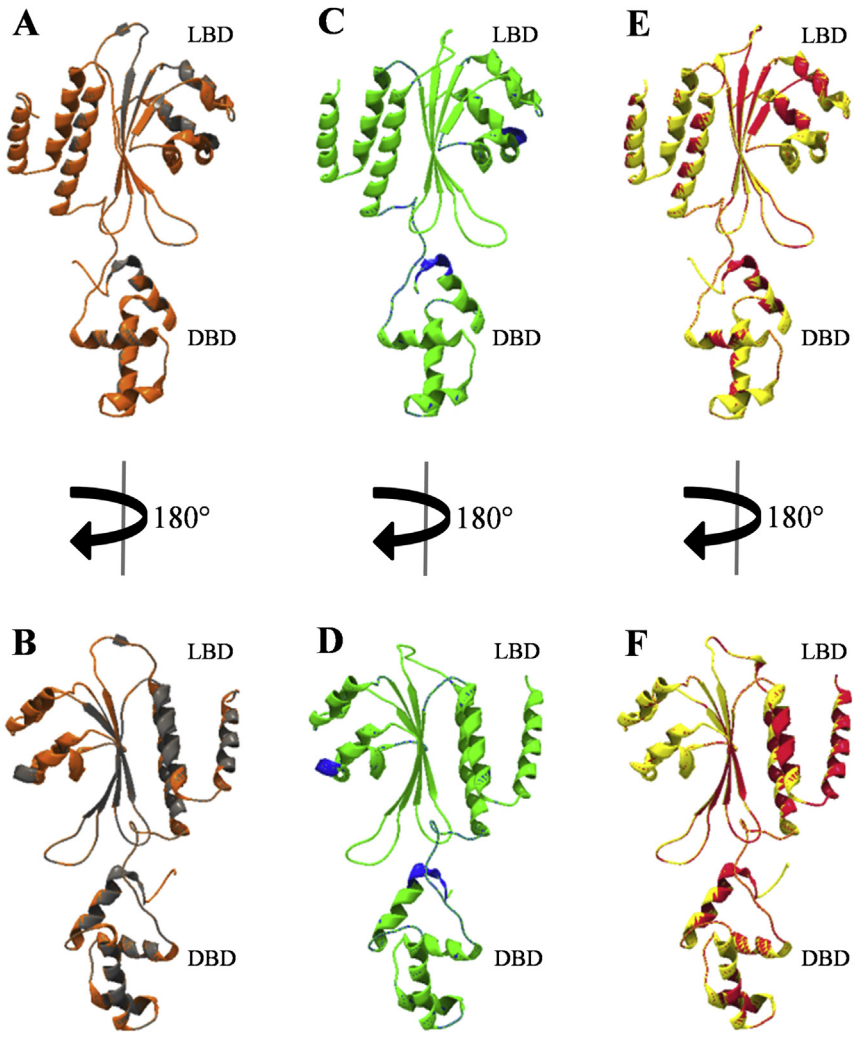

Fig. 2. Superposition of the generated macromolecular structures of SdiA protein of *Salmonella* Enteritidis PT4 578 with their respective templates of EHEC. The structures 4Y13-S of *Salmonella* Enteritidis (gray) and 4Y13 of EHEC (orange) (**A** and **B**), the structures 4Y15-S of *Salmonella* Enteritidis (blue) and 4Y15 of EHEC (green) (**C** and **D**), and the structures 4Y17-S of *Salmonella* Enteritidis (pink) and 4Y17 of EHEC (yellow) (**E** and **F**). Ligand-binding domain (LBD); DNA-binding domain (DBD). (For interpretation of the references to colour in this figure legend, the reader is referred to the web version of this article.)

Table 3
Validation of the generated macromolecular structures of SdiA proteins and their templates of EHEC.

Organism	Structure [a]	Chain	Ramachandran plot analysis			Verify3D (%) [d]	ERRAT (%) [e]
			Residues in the region (%)				
			Favored [b]	Allowed [c]	Outlier		
Salmonella Enteritidis PT4 578	4Y13-S	A	96.2	3.8	0.0	89.17	92.672
Salmonella Enteritidis PT4 578	4Y15-S	C	97.7	2.1	0.0	93.31	87.013
Salmonella Enteritidis PT4 578	4Y17-S	C	97.0	3.0	0.0	92.89	91.775
EHEC	4Y13	A	95.9	4.1	0.0	85.78	95.413
EHEC	4Y15	C	98.3	1.7	0.0	89.58	91.379
EHEC	4Y17	C	95.9	3.7	0.4	91.36	91.845

[a] The structures of *Salmonella* Enteritidis PT4 578 modeled from EHEC were identified with their template code of PDB plus the letter "S".
[b] Approximately 98.0% expected.
[c] Approximately 2.0% expected.
[d] At least 80% of the amino acid residues with score $\geq$ 0.2 indicating compatibility between an atomic model (3D) with its own amino acid sequence (1D) [52].
[e] Expressed as the percentage of the protein for which the calculated error value falls below the 95% rejection limit. Good high resolution structures generally produce values around 95% or higher. For lower resolutions (2.5 to 3 Å) the average overall quality factor is around 91% [53].

the present study. These residues would present great targets for site directed mutagenesis studies.

The 4Y13, 4Y15 and 4Y17 structures of SdiA proteins of EHEC used as templates in this study showed the highest binding affinity to 3-oxo-C12-HSL with scores of −75.66, −82.30 and −86.16, respectively (Table 5). This molecule bound to S43 and S134

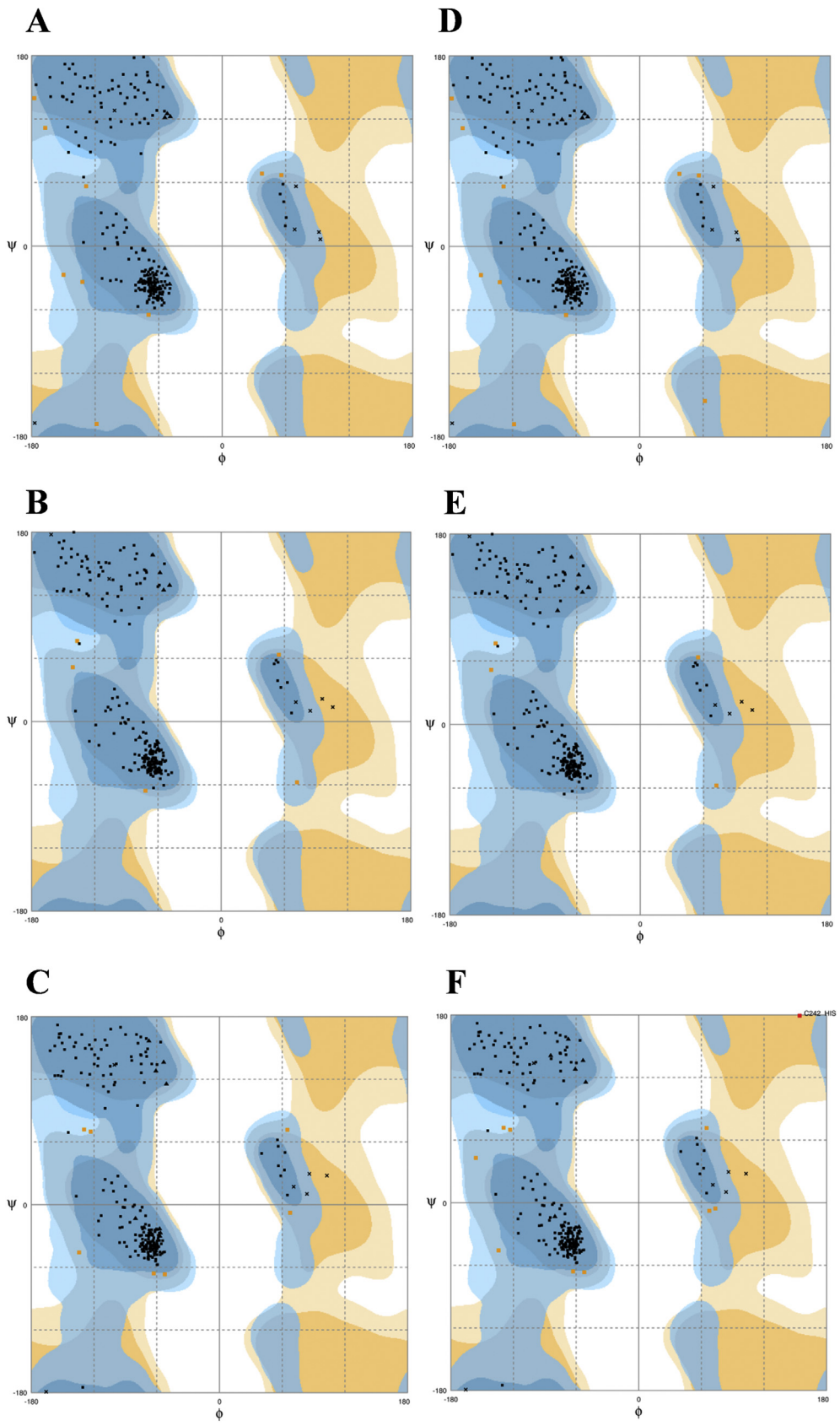

Fig. 3. Ramachandran Plot Analysis of the generated macromolecular structures of SdiA protein of *Salmonella* Enteritidis PT4 578: A chain of 4Y13-S structure **(A)**, C chain of 4Y15-S structure **(B)**, C chain of 4Y17-S structure **(C)** and their templates of EHEC: A chain of 4Y13 structure **(D)**, C chain of 4Y15 structure **(E)**, C chain of 4Y17 structure **(F)**. Black square with dark blue background, general amino acid in favored region; black triangle with dark blue background, pre and pro-proline in favored region; black cross with dark pink background, glycine in favored region; orange square with light blue background, general amino acid in allowed region; orange triangle with light blue background, pre and pro-proline in allowed region; orange cross with light pink background, glycine in allowed region; Red square or triangle or cross, general amino acid or pre and pro-proline or glycine in outlier region, respectively. (For interpretation of the references to colour in this figure legend, the reader is referred to the web version of this article.)

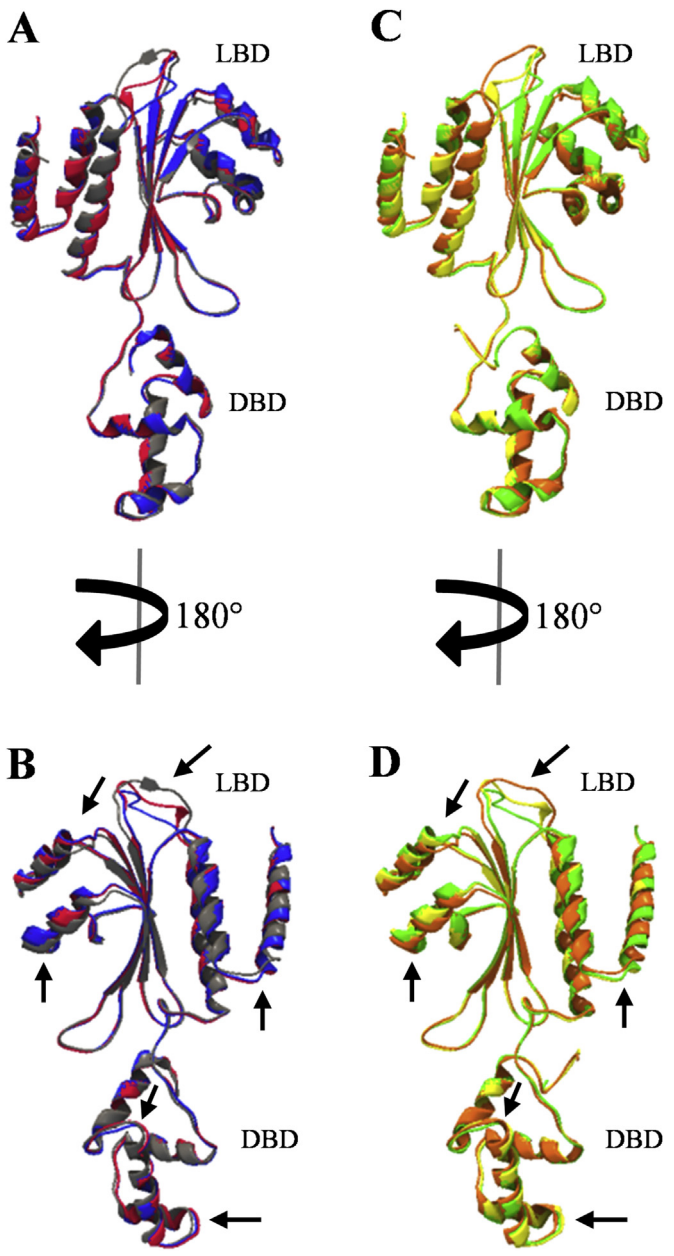

Fig. 4. Superposition of all the generated macromolecular structures of SdiA protein of *Salmonella* Enteritidis PT4 578 and their templates of EHEC separately. The 4Y13-S (gray), 4Y15-S (blue) and 4Y17-S (pink) structures of *Salmonella* (**A** and **B**), and 4Y13 (orange), 4Y15 (green) and 4Y17 (yellow) structure of EHEC (**C** and **D**). Ligand-binding domain (LBD); DNA-binding domain (DBD); Black arrows show conformational changes. (For interpretation of the references to colour in this figure legend, the reader is referred to the web version of this article.)

residues of the protein and with glycerol bounded at Q72 residue (Fig. 6B). Moreover, the S43, Y63, W67, D80 and S134 residues of 4Y15 and 4Y17 structures were common binding sites for 3-oxo-C12-HSL (Table 5). In addition, the binding affinity of the AHLs by 4Y13 structure of SdiA protein of EHEC was similar to 4Y13-S structure of SdiA protein of *Salmonella* Enteritidis (Table 5). Differently, Kim et al. [61] showed that the binding affinity of C8-HSL to SdiA of *E. coli* is stronger than that of C4-HSL and C10-HSL. Furthermore, only one brominated furanone and another non-brominated furanone were not predicted to bind to EHEC SdiA (Table 5).

The molecules with greater binding affinities to 4Y15 and 4Y17 structures of EHEC SdiA were AHLs with twelve and ten carbons with or without 3-oxo modification as well as brominated furanones with twelve and ten carbons, following by same molecules with eight carbons and OCL (Table 5). Moreover, the conformational changes of 4Y15 and 4Y17 structures of EHEC resulting from the binding with AHLs also increased the affinity to brominated furanones as observed in *Salmonella* Enteritidis predicted structures. The S43, Y63, W67, Y71, D80 and S134 residues were common binding sites when comparing the five best scores of each molecule resulting from the molecular docking with the three structures of SdiA protein of EHEC (Table 5). Yao et al. [62] showed that the Y63, W67, Y71, D80 and W95 residues of SdiA protein of the *E. coli* were binding sites for C8-HSL. Moreover, Nguyen et al. [16] also showed that the S43, F59, T61, Y63, W67, Y71, L77, D80, W107 and S134 residues of SdiA protein of the EHEC were binding sites for different AHLs and OCL, with Y63 being the most specific and presenting the highest affinity. Thus, all binding residues found in this study corroborate with those described Yao et al. [62] and Nguyen et al. [16]. In addition, we show that AHLs with longer acyl chains may also be good activators of SdiA in EHEC, and to our knowledge, this has not been tested. Interestingly, AHLs with longer chain are more stable in slightly alkaline environment such as that found in the gut where these microorganisms cause infection [63]. It would be interesting to test whether EHEC SdiA responds to C12-HSL or 3-oxo-C12-HSL as *Salmonella* does.

In general, the comparison of molecular docking results of different structures of SdiA protein of *Salmonella* Enteritidis and EHEC with the results of Gnanendra et al. [30], Yao et al. [62] and Nguyen et al. [16] showed that the W67, Y71 and D80 residues are common binding sites for different quorum sensing and quorum quenching molecules. In addition, the Y63 and S134 residues are common binding sites for SdiA proteins as described by Nguyen et al. [16], as well as the Y63 residue for Yao et al. [62]. Furthermore, these residues are conserved among many LuxR type proteins [6,16,30,50,61].

3.6. Site directed mutagenesis of predicted binding sites of the SdiA

All SdiA residues of *Salmonella* Enteritidis and EHEC found as binding sites for OCL, AHLs and furanones were point mutated to leucine residues. Then, new molecular docking for each mutant protein was performed and we finally showed that the signaling molecules did not bind to the proteins with mutated residues. These results confirm that the Y63, W67, Y71, Q72, D80 and S134 residues of the SdiA protein of *Salmonella* Enteritidis are binding sites for quorum sensing and quenching molecules (Fig. 7A and B). In EHEC, the S43, Y63, W67, Y71, Q72, D80, R111, F132 and S134 residues were also confirmed as binding sites in this mutagenic approach (Fig. 7C and D).

4. Conclusion

We have shown that the available structures of SdiA protein of EHEC provided good prototypes for modeling SdiA from *Salmonella* Enteritidis PT4 578. The molecular docking of these proteins showed that the Y63, W67, Y71, D80 and S134 residues are common binding sites for different quorum sensing and quorum quenching molecules and these residues are conserved among LuxR type proteins. In addition, the S43 residue of EHEC SdiA is a common binding site, but this residue is not conserved. The AHLs with twelve carbons have better binding affinities to SdiA, regardless of the evaluated structure. The models generated from SdiA bound to AHLs presented increased affinity to brominated furanones, indicating strong possibility for competition for binding to SdiA among

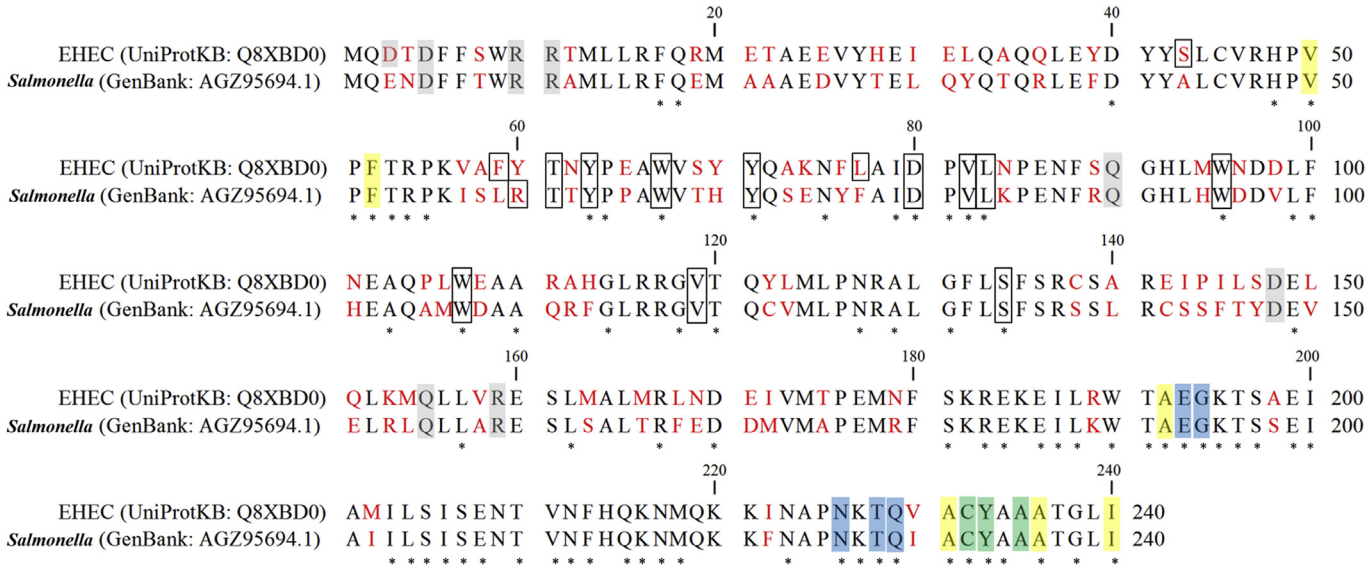

Fig. 5. Alignment of the amino acid sequences of SdiA protein of *Salmonella* Enteritidis PT4 578 (GenBank: AGZ95694.1) and EHEC (UniProtKB: Q8XBD0). Black letter, conserved amino acid residue; Red letter, non-conserved amino acid residue; asterisk, conserved amino acid residue between LuxR family protein described by Ahmer et al. [6], Gnanendra et al. [30], Kim et al. [61], Nguyen et al. [16] and Campos-Galvão et al. [50]; Gray background, amino acid residues involved in the interaction between two LBD described by Nguyen et al. [16]; Blue background, amino acid residue involved in the interaction between two DBD described by Nguyen et al. [16]; Yellow background, amino acid residue involved in the interaction between LBD-DBD described by Nguyen et al. [16]; Green background, amino acid residue involved in the interaction between DBD-DBD and LBD-DBD described by Nguyen et al. [16]; Boxed residue, amino acid residue involved in the interaction between LBD-ligand described by Gnanendra et al. [30], Yao et al. [62] and Nguyen et al. [16]. Ligand-binding domain (LBD); DNA-binding domain (DBD). (For interpretation of the references to colour in this figure legend, the reader is referred to the web version of this article.)

Table 4
Results from molecular docking of generated macromolecular structures of SdiA protein of *Salmonella* Enteritidis PT4 578 with quorum sensing and quorum quenching molecules.

Molecule	Generated macromolecular structures of SdiA protein of *Salmonella* Enteritidis								
	4Y13-S			4Y15-S			4Y17-S		
	Binding residue	Score	Rank	Binding residue	Score	Rank	Binding residue	Score	Rank
***N*-(3-oxododecanoyl)-L-homoserine lactone**	**Y63, S134, Glycerol**	**−70.32**	**1**	Y71, S134	−83.28	3	**Y63, W67, D80, S134**	**−86.30**	**1**
***N*-dodecanoyl-DL-homoserine lactone**	Y63, W67	−69.67	2	**Y63, W67, S134**	**−85.00**	**1**	Y63, W67, D80	−83.89	3
N-decanoyl-DL-homoserine lactone	Y71	−69.29	3	Y63, W67, S134	−80.68	4	W67, S134	−80.05	4
N-(3-oxodecanoyl)-L-homoserine lactone	Y63, W67, D80, S134	−66.76	4	Y63, W67, S134	−79.21	5	W67, S134	−78.85	5
N-(3-oxooctanoyl)-L-homoserine lactone	Y63	−65.65	5	Y63, W67, Y71, D80, S134	−72.13	7	Y63, W67, Y71, D80	−72.03	7
N-octanoyl-DL-homoserine lactone	Y63	−64.26	6	Y63, W67, D80, S134	−71.34	8	Y63, W67, D80	−70.89	8
1-octanoyl-*rac*-glycerol	W67, D80, Glycerol	−60.82	7	Y63, D80, S134	−62.16	11	Y63, D80	−62.94	11
4-bromo-5-(bromomethylene)-3-decyl-2(5H)-furanone	Y71	−60.55	8	Y71	−76.82	6	Y71	−74.48	6
4-bromo-5-(bromomethylene)-3-hexyl-2(5H)-furanone	W67	−60.50	9	W67	−64.85	10	W67	−63.59	10
4-bromo-5-(bromomethylene)-3-octyl-2(5H)-furanone	S134	−59.40	10	Y71	−66.33	9	Y71	−68.29	9
3-butyl-2(5H)-furanone	W67	−57.55	11	–	–	–	–	–	–
N-(3-oxohexanoyl)-L-homoserine lactone	Y63	−57.39	12	Y63, W67	−60.66	12	Y63, W67	−60.71	12
N-hexanoyl-DL-homoserine lactone	Y63, W67	−56.38	13	Y63, W67	−60.42	13	Y63, W67, D80	−60.50	13
4-bromo-5-(bromomethylene)-3-dodecyl-2(5H)-furanone	Glycerol (Q72)	−55.52	14	Y71	−83.51	2	Y71	−84.02	2
4-bromo-3-butyl-5-(dibromomethylene)furan-2(5H)-one	W67	−53.62	15	W67	−58.39	14	W67	−57.69	14
4-bromo-5-(bromomethylene)-3-butyl-2(5H)-furanone	W67	−52.17	16	Y71	−53.49	15	W67	−54.61	15
N-butyryl-DL-homoserine lactone	Y63	−45.43	17	–	–	–	–	–	–
5-bromomethylene-2(5H)-furanone	W67	−35.45	18	–	–	–	–	–	–
3-methyl-2(5H)-furanone	W67	−35.14	19	–	–	–	–	–	–
2(5H)-furanone	W67	−31.41	20	–	–	–	–	–	–
2-methyl tetrahydro-3-furanone	W67	−30.14	21	–	–	–	–	–	–
4-bromo-5-(bromomethylene)-2(5H)-furanone	–	–	–	Y71	−40.87	16	Y71	−42.32	16
4-bromo-5-(bromomethylene)-3-ethyl-2(5H)-furanone	–	–	–	–	–	–	–	–	–
5-dibromomethylene-2(5H)-furanone	–	–	–	–	–	–	–	–	–
3-ethyl-5-(dibromomethylene)furan-2(5H)-one	–	–	–	–	–	–	–	–	–
2,2-dimethyl-3(2H)-furanone	–	–	–	–	–	–	–	–	–
All binding residues of the five best score	Y63, W67, Y71, D80, S134, Glycerol (Q72), Glycerol			Y63, W67, Y71, D80, S134			Y63, W67, Y71, D80, S134		

No binding (–). The best result of all in bold.

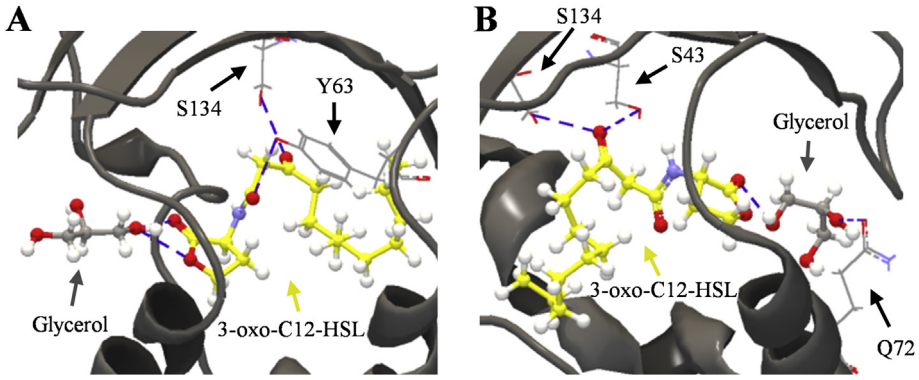

Fig. 6. Representative inspection of the binding sites the 4Y13-S structure of SdiA protein of *Salmonella* Enteritidis PT4 578 **(A)** and the 4Y13 structure of EHEC **(B)** with 3-oxo-C12-HSL and glycerol. Black arrow, the binding sistes; Gray arrow, glycerol; Yellow arrow, 3-oxo-C12-HSL; Blue dashed line, hydrogen bond. (For interpretation of the references to colour in this figure legend, the reader is referred to the web version of this article.)

Table 5
Results from molecular docking of macromolecular structures of SdiA protein of EHEC with quorum sensing and quenching molecules.

Molecule	Macromolecular structures of SdiA protein of EHEC								
	4Y13			4Y15			4Y17		
	Binding residue	Score	Rank	Binding residue	Score	Rank	Binding residue	Score	Rank
***N*-(3-oxododecanoyl)-L-homoserine lactone**	**S43, S134, Glycerol (Q72)**	**−75.66**	**1**	**S43, Y63, W67, D80, S134**	**−82.30**	**1**	**S43, Y63, W67, D80, S134**	**−86.16**	**1**
N-(3-oxodecanoyl)-L-homoserine lactone	S43, S134, Glycerol (Q72)	−72.78	2	S43, Y63, W67, D80, S134	−77.65	4	S43, Y63, W67, D80	−80.46	3
N-dodecanoyl-DL-homoserine lactone	Y63, D80, Glycerol (R111)	−72.17	3	Y63, W67, D80	−81.88	2	Y63, W67, D80	−85.53	2
N-decanoyl-DL-homoserine lactone	Y71	−72.13	4	Y63, W67, D80, S134	−78.04	3	Y63, W67, D80	−79.25	4
N-(3-oxooctanoyl)-L-homoserine lactone	S43, Y63	−67.96	5	S43, Y63, W67, D80	−70.13	7	S43, Y63, W67	−71.22	7
N-octanoyl-DL-homoserine lactone	Y63	−67.12	6	Y63, W67, S134	−68.68	8	Y63	−69.04	9
1-octanoyl-*rac*-glycerol	W67, D80, Glycerol (R111)	−63.20	7	W67, Y71, D80	−60.52	11	Y71, D80	−61.86	11
4-bromo-5-(bromomethylene)-3-dodecyl-2(5H)-furanone	S43	−62.19	8	W67	−72.98	5	W67	−78.97	5
4-bromo-5-(bromomethylene)-3-octyl-2(5H)-furanone	W67	−60.84	9	W67	−65.90	9	S43	−71.19	8
4-bromo-5-(bromomethylene)-3-decyl-2(5H)-furanone	W67	−60.68	10	S43	−72.58	6	S43	−78.75	6
4-bromo-5-(bromomethylene)-3-hexyl-2(5H)-furanone	W67	−60.52	11	W67	−60.54	10	S43	−59.95	12
N-(3-oxohexanoyl)-L-homoserine lactone	Y63, W67, Glycerol (Q72)	−60.24	12	S43, Y63, W67	−60.28	12	S43, Y63, W67	−61.96	10
N-hexanoyl-DL-homoserine lactone	Glycerol (Q72)	−58.12	13	Y63, W67	−58.46	13	Y63, W67	−59.87	13
4-bromo-3-butyl-5-(dibromomethylene)furan-2(5H)-one	W67	−57.01	14	–	–	–	–	–	–
4-bromo-5-(bromomethylene)-3-butyl-2(5H)-furanone	W67	−56.17	15	–	–	–	–	–	–
3-butyl-2(5H)-furanone	W67	−49.75	16	–	–	–	Q72	−52.42	14
N-butyryl-DL-homoserine lactone	S43	−48.33	17	S43, Y71	−45.81	14	–	–	–
3-methyl-2(5H)-furanone	Glycerol (Q72)	−38.01	18	–	–	–	–	–	–
5-dibromomethylene-2(5H)-furanone	W67	−37.99	19	S43	−40.41	17	S43	−40.02	18
2,2-dimethyl-3(2H)-furanone	Glycerol (Q72)	−37.32	20	–	–	–	S43	−33.27	20
4-bromo-5-(bromomethylene)-2(5H)-furanone	Glycerol (Q72)	−36.64	21	S43	−40.52	16	S43	−41.03	17
5-bromomethylene-2(5H)-furanone	W67	−34.62	22	S43	−34.30	18	Q72	−36.60	19
2(5H)-furanone	Glycerol (Q72)	−33.43	23	–	–	–	Q72	−32.02	21
2-methyl tetrahydro-3-furanone	Glycerol (Q72)	−32.61	24	S43	−29.58	19	–	–	–
4-bromo-5-(bromomethylene)-3-ethyl-2(5H)-furanone	–	–	–	S43	−45.04	15	S43	−48.77	15
3-ethyl-5-(dibromomethylene)furan-2(5H)-one	–	–	–	–	–	–	S43	−47.99	16
All binding residues of the five best score	S43, Y63, W67, Y71, Q72, D80, S134, Glycerol (Q72 and R111)			S43, Y63, W67, Y71, Q72, D80, F132, S134			S43, Y63, W67, Y71, D80, S134		

No binding (–). The best result of all in bold.

these molecules. Therefore, brominated furanones may be used to inhibit phenotypes controlled by quorum sensing in *Salmonella* and EHEC whenever external AHLs are present, since these inhibitors may compete with AHLs for binding to SdiA. The modeled protein from *Salmonella* as well as the approach here described may be used to test different types of quorum sensing inhibitors and guide future laboratory works.

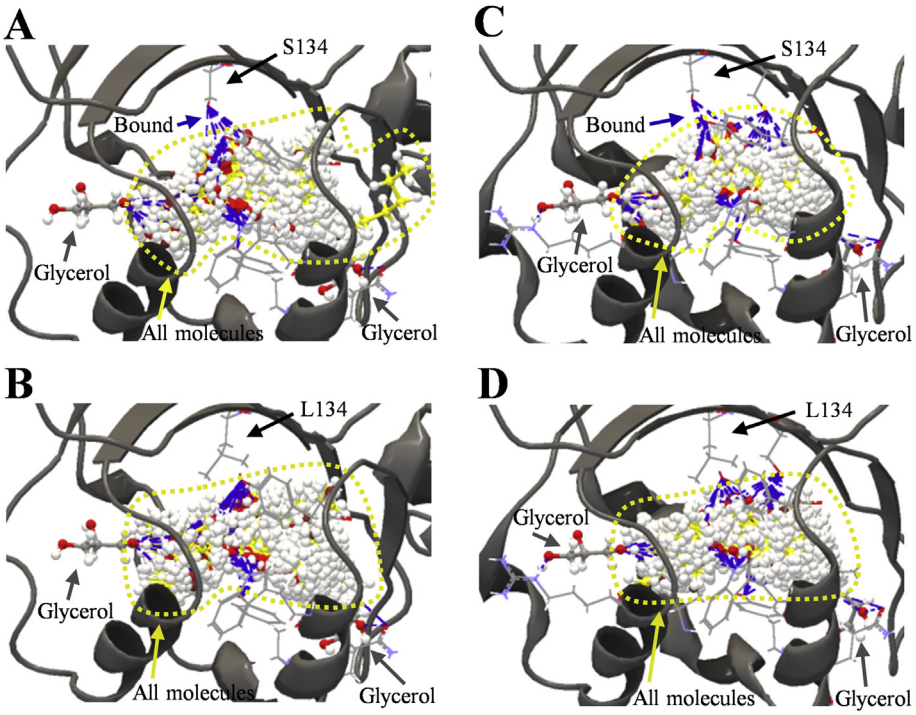

Fig. 7. Representative confirmation of the S134 residue of the 4Y13-S structure of SdiA proteins of *Salmonella* Enteritidis PT4 578 **(A** and **B)** and the 4Y13 structure of EHEC **(C** and **D)** as binding site of different molecules by *in silico* leucine scanning mutagenesis followed by new molecular docking. Black arrow, S134 or L134 residue; Gray arrow, glycerol; Yellow arrow and yellow dashed line, quorum sensing and quorum quenching molecules; Blue arrow, hydrogen bond between S134 residue and evaluated molecules. (For interpretation of the references to colour in this figure legend, the reader is referred to the web version of this article.)

Acknowledgements

Felipe Alves de Almeida was supported by a fellowship from Conselho Nacional de Desenvolvimento Científico e Tecnológico (CNPq) and this research has been supported by Fundação de Amparo à Pesquisa do Estado de Minas Gerais (FAPEMIG) and by Coordenação de Aperfeiçoamento de Pessoal de Nível Superior (CAPES). The authors acknowledge the CLC bio of the QIAGEN Company by license of the CLC Drug Discovery Workbench 2.5 software. UMP acknowledges the support from CNPq process number (457794/2014-3) for his research.

Appendix A. Supplementary data

Supplementary data related to this article can be found at http://dx.doi.org/10.1016/j.micpath.2016.08.024.

References

[1] W.C. Fuqua, S.C. Winans, E.P. Greenberg, Quorum sensing in bacteria: the LuxR-LuxI family of cell density-responsive transcriptional regulators, J. Bacteriol. 176 (1994) 269–275.
[2] U.M. Pinto, K.M. Pappas, S.C. Winans, The ABCs of plasmid replication and segregation, Nat. Rev. Microbiol. 10 (2012) 755–765, http://dx.doi.org/10.1038/nrmicro2882.
[3] H.B. Kaplan, E.P. Greenberg, Diffusion of autoinducer is involved in regulation of the *Vibrio fischeri* luminescence system, J. Bacteriol. 163 (1985) 1210–1214.
[4] J.P. Pearson, C. van Delden, B.H. Iglewski, Active efflux and diffusion are involved in transport of *Pseudomonas aeruginosa* cell-to-cell signals, J. Bacteriol. 181 (1999) 1203–1210.
[5] R.J. Case, M. Labbate, S. Kjelleberg, AHL-driven quorum-sensing circuits: their frequency and function among the Proteobacteria, ISME J. 2 (2008) 345–349, http://dx.doi.org/10.1038/ismej.2008.13.
[6] B.M. Ahmer, J. van Reeuwijk, C.D. Timmers, P.J. Valentine, F. Heffron, *Salmonella* Typhimurium encodes an SdiA homolog, a putative quorum sensor of the LuxR family, that regulates genes on the virulence plasmid, J. Bacteriol. 180 (1998) 1185–1193.
[7] B. Michael, J.N. Smith, S. Swift, F. Heffron, B.M.M. Ahmer, SdiA of *Salmonella enterica* is a LuxR homolog that detects mixed microbial communities, J. Bacteriol. 183 (2001) 5733–5742, http://dx.doi.org/10.1128/JB.183.19.5733-5742.2001.
[8] J.N. Smith, B.M.M. Ahmer, Detection of other microbial species by *Salmonella*: expression of the SdiA regulon, J. Bacteriol. 185 (2003) 1357–1366, http://dx.doi.org/10.1128/JB.185.4.1357-1366.2003.
[9] J.N. Smith, J.L. Dyszel, J.A. Soares, C.D. Ellermeier, C. Altier, S.D. Lawhon, et al., SdiA, an N-acylhomoserine lactone receptor, becomes active during the transit of *Salmonella enterica* through the gastrointestinal tract of turtles, PLoS One 3 (2008) e2826, http://dx.doi.org/10.1371/journal.pone.0002826.
[10] J.L. Dyszel, J.A. Soares, M.C. Swearingen, A. Lindsay, J.N. Smith, B.M.M. Ahmer, *E. coli* K-12 and EHEC genes regulated by SdiA, PLoS One 5 (2010) e8946, http://dx.doi.org/10.1371/journal.pone.0008946.
[11] A. Sabag-Daigle, B.M.M. Ahmer, ExpI and PhzI are descendants of the long lost cognate signal synthase for SdiA, PLoS One 7 (2012) e47720, http://dx.doi.org/10.1371/journal.pone.0047720.
[12] B.A. Doganer, L.K.Q. Yan, H. Youk, Autocrine signaling and quorum sensing: extreme ends of a common spectrum, Trends Cell Biol. 26 (2016) 262–271, http://dx.doi.org/10.1016/j.tcb.2015.11.002.
[13] N.C. Reading, V. Sperandio, Quorum sensing: the many languages of bacteria, FEMS Microbiol. Lett. 254 (2006) 1–11, http://dx.doi.org/10.1111/j.1574-6968.2005.00001.x.
[14] W.-L. Ng, B.L. Bassler, Bacterial quorum-sensing network architectures, Annu. Rev. Genet. 43 (2009) 197–222, http://dx.doi.org/10.1146/annurev-genet-102108-134304.
[15] U.M. Pinto, S.C. Winans, Dimerization of the quorum-sensing transcription factor TraR enhances resistance to cytoplasmic proteolysis, Mol. Microbiol. 73 (2009) 32–42, http://dx.doi.org/10.1111/j.1365-2958.2009.06730.x.
[16] Y. Nguyen, N.X. Nguyen, J.L. Rogers, J. Liao, J.B. MacMillan, Y. Jiang, et al., Structural and mechanistic roles of novel chemical ligands on the SdiA quorum-sensing transcription regulator, MBio 6 (2015), http://dx.doi.org/10.1128/mBio.02429-14 e02429–14.
[17] L.L. Nesse, K. Berg, L.K. Vestby, I. Olsaker, B. Djønne, *Salmonella* Typhimurium invasion of HEp-2 epithelial cells *in vitro* is increased by N-acylhomoserine lactone quorum sensing signals, Acta Vet. Scand. 53 (2011) 44, http://dx.doi.org/10.1186/1751-0147-53-44.
[18] Z. Liu, F. Que, L. Liao, M. Zhou, L. You, Q. Zhao, et al., Study on the promotion of bacterial biofilm formation by a *Salmonella* conjugative plasmid and the underlying mechanism, PLoS One 9 (2014) e109808, http://dx.doi.org/10.1371/journal.pone.0109808.
[19] M.E.M. Campos-Galvão, A.O.B. Ribon, E.F. Araújo, M.C.D. Vanetti, Changes in the *Salmonella enterica* Enteritidis phenotypes in presence of acyl homoserine lactone quorum sensing signals, J. Basic Microbiol. 55 (2015) 1–9, http://

dx.doi.org/10.1002/jobm.201500471.
[20] R. van Houdt, A. Aertsen, P. Moons, K. Vanoirbeek, C.W. Michiels, N-acyl-L-homoserine lactone signal interception by *Escherichia coli*, FEMS Microbiol. Lett. 256 (2006) 83–89, http://dx.doi.org/10.1111/j.1574-6968.2006.00103.x.
[21] J. Lee, T. Maeda, S.H. Hong, T.K. Wood, Reconfiguring the quorum-sensing regulator SdiA of *Escherichia coli* to control biofilm formation via indole and N-acylhomoserine lactones, Appl. Environ. Microbiol. 75 (2009) 1703–1716, http://dx.doi.org/10.1128/AEM.02081-08.
[22] V.K. Sharma, S.M.D. Bearson, Evaluation of the impact of quorum sensing transcriptional regulator SdiA on long-term persistence and fecal shedding of *Escherichia coli* O157:H7 in weaned calves, Microb. Pathog. 57 (2013) 21–26, http://dx.doi.org/10.1016/j.micpath.2013.02.002.
[23] J.L. Dyszel, J.N. Smith, D.E. Lucas, J.A. Soares, M.C. Swearingen, M.A. Vross, et al., *Salmonella enterica* serovar Typhimurium can detect acyl homoserine lactone production by *Yersinia enterocolitica* in mice, J. Bacteriol. 192 (2010) 29–37, http://dx.doi.org/10.1128/JB.01139-09.
[24] D.T. Hughes, D.A. Terekhova, L. Liou, C.J. Hovde, J.W. Sahl, A.V. Patankar, et al., Chemical sensing in mammalian host-bacterial commensal associations, Proc. Natl. Acad. Sci. U. S. A. 107 (2010) 9831–9836, http://dx.doi.org/10.1073/pnas.1002551107.
[25] H.M. Alvarez, A. Steinbüchel, Triacylglycerols in prokaryotic microorganisms, Appl. Microbiol. Biotechnol. 60 (2002) 367–376, http://dx.doi.org/10.1007/s00253-002-1135-0.
[26] Q. Liu, R.M.P. Siloto, R. Lehner, S.J. Stone, R.J. Weselake, Acyl-CoA:diacylglycerol acyltransferase: molecular biology, biochemistry and biotechnology, Prog. Lipid Res. 51 (2012) 350–377, http://dx.doi.org/10.1016/j.plipres.2012.06.001.
[27] L. Yang, M.T. Rybtke, T.H. Jakobsen, M. Hentzer, T. Bjarnsholt, M. Givskov, et al., Computer-aided identification of recognized drugs as *Pseudomonas aeruginosa* quorum-sensing inhibitors, Antimicrob. Agents Chemother. 53 (2009) 2432–2443, http://dx.doi.org/10.1128/AAC.01283-08.
[28] A. Grosdidier, V. Zoete, O. Michielin, SwissDock, a protein-small molecule docking web service based on EADock DSS, Nucleic Acids Res. 39 (2011) W270–W277, http://dx.doi.org/10.1093/nar/gkr366.
[29] A. Annapoorani, V. Umamageswaran, R. Parameswari, S.K. Pandian, A.V. Ravi, Computational discovery of putative quorum sensing inhibitors against LasR and RhlR receptor proteins of *Pseudomonas aeruginosa*, J. Comput. Aided. Mol. Des. 26 (2012) 1067–1077, http://dx.doi.org/10.1007/s10822-012-9599-1.
[30] S. Gnanendra, S. Anusuya, J. Natarajan, Molecular modeling and active site analysis of SdiA homolog, a putative quorum sensor for *Salmonella* Typhimurium pathogenecity reveals specific binding patterns of AHL transcriptional regulators, J. Mol. Model 18 (2012) 4709–4719, http://dx.doi.org/10.1007/s00894-012-1469-1.
[31] K.S. Musthafa, K. Balamurugan, S.K. Pandian, A.V. Ravi, 2,5-Piperazinedione inhibits quorum sensing-dependent factor production in *Pseudomonas aeruginosa* PAO1, J. Basic Microbiol. 52 (2012) 679–686, http://dx.doi.org/10.1002/jobm.201100292.
[32] S. Gnanendra, S. Mohamed, J. Natarajan, Identification of potent inhibitors for *Salmonella* Typhimurium quorum sensing via virtual screening and pharmacophore modeling, Comb. Chem. High. Throughput Screen 16 (2013) 826–839, http://dx.doi.org/10.2174/1386207311301010003.
[33] S.Y.-Y. Tan, S.-L. Chua, Y. Chen, S.A. Rice, S. Kjelleberg, T.E. Nielsen, et al., Identification of five structurally unrelated quorum-sensing inhibitors of *Pseudomonas aeruginosa* from a natural-derivative database, Antimicrob. Agents Chemother. 57 (2013) 5629–5641, http://dx.doi.org/10.1128/AAC.00955-13.
[34] C.-Y. Chang, T. Krishnan, H. Wang, Y. Chen, W.-F. Yin, Y.-M. Chong, et al., Non-antibiotic quorum sensing inhibitors acting against N-acyl homoserine lactone synthase as druggable target, Sci. Rep. 4 (2014) 1–8, http://dx.doi.org/10.1038/srep07245.
[35] V. Gopu, C.K. Meena, P.H. Shetty, Quercetin influences quorum sensing in food borne bacteria: *in-vitro* and *in-silico* evidence, PLoS One 10 (2015) 1–17, http://dx.doi.org/10.1371/journal.pone.0134684.
[36] H.-S. Kim, S.-H. Lee, Y. Byun, H.-D. Park, 6-Gingerol reduces *Pseudomonas aeruginosa* biofilm formation and virulence via quorum sensing inhibition, Sci. Rep. 5 (2015) 1–11, http://dx.doi.org/10.1038/srep08656.
[37] F.M. Husain, I. Ahmad, M.S. Khan, E. Ahmad, Q. Tahseen, M.S. Khan, et al., Sub-MICs of *Mentha piperita* essential oil and menthol inhibits AHL mediated quorum sensing and biofilm of Gram-negative bacteria, Front. Microbiol. 6 (2015) 1–12, http://dx.doi.org/10.3389/fmicb.2015.00420.
[38] V. Soheili, B.S.F. Bazzaz, N. Abdollahpour, F. Hadizadeh, Investigation of *Pseudomonas aeruginosa* quorum-sensing signaling system for identifying multiple inhibitors using molecular docking and structural analysis methodology, Microb. Pathog. 89 (2015) 73–78, http://dx.doi.org/10.1016/j.micpath.2015.08.017.
[39] A.R. Ponce-Rossi, U.M. Pinto, A.O.B. Ribon, D.M.S. Bazzolli, M.C.D. Vanetti, Quorum sensing regulated phenotypes in *Aeromonas hydrophila* ATCC 7966 deficient in AHL production, Ann. Microbiol. (2016) 1–10, http://dx.doi.org/10.1007/s13213-016-1196-4.
[40] M. Danishuddin, A. Khan, M. Faheem, P. Kalaiarasan, M. Hassan Baig, N. Subbarao, et al., Structure-based screening of inhibitors against KPC-2: designing potential drug candidates against multidrug-resistant bacteria, J. Biomol. Struct. Dyn. 32 (2014) 741–750, http://dx.doi.org/10.1080/07391102.2013.789988.
[41] F.M. Husain, I. Ahmad, M.H. Baig, M.S. Khan, M.S. Khan, I. Hassan, et al., Broad-spectrum inhibition of AHL-regulated virulence factors and biofilms by sub-inhibitory concentrations of ceftazidime, RSC Adv. 6 (2016) 27952–27962, http://dx.doi.org/10.1039/C6RA02704K.
[42] T.B. Rasmussen, M. Manefield, J.B. Andersen, L. Eberl, U. Anthoni, C. Christophersen, et al., How Delisea pulchra furanones affect quorum sensing and swarming motility in *Serratia liquefaciens* MG1, Microbiology 146 (2000) 3237–3244, http://dx.doi.org/10.1099/00221287-146-12-3237.
[43] J. Zhu, S.C. Winans, The quorum-sensing transcriptional regulator TraR requires its cognate signaling ligand for protein folding, protease resistance, and dimerization, Proc. Natl. Acad. Sci. U. S. A. 98 (2001) 1507–1512, http://dx.doi.org/10.1073/pnas.98.4.1507.
[44] M. Hentzer, K. Riedel, T.B. Rasmussen, A. Heydorn, J.B. Andersen, M.R. Parsek, et al., Inhibition of quorum sensing in *Pseudomonas aeruginosa* biofilm bacteria by a halogenated furanone compound, Microbiology 148 (2002) 87–102, http://dx.doi.org/10.1099/00221287-148-1-87.
[45] M. Manefield, T.B. Rasmussen, M. Henzter, J.B. Andersen, P. Steinberg, S. Kjelleberg, et al., Halogenated furanones inhibit quorum sensing through accelerated LuxR turnover, Microbiology 148 (2002) 1119–1127, http://dx.doi.org/10.1099/00221287-148-4-1119.
[46] M. Hentzer, H. Wu, J.B. Andersen, K. Riedel, T.B. Rasmussen, N. Bagge, et al., Attenuation of *Pseudomonas aeruginosa* virulence by quorum sensing inhibitors, EMBO J. 22 (2003) 3803–3815, http://dx.doi.org/10.1093/emboj/cdg366.
[47] J.C.A. Janssens, H. Steenackers, S. Robijns, E. Gellens, J. Levin, H. Zhao, et al., Brominated furanones inhibit biofilm formation by *Salmonella enterica* serovar Typhimurium, Appl. Environ. Microbiol. 74 (2008) 6639–6648, http://dx.doi.org/10.1128/AEM.01262-08.
[48] L.K. Vestby, K.C.S. Johannesen, I.L. Witsø, O. Habimana, A.A. Scheie, A.M. Urdahl, et al., Synthetic brominated furanone F202 prevents biofilm formation by potentially human pathogenic *Escherichia coli* O103: H2 and *Salmonella* ser. Agona on abiotic surfaces, J. Appl. Microbiol. 116 (2014) 258–268, http://dx.doi.org/10.1111/jam.12355.
[49] D. Ren, J.J. Sims, K.T. Wood, Inhibition of biofilm formation and swarming of *Escherichia coli* by (5Z)-4-bromo-5-(bromomethylene)-3-butyl-2(5H)-furanone, Environ. Microbiol. 3 (2001) 731–736, http://dx.doi.org/10.1046/j.1462-2920.2001.00249.x.
[50] M.E.M. Campos-Galvão, T.D.S. Leite, A.O.B. Ribon, E.F. Araújo, M.C.D. Vanetti, A new repertoire of informations about the quorum sensing system in *Salmonella enterica* serovar Enteritidis PT4, Genet. Mol. Res. 14 (2015) 4068–4084, http://dx.doi.org/10.4238/2015.April.27.22.
[51] S.C. Lovell, I.W. Davis, W.B. Arendall, P.I.W. de Bakker, J.M. Word, M.G. Prisant, et al., Structure validation by Cα geometry: phi, psi and Cβ deviation, Proteins 50 (2003) 437–450, http://dx.doi.org/10.1002/prot.10286.
[52] R. Lüthy, J.U. Bowie, D. Eisenberg, Assessment of protein models with three-dimensional profiles, Nature 356 (1992) 83–85, http://dx.doi.org/10.1038/356083a0.
[53] C. Colovos, T.O. Yeates, Verification of protein structures: patterns of nonbonded atomic interactions, Protein Sci. 2 (1993) 1511–1519, http://dx.doi.org/10.1002/pro.5560020916.
[54] C. Lu, L.-Z. Mi, M.J. Grey, J. Zhu, E. Graef, S. Yokoyama, et al., Structural evidence for loose linkage between ligand binding and kinase activation in the epidermal growth factor receptor, Mol. Cell. Biol. 30 (2010) 5432–5443, http://dx.doi.org/10.1128/MCB.00742-10.
[55] J.L. Miller, C.G. Tate, Engineering an ultra-thermostable β1-adrenoceptor, J. Mol. Biol. 413 (2011) 628–638, http://dx.doi.org/10.1016/j.jmb.2011.08.057.
[56] P. Anand, D. Nagarajan, S. Mukherjee, N. Chandra, ABS–Scan: *In silico* alanine scanning mutagenesis for binding site residues in protein–ligand complex, F1000Research 3 (2014) 1–18, http://dx.doi.org/10.12688/f1000research.5165.1.
[57] A. Vannini, C. Volpari, C. Gargioli, E. Muraglia, R. Cortese, R. De Francesco, et al., The crystal structure of the quorum sensing protein TraR bound to its autoinducer and target DNA, EMBO J. 21 (2002) 4393–4401, http://dx.doi.org/10.1093/emboj/cdf459.
[58] R.-G. Zhang, K.M. Pappas, J.L. Brace, P.C. Miller, T. Oulmassov, J.M. Molyneaux, et al., Structure of a bacterial quorum-sensing transcription factor complexed with pheromone and DNA, Nature 417 (2002) 971–974, http://dx.doi.org/10.1038/nature00833.
[59] K. Yamamoto, K. Yata, N. Fujita, A. Ishihama, Novel mode of transcription regulation by SdiA, an *Escherichia coli* homologue of the quorum-sensing regulator, Mol. Microbiol. 41 (2001) 1187–1198, http://dx.doi.org/10.1046/j.1365-2958.2001.02585.x.
[60] N. Abed, O. Grépinet, S. Canepa, G.A. Hurtado-Escobar, N. Guichard, A. Wiedemann, et al., Direct regulation of the *pefI-srgC* operon encoding the Rck invasin by the quorum-sensing regulator SdiA in *Salmonella* Typhimurium, Mol. Microbiol. 94 (2014) 254–271, http://dx.doi.org/10.1111/mmi.12738.
[61] T. Kim, T. Duong, C.A. Wu, J. Choi, N. Lan, S.W. Kang, et al., Structural insights into the molecular mechanism of *Escherichia coli* SdiA, a quorum-sensing receptor, Acta Crystallogr. Sect. D. Biol. Crystallogr. 70 (2014) 694–707, http://dx.doi.org/10.1107/S1399004713032355.
[62] Y. Yao, M.A. Martinez-Yamout, T.J. Dickerson, A.P. Brogan, P.E. Wright, H.J. Dyson, Structure of the *Escherichia coli* quorum sensing protein SdiA: activation of the folding switch by acyl homoserine lactones, J. Mol. Biol. 355 (2006) 262–273, http://dx.doi.org/10.1016/j.jmb.2005.10.041.
[63] E.A. Yates, B. Philipp, C. Buckley, S. Atkinson, S.R. Chhabra, R.E. Sockett, et al.,

N-acylhomoserine lactones undergo lactonolysis in a pH, temperature, and acyl chain length-dependent manner during growth of *Yersinia pseudotuberculosis* and *Pseudomonas aeruginosa*, Infect. Immun. 70 (2002) 5635–5646, http://dx.doi.org/10.1128/IAI.70.10.5635-5646.2002.

[64] H. Wu, Z. Song, M. Hentzer, J.B. Andersen, S. Molin, M. Givskov, et al., Synthetic furanones inhibit quorum-sensing and enhance bacterial clearance in *Pseudomonas aeruginosa* lung infection in mice, J. Antimicrob. Chemother. 53 (2004) 1054–1061, http://dx.doi.org/10.1093/jac/dkh223.

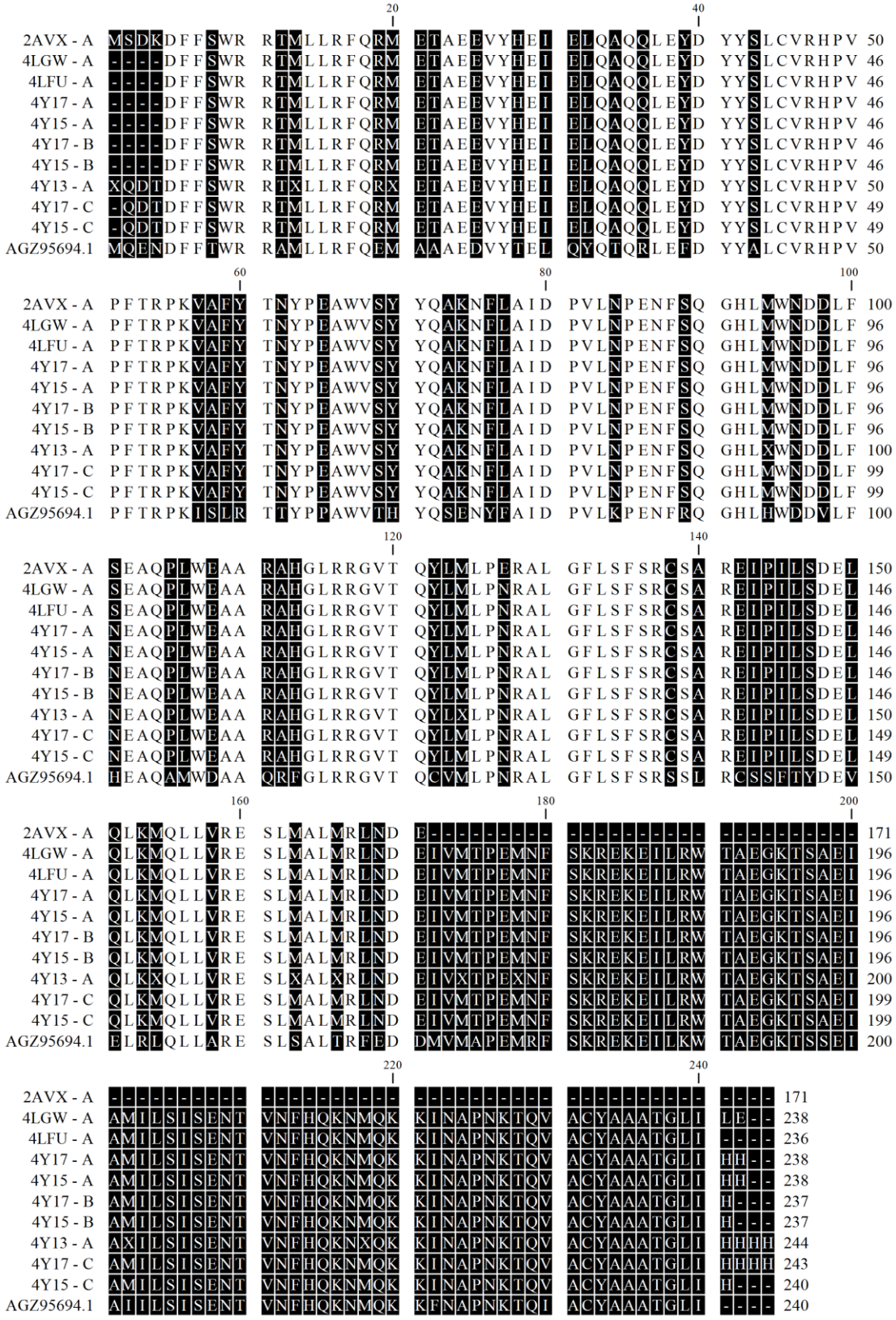

Fig. S1. Alignment of the amino acid sequences of the SdiA proteins at PDB database with more than 50 % identity with the SdiA protein of *Salmonella* Enteritidis PT4 578 (GenBank: AGZ95694.1). White background, conserved amino acid residue; black background, non-conserved amino acid residue; dash, gap.

CAPÍTULO 5

Virtual screening of plant compounds and nonsteroidal anti-inflammatory drugs for inhibition of quorum sensing and biofilm formation in *Salmonella*

Article formatted according to Microbial Pathogenesis

Virtual screening of plant compounds and nonsteroidal anti-inflammatory drugs for inhibition of quorum sensing and biofilm formation in *Salmonella*

Felipe Alves de Almeida[ab], Erika Lorena Giraldo Vargas[a], Deisy Guimarães Carneiro[a], Uelinton Manoel Pinto[c], Maria Cristina Dantas Vanetti[a]*

[a]Department of Microbiology, Universidade Federal de Viçosa, Viçosa - MG, Brazil;

[b]Department of Nutrition, Universidade Federal de Juiz de Fora, Governador Valadares - MG, Brazil;

[c]Food Research Center, Department of Food and Experimental Nutrition, Faculty of Pharmaceutical Sciences, Universidade de São Paulo, São Paulo – SP, Brazil.

*Corresponding author: Department of Microbiology, Universidade Federal de Viçosa, Viçosa – MG, 36570-900, Brazil.

Telephone: + 55 31 3899-2954

E-mail address: mvanetti@ufv.br

Abstract

Salmonella belongs to the Enterobacteriaceae family which is widely distributed in the environment due to its adaptive capacity to stress conditions. In addition, *Salmonella* is able to perform a type of cell-to-cell communication called quorum sensing, which leads to the differential gene expression. The quorum sensing system mediated by AI-1, acyl homoserine lactones (AHLs), is incomplete in *Salmonella* because the *luxI* homolog gene, which encodes for AI-1 synthase, is missing in the genome. However, a homologue of LuxR, known as SdiA, is present and allows the detection of signaling molecules produced by other species of bacteria, leading to the regulation of gene expression, mainly related to virulence and biofilm formation. Thus, in view of the importance of quorum sensing on the physiology regulation of microorganisms, the aim of the present study is to perform a virtual screening of plant compounds and nonsteroidal anti-inflammatory drugs (NASIDs) for inhibition of quorum sensing by molecular docking and biofilm formation in *Salmonella.* In general, most the plant compounds and all NSAIDs bound in, at least, one of the three structures of SdiA proteins of *Salmonella* Enteritidis PT4 578 modeled. In addition, many compounds tested had higher binding affinity than the AHLs and the furanones that are the inducers and inhibitors of the quorum sensing mechanism, respectively. The Z-phytol and lonazolac were good candidates for the *in vitro* tests of inhibition of the quorum sensing by AI-1 and biofilm formation in *Salmonella*. Thus, this study directs future prospecting of plant extracts for inhibition of quorum sensing mechanism depending on AHL and biofilm formation. In addition, the use of inhibitors of quorum sensing and biofilm formation can be combined with antibiotics for better treatment efficacy as well as the use of these compounds to design new drugs.

Keywords: anti-biofilm; lonazolac; quorum quenching; SdiA protein; Z-phytol.

1. Introduction

Salmonella belongs to the Enterobacteriaceae family which is widely distributed in the environment due to its adaptive capacity to stress conditions. This characteristic is related to the virulence factors that, in most cases, are coded in regions of the bacterial genome denominated Pathogenicity Islands (SPIs) [1-3]. In addition, *Salmonella* is able to perform a type of cell-to-cell communication called quorum sensing, which leads to the differential gene expression [4-8]. In *Salmonella,* there are different quorum sensing mechanisms depending on the type of signaling molecule used. These signaling molecules are also known as autoinducers (AIs) and the three main types used by *Salmonella* are AI-1, AI-2 and AI-3 [9, 10].

The quorum sensing system mediated by AI-1, acyl homoserine lactones (AHLs), is incomplete in *Salmonella* because the *luxI* homolog gene, which encodes for AI-1 synthase, is missing in the genome. However, a homologue of LuxR, known as SdiA, is present and allows the detection of signaling molecules produced by other species of microorganisms, leading to the regulation of gene expression [11-13].

Liu et al. [14] showed that the addition of *N*-octanoyl-DL-homoserine lactone (C8-HSL) associated with the presence of pRST98 plasmid in *Salmonella enterica* serovar Typhi, which contains the *rck* gene, increased its adhesion in HeLa cells and biofilm formation in polystyrene. Abed et al. [15] also showed that the promoter region of the *rck* operon, located on the *S. enterica* serovar Typhimurium ATCC 14018 plasmid, is regulated by the SdiA protein in the presence of AHL. The *hilA*, *invA* and *invF* genes of SPI-1 of *S. enterica* serovar Enteritidis PT4, and *glgC*, *fliF*, *lpfA* and *fimF* which are genes involved in biofilm formation were most expressed in the presence of *N*-dodecanoyl homoserine lactone (C12-AHL) [16]. The C12-HSL also increased abundance of the PheT, HtpG, PtsI, TalB, PmgI, Eno, PykF and Adi proteins and decreased the abundance of OmpA, OmpC, OmpD, GapA, Tsf, RpsB, RplE and RplB

proteins, besides altering the consumption of formate [17]. In addition, biofilm formation after 36 h of culturing in the presence of C12-HSL induced biofilm on polystyrene, under anaerobic conditions by this pathogen [16, 18].

Thus, in view of the importance of quorum sensing on the physiology regulation of microorganisms, the search for inhibitors of this mechanism became a research target. Molecules known as furanones were the first inhibitors of quorum sensing discovered and present similar structures to AHLs [19-25]. Almeida et al. [26] demonstrated, by molecular docking, that the non-brominated and brominated furanones can bind to the SdiA proteins of *Salmonella* Enteritidis and Enterohemorrhagic *Escherichia coli* (EHEC). Biofilm formation by *Salmonella* Enteritidis which was shown to be induced by C12-HSL, was then inhibited by a mixture of non-brominated furanones if added concomitantly [16, 18]. Additionally, when different furanones were added without signaling molecules, biofilm formation by *Salmonella* Typhimurium [23] and *S. enterica* serovar Agona [24] was also inhibited.

Plant compounds with quorum sensing inhibitory activity also known as quorum quenching have become an intense target of research [27-48]. Kumar et al. [36] showed that ginger compounds such as [6]-gingerol and [6]-shogaol inhibited quorum sensing in *Chromobacterium violaceum* and *Pseudomonas aeruginosa*. In addition, Kim et al. [34] showed that [6]-gingerol bound to LasR protein (homologous to LuxR) of *P. aeruginosa* by molecular docking.

Additionally, substances used in the medical field for other purposes, such as nonsteroidal anti-inflammatory drugs (NSAIDs), have been studied in relation to their ability to inhibit the quorum sensing [28, 45, 48, 49-52]. El-Mowafy et al. [49] showed by molecular docking that aspirin bound to LasR protein of *P. aeruginosa*. Soheili et al. [51] also used the same tool to search for NSAIDs capable of binding to LasR protein of

P. aeruginosa and suggested that piroxicam and meloxicam have anti-quorum sensing potential for this microorganism.

Thus, the aim of the present study is to perform a virtual screening of plant compounds and nonsteroidal anti-inflammatory drugs (NASIDs) for inhibition of quorum sensing and biofilm formation in *Salmonella.*

2. Materials and methods

The experimental strategy employed in this study for virtual screening of plant compounds and nonsteroidal anti-inflammatory drugs (NSAIDs) for inhibition of quorum sensing by AI-1 and biofilm formation by *Salmonella* is depicted on Fig. 1 and fully described herein.

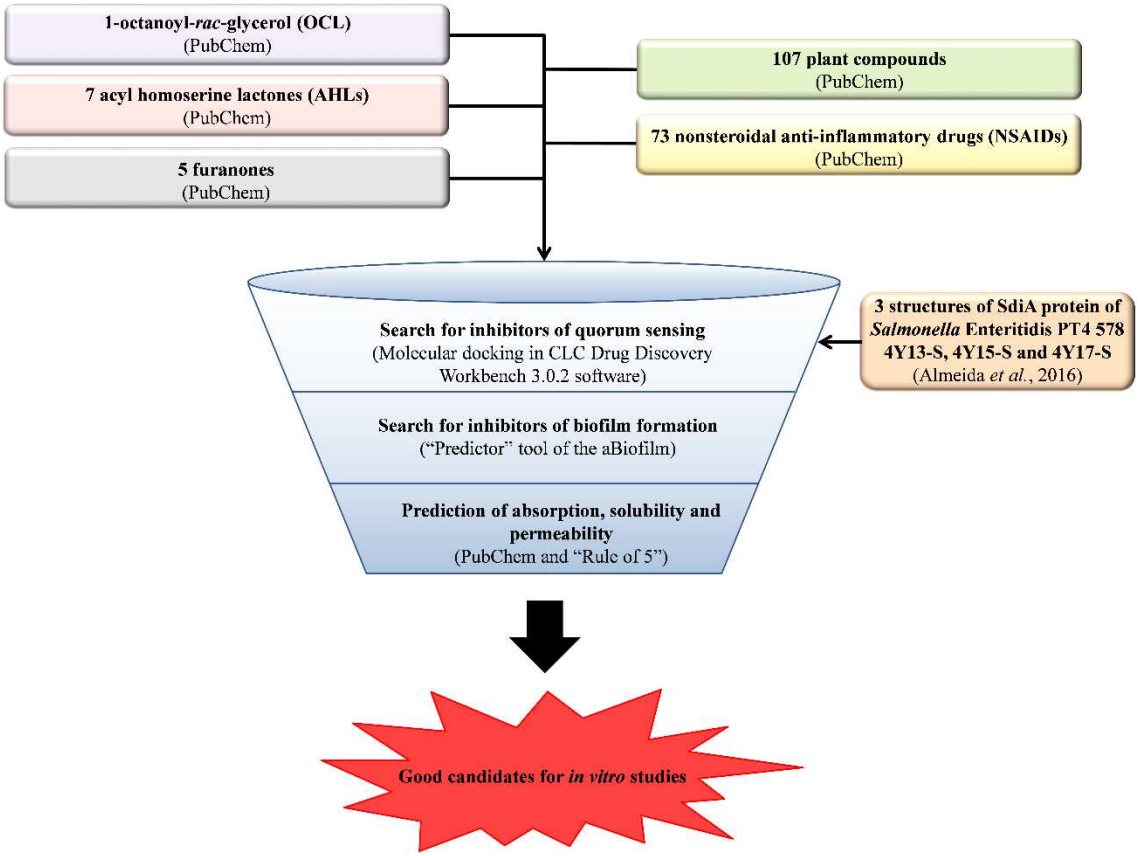

Fig. 1. Experimental strategy used for virtual screening of plant compounds and nonsteroidal anti-inflammatory drugs (NSAIDs) for inhibition of quorum sensing and biofilm formation by *Salmonella*. The databases, tools, softwares and reference used in the different steps are indicated in brackets.

2.1. Quorum sensing, quorum quenching and anti-biofilm compounds

The compounds selected for this study were 1-octanoyl-*rac*-glycerol (OCL), seven acyl homoserine lactones (AHLs), five furanones, 107 plant compounds and 73 NSAIDs, totaling 193 compounds (Table 1). These compounds were selected based on previous studies or structural similarity to compounds already studied with anti-quorum sensing activity. The structures of these molecules were obtained from the Compound Identifier of PubChem database (PubChem CID; https://pubchem.ncbi.nlm.nih.gov/). In addition, the plant componds were classified according to their main funcional group and the classification of NSAIDs was obtained from KEGG Drug database (http://www.genome.jp/kegg/drug/) (Table 1).

Table 1. Quorum sensing and quorum quenching compounds used for virtual screening of the inhibitors of quorum sensing and biofilm formation by *Salmonella*.

Group	Classification	Molecule	Pubchem CID	References of studies with quorum sensing in bacteria	Total
OCL	OCL	1-octanoyl-*rac*-glycerol	3033877	[26, 53]	1
AHL	Unmodified in 3-oxo	*N*-butyryl-DL-homoserine lactone	443433	[21, 26]	7
		N-hexanoyl-DL-homoserine lactone	3462373	[16, 21, 26, 54]	
		N-octanoyl-DL-homoserine lactone	3474204	[16, 21, 26, 54]	
		N-dodecanoyl-DL-homoserine lactone	11565426	[16, 26, 54]	
	Modified in 3-oxo	*N*-(3-oxohexanoyl)-L-homoserine lactone	688505	[21, 25, 26, 53, 55]	
		N-(3-oxooctanoyl)-L-homoserine lactone	127293	[21, 26, 53]	
		N-(3-oxododecanoyl)-L-homoserine lactone	3246941	[26, 55]	
Furanone	Non-brominated	2,2-dimethyl-3(2H)-furanone	147604	[26, 54]	5
		3-butyl-2(5H)-furanone	11768654	[23, 26]	
	Brominated	4-bromo-5-(bromomethylene)-3-butyl-2(5H)-furanone	9839657	[23, 26]	
		4-bromo-5-(bromomethylene)-3-hexyl-2(5H)-furanone	16127328	[23, 26]	
		4-bromo-5-(bromomethylene)-3-dodecyl-2(5H)-furanone	10180544	[23, 26]	
Plant	Ajoene	E-ajoene	5386591	[32, 42]	107
		Z-ajoene	9881148	[32, 42]	
	Alcohol	1-hydroxyoctane	957	[31]	
		1-methylcyclohexanol	11550	[31]	
		2-methylcyclohexanol	11418	[31]	
		3-methylcyclohexanol	11566	[31]	
		4-methylcyclohexanol	11524	[31]	
		Trans-2-methylcyclohexanol	24004	[31]	
	Amino acid	2-amino-4-chlorobenzoic acid (4CABA)	66646	[27, 37]	
		2-amino-6-chlorobenzoic acid (6CABA)	75071	[27, 37]	
		2-amino-6-fluorobenzoic acid (6FABA)	521142	[27, 37]	
		Anthranilic acid (AA)	227	[27, 37]	
		R-canavanine	222546	[33]	
		S-canavanine	439202	[33]	
		RS-canavanine	275	[33]	

Table 1. Continuation.

Group	Classification	Molecule	Pubchem CID	References of studies with quorum sensing in bacteria	Total
Plant	Aminobenzoic ester	Methyl anthranilate (MA)	8635	[27, 37]	
	Aromatic aldehyde	Vanillin	1183	[45]	
	Aromatic ether	Butyl trityl ether	348962	[41]	
	C_{13}-norisoprenoid	E-alfa-damascenone	68473438	[41]	
		Z-alfa-damascenone	91668178	[41]	
		E-beta-damascenone	5366074	[41]	
		Z-beta-damascenone	12309006	[41]	
	Chalcone	Cardamonin	641785	[41]	
	Coumarin	Coumarin	323	[41]	
	Cyclitol	R-quinic acid	6508	[41]	
		S-quinic acid	37439	[41]	
	Fatty acid	Linolenic acid	5280934	[41]	
		Malvalic acid	10416	[41]	
		Margaric acid	10465	[41]	
		Palmitic acid	985	[41]	
		Punicic acid	5281126	[41]	
	Flavonoid	7,8-dihydroxy-4'-methoxyisoflavone (Isoflavone)	5481240	[41]	
		Acacetin	5280442	[41]	
		Astragalin	5282102	[41]	
		R-catechin	73160	[40, 47]	
		S-catechin	9064	[40, 47]	
		RS-catechin	1203	[47]	
		Chrysin	5281607	[46]	
		R-epicatechin	72276	[44]	
		S-epicatechin	182232	[44]	
		Isosakuranetin	160481	[46]	
		Kaempferol	5280863	[46]	
		Luteolin	5280445	[46]	
		Myricetin	5281672	[46]	
		Pinobanksin	73202	[46]	
		Pinocembrin	68071	[46]	
		Poriol	301798	[41]	

Table 1. Continuation.

Group	Classification	Molecule	Pubchem CID	References of studies with quorum sensing in bacteria	Total
Plant	Flavonoid	Quercetin	5280343	[46]	
		Retusin (Flavonol)	5352005	[41]	
		Rutin	5280805	[35, 44]	
		Tricetin	5281701	[46]	
	Furanocoumarin	Imperatorin (Ammidin)	10212	[41]	
	Isothiocyanate	Iberin	10455	[32]	
	Methoxy phenol	[6]-gingerol	442793	[34, 36]	
		[8]-gingerol	168114	This study	
		[10]-gingerol	168115	This study	
		[6]-isoshogaol	11694761	This study	
		[8]-isoshogaol	91715793	This study	
		[10]-isoshogaol	53379231	This study	
		[12]-isoshogaol	91715817	This study	
		[6]-shogaol	5281794	[36]	
		[8]-shogaol	6442560	This study	
		[10]-shogaol	6442612	This study	
		Zingerone (Vanillylacetone)	31211	[36]	
	Monoterpene	R-limonene	440917	[31]	
		S-limonene	439250	[31]	
		RS-limonene	22311	[31]	
	Oxygenated diterpene	E-phytol	5280435	[41]	
		Z-phytol	6430833	[41]	
	Oxygenated monoterpene	R-isomenthone	70962	[31]	
		S-isomenthone	6432469	[31]	
		R-isopulegol	170833	[31]	
		S-isopulegol	1268090	[31]	
		RS-isopulegol	24585	[31]	
		R-lavandulol	5464156	[31]	
		S-lavandulol	68133	[31]	
		RS-lavandulol	94060	[31]	

Table 1. Continuation.

Group	Classification	Molecule	Pubchem CID	References of studies with quorum sensing in bacteria	Total
Plant	Oxygenated monoterpene	R-menthol	16666	[31]	
		S-menthol	165675	[31]	
		RS-menthol	1254	[31]	
		R-menthone	26447	[31]	
		S-menthone	443159	[31]	
		RS-menthone	6986	[31]	
		R-menthyl acetate	220674	[31]	
		S-menthyl acetate	62335	[31]	
		RS-menthyl acetate	27867	[31]	
		R-neoisomenthol	19244	[31]	
		S-neoisomenthol	1715097	[31]	
		R-piperitone	107561	[31]	
		S-piperitone	61362	[31]	
		RS-piperitone	6987	[31]	
	Oxygenated sesquiterpene	E,E-farnesol	445070	[29, 30]	
		E,Z-farnesol	1549109	[29, 30]	
		Z,E-farnesol	1549108	[29, 30]	
		Z,Z-farnesol	1549107	[41]	
		R-norpatchoulenol	57124935	[41]	
		S-norpatchoulenol	14682250	[41]	
	Phenolic	Pyrogallol	1057	This study	
	Phenolic acid	Ellagic acid	5281855	[44]	
		Gallic acid	370	[44]	
		Salicylic acid	338	[28, 45, 48]	
	Phenylpropanoid	Caffeic acid	689043	[44, 46]	
		Cinnamic acid	444539	[41]	
		Ferulic acid	445858	[44, 46]	
		p-coumaric acid	637542	[40, 46]	
		Trans-cinnamaldehyde	637511	[28]	
	Terpenoid	Callicarpenal	11107286	[31]	

Table 1. Continuation.

Group	Classification	Molecule	Pubchem CID	References of studies with quorum sensing in bacteria	Total
NSAID	Acetic acid derivative	Aceclofenac	71771	This study	73
		Acemetacin	1981	This study	
		Alclofenac	30951	This study	
		Bufexamac	2466	This study	
		Diclofenac	3033	[51, 52]	
		Difenpiramide	100472	This study	
		Etodolac	3308	This study	
		Fentiazac	28871	This study	
		Glucametacin	46174088	This study	
		Indomethacin	3715	[51]	
		Ketorolac	3826	[51]	
		Lonazolac	68706	[50]	
		Oxametacin	33675	This study	
		Sulindac	1548887	[51]	
		Tolmetin	5509	[51]	
		Zomepirac	5733	This study	
	Anilide derivative	Paracetamol (Acetaminophen)	1983	This study	
	Anilinonicotinic acid derivative	Clonixin	28718	This study	
		Flunixin	38081	This study	
		Morniflumate	72106	This study	
		Niflumic acid	4488	This study	
	Enolic acid derivative (Oxicam)	Droxicam	65679	This study	
		Isoxicam	54677972	This study	
		Lornoxicam	54690031	This study	
		Meloxicam	54677470	[51]	
		Piroxicam	54676228	[51, 52]	
		Tenoxicam	54677971	This study	
	Fenamic acid derivative	Flufenamic acid	3371	This study	
		Meclofenamic acid	4037	This study	
		Mefenamic acid	4044	This study	
		Tolfenamic acid	610479	This study	

Table 1. Continuation.

Group	Classification	Molecule	Pubchem CID	References of studies with quorum sensing in bacteria	Total
NSAID	Propionic acid derivative	Alminoprofen	2097	This study	
		Benoxaprofen	39941	This study	
		Dexibuprofen	39912	This study	
		Dexketoprofen	667550	This study	
		Fenbufen	3335	This study	
		Fenoprofen	3342	This study	
		Flunoxaprofen	68869	This study	
		Flurbiprofen	3394	This study	
		Ibuprofen	3672	[51, 52]	
		Ibuproxam	68704	This study	
		Indoprofen	3718	This study	
		Ketoprofen	3825	[52]	
		Loxoprofen	3965	This study	
		Naproxen	156391	[51, 52]	
		Oxaprozin	4614	This study	
		Suprofen	5359	This study	
		Tiaprofenic acid	5468	This study	
	Pyrazolone derivative	Aminopyrine (Aminophenazone)	6009	This study	
		Azapropazone	26098	This study	
		Dipyrone (Metamizole)	3111	This study	
		Feprazone	35455	This study	
		Ketophenylbutazone (Kebutazone)	3824	This study	
		Mofebutazone	16639	This study	
		Nifenazone	4487	This study	
		Oxyphenbutazone	4641	This study	
		Phenylbutazone	4781	This study	
		Suxibuzone	5362	This study	

Table 1. Continuation.

Group	Classification	Molecule	Pubchem CID	References of studies with quorum sensing in bacteria	Total
NSAID	Salicylic acid derivative	Aspirin (Acetylsalicylic acid)	2244	[49, 51]	
		Benorilate	21102	This study	
		Diflunisal	3059	This study	
		Olsalazine	6003770	This study	
		Salicylamide	5147	This study	
		Salicylic acid	338	[28, 45, 48]	
	Selective COX2 inhibitor (Coxibs)	Celecoxib	2662	[51]	
		Etoricoxib	123619	This study	
		Firocoxib	208910	This study	
		Lumiracoxib	151166	This study	
		Nabumetone	4409	This study	
		Parecoxib	119828	This study	
		Rofecoxib	5090	This study	
		Valdecoxib	119607	This study	
	Sulfonamide derivative	Nimesulide	4495	This study	
Total					**193**

The number in brackets indicates the size of the carbon chain.

2.2. Search for inhibitors of AI-1 type quorum sensing in *Salmonella*

2.2.1. Macromolecular structures of SdiA protein of *Salmonella* Enteritidis

The SdiA protein of *S. enterica* serovar Enteritidis PT4 578 (GenBank: AGZ95694.1) was modeled and validated (4Y13-S, 4Y15-S and 4Y17-S) from the SdiA protein of Enterohemorrhagic *E. coli* (EHEC; PDB: 4Y13, 4Y15 and 4Y17; [53]) using CLC Drug Discovery Workbench 2.5 software (http://www.clcbio.com/products/clc-drug-discovery-workbench/) by Almeida et al. [26] and was used for molecular docking.

2.2.2. Molecular docking of SdiA protein of *Salmonella* Enteritidis with different compounds

The molecular docking of SdiA protein of *Salmonella* Enteritidis PT4 578 was performed with quorum sensing and potential quorum quenching compounds of the AI-1 QS system (Table 1) by using the "Dock Ligands" tool of the CLC Drug Discovery Workbench 3.0.2 software (http://www.clcbio.com/products/clc-drug-discovery-workbench/), with 1,000 interactions for each compound being performed. The generated score mimics the potential energy change when the protein and the compound come together based on hydrogen bonds, metal ions and steric interactions, where lower scores (more negative) correspond to higher binding affinities. The five best scores of the docking were used in each macromolecular structure, allowing the inspection of the binding sites of SdiA with compounds and cofactors [26].

2.3. Search for inhibitors of biofilm formation

The search for inhibitors of biofilm formation was performed with compounds of Table 1 by using the "Predictor" tool of the "aBiofilm" resource (http://bioinfo.imtech.res.in/manojk/abiofilm/; [56]). The compounds were classified

according to the "inhibition efficiency color gradient" scale which describes the activity of inhibiting biofilm formation as high in shades of green (60-100%) or low in shades of pink (< 20%), as well as the confidence score of the result with high confidence in dark green (H2) and dark pink (L2), medium confidence in green (H1) and pink (L1) or low confidence in light green (H0) and light pink (L0).

2.4. Prediction of absorption, solubility and permeability of evaluated compounds

All compounds from Table 1 were also classified according the “rule of 5”. This classification establishes four parameters of the compounds as molecular weight (weight), octanol-water partition coefficient (log P), the number of H-bond donors (H-bond donors) and the number of H-bond acceptors (H-bond acceptors) which are associated with their absorption, solubility and permeability. It is noteworthy that there are not five parameters, but the cutoffs for each of the four parameters are all close to 5 or a multiple of 5. Thus, the compounds with better absorption, solubility and permeability are more likely when the weight is less than 500, the LogP is less than 5, H-bond donors less than 5 and H-bond acceptors 10. If two or more parameters are out of range, it is possible that the compound exhibits poor absorption, solubility and permeability [57].

3. Results and discussion

3.1. Potential inhibitors of AI-1 type quorum sensing in *Salmonella*

In this study, three macromolecular structures of SdiA protein of *Salmonella* Enteritidis PT4 578 were used on molecular docking. It is noteworthy that *Salmonella* SdiA structure is not available in the PDB database and the macromolecular structures used in this study were generated by us based on structures of SdiA protein of EHEC [26]. Nguyen et al. [53] observed conformational changes of SdiA protein of EHEC

when complexed with different compounds. They named the SdiA structure of *E. coli* as 4Y13 when the protein was bound to 1-octanoyl-*rac*-glycerol (OCL), 4Y15 structure for this protein bound to *N*-(3-oxo-hexanoyl)-L-homoserine lactone (3-oxo-C6-HSL) and, 4Y17 structure for the protein bound to *N*-(3-oxo-octanoyl)-L-homoserine lactone (3-oxo-C8-HSL). Likewise, the modeled structures of SdiA of *Salmonella* were named 4Y13-S, 4Y15-S and 4Y17-S. Then, considering three different macromolecular structure arrangements of SdiA protein of *Salmonella* Enteritidis, it was observed that binding affinities with the evaluated compounds were different (Tables 2 and 3). In our previous study it was also shown, by molecular docking, that these structures have different affinities for different AHLs and furanones [26].

3.1.1. Plant compounds

The farnesol isomers (-70.17, -69.46, -69.20 and -68.32) and malvalic acid (-69.39) showed the highest binding affinities with the modeled 4Y13-S structure which was complexed with OCL, among the 107 compounds of plants tested (Table 2).

Table 2. Results of molecular docking of macromolecular structures of SdiA protein of *Salmonella* Enteritidis PT4 578 with plant compounds.

Group	Classification	Molecule	Structures of modeled SdiA protein of *Salmonella* Enteritidis PT4 578								
			4Y13-S			4Y15-S			4Y17-S		
			Binding residue	Score	Rank	Binding residue	Score	Rank	Binding residue	Score	Rank
Plant	**Oxygenated diterpene**	**Z-phytol**	**Q72, Glycerol (Q72)**	**-67.90**	**8**	**F132, S134**	**-82.63**	**6**	**F132, S134**	**-87.89**	**1**
AHL	**Modified in 3-oxo**	***N*-(3-oxododecanoyl)-L-homoserine lactone**	**Y63, W67, S134**	**-67.99**	**6**	**Y63, W67, D80, S134**	**-86.07**	**1**	**W67, S134**	**-86.15**	**2**
AHL	**Unmodified in 3-oxo**	***N*-dodecanoyl-DL-homoserine lactone**	**Y63, W67**	**-67.61**	**9**	**Y63, W67**	**-85.38**	**2**	**Y63, W67, D80**	**-85.75**	**3**
Plant	**Methoxy phenol**	**[12]-isoshogaol**	**T61, Glycerol (Q72)**	**-57.63**	**29**	**Y71, S134**	**-85.31**	**3**	**Y71, D80, S134**	**-85.70**	**4**
Plant	**Methoxy phenol**	**[8]-gingerol**	**Y63, W67**	**-60.51**	**23**	**D80, S134**	**-81.52**	**9**	**D80, S134**	**-84.64**	**5**
Plant	**Oxygenated diterpene**	**E-phytol**	**Q72, Glycerol (Q72)**	**-67.33**	**11**	**A43, F132, S134**	**-82.45**	**7**	**M106**	**-84.34**	**6**
Plant	**Methoxy phenol**	**[10]-gingerol**	**Y63, F132, S134, Glycerol**	**-56.29**	**32**	**Y63, S134**	**-81.61**	**8**	**D80, S134**	**-83.17**	**7**
Plant	**Methoxy phenol**	**[8]-shogaol**	**Y71, Glycerol**	**-64.77**	**16**	**A43, F132, S134**	**-80.61**	**11**	**Y71**	**-82.82**	**8**
Plant	**Methoxy phenol**	**[8]-isoshogaol**	**Glycerol**	**-60.75**	**21**	**A43, W67, F132, S134**	**-76.82**	**15**	**W67**	**-82.66**	**9**
Plant	**Fatty acid**	**Punicic acid**	**Q72, Glycerol (Q72)**	**-64.87**	**14**	**A43, F132, S134**	**-80.66**	**10**	**D80**	**-81.65**	**10**
Plant	**Methoxy phenol**	**[10]-shogaol**	**Y71, Glycerol**	**-54.10**	**36**	**A43, F132, S134**	**-83.39**	**5**	**S134**	**-80.80**	**11**
Plant	**Fatty acid**	**Malvalic acid**	**Y63, W67**	**-69.39**	**3**	**Y63, S134**	**-79.20**	**12**	**D80, S134**	**-80.07**	**12**
Furanone	**Brominated**	**4-bromo-5-(bromomethylene)-3-dodecyl-2(5H)-furanone**	**Y71**	**-60.31**	**25**	**Y71**	**-83.64**	**4**	**Y71**	**-80.04**	**13**
Plant	**Methoxy phenol**	**[10]-isoshogaol**	**Y71, Glycerol (Q72)**	**-57.88**	**27**	**S134**	**-75.94**	**16**	**D80, S134**	**-79.81**	**14**
Plant	**Methoxy phenol**	**[6]-gingerol**	**D80, S134**	**-61.34**	**20**	**D80, S134**	**-77.28**	**13**	**Y63, S134**	**-78.60**	**15**
Plant	**Fatty acid**	**Margaric acid**	**Glycerol**	**-67.57**	**10**	**A43, F132, S134**	**-74.93**	**18**	**Y63, W67**	**-78.52**	**16**
Plant	**Methoxy phenol**	**[6]-shogaol**	**S134**	**-67.94**	**7**	**S134**	**-77.20**	**14**	**S134**	**-78.22**	**17**
Plant	**Methoxy phenol**	**[6]-isoshogaol**	**Glycerol (Q72), Glycerol**	**-61.81**	**19**	**A43, Y63, W67, F132, S134**	**-74.98**	**17**	**Y63**	**-76.38**	**18**
Plant	**Fatty acid**	**Palmitic acid**	**D80, Glycerol**	**-64.19**	**17**	**Y63, S134**	**-74.24**	**19**	**Y63, W67**	**-74.16**	**19**
Plant	Furanocoumarin	Imperatorin (Ammidin)	W67, S134	-62.31	18	W67	-72.26	22	W67	-73.39	20
Plant	**Oxygenated**	**E,Z-farnesol**	**Q72, Glycerol (Q72)**	**-69.46**	**2**	**M106**	**-71.73**	**24**	**L44, R60**	**-72.38**	**21**
AHL	Modified in 3-oxo	*N*-(3-oxooctanoyl)-L-homoserine lactone	Y63	-65.60	13	Y63, W67, Y71, D80, S134	-72.61	20	Y63, W67, Y71, D80	-72.03	22
AHL	Unmodified in 3-oxo	*N*-octanoyl-DL-homoserine lactone	Y63	-66.19	12	Y63, W67, D80, S134	-71.90	23	Y63, W67, D80	-71.07	23
Plant	Flavonoid	Pinobanksin	Y63, V68, W67	-53.75	37	W67, D80	-69.02	27	S134	-68.98	24
Plant	Flavonoid	Poriol	M106, S134, Glycerol	-50.36	44	M106, S134	-68.12	29	S134	-68.15	25
Plant	Flavonoid	Retusin (Flavonol)	Glycerol	-35.53	90	W67	-63.95	35	S134	-66.39	26
Plant	Chalcone	Cardamonin	V68, Q72	-54.12	35	L44, R60, Y71	-66.37	31	L44, R60, Y71	-66.15	27
Plant	Flavonoid	Kaempferol	W67	-46.98	56	W67, D80	-66.26	32	S134	-65.99	28
Plant	Flavonoid	R-epicatechin	W67, D80, Glycerol	-55.31	33	Y71	-60.23	43	Y71, D80	-63.72	29
Plant	Flavonoid	RS-catechin	W67, D80, Glycerol	-55.27	34	Y71	-60.21	44	Y71, D80	-63.71	30

Table 2. Continuation.

Group	Classification	Molecule	Structures of SdiA protein of *Salmonella* Enteritidis PT4 578 modeled								
			4Y13-S			4Y15-S			4Y17-S		
			Binding residue	Score	Rank	Binding residue	Score	Rank	Binding residue	Score	Rank
OCL	Monoacylglycerol	1-octanoyl-*rac*-glycerol	Y63, D80, Glycerol	-60.68	22	D80, S134	-61.30	38	Y63, W67, D80, S134	-63.62	31
Furanone	**Brominated**	**4-bromo-5-(bromomethylene)-3-hexyl-2(5H)-furanone**	**W67**	**-60.37**	**24**	**W67**	**-64.03**	**34**	**W67**	**-63.53**	**32**
Plant	Flavonoid	S-catechin	Y63, W67, V68, D80	-52.55	39	W67, D80	-60.93	40	D80, S134	-63.32	33
Plant	Flavonoid	Quercetin	Y63, W67, V68, D80, Glycerol	-46.59	58	W67, D80	-63.16	36	D80, S134	-63.30	34
Plant	Ajoene	E-ajoene	Y63	-57.84	28	Y71	-62.16	37	W67	-62.95	35
Plant	Flavonoid	R-catechin	D80, Glycerol	-49.69	45	W67, D80	-68.69	28	S134	-62.94	36
Plant	Flavonoid	S-epicatechin	Y63, Glycerol	-48.16	53	Y63, W67	-64.61	33	Y63	-62.81	37
Plant	Flavonoid	7,8-dihydroxy-4'-methoxyisoflavone (Isoflavone)	W67, Glycerol	-38.28	82	A43, L44, S134	-60.64	41	W67, Y71	-61.12	38
AHL	Modified in 3-oxo	*N*-(3-oxohexanoyl)-L-homoserine lactone	Y63	-57.45	30	Y63, W67	-60.57	42	Y63, W67	-60.87	39
AHL	Unmodified in 3-oxo	*N*-hexanoyl-DL-homoserine lactone	Y63, W67	-56.37	31	Y63, W67	-60.00	45	Y63, W67, D80	-60.57	40
Plant	Ajoene	Z-ajoene	W67	-58.24	26	Y63, W67	-61.10	39	Y63, W67	-60.27	41
Plant	Oxygenated monoterpene	RS-menthyl acetate	-	-	-	Y71	-58.27	46	Y71	-59.69	42
Plant	Flavonoid	Myricetin	Y63, W67, V68, D80, Glycerol	-40.94	75	D80, S134	-52.02	56	D80, S134	-59.53	43
Plant	Oxygenated monoterpene	S-menthyl acetate	Y63, W67	-51.37	43	Y63, W67	-57.08	48	Y63, W67	-58.83	44
Plant	Oxygenated monoterpene	R-menthyl acetate	W67	-52.81	38	Y71	-54.45	53	Y71	-57.93	45
Plant	Flavonoid	Tricetin	M106, Glycerol	-42.56	68	M106	-56.68	49	D80	-57.17	46
Plant	Oxygenated monoterpene	R-lavandulol	D80	-48.76	49	Y71, D80	-54.49	52	L44, R60	-56.91	47
Plant	Methoxy phenol	Zingerone (Vanillylacetone)	Glycerol (Q72), Glycerol	-52.53	40	A43, F132, S134	-57.51	47	A43, S134	-56.35	48
Plant	Oxygenated monoterpene	S-lavandulol	Y63	-48.90	48	Y71, D80	-54.87	50	Y71, D80	-56.26	49
Plant	Oxygenated monoterpene	RS-lavandulol	D80	-48.65	50	Y71, D80	-54.85	51	L44, R60	-55.89	50
Furanone	Brominated	4-bromo-5-(bromomethylene)-3-butyl-2(5H)-furanone	W67	-52.34	41	Y71	-53.56	54	W67	-54.65	51
Plant	Terpenoid	Callicarpenal	Glycerol	-48.35	52	-	-	-	Y63	-54.47	52
Plant	Alcohol	1-hydroxyoctane	Q72, Glycerol (Q72)	-44.76	64	L44, R60	-49.19	62	L44, R60	-50.62	53
Plant	Phenylpropanoid	*p*-coumaric acid	Y63, D80	-46.25	61	D80	-49.56	61	Y63, D80	-49.94	54
Plant	Phenylpropanoid	Cinnamic acid	D80	-46.55	59	D80	-50.28	59	D80, S134	-49.90	55
Plant	Phenolic acid	Ellagic acid	W67, F132, S134	-30.03	97	W67, S134	-47.73	67	W67, S134	-49.83	56
Plant	Coumarin	Coumarin	W67	-47.52	55	W67	-50.91	57	W67	-49.40	57
Plant	Phenylpropanoid	Ferulic acid	D80, Glycerol	-46.77	57	A43, F132, S134	-49.70	60	D80	-49.15	58

Table 2. Continuation.

Group	Classification	Molecule	Structures of SdiA protein of *Salmonella* Enteritidis PT4 578 modeled								
			4Y13-S			4Y15-S			4Y17-S		
			Binding residue	Score	Rank	Binding residue	Score	Rank	Binding residue	Score	Rank
Plant	Oxygenated monoterpene	R-piperitone	W67	-43.99	67	Y71	-48.61	66	Y71	-47.42	59
Plant	Oxygenated monoterpene	RS-piperitone	W67	-44.02	66	Y71	-48.62	65	Y71	-47.33	60
Plant	Oxygenated monoterpene	R-isomenthone	W67	-41.48	73	Y71	-47.38	69	Y71	-47.19	61
Plant	Oxygenated monoterpene	S-isomenthone	W67	-41.59	72	-	-	-	Y71	-46.58	62
Plant	Oxygenated monoterpene	RS-menthone	W67	-41.80	71	-	-	-	Y71	-46.46	63
Plant	Phenylpropanoid	Caffeic acid	Glycerol	-45.78	62	A43, F132, S134	-46.14	70	V68, Y71, D80, S134	-45.21	64
Plant	Amino acid	2-amino-4-chlorobenzoic acid (4CABA)	W67	-42.43	69	Y71, D80	-45.64	71	Y71, D80	-44.53	65
Plant	Aromatic aldehyde	Vanillin	W67, D80	-40.90	76	W67	-43.53	73	Y71, D80, S134	-43.98	66
Plant	Phenolic acid	Salicylic acid	Y71, D80, Glycerol (Q72)	-38.80	80	W67, Y71, D80	-43.91	72	W67, Y71, D80	-43.23	67
Plant	Amino acid	Anthranilic acid (AA)	Y71, D80, Glycerol (Q72)	-38.89	79	Y71, D80	-42.31	77	Y71, D80	-42.74	68
Plant	Amino acid	2-amino-6-chlorobenzoic acid (6CABA)	W67, D80	-35.55	89	Y71, D80	-42.96	75	W67	-42.67	69
Plant	Amino acid	2-amino-6-fluorobenzoic acid (6FABA)	W67, D80	-37.28	83	Y71, D80	-42.82	76	W67	-41.46	70
Plant	Phenolic acid	Gallic acid	D80, S134, Glycerol	-36.21	87	Y71, D80	-39.80	78	Y71, D80	-39.93	71
Plant	Cyclitol	R-quinic acid	Y63, D80, Glycerol	-38.28	81	Y63, W67, Y71, D80, S134	-36.41	84	Y63, W67, D80, S134	-38.61	72
Plant	Flavonoid	Astragalin	Y63, W67, Q72, D80, S134, Glycerol (Q72), Glycerol	-13.42	100	L44, W67, F132, S134	-36.15	85	A43, L44, R60, W67, Y71, D80, S134	-38.25	73
Plant	Cyclitol	S-quinic acid	Y63, W67, Y71, D80, S134, Glycerol	-35.89	88	Y63, Y71, D80, S134	-37.87	81	Y63, Y71, D80	-37.68	74
Plant	Alcohol	4-methylcyclohexanol	D80	-35.09	91	D80	-38.51	80	Y71, D80	-37.42	75
Plant	Phenolic	Pyrogallol	Glycerol (Q72)	-34.86	94	W67	-36.82	83	Y63, W67, D80	-36.95	76
Plant	Amino acid	RS-canavanine	W67, V68, Glycerol (Q72)	-34.91	93	F132, S134	-34.50	88	D80	-36.22	77
Plant	Amino acid	S-canavanine	W67, V68, Glycerol (Q72)	-35.05	92	S134	-35.49	86	D80	-36.21	78
Plant	Amino acid	R-canavanine	W67, D80, Glycerol	-36.39	86	Y71, S134	-35.25	87	Y71, S134	-34.89	79
Plant	Oxygenated sesquiterpene	S-norpatchoulenol	Y71, D80	-20.92	99	Y71, D80	-29.28	89	Y63	-31.17	80
Plant	Oxygenated sesquiterpene	R-norpatchoulenol	Y71, D80	-20.94	98	Y71, D80	-29.15	90	Y63	-31.04	81
Plant	Flavonoid	Rutin	A43, C45, L59, Y71, Q72, S134, Glycerol (Q72), Glycerol	43.77	101	I57, W67, V68, Y71, Q72, D80, S134	23.37	91	I57, T61, V68, Y71, Q72, D80, S134	5.12	82
Plant	**Oxygenated**	**Z,E-farnesol**	**Q72, Glycerol (Q72)**	**-69.20**	**4**	**L44, R60**	**-72.30**	**21**	**-**	**-**	**-**
Plant	**Oxygenated**	**Z,Z-farnesol**	**Q72, Glycerol (Q72)**	**-70.17**	**1**	**L44, R60**	**-70.68**	**25**	**-**	**-**	**-**
Plant	Flavonoid	Chrysin	-	-	-	W67	-69.94	26	-	-	-
Plant	Flavonoid	Pinocembrin	-	-	-	S134	-67.81	30	-	-	-

Table 2. Continuation.

Group	Classification	Molecule	Structures of SdiA protein of *Salmonella* Enteritidis PT4 578 modeled								
			4Y13-S			4Y15-S			4Y17-S		
			Binding residue	Score	Rank	Binding residue	Score	Rank	Binding residue	Score	Rank
Plant	C_{13}-norisoprenoid	E-alfa-damascenone	W67	-48.62	51	Y71	-52.60	55	-	-	-
Plant	C_{13}-norisoprenoid	Z-alfa-damascenone	W67	-44.72	65	Y63	-50.86	58	-	-	-
Plant	Phenylpropanoid	Trans-cinnamaldehyde	S134	-45.17	63	W67	-49.14	63	-	-	-
Plant	**Oxygenated**	**S-Isopulegol**	**Glycerol (Q72)**	**-46.49**	**60**	**W67**	**-48.83**	**64**	**-**	**-**	**-**
Plant	**C_{13}-norisoprenoid**	**E-beta-damascenone**	**-**	**-**	**-**	**Y71**	**-47.53**	**68**	**-**	**-**	**-**
Plant	Oxygenated monoterpene	S-menthone	W67	-38.97	78	Y71	-43.28	74	-	-	-
Plant	Isothiocyanate	Iberin	Glycerol	-40.48	77	S134	-39.52	79	-	-	-
Plant	Alcohol	3-methylcyclohexanol	-	-	-	Y63	-37.71	82	-	-	-
Plant	**Oxygenated**	**E,E-farnesol**	**Q72, Glycerol (Q72)**	**-68.32**	**5**	**-**	**-**	**-**	**-**	**-**	**-**
Plant	Fatty acid	Linolenic acid	D80, Glycerol	-64.82	15	-	-	-	-	-	-
Plant	Flavonoid	Luteolin	Glycerol	-51.56	42	-	-	-	-	-	-
Plant	Flavonoid	Acacetin	Glycerol	-49.62	46	-	-	-	-	-	-
Plant	Flavonoid	Isosakuranetin	Glycerol	-49.43	47	-	-	-	-	-	-
Furanone	Non-brominated	3-butyl-2(5H)-furanone	W67	-47.66	54	-	-	-	-	-	-
Plant	Oxygenated monoterpene	S-piperitone	W67	-42.41	70	-	-	-	-	-	-
Plant	Oxygenated monoterpene	R-menthone	W67	-40.98	74	-	-	-	-	-	-
Plant	Alcohol	2-methylcyclohexanol	Glycerol (Q72)	-36.67	84	-	-	-	-	-	-
Plant	Alcohol	Trans-2-methylcyclohexanol	Glycerol (Q72)	-36.64	85	-	-	-	-	-	-
Plant	Aromatic ether	Butyl trityl ether	Y71	-34.84	95	-	-	-	-	-	-
Furanone	Non-brominated	2,2-dimethyl-3(2H)-furanone	W67	-34.08	96	-	-	-	-	-	-
Plant	**Alcohol**	**1-methylcyclohexanol**	**-**	**-**	**-**	**-**	**-**	**-**	**-**	**-**	**-**
Plant	**Aminobenzoic ester**	**Methyl anthranilate (MA)**	**-**	**-**	**-**	**-**	**-**	**-**	**-**	**-**	**-**
AHL	**Unmodified in 3-oxo**	***N*-butyryl-DL-homoserine lactone**	**-**	**-**	**-**	**-**	**-**	**-**	**-**	**-**	**-**
Plant	**Oxygenated**	**R-isopulegol**	**-**	**-**	**-**	**-**	**-**	**-**	**-**	**-**	**-**
Plant	**Monoterpene**	**R-limonene**	**-**	**-**	**-**	**-**	**-**	**-**	**-**	**-**	**-**
Plant	**Oxygenated**	**R-menthol**	**-**	**-**	**-**	**-**	**-**	**-**	**-**	**-**	**-**
Plant	**Oxygenated**	**R-neoisomenthol**	**-**	**-**	**-**	**-**	**-**	**-**	**-**	**-**	**-**
Plant	**Oxygenated**	**RS-isopulegol**	**-**	**-**	**-**	**-**	**-**	**-**	**-**	**-**	**-**
Plant	**Monoterpene**	**RS-limonene**	**-**	**-**	**-**	**-**	**-**	**-**	**-**	**-**	**-**
Plant	**Oxygenated**	**RS-menthol**	**-**	**-**	**-**	**-**	**-**	**-**	**-**	**-**	**-**

Table 2. Continuation.

Group	Classification	Molecule	Structures of SdiA protein of *Salmonella* Enteritidis PT4 578 modeled								
			4Y13-S			4Y15-S			4Y17-S		
			Binding residue	Score	Rank	Binding residue	Score	Rank	Binding residue	Score	Rank
Plant	**Monoterpene**	**S-limonene**	-	-	-	-	-	-	-	-	-
Plant	**Oxygenated**	**S-menthol**	-	-	-	-	-	-	-	-	-
Plant	**Oxygenated**	**S-neoisomenthol**	-	-	-	-	-	-	-	-	-
Plant	**C_{13}-norisoprenoid**	**Z-beta-damascenone**	-	-	-	-	-	-	-	-	-

No binding (-);
Main results discussed in the text are shown in bold.

The scores were -70.17 for Z,Z-farnesol, -69.46 for E,Z-farnesol, -69.39 for malvalic acid, -69.20 for Z,E-farnesol and -68.32 for E,E-farnesol, which were actually greater than the score of -60.68 for OCL. In addition, the scores were higher than those of the AI-1 quorum sensing molecules that, preferentially, bind to this structure with -67.99 for *N*-(3-oxododecanoyl)-L-homoserine lactone (3-oxo-C12-HSL) and -67.61 for C12-HSL. Furanones, that are recognized competitors of AHLs, also showed affinities lower than farnesol isomers for structures of SdiA protein, -60.37 for 4-bromo-5-(bromomethylene)-3-hexyl-2(5H)-furanone and -60.31 for 4-bromo-5-(bromomethylene)-3-dodecyl-2(5H)-furanone. Interestingly, farnesol is produced by *Candida albicans* and acts as an intra and interspecies signaling molecule [29, 30, 58, 59]. This compound inhibits the production of *Pseudomonas aeruginosa* quinolone signal (PQS; 2-heptyl-3-hydroxy-4-quinolone) by inhibiting transcription of the *pqs* operon [29], but it increases the levels of *N*-butyryl-homoserine lactone (C4-HSL) in this same species [30].

On the other hand, the modeled 4Y15-S structure which is complexed with 3-oxo-C6-HSL showed the highest binding affinities with 3-oxo-C12-HSL (-86.07) and C12-HSL (-85.38) (Table 2). Interestingly, the plant compound with the highest affinity for this structure was isoshogaol with 12 carbons (-85.31), which is the size of the AHLs carbon chains presenting higher affinity. In general, the compounds classified as methoxy phenol as isoshogaol (-85.31, -76.82, -75.94 and -74.98), shogaol (-83.39, -80.61 ando -77.20) and gingerol (-81.61, -81.52 and -77.28) with carbon chain size ranging from six to 10 or 12, as well as the fatty acids as punicic (-80.66), malvalic (-79.20), margaric (-74.93) and palmitic (-74.24) acids had high binding affinities to the 4Y15-S structure. However, these compounds had no greater affinity than that of the 4-bromo-5-(bromomethylene)-3-dodecyl-2(5H)-furanone (-83.64).

The modeled 4Y17-S structure complexed with 3-oxo-C8-HSL showed the highest binding affinity with the Z-phytol (-87.89) followed by the 3-oxo-C12-HSL (-86.15), C12-HSL (-85.75) and [12]-isoshogaol (-85.70), similarly to what was observed in 4Y15-S structure (Table 2). In addition, the compounds classified as methoxy phenol and fatty acid had high binding affinities to the 4Y17-S structure as to the 4Y15-S. Interestingly, compounds classified as methoxy phenol such as [6]-gingerol and [6]-shogaol, components of ginger (*Zingiber officinale* Roscoe), inhibited quorum sensing in *Chromobacterium violaceum* and *P. aeruginosa* [36]. In addition, Kim et al. [60] has demonstrated binding between [6]-gingerol and LasR protein of *P. aeruginosa* by molecular docking. It is noteworthy that no studies evaluating the inhibition of quorum sensing by compounds classified as methoxy phenol such as isoshogaol, shogaol and gingerol with different carbon chain sizes have been reported so far (Table 1). On the other hand, Priyanka et al. [41] showed, by molecular docking, that the binding scores between phytol and fatty acids such as punicic, malvalic, margaric and palmitic acids with two proteins homologous to LuxR, SdiA protein of *Enterobacter aerogens* and CviR protein of *C. violaceum*, were low. These authors used the pseudo phytol structure (Pubchem CID 6437979) and in the present study we used the Z-phytol and E-phytol structures. However, the differences in binding affinity between the same compounds with different proteins homologous to LuxR may be related to the variations in primary sequence of the proteins [16, 26, 53, 60-62].

The molecule C4-HSL was the only AHL that did not bind to any of the SdiA protein structures under study, as well as, the plant compounds: methyl anthranilate (MA), 1-methylcyclohexanol, Z-beta-damascenone, RS-limonene, S-limonene, R-limonene, RS-menthol, R-menthol, S-menthol, R-neoisomenthol, S-neoisomenthol, RS-isopulegol and R-isopulegol (Table 2). However, the isomers of two of these compounds were able to bind with low binding affinity in at least one of the structures,

such as E-beta-damascenone which bound to 4Y15-S structure (-47.53) and S-isopulegol which bound to 4Y13-S and 4Y15-S structures (-46.49 and -48.83, respectively). Priyanka et al. [41] also showed that E-beta-damascenone bound to the SdiA protein of *E. aerogens* and the CviR protein of *C. violaceum,* confirming our findings.

The global analysis of the binding affinities between plant compounds with the three structures of SdiA protein showed that Z-phytol is a good candidate for *in vitro* studies of quorum sensing inhibition in *Salmonella*, since it was ranked in eighth for the structure 4Y13-S (-67.90), sixth for the structure 4Y15-S (-82.63) and first for the structure 4Y17-S (-87.89) (Table 2), showing consistency of high binding affinities across all modeled strucutres. This compound bound to Q72 residue of the 4Y13-S structure and with glycerol (Fig. 2A). On the other hand, this molecule bound to F132 and S134 residues in the 4Y15-S and 4Y17-S structures (Fig. 2B and 2C). In addition, the S134 residue was also the binding site of the 3-oxo-C12-HSL in the three structures evaluated and could compete with the Z-phytol to bind to this residue (Fig. 2D, 2E, 2F).

The compounds methoxy phenol and fatty acids had high binding affinities to the 4Y15-S and 4Y17-S structures and, therefore, also become good candidates for *in vitro* quorum quenching studies (Table 2). In addition, these compounds with higher binding affinity most often bind to hydrophobic amino acid residues of the SdiA protein such as alanine (A43), methionine (M106), phenylalanine (F132), tryptophan (W67) and tyrosine (Y63 and Y71) (Table 2). Priyanka et al. [41] also showed that the amino acid residues tryptophan, aspartate and tyrosine of the CviR protein from *E. aerogens* were the major binding sites of plant compounds.

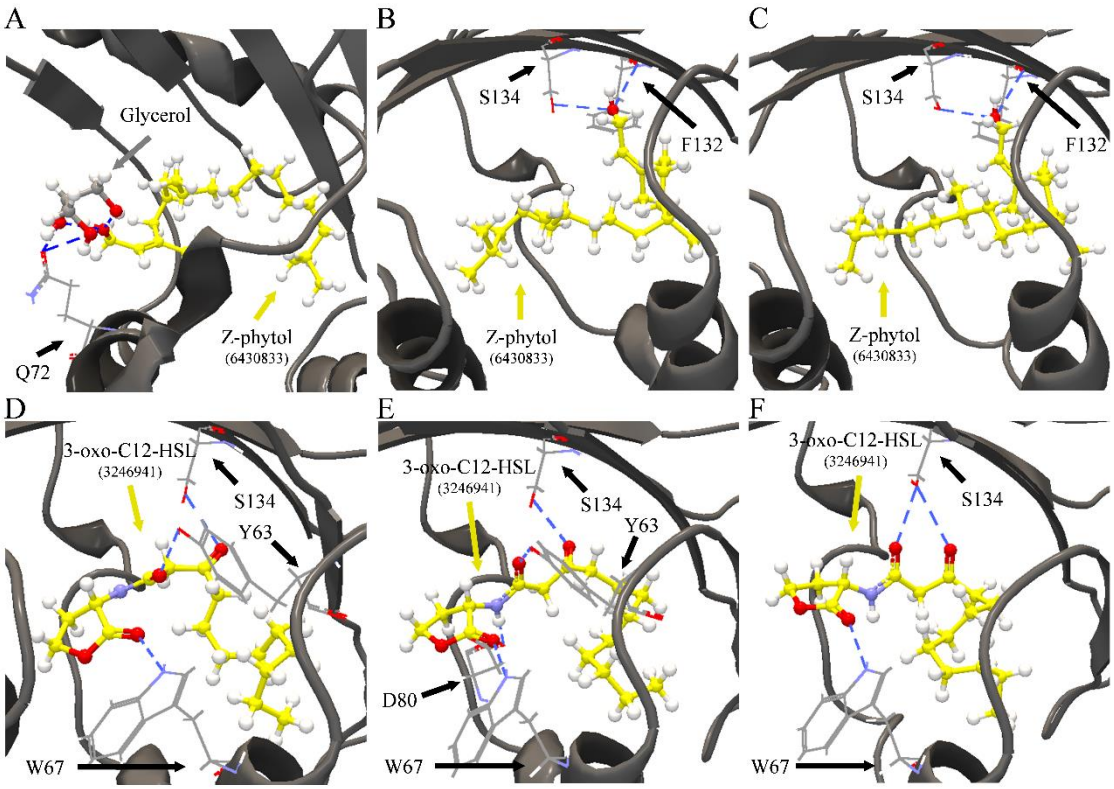

Fig. 2. Molecular docking of 4Y13-S **(A and D)**, 4Y15-S **(B and E)** and 4Y17-S **(C and F)** structures of SdiA protein of *Salmonella* Enteritidis PT4 578 with Z-phytol and 3-oxo-C12-HSL, respectively. Black arrow indicates the binding site; Gray arrow, glycerol; Yellow arrow, Z-phytol or 3-oxo-C12-HSL; Blue dashed line, hydrogen bond.

3.1.2. NSAIDs

The 73 NSAIDs compounds evaluated were able to bind to at least one of the modeled structures of the SdiA protein of *Salmonella* Enteritidis PT4 578. Thus, all NSAIDs could able to compete with OCL, AHLs and furanones for binding to this protein (Table 3).

The dipyrone (metamizole) showed the highest binding affinity (-70.32) with the modeled 4Y13-S structure complexed with OCL among the 73 NSAIDs tested compounds. In addition, the score for dypirone was higher than that for C12-HSL (-70.07) and 3-oxo-C12-HSL (-68.87), as well as for the furanone 4-bromo-5-(bromomethylene)-3-hexyl-2(5H)-furanone (-64.69). However, other NSAIDs such as niflumic acid (-69.52) and lonazolac (-69.20) also showed high binding affinity to this structure, comparable to that of the C12-HSL (-70.07) which showed the highest

affinity (Table 3). Interestingly, the lonazolac which is classified as acetic acid derivative was the compound that showed the highest binding affinity to 4Y15-S and 4Y17-S structures (-86.90 and -87.33, respectively) (Table 3).

Another compound classified as acetic acid derivative, the acemetacin (-85.71), also showed binding affinity to 4Y15-S structure greater than 3-oxo-C12-HSL (-85.18), C12-HSL (-82.89) and furanone 4-bromo-5-(bromomethylene)-3-dodecyl-2(5H)-furanone (-82.35) (Table 3). Other NSAIDs classified as acetic acid derivative such as fentiazac (-84.03), oxametacin (-80.32), aceclofenac (-77.67), sulindac (-75.62) and indomethacin (-74.27), as well as some classified as pyrazolone derivative including feprazone (-83.47), phenylbutazone (-79.49), ketophenylbutazone (-78.37), dipyrone (-73.25) and aminopyrine (-73.11) showed good binding affinities to 4Y15-S structure (Table 3).

The binding affinities observed between the 4Y17-S structure and the NSAIDs resemble those found for the 4Y15-S structure, except for azapropazone of the class of pyrozalone derivatives which does not bind to the 4Y15-S, but showed good binding affinity to 4Y17-S (-75.46) (Table 3). Soheili et al. [51] also showed by molecular docking that sulindac presented good inhibition constant against LasR protein of *P. aeruginosa*. On the other hand, indomethacin was not active against either LasR protein.

Table 3. Results from molecular docking of macromolecular structures of SdiA protein of *Salmonella* Enteritidis PT4 578 with nonsteroidal anti-inflammatory drugs (NSAIDs).

Group	Classification	Molecule	Structures of modeled SdiA protein of *Salmonella* Enteritidis PT4 578								
			4Y13-S			4Y15-S			4Y17-S		
			Binding residue	Score	Rank	Binding residue	Score	Rank	Binding residue	Score	Rank
NSAID	**Acetic acid derivative**	**Lonazolac**	**S134**	**-69.20**	**4**	**W67, Y71, D80**	**-86.90**	**1**	**W67, Y71, D80**	**-87.33**	**1**
AHL	**Unmodified in 3-oxo**	***N*-dodecanoyl-DL-homoserine lactone**	**Y63, D80, Glycerol**	**-70.07**	**2**	**Y63, W67, D80**	**-82.89**	**6**	**Y63, W67, D80**	**-86.53**	**2**
NSAID	**Acetic acid derivative**	**Acemetacin**	**Q72, Glycerol (Q72)**	**-50.07**	**58**	**L44, R60, Y63, W67**	**-85.71**	**2**	**L44, R60, Y63, W67**	**-86.36**	**3**
AHL	**Modified in 3-oxo**	***N*-(3-oxododecanoyl)-L-homoserine**	**Y63, W67, S134**	**-68.87**	**5**	**Y63, W67, D80, S134**	**-85.18**	**3**	**Y63, W67, Y71, D80, S134**	**-85.66**	**4**
NSAID	**Acetic acid derivative**	**Fentiazac**	**S134**	**-64.68**	**15**	**A43, S134**	**-84.03**	**4**	**A43, S134**	**-85.41**	**5**
NSAID	**Pyrazolone derivative**	**Feprazone**	**W67**	**-49.31**	**60**	**W67**	**-83.47**	**5**	**W67**	**-83.66**	**6**
NSAID	Propionic acid derivative*?	Oxaprozin	W67, D80, Glycerol	-68.15	7	W67, D80	-79.71	9	W67, D80	-82.57	7
Furanone	**Brominated**	**4-bromo-5-(bromomethylene)-3-dodecyl-2(5H)-furanone**	**Glycerol (Q72)**	**-57.26**	**38**	**Y71**	**-82.35**	**7**	**Y71**	**-80.30**	**8**
NSAID	**Acetic acid derivative**	**Oxametacin**	**A43, Y63, W67, F132, S134**	**-55.21**	**47**	**A43, Y63, W67, F132, S134**	**-80.32**	**8**	**A43, Y63, W67, F132, S134**	**-79.93**	**9**
NSAID	**Pyrazolone derivative**	**Ketophenylbutazone (Kebutazone)**	**W67**	**-49.76**	**59**	**W67**	**-78.37**	**11**	**W67**	**-79.22**	**10**
NSAID	**Pyrazolone derivative**	**Phenylbutazone**	**W67**	**-48.85**	**63**	**S134**	**-79.49**	**10**	**W67**	**-79.02**	**11**
NSAID	Anilinonicotinic acid derivative	Morniflumate	Y63, W67, S134	-49.19	61	W67	-73.12	17	Y71	-78.64	12
NSAID	Propionic acid derivative	Flunoxaprofen	D80, Glycerol	-53.45	51	W67, M106	-71.50	24	W67, V68	-76.18	13
NSAID	**Acetic acid derivative**	**Aceclofenac**	**Y63, D80, Glycerol**	**-62.56**	**24**	**Y63, W67, D80**	**-77.67**	**12**	**Y63, W67, D80**	**-75.65**	**14**
NSAID	**Pyrazolone derivative**	**Azapropazone**	**W67, S134**	**-54.38**	**49**	**-**	**-**	**-**	**W67**	**-75.46**	**15**
NSAID	**Acetic acid derivative**	**Sulindac**	**V68, Glycerol (Q72), Glycerol**	**-42.83**	**70**	**L44, R60**	**-75.62**	**13**	**L44, R60**	**-74.95**	**16**
NSAID	Propionic acid derivative	Fenbufen	V68, Glycerol (Q72)	-67.66	9	L44, R60	-72.99	19	L44, R60	-74.29	17
NSAID	Anilinonicotinic acid derivative	Niflumic acid	Y63, S134	-69.52	3	Y71, D80	-71.19	25	Y63, S134	-74.04	18
NSAID	**Acetic acid derivative**	**Indomethacin**	**L44, R60, T61, S134**	**-56.46**	**43**	**L44, R60, S134**	**-74.27**	**14**	**L44, R60, S134**	**-73.93**	**19**
NSAID	**Pyrazolone derivative**	**Dipyrone (Metamizole)**	**W67**	**-70.32**	**1**	**W67**	**-73.25**	**16**	**W67**	**-73.78**	**20**
NSAID	**Pyrazolone derivative**	**Aminopyrine (Aminophenazone)**	**-**	**-**	**-**	**W67**	**-73.11**	**18**	**W67**	**-73.34**	**21**
NSAID	Propionic acid derivative	Ketoprofen	Y71, D80, Glycerol	-68.09	8	Y71, D80	-71.80	23	D80	-72.64	22
AHL	Modified in 3-oxo	*N*-(3-oxooctanoyl)-L-homoserine lactone	Y63	-65.60	13	Y63, W67, Y71, D80, S134	-72.61	20	Y63, W67, Y71, D80	-72.03	23
NSAID	Salicylic acid derivative	Benorilate	Y63, W67, Glycerol (Q72)	-43.80	69	Y71	-71.11	26	Y71	-72.00	24
AHL	Unmodified in 3-oxo	*N*-octanoyl-DL-homoserine lactone	Y63	-66.19	11	Y63, W67, D80, S134	-71.90	21	Y63, W67, D80	-71.07	25
NSAID	Propionic acid derivative	Benoxaprofen	Glycerol	-52.75	52	W67, L115	-68.19	30	W67, V68	-69.79	26
NSAID	Pyrazolone derivative	Mofebutazone	W67, S134	-63.73	19	W67	-68.80	29	W67	-67.78	27
NSAID	Propionic acid derivative	Tiaprofenic acid	D80, Glycerol	-63.91	17	Y71	-69.85	28	D80	-67.60	28

Table 3. Continuation.

Group	Classification	Molecule	Structures of SdiA protein of *Salmonella* Enteritidis PT4 578 modeled								
			4Y13-S			4Y15-S			4Y17-S		
			Binding residue	Score	Rank	Binding residue	Score	Rank	Binding residue	Score	Rank
NSAID	Enolic acid derivative	Lornoxicam	Y63, S134, Glycerol (Q72)	-39.53	76	Y63, W67, Y71	-73.80	15	Y63, W67, Y71	-67.35	29
NSAID	Propionic acid derivative	Loxoprofen	D80, Glycerol	-62.76	22	D80	-62.99	44	D80	-67.10	30
NSAID	Acetic acid derivative	Zomepirac	D80, Glycerol	-52.66	53	-	-	-	L44	-67.08	31
NSAID	Acetic acid derivative	Diclofenac	D80, Glycerol	-60.01	29	Y63, W67	-67.14	33	Y63, W67	-66.77	32
NSAID	Fenamic acid derivative	Mefenamic acid	S134	-57.20	39	Y71, D80	-66.23	36	Y71, D80	-66.56	33
NSAID	Acetic acid derivative	Etodolac	Q72, Glycerol (Q72)	-55.92	46	A43, S134	-58.17	59	V68	-66.12	34
NSAID	Propionic acid derivative	Fenoprofen	D80, Glycerol	-65.85	12	W67	-66.75	34	D80	-66.05	35
NSAID	Propionic acid derivative	Dexketoprofen	Y71, D80, Glycerol	-65.05	14	Y63, S134	-67.86	32	Y63, S134	-65.90	36
NSAID	Pyrazolone derivative	Nifenazone	-	-	-	Y63, W67	-62.97	45	W67	-65.41	37
NSAID	Anilinonicotinic acid derivative	Clonixin	W67, S134	-54.73	48	Y71, D80	-63.09	43	Y71, D80	-65.33	38
NSAID	Propionic acid derivative	Naproxen	D80. Glycerol (Q72). Glycerol	-63.37	20	Y63, W67	-63.52	41	D80	-64.90	39
NSAID	Selective COX2 inhibitor	Celecoxib	V68, Glycerol (Q72)	-52.42	54	A43, F132, S134	-58.19	58	W67, V68	-64.86	40
NSAID	Enolic acid derivative	Tenoxicam	Y63, S134, Glycerol (Q72)	-39.96	75	Y63, Y71	-70.88	27	Y63, W67, Y71	-64.85	41
NSAID	Fenamic acid derivative	Tolfenamic acid	S134	-56.41	44	Y71, D80	-64.46	39	Y71, D80	-64.67	42
NSAID	Enolic acid derivative	Piroxicam	Y63, W67, S134	-46.52	65	W67, Y71	-63.79	40	W67, Y71	-64.30	43
OCL	OCL	1-octanoyl-*rac*-glycerol	Y63, D80, Glycerol	-59.31	33	Y63, W67, D80	-61.94	46	W67, D80, S134	-64.17	44
NSAID	Enolic acid derivative	Isoxicam	Glycerol	-32.73	78	-	-	-	W67	-63.92	45
Furanone	**Brominated**	**4-bromo-5-(bromomethylene)-3-hexyl-2(5H)-furanone**	**W67**	**-60.40**	**27**	**W67**	**-64.69**	**37**	**W67**	**-63.85**	**46**
NSAID	Propionic acid derivative	Ibuproxam	V68	-59.75	31	A43, F132, S134	-61.50	47	A43, F132, S134	-63.51	47
NSAID	Enolic acid derivative	Meloxicam	Y63, S134, Glycerol (Q72)	-40.37	74	Y71	-63.28	42	W67, Y71	-63.42	48
NSAID	Propionic acid derivative	Dexibuprofen	D80	-58.95	34	W67	-61.27	48	Y71, D80, S134	-63.34	49
NSAID	Selective COX2 inhibitor	Valdecoxib	S134, Glycerol (Q72)	-50.64	57	D80	-58.82	56	D80	-63.22	50
NSAID	Pyrazolone derivative	Oxyphenbutazone	V82, T120	-45.61	67	F132, S134	-64.51	38	F132, S134	-62.64	51
NSAID	Acetic acid derivative	Alclofenac	D80, Glycerol	-56.14	45	Y63, D80, S134	-61.00	50	S134	-62.15	52
NSAID	Acetic acid derivative	Bufexamac	Glycerol	-58.31	36	A43, W67, F132, S134	-61.25	49	A43, W67, F132, S134	-61.46	53
NSAID	Enolic acid derivative	Droxicam	Glycerol (Q72)	-31.76	79	W67	-58.25	57	W67	-61.01	54
AHL	Modified in 3-oxo	*N*-(3-oxohexanoyl)-L-homoserine lactone	Y63	-57.70	37	Y63, W67	-60.17	52	Y63, W67	-60.79	55
AHL	Unmodified in 3-oxo	*N*-hexanoyl-DL-homoserine lactone	Y63, W67	-56.47	42	Y63, W67	-60.43	51	Y63, W67	-60.62	56
NSAID	Propionic acid derivative	Ibuprofen	Glycerol (Q72)	-59.71	32	Y71, D80	-59.70	55	Y63, D80	-60.37	57
NSAID	Selective COX2 inhibitor	Lumiracoxib	W67, S134	-59.79	30	D80, S134	-59.88	54	D80, S134	-58.84	58

Table 3. Continuation.

Group	Classification	Molecule	Structures of SdiA protein of *Salmonella* Enteritidis PT4 578 modeled								
			4Y13-S			4Y15-S			4Y17-S		
			Binding residue	Score	Rank	Binding residue	Score	Rank	Binding residue	Score	Rank
NSAID	Sulfonamide derivative	Nimesulide	S134	-60.19	28	Y63, S134	-59.98	53	W67, S134	-57.92	59
Furanone	Brominated	4-bromo-5-(bromomethylene)-3-butyl-2(5H)-furanone	W67	-52.18	55	Y71	-53.52	60	W67	-54.70	60
NSAID	Salicylic acid derivative	Olsalazine	D80, Glycerol	-53.56	50	Y71	-52.17	61	Y71	-54.16	61
NSAID	Selective COX2 inhibitor	Etoricoxib	S134, Glycerol (Q72)	-51.15	56	S134	-47.80	64	S134	-54.15	62
NSAID	Fenamic acid derivative	Meclofenamic acid	Y71, Glycerol (Q72)	-49.07	62	D80, S134	-50.05	63	D80, S134	-53.82	63
NSAID	Salicylic acid derivative	Aspirin (Acetylsalicylic acid)	W67, S134	-41.10	71	Y71	-50.45	62	Y71, D80	-51.62	64
NSAID	Salicylic acid derivative	Salicylamide	W67, Y71, D80	-40.38	72	W67	-45.01	65	W67	-44.84	65
NSAID	Anilide derivative	Paracetamol (Acetaminophen)	W67	-40.37	73	W67	-44.42	66	W67	-44.11	66
NSAID	Acetic acid derivative	Glucametacin	T61, Q72	-28.75	81	Y63, D80, S134	-40.46	69	Y71, L115	-43.79	67
NSAID	Pyrazolone derivative	Suxibuzone	Q72, Glycerol (Q72)	-21.73	82	Y63, W67, Y71, M106, S134	-41.03	68	W67, Y71, S134	-43.65	68
NSAID	Salicylic acid derivative	Salicylic acid	Y71, D80, Glycerol (Q72)	-38.69	77	W67, Y71, D80	-43.90	67	W67, Y71, D80	-43.12	69
NSAID	Fenamic acid derivative	Flufenamic acid	Y63, W67, S134	-67.05	10	Y71, D80	-71.84	22	-	-	-
NSAID	Propionic acid derivative	Flurbiprofen	V68, Glycerol (Q72)	-63.73	18	Y71	-68.10	31	-	-	-
NSAID	Anilinonicotinic acid derivative	Flunixin	Y63, S134	-63.98	16	Y71, D80	-66.45	35	-	-	-
NSAID	Selective COX2 inhibitor	Nabumetone	Glycerol	-68.60	6	-	-	-	-	-	-
NSAID	Propionic acid derivative	Alminoprofen	V68, D80, Glycerol (Q72)	-62.94	21	-	-	-	-	-	-
NSAID	Propionic acid derivative	Indoprofen	V68, Glycerol (Q72)	-62.66	23	-	-	-	-	-	-
NSAID	Propionic acid derivative	Suprofen	V68, Glycerol (Q72)	-61.92	25	-	-	-	-	-	-
NSAID	Acetic acid derivative	Tolmetin	Glycerol (Q72)	-60.97	26	-	-	-	-	-	-
NSAID	Acetic acid derivative	Ketorolac	V68, Glycerol (Q72)	-58.50	35	-	-	-	-	-	-
NSAID	Acetic acid derivative	Difenpiramide	Glycerol (Q72)	-56.81	40	-	-	-	-	-	-
NSAID	Salicylic acid derivative	Diflunisal	Glycerol	-56.62	41	-	-	-	-	-	-
Furanone	Non-brominated	3-butyl-2(5H)-furanone	W67	-47.65	64	-	-	-	-	-	-
NSAID	Selective COX2 inhibitor	Rofecoxib	Glycerol	-45.98	66	-	-	-	-	-	-
NSAID	Selective COX2 inhibitor	Firocoxib	Y63, W67, Glycerol (Q72)	-44.01	68	-	-	-	-	-	-
NSAID	Selective COX2 inhibitor	Parecoxib	S134	-30.54	80	-	-	-	-	-	-
Furanone	Non-brominated	2,2-dimethyl-3(2H)-furanone	-	-	-	-	-	-	-	-	-
AHL	Unmodified in 3-oxo	*N*-butyryl-DL-homoserine lactone	-	-	-	-	-	-	-	-	-

No binding (-);
*?Main results discussed in the text are shown in bold.

The global analysis of the binding affinities between NSAIDs with the three structures of SdiA protein showed that lonazolac is a good candidate for the *in vitro* study of inhibition of quorum sensing in *Salmonella*, since it showed consistent good ranking across all modeled structures being ranked in fourth for the structure 4Y13-S (-69.20), first for 4Y15-S (-86.90) and 4Y17-S (-87.33) structures (Table 3). This compound bound to S134 residue of the 4Y13-S structure (Fig. 3A), and to W67, Y71 and D80 residues in the 4Y15-S and 4Y17-S structures (Fig. 3B and 3C). In addition, the D80 residue was also the binding site of the C12-HSL in the three structures evaluated and could compete with the lonazolac to bind to this residue (Fig. 3D, 3E, 3F). The potential for lonazolac for inhibition of quorum sensing has never been evaluated neither *in silico* nor *in vitro*. However, it was cited in a patent for studies of inhibitors of quorum sensing in bacteria deposited by Mathee et al. [50] in the United States of America.

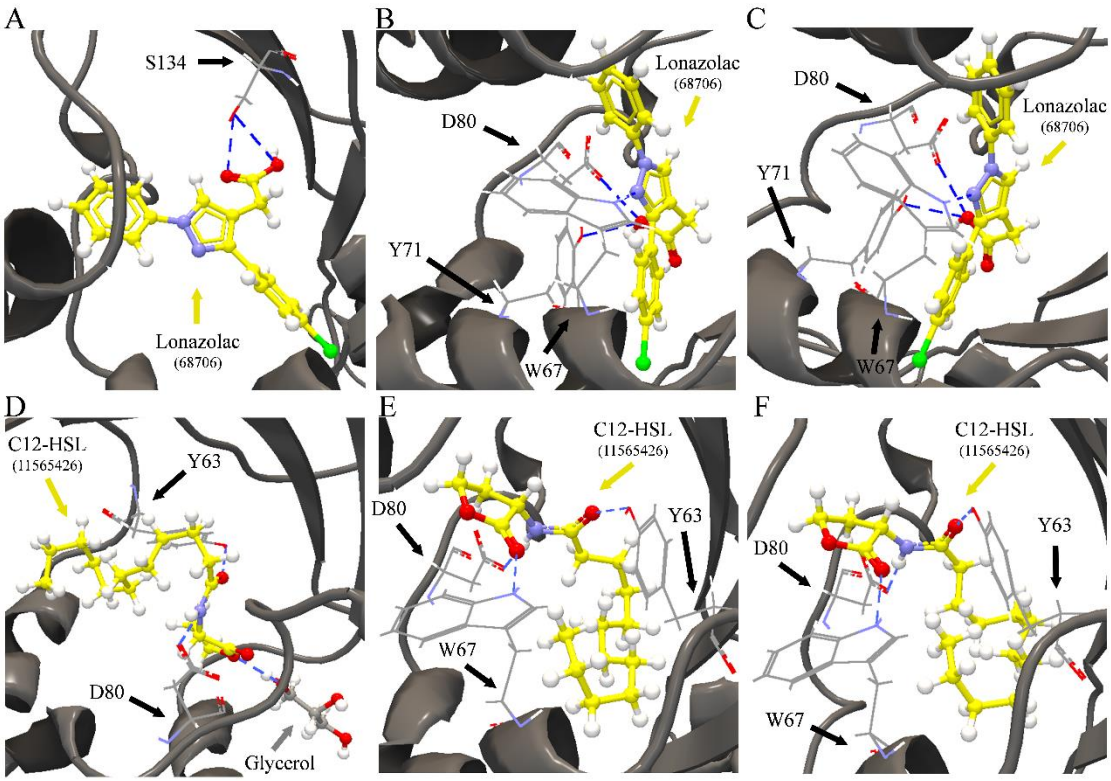

Fig. 3. Molecular docking of 4Y13-S **(A and D)**, 4Y15-S **(B and E)** and 4Y17-S **(C and F)** structures of SdiA protein of *Salmonella* Enteritidis PT4 578 with lonazolac and C12-HSL, respectively. Black arrow, the binding site; Yellow arrow, lonazolac or C12-HSL; Gray arrow, glycerol; Blue dashed line, hydrogen bond.

Interestingly, NSAIDs with higher binding affinity for the SdiA protein of *Salmonella* Enteritidis also had hydrophobic amino acid residues such as alanine (A43), leucine (L44), phenylalanine (F132), tryptophan (W67) and tyrosine (Y63 and Y71) as well as observed for the plant compounds (Table 3).

3.2. Potential inhibitors of *Salmonella* biofilm formation

3.2.1. OCL, AHLs and furanones

The molecules OCL and C4-HSL were the only compounds classified in OCL, AHLs and furanones groups that showed low activity at inhibiting biofilm formation based on *in silico* results as shown in Table 4 and Fig. S1 (Supplementary material).

Some AHL molecules have shown an abitility to enhance biofilm formation by *Salmonella.* The presence of C12-HSL or a mixture of AHLs with carbon chains ranging from six to 12 induced biofilm formation on a polystyrene surface by *Salmonella* Enteritidis PT4 578 in anaerobic TSB [16]. On the other hand, when a mixture of the non-brominated furanones including 3-methyl-2(5H)-furanone, 2-methyltetrahydro-3-furanone, 2(5H)-furanone and 2,2-dimethyl-3(2H)-furanone were added to the growth medium, there was no biofilm formation under the same conditions. These results corroborate with those found by us showing that C12-HSL does not stimulate initial adhesion on polystyrene but enhanced biofilm formation after 36 h incubation [18]. Janssens et al. [23] showed that the presence of different brominated furanones inhibited biofilm formation by *Salmonella* Typhimurium on polystyrene after 48 h of incubation at 16 °C in aerobic conditions, when compared to the control treatment. In addition, Vestby et al. [24] also reported the inhibitory effect of a synthetic furanone on the biofilm formation by *Salmonella* Agona on polystyrene without bactericidal effect.

Table 4. Results of the *in silico* inhibition potential of biofilm formation and the violation of "rule of 5" for plant compounds and nonsteroidal anti-inflammatory drugs (NSAIDs) grouped according to their classification.

Group	Classification	Number of compounds		
		Inhibition of the biofilm		Violation of "rule of 5"
		High	Low	
OCL	Monoacylglycerol	0	1	-
AHL	Unmodified in 3-oxo	3	1	1
	Modified in 3-oxo	3	0	-
Furanone	Non-brominated	2	0	-
	Brominated	3	0	2
Plant	Ajoene	0	2	-
	Alcohol	5	1	-
	Amino acid	0	7	3
	Aminobenzoic ester	0	1	-
	Aromatic aldehyde	0	1	-
	Aromatic ether	1	0	1
	C_{13}-norisoprenoid	4	0	-
	Chalcone	1	0	-
	Coumarin	1	0	-
	Cyclitol	2	0	-
	Fatty acid	4	1	5
	Flavonoid	20	0	3
	Furanocoumarin	1	0	1
	Isothiocyanate	0	1	-
	Methoxy phenol	11	0	6
	Monoterpene	3	0	-
	Oxigenated diterpene	2	0	2
	Oxigenated monoterpene	22	0	-
	Oxigenated sesquiterpene	6	0	-
	Phenolic	0	1	-
	Phenolic acid	1	2	-
	Phenylpropanoid	4	1	-
	Terpenoid	1	0	-
NSAID	Acetic acid derivative	15	1	1
	Anilide derivative	1	0	-
	Anilinonicotinic acid derivative	3	1	-
	Enolic acid derivative	4	2	-
	Fenamic acid derivative	3	1	1
	Propionic acid derivative	11	6	6
	Pyrazolone derivative	2	8	-
	Salicylic acid derivative	3	3	-
	Selective COX2 inhibitor	7	1	-
	Sulfonamide derivative	0	1	-

Not violated the "rule of 5" (-).

3.2.2. Plant compounds

Of the 107 plant compounds under investigation, 89 (83.2%) showed high activity for inhibiting the formation of biofilm and 18 (16.8%) showed low activity on this phenotype (Table 4 and Fig. S1). Among the compounds with high inhibitory activity are those classified as flavonoids, methoxy phenol and monoterpene

oxygenated. The activity of compound classified as methoxy phenol such as [6]-gingerol on reduced biofilm formation and virulence of *P. aeruginosa* has already been demonstrated [34].

Among the compounds with low inhibitory activity upon biofilm formation are those classified as ajoene, alcohol, amino acid, aminobenzoic ester, aromatic aldehyde, fatty acid, isothiocyanate, isothiocyanate, phenolic, phenolic acid and phenylpropanoid. All compounds classified as amino acid such as 2-amino-4-chlorobenzoic acid (4CABA), 2-amino-6-chlorobenzoic acid (6CABA), 2-amino-6-fluorobenzoic acid (6FABA), anthranilic acid (AA) and three isomers of canavanine showed low activity *in silico* as inhibitors of biofilm formation. Jakobsen et al. [32] showed that the treatment of the *P. aeruginosa* biofilm with ajoene did not kill the cells, but when associated with tobramycin, it caused cell death. However, treatment with ajoene altered the synthesis of C4-HSL and 3-oxo-C12-HSL by *P. aeruginosa*, likewise the expression of genes controlled by quorum sensing was decreased.

3.2.3. NSAIDs

Of the 73 NSAIDs, 49 (67.1%) showed high activity for inhibiting biofilm formation (Table 4 and Fig. S1). Among the 16 NSAIDs classified as acetic acid derivative only one presented low activity, and of the 17 compounds derived from propionic acid, six presented low activity. On the other hand, among the 10 NSAIDs classified as pyrazolone derivative only two presented high activity. Reslinski et al. [63] showed that biofilm formation by 70 strains of *Staphylococcus aureus* and 70 strains of *E. coli* on the surface of monofilament polypropylene mesh was reduced in the presence of diclofenac and ibuprofen. These results differ from those predicted in this study, since the diclofenac showed high activity for inhibiting biofilm formation and ibuprofen showed low activity (Table 4 and Fig. S1).

3.3. Prediction of absorption, solubility and permeability of compounds

3.3.1. OCL, AHLs and furanones

The molecule C12-HSL and two brominated furanones, 4-bromo-5-(bromomethylene)-3-hexyl-2(5H)-furanone and 4-bromo-5-(bromomethylene)-3-dodecyl-2(5H)-furanone violated the LogP parameter of the "rule of 5" (Table 4 and Fig. S1). The compounds with LogP greater than 5 indicate their lipolytic character, in other words, they have a greater ability to dissolve in non-aqueous solutions. According to the Cayman Chemical Company (Ann Arbor, Michigan, United States of America), the solubility of C12-HSL in organic solvents such as dimethyl sulfoxide (DMSO) and dimethyl formamide (DMF) is approximately 30 $mg.mL^{-1}$. However in phosphate-buffered saline (PBS), pH 7.2, is approximately 10 $mg.mL^{-1}$. Nevertheless, only when the compound violates two or more parameters from "rule of 5" that it is possible to exhibit poor absorption, solubility and permeability [57].

3.3.2. Plant compounds

Of the 107 plant compounds being tested, 86 (80.4%) did not violate any of the parameters from "rule of 5" and 19 (17.8%) violated the LogP or the H-bond donors (Table 4 and Fig. S1). Among the compounds that violated the LogP are those classified as aromatic ether, furanocoumarin, methoxy phenol and oxygenated diterpene, and all fatty acids such as linolenic, malvalic, margaric, palmitic and punicic acids. The compounds that violated the H-bond donors are three isomers of canavanine and myricetin. On the other hand, only two compounds classified as flavonoid as astragalin and rutin violated two and three parameters, respectively (Table 4 and Fig. S1). These compounds can exhibit poor absorption, solubility and permeability because they violate two or more parameters from "rule of 5".

3.3.3. NSAIDs

Of the 73 NSAIDs, 71 (97.3%) did not violate any of the parameters from "rule of 5" and 2 (2.7%) violated the LogP or the weight, exemplified by meclofenamic acid and glucametacin, respectively (Table 4 and Fig. S1). The higher number of compounds that did not violate the parameters of the “rule of 5” is probably explained by the fact that many of these molecules are already used in the clinic, confirmed by many previous studies that they, do not present solubility problems. This actually gives us confidence that our results are reliable.

3.4. Compilation of the data

3.4.1. Z-phytol is a good candidate

In general, most of the plant compounds that showed higher binding affinities with of structures of SdiA protein of *Salmonella* Enteritidis PT4 578 violated the LogP parameter of the "rule of 5", but were predicted to have high inhibition efficiency of biofilm formation (Table 5). It is noteworthy that C12-HSL, which has higher binding affinity to the structures of the SdiA protein, also violated the LogP parameter.

The plant compound Z-phytol is a promising candidate for the *in vitro* quorum sensing inhibition tests and biofilm formation. In addition, the compounds classified as methoxy phenol such as isoshogaol, shogaol and gingerol, with the carbon chain size ranging from six to 12, as well as the fatty acids as punicic, malvalic, margaric and palmitic acids are also good candidates for *in vitro* studies (Table 5). Such binding affinity between compounds with low water solubility, that is, high octanol-water partition coefficient, can be correlated with the characteristics of the ligand-binding domain (LDB) of the SdiA protein of *Salmonella* Enteritidis. In the SdiA protein of EHEC, the acyl chain of the AHLs is stabilize by hydrophobic residues of the LDB [53]. Chai and Winans [64] reported that the binding pocket of TraR protein (a

homologue of LuxR) of *Agrobacterium tumefaciens* is hydrophobic. Ponce-Rossi et al. [65] also showed that the AHL bound in hydrophobic pocket of the modeled structure of AhyR protein (a homologue of LuxR) of *Aeromonas hydrophila* by molecular docking. Thus, the most hydrophobic compounds are the better candidates for inhibition of the quorum sensing mechanism and for biofilm formation, indicating that the use of non-polar solvents in the process of extracting plant material is more indicative for success in the *in vitro* tests.

The molecule phytol is found in all green vegetables and is present in vitamin K, vitamin E, and other tocopherols [66]. This compound has shown antimicrobial activity against *S. aureus* [67] and *Mycobacterium tuberculosis* [68, 69], as well as against *Schistosomiasis mansoni* [70]. In addition, phytol and its derivatives have no cumulative inflammatory or toxic effects even in immuno-compromised mice [71]. Thus, phytol obtained from vegetables could be used for inhibition of quorum sensing and biofilm formation in *Salmonella* based on the results of the present study and described in the literature.

Table 5. Compilation of the data of inhibition potential *in silico* of the quorum sensing and biofilm, as well as the characteristic of plant compounds.

Group	Classification	Molecule	Molecular doking of structures			aBiofilm	Parameter violated from the "rule of 5"
			4Y13-S	4Y15-S	4Y17-S		
Plant	**Oxygenated diterpene**	**Z-phytol**	**8**	**6**	**1**	**H0**	**LogP**
AHL	Modified in 3-oxo	*N*-(3-oxododecanoyl)-L-homoserine lactone	6	1	2	H2	-
AHL	Unmodified in 3-oxo	*N*-dodecanoyl-DL-homoserine lactone	9	2	3	H2	LogP
Plant	Methoxy phenol	[12]-isoshogaol	29	3	4	H2	LogP
Plant	Methoxy phenol	[8]-gingerol	23	9	5	H2	-
Plant	Oxygenated diterpene	E-phytol	11	7	6	H0	LogP
Plant	Methoxy phenol	[10]-gingerol	32	8	7	H2	LogP
Plant	Methoxy phenol	[8]-shogaol	16	11	8	H2	LogP
Plant	Methoxy phenol	[8]-isoshogaol	21	15	9	H2	LogP
Plant	Fatty acid	Punicic acid	14	10	10	L2	LogP
Plant	Methoxy phenol	[10]-shogaol	36	5	11	H2	LogP
Plant	Fatty acid	Malvalic acid	3	12	12	H2	LogP
Furanone	Brominated	4-bromo-5-(bromomethylene)-3-dodecyl-2(5H)-furanone	25	4	13	H2	LogP
Plant	Methoxy phenol	[10]-isoshogaol	27	16	14	H2	LogP
Plant	Methoxy phenol	[6]-gingerol	20	13	15	H2	-
Plant	Fatty acid	Margaric acid	10	18	16	H1	LogP
Plant	Methoxy phenol	[6]-shogaol	7	14	17	H2	-
Plant	Methoxy phenol	[6]-isoshogaol	19	17	18	H2	-
Plant	Fatty acid	Palmitic acid	17	19	19	H1	LogP
Plant	Furanocoumarin	Imperatorin (Ammidin)	18	22	20	H2	LogP
Plant	Oxygenated sesquiterpene	E,Z-farnesol	2	24	21	H0	-
AHL	Modified in 3-oxo	*N*-(3-oxooctanoyl)-L-homoserine lactone	13	20	22	H2	-
AHL	Unmodified in 3-oxo	*N*-octanoyl-DL-homoserine lactone	12	23	23	H2	-
Plant	Flavonoid	Pinobanksin	37	27	24	H2	-
Plant	Flavonoid	Poriol	44	29	25	H2	-
Plant	Flavonoid	Retusin (Flavonol)	90	35	26	H2	-
Plant	Chalcone	Cardamonin	35	31	27	H2	-
Plant	Flavonoid	Kaempferol	56	32	28	H2	-
Plant	Flavonoid	R-epicatechin	33	43	29	H2	-
Plant	Flavonoid	RS-catechin	34	44	30	H2	-
OCL	Monoacylglycerol	1-octanoyl-*rac*-glycerol	22	38	31	L1	-
Furanone	Brominated	4-bromo-5-(bromomethylene)-3-hexyl-2(5H)-furanone	24	34	32	H2	LogP
Plant	Flavonoid	S-catechin	39	40	33	H2	-
Plant	Flavonoid	Quercetin	58	36	34	H2	-
Plant	Ajoene	E-ajoene	28	37	35	L2	-
Plant	Flavonoid	R-catechin	45	28	36	H2	-
Plant	Flavonoid	S-epicatechin	53	33	37	H2	-
Plant	Flavonoid	7,8-dihydroxy-4'-methoxyisoflavone (Isoflavone)	82	41	38	H2	-
AHL	Modified in 3-oxo	*N*-(3-oxohexanoyl)-L-homoserine lactone	30	42	39	H2	-
AHL	Unmodified in 3-oxo	*N*-hexanoyl-DL-homoserine lactone	31	45	40	H2	-
Plant	Ajoene	Z-ajoene	26	39	41	L2	-
Plant	Oxygenated monoterpene	RS-menthyl acetate	-	46	42	H2	-
Plant	Flavonoid	Myricetin	75	56	43	H2	H-bond donors
Plant	Oxygenated monoterpene	S-menthyl acetate	43	48	44	H2	-
Plant	Oxygenated monoterpene	R-menthyl acetate	38	53	45	H2	-
Plant	Flavonoid	Tricetin	68	49	46	H2	-
Plant	Oxygenated monoterpene	R-lavandulol	49	52	47	H0	-
Plant	Methoxy phenol	Zingerone (Vanillylacetone)	40	47	48	H2	-
Plant	Oxygenated monoterpene	S-lavandulol	48	50	49	H0	-
Plant	Oxygenated monoterpene	RS-lavandulol	50	51	50	H0	-
Furanone	Brominated	4-bromo-5-(bromomethylene)-3-butyl-2(5H)-furanone	41	54	51	H2	-
Plant	Terpenoid	Callicarpenal	52	-	52	H2	-
Plant	Alcohol	1-hydroxyoctane	64	62	53	H2	-
Plant	Phenylpropanoid	*p*-coumaric acid	61	61	54	H2	-
Plant	Phenylpropanoid	Cinnamic acid	59	59	55	H2	-
Plant	Phenolic acid	Ellagic acid	97	67	56	H2	-
Plant	Coumarin	Coumarin	55	57	57	H2	-
Plant	Phenylpropanoid	Ferulic acid	57	60	58	H2	-
Plant	Oxygenated monoterpene	R-piperitone	67	66	59	H2	-
Plant	Oxygenated monoterpene	RS-piperitone	66	65	60	H2	-
Plant	Oxygenated monoterpene	R-isomenthone	73	69	61	H2	-

Table 5. Continuation.

Group	Classification	Molecule	Molecular doking of structures			aBiofilm	Parameter violated from the "rule of 5"
			4Y13-S	4Y15-S	4Y17-S		
Plant	Oxygenated monoterpene	S-isomenthone	72	-	62	H2	-
Plant	Oxygenated monoterpene	RS-menthone	71	-	63	H2	-
Plant	Phenylpropanoid	Caffeic acid	62	70	64	H2	-
Plant	Amino acid	2-amino-4-chlorobenzoic acid (4CABA)	69	71	65	L0	-
Plant	Aromatic aldehyde	Vanillin	76	73	66	L1	-
Plant	Phenolic acid	Salicylic acid	80	72	67	L1	-
Plant	Amino acid	Anthranilic acid (AA)	79	77	68	L1	-
Plant	Amino acid	2-amino-6-chlorobenzoic acid (6CABA)	89	75	69	L2	-
Plant	Amino acid	2-amino-6-fluorobenzoic acid (6FABA)	83	76	70	L0	-
Plant	Phenolic acid	Gallic acid	87	78	71	L0	-
Plant	Cyclitol	R-quinic acid	81	84	72	H0	-
Plant	Flavonoid	Astragalin	100	85	73	H2	H-bond donors and acceptors
Plant	Cyclitol	S-quinic acid	88	81	74	H0	-
Plant	Alcohol	4-methylcyclohexanol	91	80	75	L1	-
Plant	Phenolic	Pyrogallol	94	83	76	L0	-
Plant	Amino acid	RS-canavanine	93	88	77	L1	H-bond donors
Plant	Amino acid	S-canavanine	92	86	78	L1	H-bond donors
Plant	Amino acid	R-canavanine	86	87	79	L1	H-bond donors
Plant	Oxygenated sesquiterpene	S-norpatchoulenol	99	89	80	H2	-
Plant	Oxygenated sesquiterpene	R-norpatchoulenol	98	90	81	H2	-
Plant	Flavonoid	Rutin	101	91	82	H2	Weight, H-bond donors and acceptors
Plant	Oxygenated sesquiterpene	Z,E-farnesol	4	21	-	H0	-
Plant	Oxygenated sesquiterpene	Z,Z-farnesol	1	25	-	H0	-
Plant	Flavonoid	Chrysin	-	26	-	H2	-
Plant	Flavonoid	Pinocembrin	-	30	-	H2	-
Plant	C_{13}-norisoprenoid	E-alfa-damascenone	51	55	-	H2	-
Plant	C_{13}-norisoprenoid	Z-alfa-damascenone	65	58	-	H2	-
Plant	Phenylpropanoid	Trans-cinnamaldehyde	63	63	-	L2	-
Plant	Oxygenated monoterpene	S-isopulegol	60	64	-	H2	-
Plant	C_{13}-norisoprenoid	E-beta-damascenone	-	68	-	H2	-
Plant	Oxygenated monoterpene	S-menthone	78	74	-	H2	-
Plant	Isothiocyanate	Iberin	77	79	-	L0	-
Plant	Alcohol	3-methylcyclohexanol	-	82	-	H2	-
Plant	Oxygenated sesquiterpene	E,E-farnesol	5	-	-	H0	-
Plant	Fatty acid	Linolenic acid	15	-	-	H1	LogP
Plant	Flavonoid	Luteolin	42	-	-	H2	-
Plant	Flavonoid	Acacetin	46	-	-	H2	-
Plant	Flavonoid	Isosakuranetin	47	-	-	H2	-
Furanone	Non-brominated	3-butyl-2(5H)-furanone	54	-	-	H1	-
Plant	Oxygenated monoterpene	S-piperitone	70	-	-	H2	-
Plant	Oxygenated monoterpene	R-menthone	74	-	-	H2	-
Plant	Alcohol	2-methylcyclohexanol	84	-	-	H2	-
Plant	Alcohol	Trans-2-methylcyclohexanol	85	-	-	H2	-
Plant	Aromatic ether	Butyl trityl ether	95	-	-	H2	LogP
Furanone	Non-brominated	2,2-dimethyl-3(2H)-furanone	96	-	-	H1	-
Plant	Alcohol	1-methylcyclohexanol	-	-	-	H2	-
Plant	Aminobenzoic ester	Methyl anthranilate (MA)	-	-	-	L1	-
AHL	Unmodified in 3-oxo	*N*-butyryl-DL-homoserine lactone	-	-	-	L0	-
Plant	Oxygenated monoterpene	R-isopulegol	-	-	-	H2	-
Plant	Monoterpene	R-limonene	-	-	-	H2	-
Plant	Oxygenated monoterpene	R-menthol	-	-	-	H2	-
Plant	Oxygenated monoterpene	R-neoisomenthol	-	-	-	H2	-
Plant	Oxygenated monoterpene	RS-isopulegol	-	-	-	H2	-
Plant	Monoterpene	RS-limonene	-	-	-	H2	-
Plant	Oxygenated monoterpene	RS-menthol	-	-	-	H2	-
Plant	Monoterpene	S-limonene	-	-	-	H2	-
Plant	Oxygenated monoterpene	S-menthol	-	-	-	H2	-
Plant	Oxygenated monoterpene	S-neoisomenthol	-	-	-	H2	-
Plant	C_{13}-norisoprenoid	Z-beta-damascenone	-	-	-	H2	-

Molecular docking = Binding affinity scale between SdiA protein and the plant compounds with a color ramp ranging from dark pink (higher affinity) to dark green (lower affinity) and hyphen for no binding;
aBiofilm = High (H) or low inhibition of biofilm formation (L) and high (H2 or L2), medium (H1 or L1) or low confidence (H0 or L0);
Parameter violated from the "rule of 5" = - (not violated any of the parameters), yellow (violated one parameter), orange (violated two parameters) and red (violated three parameters);
The best plant compound in bold.

3.4.2. Lonazolac is a good candidate

The compound lonazolac was the NSAID acetic acid derivative that showed good binding affinities with the three modeled structures of the SdiA and was predicted to have high inhibition efficiency of biofilm formation, without violating any of the "rule of 5" parameters (Table 6).

Based on the results of the present study, lonazolac was considered a good candidate for the *in vitro* tests as a quorum quenching substance and for inhibition of biofilm formation by *Salmonella*. In addition, other acetic acid derivatives including acemetacin, fentiazac, oxametacin, aceclofenac and indomethacin may be good candidates, considering their binding affinity to the SdiA protein structures as well as the predicted high inhibition of biofilm formation efficiency (Table 6). On the other hand, the NSADIs classified as pyrazolone derivative as feprazone, phenylbutazone, ketophenylbutazone, dipyrone and aminopyrine, which exhibit high binding affinity, have been predicted to have low inhibition of biofilm formation (Table 6).

Lonazolac is a nonsteroidal anti-inflammatory acetic acid derivative which has a 50% effective dose (ED 50) equivalent to diclofenac [72]. Ismail et al. [73] created new molecules from the structure of lonazolac and could be used in future studies. This compound also was cited in a patent for studies of inhibitors of quorum sensing in bacteria [50], but there are few studies with this compound.

Table 6. Compilation of the data of inhibition potential *in silico* of the quorum sensing and biofilm, as well as the characteristic of NSAIDs.

Group	Classification	Molecule	Molecular doking of structures			aBiofilm	Parameter violated from the "rule of 5"
			4Y13-S	4Y15-S	4Y17-S		
NSAID	**Acetic acid derivative**	**Lonazolac**	**4**	**1**	**1**	**H0**	-
AHL	Unmodified in 3-oxo	*N*-dodecanoyl-DL-homoserine lactone	2	6	2	H2	LogP
NSAID	Acetic acid derivative	Acemetacin	58	2	3	H0	-
AHL	Modified in 3-oxo	*N*-(3-oxododecanoyl)-L-homoserine lactone	5	3	4	H2	-
NSAID	Acetic acid derivative	Fentiazac	15	4	5	H2	-
NSAID	Pyrazolone derivative	Feprazone	60	5	6	L2	-
NSAID	Propionic acid derivative	Oxaprozin	7	9	7	L2	-
Furanone	Brominated	4-bromo-5-(bromomethylene)-3-dodecyl-2(5H)-furanone	38	7	8	H2	LogP
NSAID	Acetic acid derivative	Oxametacin	47	8	9	H2	-
NSAID	Pyrazolone derivative	Ketophenylbutazone (Kebutazone)	59	11	10	L2	-
NSAID	Pyrazolone derivative	Phenylbutazone	63	10	11	L1	-
NSAID	Anilinonicotinic acid derivative	Morniflumate	61	17	12	H0	-
NSAID	Propionic acid derivative	Flunoxaprofen	51	24	13	H1	-
NSAID	Acetic acid derivative	Aceclofenac	24	12	14	H2	-
NSAID	Pyrazolone derivative	Azapropazone	49	-	15	H1	-
NSAID	Acetic acid derivative	Sulindac	70	13	16	L0	-
NSAID	Propionic acid derivative	Fenbufen	9	19	17	L1	-
NSAID	Anilinonicotinic acid derivative	Niflumic acid	3	25	18	H0	-
NSAID	Acetic acid derivative	Indomethacin	43	14	19	H2	-
NSAID	Pyrazolone derivative	Dipyrone (Metamizole)	1	16	20	L2	-
NSAID	Pyrazolone derivative	Aminopyrine (Aminophenazone)	-	18	21	L2	-
NSAID	Propionic acid derivative	Ketoprofen	8	23	22	H0	-
AHL	Modified in 3-oxo	*N*-(3-oxooctanoyl)-L-homoserine lactone	13	20	23	H2	-
NSAID	Salicylic acid derivative	Benorilate	69	26	24	H0	-
AHL	Unmodified in 3-oxo	*N*-octanoyl-DL-homoserine lactone	11	21	25	H2	-
NSAID	Propionic acid derivative	Benoxaprofen	52	30	26	H1	-
NSAID	Pyrazolone derivative	Mofebutazone	19	29	27	L2	-
NSAID	Propionic acid derivative	Tiaprofenic acid	17	28	28	H2	-
NSAID	Enolic acid derivative (Oxicam)	Lornoxicam	76	15	29	L0	-
NSAID	Propionic acid derivative	Loxoprofen	22	44	30	H1	-
NSAID	Acetic acid derivative	Zomepirac	53	-	31	H0	-
NSAID	Acetic acid derivative	Diclofenac	29	33	32	H1	-
NSAID	Fenamic acid derivative	Mefenamic acid	39	36	33	L2	-
NSAID	Acetic acid derivative	Etodolac	46	59	34	H1	-
NSAID	Propionic acid derivative	Fenoprofen	12	34	35	H0	-
NSAID	Propionic acid derivative	Dexketoprofen	14	32	36	H0	-
NSAID	Pyrazolone derivative	Nifenazone	-	45	37	L2	-
NSAID	Anilinonicotinic acid derivative	Clonixin	48	43	38	H1	-
NSAID	Propionic acid derivative	Naproxen	20	41	39	H1	-
NSAID	Selective COX2 inhibitor (Coxibs)	Celecoxib	54	58	40	H0	-
NSAID	Enolic acid derivative (Oxicam)	Tenoxicam	75	27	41	L0	-
NSAID	Fenamic acid derivative	Tolfenamic acid	44	39	42	H1	-
NSAID	Enolic acid derivative (Oxicam)	Piroxicam	65	40	43	H0	-
OCL	OCL	1-octanoyl-*rac*-glycerol	33	46	44	L1	-
NSAID	Enolic acid derivative (Oxicam)	Isoxicam	78	-	45	H1	-
Furanone	Brominated	4-bromo-5-(bromomethylene)-3-hexyl-2(5H)-furanone	27	37	46	H2	LogP
NSAID	Propionic acid derivative	Ibuproxam	31	47	47	L0	-
NSAID	Enolic acid derivative (Oxicam)	Meloxicam	74	42	48	H2	-
NSAID	Propionic acid derivative	Dexibuprofen	34	48	49	L0	-
NSAID	Selective COX2 inhibitor (Coxibs)	Valdecoxib	57	56	50	H1	-
NSAID	Pyrazolone derivative	Oxyphenbutazone	67	38	51	H1	-
NSAID	Acetic acid derivative	Alclofenac	45	50	52	H0	-
NSAID	Acetic acid derivative	Bufexamac	36	49	53	H1	-
NSAID	Enolic acid derivative (Oxicam)	Droxicam	79	57	54	H2	-
AHL	Modified in 3-oxo	*N*-(3-oxohexanoyl)-L-homoserine lactone	37	52	55	H2	-
AHL	Unmodified in 3-oxo	*N*-hexanoyl-DL-homoserine lactone	42	51	56	H2	-
NSAID	Propionic acid derivative	Ibuprofen	32	55	57	L0	-
NSAID	Selective COX2 inhibitor (Coxibs)	Lumiracoxib	30	54	58	L1	-
NSAID	Sulfonamide derivative	Nimesulide	28	53	59	L1	-
Furanone	Brominated	4-bromo-5-(bromomethylene)-3-butyl-2(5H)-furanone	55	60	60	H2	-
NSAID	Salicylic acid derivative	Olsalazine	50	61	61	H0	-

Table 6. Continuation.

Group	Classification	Molecule	Molecular doking of structures			aBiofilm	Parameter violated from the "rule of 5"
			4Y13-S	4Y15-S	4Y17-S		
NSAID	Selective COX2 inhibitor (Coxibs)	Etoricoxib	56	64	62	H0	-
NSAID	Fenamic acid derivative	Meclofenamic acid	62	63	63	H2	LogP
NSAID	Salicylic acid derivative	Aspirin (Acetylsalicylic acid)	71	62	64	L1	-
NSAID	Salicylic acid derivative	Salicylamide	72	65	65	L1	-
NSAID	Anilide derivative	Paracetamol (Acetaminophen)	73	66	66	H2	-
NSAID	Acetic acid derivative	Glucametacin	81	69	67	H1	Weight
NSAID	Pyrazolone derivative	Suxibuzone	82	68	68	L1	-
NSAID	Salicylic acid derivative	Salicylic acid	77	67	69	L1	-
NSAID	Fenamic acid derivative	Flufenamic acid	10	22	-	H0	-
NSAID	Propionic acid derivative	Flurbiprofen	18	31	-	H1	-
NSAID	Anilinonicotinic acid derivative	Flunixin	16	35	-	L2	-
NSAID	Selective COX2 inhibitor (Coxibs)	Nabumetone	6	-	-	H1	-
NSAID	Propionic acid derivative	Alminoprofen	21	-	-	H0	-
NSAID	Propionic acid derivative	Indoprofen	23	-	-	L2	-
NSAID	Propionic acid derivative	Suprofen	25	-	-	H1	-
NSAID	Acetic acid derivative	Tolmetin	26	-	-	H1	-
NSAID	Acetic acid derivative	Ketorolac	35	-	-	H2	-
NSAID	Acetic acid derivative	Difenpiramide	40	-	-	H2	-
NSAID	Salicylic acid derivative	Diflunisal	41	-	-	H2	-
Furanone	Non-brominated	3-butyl-2(5H)-furanone	64	-	-	H1	-
NSAID	Selective COX2 inhibitor (Coxibs)	Rofecoxib	66	-	-	H1	-
NSAID	Selective COX2 inhibitor (Coxibs)	Firocoxib	68	-	-	H0	-
NSAID	Selective COX2 inhibitor (Coxibs)	Parecoxib	80	-	-	H0	-
Furanone	Non-brominated	2,2-dimethyl-3(2H)-furanone	-	-	-	H1	-
AHL	Unmodified in 3-oxo	*N*-butyryl-DL-homoserine lactone	-	-	-	L0	-

Molecular docking = Binding affinity scale between SdiA protein and the NSAIDs with a color ramp ranging from dark pink (higher affinity) to dark green (lower affinity) and hyphen for no binding;
aBiofilm = High (H) or low inhibition of biofilm formation (L) and high (H2 or L2), medium (H1 or L1) or low confidence (H0 or L0);
Parameter violated from the "rule of 5" = - (not violated any of the parameters) and yellow (violated one parameter);
The best plant compound in bold.

4. Conclusions and perspectives

In general, most the plant compounds and all nonsteroidal anti-inflammatory drugs (NSAIDs) bound in at least one of three structures of the SdiA proteins of *Salmonella* Enteritidis PT4 578 modeled. In addition, many compounds tested had higher binding affinity than the AHLs and the furanones, that are, the inducers and inhibitors of the quorum sensing mechanism, respectively. The Z-phytol and lonazolac were good candidates for the *in vitro* tests of inhibition of the quorum sensing by AI-1 and biofilm formation in *Salmonella*.

Thus, this study directs future prospecting of plant extracts for inhibition of quorum sensing mechanism depending on AHL and biofilm formation. The physico-chemical characteristics of the compounds with the greatest *in silico* potential will inform which type of separation and solvent will be more likely to be able to extract

them, and even which part of the plant or which kind of plant to choose. In addition, the use of inhibitors of quorum sensing and biofilm formation can be combined with antibiotics for better treatment efficacy until the use of these compounds to design new drugs.

Acknowledgements

Felipe Alves de Almeida was supported by a fellowship from Conselho Nacional de Desenvolvimento Científico e Tecnológico (CNPq) and this research has been supported by Fundação de Amparo à Pesquisa do Estado de Minas Gerais (FAPEMIG), Brazil and by Coordenação de Aperfeiçoamento de Pessoal de Nível Superior (CAPES). The authors acknowledge the CLC bio of the QIAGEN Company by license of the CLC Drug Discovery Workbench 3.0.2 software.

References

[1] T.J. Humphrey, A. Williams, K. McAlpine, F. Jorgensen, C. O'Byrne. Pathogenicity in isolates of *Salmonella enterica* serotype Enteritidis PT4 which differ in RpoS expression: effects of growth phase and low temperature, Epidemiol. Infect. 121 (1998) 295-301.

[2] T.J. Humphrey, A. Williams, K. McAlpine, M.S. Lever, J. Guard-Petter, J.M. Cox. Isolates of *Salmonella enterica* Enteritidis PT4 with enhanced heat and acid tolerance are more virulent in mice and more invasive in chickens, Epidemiol. Infect. 117 (1996) 79-88, http://doi.org/10.1017/S0950268800001151.

[3] S.Y. Ong, F.L. Ng, S.S. Badai, A. Yuryev, M. Alam. Analysis and construction of pathogenicity island regulatory pathways in *Salmonella enterica* serovar Typhi, J. Integr. Bioinform. 7 (2010) 145-78, http://doi.org/10.2390/biecoll-jib-2010-145.

[4] W.C. Fuqua, M.R. Parsek, E.P. Greenberg. Regulation of gene expression by cell-to-cell communication: acyl-homoserine lactone quorum sensing, Annu. Rev. Genet. 35 (2001) 439-68, http://doi.org/10.1146/annurev.genet.35.102401.090913.

[5] W.C. Fuqua, S.C. Winans, E.P. Greenberg. Census and consensus in bacterial ecosystems: the LuxR-LuxI family of quorum-sensing transcriptional regulators, Annu. Rev. Microbiol. 50 (1996) 727-51, http://doi.org/10.1146/annurev.micro.50.1.727.

[6] J.L. Smith, P.M. Fratamico, J.S. Novak. Quorum sensing: a primer for food microbiologists, J. Food Prot. 67 (2004) 1053-70, http://doi.org/10.4315/0362-028X-67.5.1053.

[7] L. Keller, M.G. Surette. Communication in bacteria: an ecological and evolutionary perspective, Nat. Rev. Microbiol. 4 (2006) 249-58, http://doi.org/10.1038/nrmicro1383.

[8] M.S. Ammor, C. Michaelidis, G.J. Nychas. Insights into the role of quorum sensing in food spoilage, J. Food Prot. 71 (2008) 1510-25, http://doi.org/10.4315/0362-028X-71.7.1510.

[9] B.M. Ahmer. Cell-to-cell signalling in *Escherichia coli* and *Salmonella enterica*, Mol. Microbiol. 52 (2004) 933-45, http://doi.org/10.1111/j.1365-2958.2004.04054.x.

[10] M. Walters, V. Sperandio. Quorum sensing in *Escherichia coli* and *Salmonella*, IJMM. 296 (2006) 125-31, http://doi.org/10.1016/j.ijmm.2006.01.041.

[11] B. Michael, J.N. Smith, S. Swift, F. Heffron, B.M. Ahmer. SdiA of *Salmonella enterica* is a LuxR homolog that detects mixed microbial communities, J. Bacteriol. 183 (2001) 5733-42, http://doi.org/10.1128/JB.183.19.5733-5742.2001.

[12] J.N. Smith, B.M. Ahmer. Detection of other microbial species by *Salmonella*: expression of the SdiA regulon, J. Bacteriol. 185 (2003) 1357-66, http://doi.org/10.1128/JB.185.4.1357–1366.2003.

[13] H. Steenackers, K. Hermans, J. Vanderleyden, S.C.J. De Keersmaecker. *Salmonella* biofilms: An overview on occurrence, structure, regulation and eradication, Food Res. Int. 45 (2012) 502-31, http://doi.org/10.1016/j.foodres.2011.01.038.

[14] Z. Liu, F. Que, L. Liao, M. Zhou, L. You, Q. Zhao, et al. Study on the promotion of bacterial biofilm formation by a *Salmonella* conjugative plasmid and the underlying mechanism, PloS One. 9 (2014) e109808-19, http://doi.org/10.1371/journal.pone.0109808.

[15] N. Abed, O. Grepinet, S. Canepa, G.A. Hurtado-Escobar, N. Guichard, A. Wiedemann, et al. Direct regulation of the *pefI-srgC* operon encoding the Rck invasin by the quorum-sensing regulator SdiA in *Salmonella* Typhimurium, Mol. Microbiol. 94 (2014) 254-71, http://doi.org/10.1111/mmi.12738.

[16] M.E.M. Campos-Galvão, T.D. Leite, A.O. Ribon, E.F. Araujo, M.C.D. Vanetti. A new repertoire of informations about the quorum sensing system in *Salmonella enterica* serovar Enteritidis PT4, Genet. Mol. Res. 14 (2015) 4068-84, http://doi.org/10.4238/2015.April.27.22.

[17] F.A. Almeida, N.J. Pimentel-Filho, L.C. Carrijo, C.B.P. Bento, M.C. Baracat-Pereira, U.M. Pinto, et al. Acyl homoserine lactone changes the abundance of proteins and the levels of organic acids associated with stationary phase in *Salmonella* Enteritidis, Microb. Pathog. 102 (2017) 148-59, http://doi.org/10.1016/j.micpath.2016.11.027.

[18] F.A. Almeida, N.J. Pimentel-Filho, U.M. Pinto, H.C. Mantovani, L.L. Oliveira, M.C.D. Vanetti. Acyl homoserine lactone-based quorum sensing stimulates biofilm

formation by *Salmonella* Enteritidis in anaerobic conditions, Arch. Microbiol. 199 (2017) 475-86, http://doi.org/10.1007/s00203-016-1313-6.

[19] T.B. Rasmussen, M. Manefield, J.B. Andersen, L. Eberl, U. Anthoni, C. Christophersen, et al. How *Delisea pulchra* furanones affect quorum sensing and swarming motility in *Serratia liquefaciens* MG1, Microbiology. 146 Pt 12 (2000) 3237-44, http://doi.org/10.1099/00221287-146-12-3237.

[20] M. Zhu, S. Takenaka, M. Sato, E. Hoshino. Influence of starvation and biofilm formation on acid resistance of *Streptococcus mutans*, Oral. Microbiol. Immunol. 16 (2001) 24-7, http://doi.org/10.1034/j.1399-302x.2001.160104.x.

[21] M. Hentzer, K. Riedel, T.B. Rasmussen, A. Heydorn, J.B. Andersen, M.R. Parsek, et al. Inhibition of quorum sensing in *Pseudomonas aeruginosa* biofilm bacteria by a halogenated furanone compound, Microbiology. 148 (2002) 87-102, http://doi.org/10.1099/00221287-148-1-87.

[22] M. Hentzer, M. Givskov. Pharmacological inhibition of quorum sensing for the treatment of chronic bacterial infections, J. Clin. Invest. 112 (2003) 1300-7, http://doi.org/10.1172/JCI20074.

[23] J.C. Janssens, H. Steenackers, S. Robijns, E. Gellens, J. Levin, H. Zhao, et al. Brominated furanones inhibit biofilm formation by *Salmonella enterica* serovar Typhimurium, Appl. Environ. Microbiol. 74 (2008) 6639-48, http://doi.org/10.1128/AEM.01262-08.

[24] L.K. Vestby, K.C. Johannesen, I.L. Witso, O. Habimana, A.A. Scheie, A.M. Urdahl, et al. Synthetic brominated furanone F202 prevents biofilm formation by potentially human pathogenic *Escherichia coli* O103:H2 and *Salmonella* ser. Agona on abiotic surfaces, J. Appl. Microbiol. 116 (2014) 258-68, http://doi.org/10.1111/jam.12355.

[25] M. Manefield, T.B. Rasmussen, M. Henzter, J.B. Andersen, P. Steinberg, S. Kjelleberg, et al. Halogenated furanones inhibit quorum sensing through accelerated LuxR turnover, Microbiology. 148 (2002) 1119-27, http://doi.org/10.1099/00221287-148-4-1119.

[26] F.A. Almeida, U.M. Pinto, M.C.D. Vanetti. Novel insights from molecular docking of SdiA from *Salmonella* Enteritidis and *Escherichia coli* with quorum sensing and quorum quenching molecules, Microb. Pathog. 99 (2016) 178-90, http://doi.org/10.1016/j.micpath.2016.08.024.

[27] M.W. Calfee, J.P. Coleman, E.C. Pesci. Interference with *Pseudomonas* quinolone signal synthesis inhibits virulence factor expression by *Pseudomonas aeruginosa*, Proc. Natl. Acad. Sci. U S A. 98 (2001) 11633-7, http://doi.org/10.1073/pnas.201328498.

[28] C.Y. Chang, T. Krishnan, H. Wang, Y. Chen, W.F. Yin, Y.M. Chong, et al. Non-antibiotic quorum sensing inhibitors acting against *N*-acyl homoserine lactone synthase as druggable target, Sci. Rep. 4 (2014) 7245-52, http://doi.org/10.1038/srep07245.

[29] C. Cugini, M.W. Calfee, J.M. Farrow, 3rd, D.K. Morales, E.C. Pesci, D.A. Hogan. Farnesol, a common sesquiterpene, inhibits PQS production in *Pseudomonas*

aeruginosa, Mol. Microbiol. 65 (2007) 896-906, http://doi.org/10.1111/j.1365-2958.2007.05840.x.

[30] C. Cugini, D.K. Morales, D.A. Hogan. *Candida albicans*-produced farnesol stimulates *Pseudomonas* quinolone signal production in LasR-defective *Pseudomonas aeruginosa* strains, Microbiology. 156 (2010) 3096-107, http://doi.org/10.1099/mic.0.037911-0.

[31] F.M. Husain, I. Ahmad, M.S. Khan, E. Ahmad, Q. Tahseen, M.S. Khan, et al. Sub-MICs of *Mentha piperita* essential oil and menthol inhibits AHL mediated quorum sensing and biofilm of Gram-negative bacteria, Front. Microbiol. 6 (2015) 420-31, http://doi.org/10.3389/fmicb.2015.00420.

[32] T.H. Jakobsen, S.K. Bragason, R.K. Phipps, L.D. Christensen, M. Van Gennip, M. Alhede, et al. Food as a source for quorum sensing inhibitors: iberin from horseradish revealed as a quorum sensing inhibitor of *Pseudomonas aeruginosa*, Appl. Environ. Microbiol. 78 (2012) 2410-21, http://doi.org/10.1128/AEM.05992-11.

[33] N.D. Keshavan, P.K. Chowdhary, D.C. Haines, J.E. Gonzalez. L-Canavanine made by *Medicago sativa* interferes with quorum sensing in *Sinorhizobium meliloti*, J. Bacteriol. 187 (2005) 8427-36, http://doi.org/10.1128/JB.187.24.8427-8436.2005.

[34] H.S. Kim, S.H. Lee, Y. Byun, H.D. Park. 6-Gingerol reduces *Pseudomonas aeruginosa* biofilm formation and virulence via quorum sensing inhibition, Sci. Rep. 5 (2015) 8656-66, http://doi.org/10.1038/srep08656.

[35] H. Kordbacheh, F. Eftekhar, S.N. Ebrahimi. Anti-quorum sensing activity of *Pistacia atlantica* against *Pseudomonas aeruginosa* PAO1 and identification of its bioactive compounds, Microb. Pathog. 110 (2017) 390-8, http://doi.org/10.1016/j.micpath.2017.07.018.

[36] N.V. Kumar, P.S. Murthy, J.R. Manjunatha, B.K. Bettadaiah. Synthesis and quorum sensing inhibitory activity of key phenolic compounds of ginger and their derivatives, Food Chem. 159 (2014) 451-7, http://doi.org/10.1016/j.foodchem.2014.03.039.

[37] B. Lesic, F. Lepine, E. Deziel, J. Zhang, Q. Zhang, K. Padfield, et al. Inhibitors of pathogen intercellular signals as selective anti-infective compounds, PLoS Pathog. 3 (2007) 1229-39, http://doi.org/10.1371/journal.ppat.0030126.

[38] B.D.A Oliveira, A.C. Rodrigues, M.C. Bertoldi, J.G. Taylor, U.M. Pinto. Microbial control and quorum sensing inhibition by phenolic compounds of acerola (*Malpighia emarginata*), IFRJ. 24 (2017) 2228-37.

[39] B.D.A. Oliveira, A.C. Rodrigues, B.M.I. Cardoso, A.L.C.C. Ramos, M.C. Bertoldi, J.G. Taylor, et al. Antioxidant, antimicrobial and anti-quorum sensing activities of *Rubus rosaefolius* phenolic extract, Ind. Crops Prod. 84 (2016) 59-66, http://doi.org/10.1016/j.indcrop.2016.01.037.

[40] K. Ponnusamy, D. Paul, J.H. Kweon. Inhibition of quorum sensing mechanism and *Aeromonas hydrophila* biofilm formation by vanillin, Environ. Eng. Sci. 26 (2009) 1359-63, http://doi.org/10.1089/ees.2008.0415.

[41] S. Priyanka, J.V. Priya, S.V. Rajesh, G. Prabhakaran, T.S. Gnanendra. Quorum sensing activity of *Couroupita Guianesis* against *Enterobacter aerogens*: *in silico* studies, Int. J. Adv. Sci. Eng. 1 (2015) 1-6.

[42] T.B. Rasmussen, T. Bjarnsholt, M.E. Skindersoe, M. Hentzer, P. Kristoffersen, M. Kote, et al. Screening for quorum-sensing inhibitors (QSI) by use of a novel genetic system, the QSI selector, J. Bacteriol. 187 (2005) 1799-814, http://doi.org/10.1128/JB.187.5.1799-1814.2005.

[43] A.C. Rodrigues, F.G. Zola, B.D.A. Oliveira, N.T. Sacramento, E.R. da Silva, M.C. Bertoldi, et al. Quorum quenching and microbial control through phenolic extract of *Eugenia* uniflora fruits, J. Food Sci. 81 (2016) M2538-44, http://doi.org/10.1111/1750-3841.13431.

[44] B.N. Singh, B.R. Singh, R.L. Singh, D. Prakash, B.K. Sarma, H.B. Singh. Antioxidant and anti-quorum sensing activities of green pod of *Acacia nilotica* L, Food Chem. Toxicol. 47 (2009) 778-86, http://doi.org/https://doi.org/10.1016/j.fct.2009.01.009.

[45] M.E. Skindersoe, M. Alhede, R. Phipps, L. Yang, P.O. Jensen, T.B. Rasmussen, et al. Effects of antibiotics on quorum sensing in *Pseudomonas aeruginosa*, Antimicrob. Agents Chemother. 52 (2008) 3648-63, http://doi.org/10.1128/AAC.01230-07.

[46] P. Truchado, A. Gil-Izquierdo, F. Tomas-Barberan, A. Allende. Inhibition by chestnut honey of *N*-Acyl-L-homoserine lactones and biofilm formation in *Erwinia carotovora*, *Yersinia enterocolitica*, and *Aeromonas hydrophila*, J. Agric. Food Chem. 57 (2009) 11186-93, http://doi.org/10.1021/jf9029139.

[47] O.M. Vandeputte, M. Kiendrebeogo, S. Rajaonson, B. Diallo, A. Mol, M. El Jaziri, et al. Identification of catechin as one of the flavonoids from *Combretum albiflorum* bark extract that reduces the production of quorum-sensing-controlled virulence factors in *Pseudomonas aeruginosa* PAO1, Appl. Environ. Microbiol. 76 (2010) 243-53, http://doi.org/10.1128/AEM.01059-09.

[48] Y.H. Yang, T.W. Kim, S.H. Park, K. Lee, H.Y. Park, E. Song, et al. Cell-free *Escherichia coli*-based system to screen for quorum-sensing molecules interacting with quorum receptor proteins of *Streptomyces coelicolor*, Appl. Environ. Microbiol. 75 (2009) 6367-72, http://doi.org/10.1128/AEM.00019-09.

[49] S.A. El-Mowafy, M.I. Shaaban, K.H. Abd El Galil. Sodium ascorbate as a quorum sensing inhibitor of *Pseudomonas aeruginosa*, J. Appl. Microbiol. 117 (2014) 1388-99, http://doi.org/10.1111/jam.12631.

[50] K. Mathee, A.L. Adonizio, F. Ausubel, J. Clardy, B. Bennett, K. Downum. Use of ellagitannins as inhibitors of bacterial quorum sensing, WO2009114810A2. The Florida International Uinversity Board of Trustees (2013).

[51] V. Soheili, B.S. Bazzaz, N. Abdollahpour, F. Hadizadeh. Investigation of *Pseudomonas aeruginosa* quorum-sensing signaling system for identifying multiple inhibitors using molecular docking and structural analysis methodology, Microb. Pathog. 89 (2015) 73-8, http://doi.org/10.1016/j.micpath.2015.08.017.

[52] S. Ulusoy, G. Bosgelmez-Tinaz. Nonsteroidal anti-inflammatory drugs reduce the production of quorum sensing regulated virulence factors and swarm in motility in human pathogen *Pseudomonas aeruginosa*, Drug Res. (Stuttg). 63 (2013) 409-13, http://doi.org/10.1055/s-0033-1343430.

[53] Y. Nguyen, N.X. Nguyen, J.L. Rogers, J. Liao, J.B. MacMillan, Y. Jiang, et al. Structural and mechanistic roles of novel chemical ligands on the SdiA quorum-sensing transcription regulator, MBio. 6 (2015) e02429-38, http://doi.org/10.1128/mBio.02429-14.

[54] M.E.M. Campos-Galvão, A.O. Ribon, E.F. Araujo, M.C.D. Vanetti. Changes in the *Salmonella enterica* Enteritidis phenotypes in presence of acyl homoserine lactone quorum sensing signals, J. Basic. Microbiol. 56 (2015) 493-501, http://doi.org/10.1002/jobm.201500471.

[55] H. Wu, Z. Song, M. Hentzer, J.B. Andersen, S. Molin, M. Givskov, et al. Synthetic furanones inhibit quorum-sensing and enhance bacterial clearance in *Pseudomonas aeruginosa* lung infection in mice, J. Antimicrob. Chemother. 53 (2004) 1054-61, http://doi.org/10.1093/jac/dkh223.

[56] A. Rajput, A. Thakur, S. Sharma, M. Kumar. aBiofilm: a resource of anti-biofilm agents and their potential implications in targeting antibiotic drug resistance, Nucleic Acids Res. 46 (2018) D894-900, http://doi.org/10.1093/nar/gkx1157.

[57] J. Lipinski. Automated solid phase dynamic extraction-extraction of organics using a wall coated syringe needle, Fresenius J. Anal. Chem. 369 (2001) 57-62, http://doi.org/10.1007/s002160000618.

[58] D.A. Hogan. Talking to themselves: autoregulation and quorum sensing in fungi, Eukaryot. Cell. 5 (2006) 613-9, http://doi.org/10.1128/EC.5.4.613-619.2006.

[59] K.W. Nickerson, A.L. Atkin, J.M. Hornby. Quorum sensing in dimorphic fungi: farnesol and beyond, Appl. Environ. Microbiol. 72 (2006) 3805-13, http://doi.org/10.1128/AEM.02765-05.

[60] A.L. Kim, S.Y. Park, C.H. Lee, C.H. Lee, J.K. Lee. Quorum quenching bacteria isolated from the sludge of a wastewater treatment plant and their application for controlling biofilm formation, J. Microbiol. Biotechnol. 24 (2014) 1574-82, http://doi.org/10.4014/jmb.1407.07009.

[61] B.M. Ahmer, J. Van Reeuwijk, C.D. Timmers, P.J. Valentine, F. Heffron. *Salmonella* Typhimurium encodes an SdiA homolog, a putative quorum sensor of the LuxR family, that regulates genes on the virulence plasmid, J. Bacteriol. 180 (1998) 1185-93.

[62] S. Gnanendra, S. Mohamed, J. Natarajan. Identification of potent inhibitors for *Salmonella* Typhimurium quorum sensing via virtual screening and pharmacophore modeling, Comb. Chem. High Throughput Screen. 16 (2013) 826-39, http://doi.org/http://dx.doi.org/10.2174/1386207311301010003.

[63] A. Reslinski, S. Dabrowiecki, K. Glowacka. The impact of diclofenac and ibuprofen on biofilm formation on the surface of polypropylene mesh, Hernia. 19 (2015) 179-85, http://doi.org/10.1007/s10029-013-1200-x.

[64] Y. Chai, S.C. Winans. Site-directed mutagenesis of a LuxR-type quorum-sensing transcription factor: alteration of autoinducer specificity, Mol. Microbiol. 51 (2004) 765–76, http://doi.org/10.1046/j.1365-2958.2003.03857.x.

[65] A.R. Ponce-Rossi, U.M. Pinto, A.O.B. Ribon, D.M.S Bazzolli, M.C.D. Vanetti. Quorum sensing regulated phenotypes in *Aeromonas hydrophila* ATCC 7966 deficient in AHL production, Ann. Microbiol. 66 (2016) 1117–26, http://doi.org/10.1007/s13213-016-1196-4.

[66] W. Vetter, M. Schroder, K. Lehnert. Differentiation of refined and virgin edible oils by means of the *trans*- and *cis*-phytol isomer distribution, J. Agric. Food Chem. 60 (2012) 6103-7, http://doi.org/10.1021/jf301373k.

[67] Y. Inoue, T. Hada, A. Shiraishi, K. Hirose, H. Hamashima, S. Kobayashi. Biphasic effects of geranylgeraniol, teprenone, and phytol on the growth of *Staphylococcus aureus*, Antimicrob. Agents Chemother. 49 (2005) 1770-4, http://doi.org/10.1128/AAC.49.5.1770-1774.2005.

[68] M.S. Rajab, C.L. Cantrell, S.G. Franzblau, N.H. Fischer. Antimycobacterial activity of (E)-phytol and derivatives: a preliminary structure-activity study, Planta Med. 64 (1998) 2-4, http://doi.org/10.1055/s-2006-957354.

[69] D. Saikia, S. Parihar, D. Chanda, S. Ojha, J.K. Kumar, C.S. Chanotiya, et al. Antitubercular potential of some semisynthetic analogues of phytol, Bioorg. Med. Chem. Lett. 20 (2010) 508-12, http://doi.org/10.1016/j.bmcl.2009.11.107.

[70] J. Moraes, R.N. de Oliveira, J.P. Costa, A.L. Junior, D.P. de Sousa, R.M. Freitas, et al. Phytol, a diterpene alcohol from chlorophyll, as a drug against neglected tropical disease *Schistosomiasis mansoni*, PLoS Negl. Trop. Dis. 8 (2014) e2617-28, http://doi.org/10.1371/journal.pntd.0002617.

[71] R.R. Chowdhury, S.K. Ghosh. Phytol-derived novel isoprenoid immunostimulants, Front. Immunol. 3 (2012) 49-59, http://doi.org/10.3389/fimmu.2012.00049.

[72] R. Riedel. Synthesis and physico-chemical properties of lonazolac-Ca, a new antiphlogistic/antirheumatic agent, Arzneimittel-Forschung. 31 (1981) 655-65.

[73] M.A.H. Ismail, J. Lehmann, D.A.A.E. Ella, A. Albohy, K.A.M. Abouzid. Lonazolac analogues: molecular modeling, synthesis, and *in vivo* anti-inflammatory activity, Med. Chem. Res. 18 (2009) 725-44, http://doi.org/10.1007/s00044-009-9163-2.

Supplementary material

Fig. S1. Results of the *in silico* inhibition potential of biofilm formation and the "rule of 5" for plant compounds and nonsteroidal anti-inflammatory drugs (NSAIDs).

Group	Classification	Molecule	Inhibition of the biofilm		The "rule of 5"				
			Low/High	Confidence	Weight	LogP	H-bond donors	H-bond acceptors	Parameter violated
OCL	OCL	1-octanoyl-*rac*-glycerol	Low	L1	218.29	1.81	2	4	-
AHL	Unmodified in 3-oxo	*N*-butyryl-DL-homoserine lactone	Low	L0	171.20	1.01	1	4	-
		N-hexanoyl-DL-homoserine lactone	High	H2	199.25	2.10	1	4	-
		N-octanoyl-DL-homoserine lactone	High	H2	227.30	3.18	1	4	-
		N-dodecanoyl-DL-homoserine lactone	High	H2	283.41	5.35	1	4	LogP
	Modified in 3-oxo	*N*-(3-oxohexanoyl)-L-homoserine lactone	High	H2	213.23	0.31	1	5	-
		N-(3-oxooctanoyl)-L-homoserine lactone	High	H2	241.29	1.39	1	5	-
		N-(3-oxododecanoyl)-L-homoserine lactone	High	H2	297.39	3.56	1	5	-
Furanone	Non-brominated	2,2-dimethyl-3(2H)-furanone	High	H1	112.13	0.65	0	2	-
		3-butyl-2(5H)-furanone	High	H1	140.18	2.11	0	2	-
	Brominated	4-bromo-5-(bromomethylene)-3-butyl-2(5H)-furanone	High	H2	309.98	4.92	0	2	-
		4-bromo-5-(bromomethylene)-3-hexyl-2(5H)-furanone	High	H2	338.04	6.00	0	2	LogP
		4-bromo-5-(bromomethylene)-3-dodecyl-2(5H)-furanone	High	H2	422.20	9.25	0	2	LogP
Plant	Ajoene	E-ajoene	Low	L2	234.39	1.72	0	1	-
		Z-ajoene	Low	L2	234.39	1.72	0	1	-
	Alcohol	1-hydroxyoctane	High	H2	130.23	2.96	1	1	-
		1-methylcyclohexanol	High	H2	114.19	1.54	1	1	-
		2-methylcyclohexanol	High	H2	114.19	1.79	1	1	-
		3-methylcyclohexanol	High	H2	114.19	1.79	1	1	-
		4-methylcyclohexanol	Low	L1	114.19	1.60	1	1	-
		Trans-2-methylcyclohexanol	High	H2	114.19	1.79	1	1	-

Fig. S1. Continuation.

Group	Classification	Molecule	Inhibition of the biofilm		The "rule of 5"				
			Low/High	Confidence	Weight	LogP	H-bond donors	H-bond acceptors	Parameter violated
Plant	Amino acid	2-amino-4-chlorobenzoic acid (4CABA)	Low	L0	171.58	2.66	3	3	-
		2-amino-6-chlorobenzoic acid (6CABA)	Low	L2	171.58	2.66	3	3	-
		2-amino-6-fluorobenzoic acid (6FABA)	Low	L0	155.13	2.13	3	3	-
		Anthranilic acid (AA)	Low	L1	137.14	2.03	3	3	-
		R-canavanine	Low	L1	176.18	-1.31	7	7	H-bond donors
		S-canavanine	Low	L1	176.18	-1.31	7	7	H-bond donors
		RS-canavanine	Low	L1	176.18	-1.31	7	7	H-bond donors
	Aminobenzoic ester	Methyl anthranilate (MA)	Low	L1	151.17	2.15	2	3	-
	Aromatic aldehyde	Vanillin	Low	L1	152.15	1.00	1	3	-
	Aromatic ether	Butyl trityl ether	High	H2	316.44	6.00	0	1	LogP
	C_{13}-norisoprenoid	E-alfa-damascenone	High	H2	190.29	3.18	0	1	-
		Z-alfa-damascenone	High	H2	190.29	3.18	0	1	-
		E-beta-damascenone	High	H2	190.29	3.19	0	1	-
		Z-beta-damascenone	High	H2	190.29	3.19	0	1	-
	Chalcone	Cardamonin	High	H2	270.28	2.95	2	4	-
	Coumarin	Coumarin	High	H2	146.15	3.17	0	2	-
	Cyclitol	R-quinic acid	High	H0	192.17	-1.82	5	6	-
		S-quinic acid	High	H0	192.17	-1.82	5	6	-
	Fatty acid	Linolenic acid	High	H1	278.44	6.46	1	2	LogP
		Malvalic acid	High	H2	280.45	6.53	1	2	LogP
		Margaric acid	High	H1	270.46	8.22	1	2	LogP
		Palmitic acid	High	H1	256.43	7.68	1	2	LogP
		Punicic acid	Low	L2	278.44	6.95	1	2	LogP

Fig. S1. Continuation.

Group	Classification	Molecule	Inhibition of the biofilm		The "rule of 5"				
			Low/High	Confidence	Weight	LogP	H-bond donors	H-bond acceptors	Parameter violated
Plant	Flavonoid	7,8-dihydroxy-4'-methoxyisoflavone (Isoflavone)	High	H2	284.27	4.02	2	5	-
		Acacetin	High	H2	284.27	4.61	2	5	-
		Astragalin	High	H2	448.38	1.57	7	11	H-bond donors and acceptors
		R-catechin	High	H2	290.27	1.41	5	6	-
		S-catechin	High	H2	290.27	1.41	5	6	-
		RS-catechin	High	H2	290.27	1.41	5	6	-
		Chrysin	High	H2	254.24	4.64	2	4	-
		R-epicatechin	High	H2	290.27	1.41	5	6	-
		S-epicatechin	High	H2	290.27	1.41	5	6	-
		Isosakuranetin	High	H2	286.28	2.71	2	5	-
		Kaempferol	High	H2	286.24	3.93	4	6	-
		Luteolin	High	H2	286.24	3.93	4	6	-
		Myricetin	High	H2	318.24	3.22	6	8	H-bond donors
		Pinobanksin	High	H2	272.26	1.64	3	5	-
		Pinocembrin	High	H2	256.26	2.74	2	4	-
		Poriol	High	H2	286.28	2.20	3	5	-
		Quercetin	High	H2	302.24	3.57	5	7	-
		Retusin (Flavonol)	High	H2	358.35	4.88	1	7	-
		Rutin	High	H2	610.52	0.12	10	16	Weight, H-bond donors and acceptors
		Tricetin	High	H2	302.24	3.57	5	7	-
	Furanocoumarin	Imperatorin (Ammidin)	High	H2	270.28	5.04	0	4	LogP
	Isothiocyanate	Iberin	Low	L0	163.25	1.05	0	2	-

Fig. S1. Continuation.

Group	Classification	Molecule	Inhibition of the biofilm		The "rule of 5"				
			Low/High	Confidence	Weight	LogP	H-bond donors	H-bond acceptors	Parameter violated
Plant	Methoxy phenol	[6]-gingerol	High	H2	294.39	3.65	2	4	-
		[8]-gingerol	High	H2	322.44	4.74	2	4	-
		[10]-gingerol	High	H2	350.50	5.82	2	4	LogP
		[6]-isoshogaol	High	H2	276.38	4.15	1	3	-
		[8]-isoshogaol	High	H2	304.43	5.23	1	3	LogP
		[10]-isoshogaol	High	H2	332.48	6.32	1	1	LogP
		[12]-isoshogaol	High	H2	360.54	7.40	1	3	LogP
		[6]-shogaol	High	H2	276.38	4.33	1	3	-
		[8]-shogaol	High	H2	304.43	5.42	1	3	LogP
		[10]-shogaol	High	H2	332.48	6.50	1	3	LogP
		Zingerone (Vanillylacetone)	High	H2	194.23	1.45	1	3	-
	Monoterpene	R-limonene	High	H2	136.24	3.36	0	0	-
		S-limonene	High	H2	136.24	3.36	0	0	-
		RS-limonene	High	H2	136.24	3.36	0	0	-
	Oxygenated diterpene	E-phytol	High	H0	296.54	8.19	1	1	LogP
		Z-phytol	High	H0	296.54	8.19	1	1	LogP
	Oxygenated monoterpene	R-isomenthone	High	H2	154.25	2.74	0	1	-
		S-isomenthone	High	H2	154.25	2.74	0	1	-
		R-isopulegol	High	H2	154.25	2.95	1	1	-
		S-isopulegol	High	H2	154.25	2.95	1	1	-
		RS-isopulegol	High	H2	154.25	2.95	1	1	-
		R-lavandulol	High	H0	154.25	3.02	1	1	-
		S-lavandulol	High	H0	154.25	3.02	1	1	-
		RS-lavandulol	High	H0	154.25	3.02	1	1	-
		R-menthol	High	H2	156.27	3.02	1	1	-
		S-menthol	High	H2	156.27	3.02	1	1	-
		RS-menthol	High	H2	156.27	3.02	1	1	-

Fig. S1. Continuation.

Group	Classification	Molecule	Inhibition of the biofilm		The "rule of 5"				
			Low/High	Confidence	Weight	LogP	H-bond donors	H-bond acceptors	Parameter violated
Plant	Oxygenated monoterpene	R-menthone	High	H2	154.25	2.74	0	1	-
		S-menthone	High	H2	154.25	2.74	0	1	-
		RS-menthone	High	H2	154.25	2.74	0	1	-
		R-menthyl acetate	High	H2	198.31	3.59	0	2	-
		S-menthyl acetate	High	H2	198.31	3.59	0	2	-
		RS-menthyl acetate	High	H2	198.31	3.59	0	2	-
		R-neoisomenthol	High	H2	156.27	3.02	1	1	-
		S-neoisomenthol	High	H2	156.27	3.02	1	1	-
		R-piperitone	High	H2	152.24	2.18	0	1	-
		S-piperitone	High	H2	152.24	2.18	0	1	-
		RS-piperitone	High	H2	152.24	2.18	0	1	-
	Oxygenated sesquiterpene	E,E-farnesol	High	H0	222.37	4.76	1	1	-
		E,Z-farnesol	High	H0	222.37	4.76	1	1	-
		Z,E-farnesol	High	H0	222.37	4.76	1	1	-
		Z,Z-farnesol	High	H0	222.37	4.76	1	1	-
		R-norpatchoulenol	High	H2	206.33	3.46	1	1	-
		S-norpatchoulenol	High	H2	206.33	3.46	1	1	-
	Phenolic	Pyrogallol	Low	L0	126.11	0.85	3	3	-
	Phenolic acid	Ellagic acid	High	H2	302.19	3.61	4	8	-
		Gallic acid	Low	L0	170.12	0.58	4	5	-
		Salicylic acid	Low	L1	138.12	1.84	2	3	-
	Phenylpropanoid	Caffeic acid	High	H2	180.16	1.58	3	4	-
		Cinnamic acid	High	H2	148.16	2.29	1	2	-
		Ferulic acid	High	H2	194.19	1.91	2	4	-
		p-coumaric acid	High	H2	164.16	1.94	2	3	-
		Trans-cinnamaldehyde	Low	L2	132.16	1.81	0	1	-
	Terpenoid	Callicarpenal	High	H2	234.38	4.17	0	1	-

Fig. S1. Continuation.

Group	Classification	Molecule	Inhibition of the biofilm		The "rule of 5"				
			Low/High	Confidence	Weight	LogP	H-bond donors	H-bond acceptors	Parameter violated
NSAID	Acetic acid derivative	Aceclofenac	High	H2	354.18	4.10	2	5	-
		Acemetacin	High	H0	415.83	3.92	1	7	-
		Alclofenac	High	H0	226.66	3.18	1	3	-
		Bufexamac	High	H1	223.27	2.42	2	4	-
		Diclofenac	High	H1	296.15	4.74	2	3	-
		Difenpiramide	High	H2	288.35	4.14	1	3	-
		Etodolac	High	H1	287.36	3.37	2	4	-
		Fentiazac	High	H2	329.80	4.96	1	3	-
		Glucametacin	High	H1	518.95	1.89	5	10	Weight
		Indomethacin	High	H2	357.79	4.76	1	5	-
		Ketorolac	High	H2	255.27	2.25	1	4	-
		Lonazolac	High	H0	312.75	4.20	1	4	-
		Oxametacin	High	H2	372.80	3.82	2	6	-
		Sulindac	Low	L0	356.41	4.41	1	3	-
		Tolmetin	High	H1	257.29	2.76	1	4	-
		Zomepirac	High	H0	291.73	3.38	1	4	-
	Anilide derivative	Paracetamol (Acetaminophen)	High	H2	151.17	1.34	2	3	-
	Anilinonicotinic acid derivative	Clonixin	High	H1	262.69	3.99	2	4	-
		Flunixin	Low	L2	296.25	4.25	2	4	-
		Morniflumate	High	H0	395.38	3.68	1	6	-
		Niflumic acid	High	H0	282.22	3.89	2	4	-
	Enolic acid derivative	Droxicam	High	H2	357.34	1.78	0	8	-
		Isoxicam	High	H1	335.33	1.89	2	8	-
		Lornoxicam	Low	L0	371.81	2.10	2	7	-
		Meloxicam	High	H2	351.39	2.47	2	7	-
		Piroxicam	High	H0	331.35	1.97	2	7	-
		Tenoxicam	Low	L0	337.37	1.13	2	7	-

Fig. S1. Continuation.

Group	Classification	Molecule	Inhibition of the biofilm		The "rule of 5"				
			Low/High	Confidence	Weight	LogP	H-bond donors	H-bond acceptors	Parameter violated
NSAID	Fenamic acid derivative	Flufenamic acid	High	H0	281.23	4.62	2	3	-
		Meclofenamic acid	High	H2	296.15	5.36	2	3	LogP
		Mefenamic acid	Low	L2	241.29	4.47	2	3	-
		Tolfenamic acid	High	H1	261.70	4.73	2	3	-
	Propionic acid derivative	Alminoprofen	High	H0	219.28	3.52	2	3	-
		Benoxaprofen	High	H1	301.73	4.40	1	4	-
		Dexibuprofen	Low	L0	206.29	3.86	1	2	-
		Dexketoprofen	High	H0	254.29	3.61	1	3	-
		Fenbufen	Low	L1	254.29	3.22	1	3	-
		Fenoprofen	High	H0	242.27	3.80	1	3	-
		Flunoxaprofen	High	H1	285.27	3.87	1	4	-
		Flurbiprofen	High	H1	244.27	4.00	1	2	-
		Ibuprofen	Low	L0	206.29	3.86	1	2	-
		Ibuproxam	Low	L0	221.30	3.12	2	3	-
		Indoprofen	Low	L2	281.31	3.06	1	4	-
		Ketoprofen	High	H0	254.29	3.61	1	3	-
		Loxoprofen	High	H1	246.31	2.73	1	3	-
		Naproxen	High	H1	230.26	3.49	1	3	-
		Oxaprozin	Low	L2	293.32	4.01	1	4	-
		Suprofen	High	H1	260.31	3.63	1	3	-
		Tiaprofenic acid	High	H2	260.31	3.66	1	3	-

Fig. S1. Continuation.

Group	Classification	Molecule	Inhibition of the biofilm		The "rule of 5"				
			Low/High	Confidence	Weight	LogP	H-bond donors	H-bond acceptors	Parameter violated
NSAID	Pyrazolone derivative	Aminopyrine (Aminophenazone)	Low	L2	231.30	2.32	0	4	-
		Azapropazone	High	H1	300.36	4.31	0	6	-
		Dipyrone (Metamizole)	Low	L2	311.36	1.30	1	7	-
		Feprazone	Low	L2	320.39	4.75	0	4	-
		Ketophenylbutazone (Kebutazone)	Low	L2	322.36	2.80	0	5	-
		Mofebutazone	Low	L2	232.28	3.02	1	4	-
		Nifenazone	Low	L2	308.34	2.16	1	6	-
		Oxyphenbutazone	High	H1	324.38	4.41	1	5	-
		Phenylbutazone	Low	L1	308.38	4.76	0	4	-
		Suxibuzone	Low	L1	438.48	4.65	1	8	-
	Salicylic acid derivative	Aspirin (Acetylsalicylic acid)	Low	L1	180.16	1.40	1	4	-
		Benorilate	High	H0	313.31	2.85	1	6	-
		Diflunisal	High	H2	250.20	3.67	2	3	-
		Olsalazine	High	H0	302.24	4.71	4	8	-
		Salicylamide	Low	L1	137.14	0.64	3	3	-
		Salicylic acid	Low	L1	138.12	1.84	2	4	-
	Selective COX2 inhibitor	Celecoxib	High	H0	381.37	3.32	2	5	-
		Etoricoxib	High	H0	358.84	3.33	0	4	-
		Firocoxib	High	H0	336.40	2.15	0	5	-
		Lumiracoxib	Low	L1	293.72	4.57	2	3	-
		Nabumetone	High	H1	228.29	3.06	0	2	-
		Parecoxib	High	H0	370.42	3.83	1	6	-
		Rofecoxib	High	H1	314.35	2.27	0	4	-
		Valdecoxib	High	H1	314.36	2.54	2	5	-
	Sulfonamide derivative	Nimesulide	Low	L1	308.31	2.83	1	7	-

High (H) or low inhibition of biofilm formation (L) and high (H2 or L2), medium (H1 or L1) or low confidence (H0 or L0);
Not violated the "rule of 5" (-).

CONCLUSÕES GERAIS

As análises globais dos perfis de proteínas, ácidos graxos e ácidos orgânicos extracelulares ao longo do tempo de cultivo de *S. enterica* sorovar Enteritidis PT4 578 em anaerobiose na presença e ausência de *N*-dodecanoil homoserina lactona (C12-HSL), mostrou que estes perfis foram alterados na presença da molécula autoindutora. Além disso, os perfis de proteínas e ácidos graxos variam menos ao longo do tempo de cultivo na presença de C12-HSL, ou seja, os perfis de ácidos graxos e proteínas de células cultivadas por 4 h (fase logarítmica) e por 36 h (fase estacionária) na presença do AI-1 foram menos dispersos. Estes resultados indicam que as células na presença de C12-HSL estão mais preparadas para os estresses de fase estacionária, por haver a antecipação das alterações celulares que ocorrem nesta fase. Um outro fato interessante é que as proteínas relacionadas ao processo de oxirredução, principalmente proteínas tiol, e a quantidade de tiol celular livre foram maiores em células cultivadas na presença de C12-HSL, indicando que este patógeno está mais preparado para uma possível condição de estresse oxidativo.

Considerando que AHL parece preparar as células para possíveis condições de estresse, entender como estes AI-1 se ligam à proteína SdiA e também realizar a prospecção de inibidores deste mecanismo se torna necessário. Assim, a proteína SdiA de *Salmonella* Enteritidis foi modelada e verificou-se que as AHLs com mais carbonos têm mais afinidade a esta proteína, principalmente as AHLs com 12 carbonos. Além disso, as furanonas que são inibidores do mecanismo de *quorum sensing* conhecidos também foram capazes de ligar a SdiA de *Salmonella* com alta afinidade. A prospecção de inibidores entre compostos de planta e anti-inflamatórios não esteroides (AINEs) por *docking* molecular também mostrou que a maioria dos compostos analisados foi capaz de ligar a proteína SdiA de *Salmonella*, com destaque para o Z-fitol e o lonazolaco.

PERSPECTIVAS

Os resultados do presente trabalho indicam caminhos para determinar as vias e, ou macromoléculas chaves do metabolismo influenciadas pelo mecanismo de *quorum sensing* por AI-1 em *Salmonella.* Além disso, os resultados obtidos *in silico* indicam potenciais compostos inibidores do *quorum sensing* para serem avaliados *in vitro*.